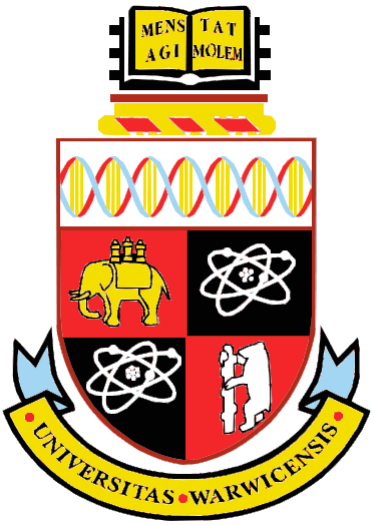

Conventional and Ultrasonic Assisted Drilling of Carbon Fibre Reinforced Polymer/ Titanium Alloy Stacks

By

Aishah Najiah Dahnel

A thesis submitted in partial fulfilment of the requirements for the degree of
Doctor of Philosophy in Engineering

WMG, University of Warwick

August 2017

Abstract

Drilling through Carbon Fibre Reinforced Polymer (CFRP) / Titanium (Ti) stacks is important for mechanical assembly of aircraft, however, there are concerns over rapid tool failure and part damage, which lead to reduced productivity and hole quality. Limited research has shown that Ultrasonic Assisted Drilling (UAD) has potential to improve hole quality when drilling CFRP and Ti individually. This has attracted the attention of aircraft manufacturers to evaluate the performance of UAD for CFRP/Ti stacks applications. This thesis presents three main studies of experimental work, which investigate tool wear mechanisms that govern tool life and hole quality when drilling CFRP/Ti stacks in a single continuous operation (one-shot) using carbide (WC-Co) drills. Study 1 involved conventional drilling of CFRP/Ti stacks as opposed to drilling CFRP and Ti individually using constant cutting parameters (cutting speed = 50 m/min; feed rate = 0.05 mm/rev). Study 2 and 3 investigate the effect of cutting parameters (cutting speeds = 25, 50, and 75 m/min; feed rates = 0.025, 0.05, and 0.075 mm/rev) during conventional drilling and UAD of CFRP/Ti stacks, and the performance of UAD was also evaluated. The hole quality was assessed in terms of hole diameter, CFRP damage (delamination and pull-out) and Ti surface integrity (burr formation, roughness, and hardness). The rapid tool failure when drilling CFRP/Ti stacks was found to be due to complex tool wear mechanisms, i.e. strong Ti adhesion on the abraded cutting edges and hence cutting edge fragmentation as the adhered Ti detached. Holes with inconsistent diameters, 22% – 62% more CFRP entrance delamination, 170% – 530% more CFRP pull-out and 720% higher Ti burr (after 80 holes) were observed when one-shot drilling of CFRP/Ti stacks compared to the case of drilling the materials individually (Study 1). It was shown (in Study 2 and 3) that using a low cutting speed and a high feed rate is important for better tool life during both conventional and UAD of CFRP/Ti stacks, although this does not completely resolve hole quality issues. Ti adhesion reduced, hence cutting edges wore uniformly and gradually, which resulted in a longer tool life, consistent hole diameter and reduced Ti burr when drilling CFRP/Ti stacks with reduced cutting speed and increased feed rate due to lower heat generation and contact time. However, CFRP damage when drilling CFRP/Ti stacks was not significantly affected by cutting parameters and tool wear, rather it was found to be substantially influenced by Ti chips evacuating through the CFRP. The application of UAD on CFRP/Ti stacks did not provide any significant advantage in tool wear / life compared to conventional drilling within the range of cutting parameters and cutting tool used, although there was slight improvement in hole quality. The cutting force profiles and Ti chip morphology indicated that UAD exhibited continuous cutting, i.e. the tool did not disengage from the workpiece during drilling. Even though the use of UAD was beneficial to produce more consistent hole diameter (between CFRP and Ti of the stacks), 33% lower machined Ti surface roughness and a marginal increase in Ti hardness compared to conventional drilling, there was no significant improvement in CFRP damage and Ti burr height. When drilling CFRP/Ti stacks, tool life and productivity could not be improved by the application of ultrasonic assistance using the range of parameters investigated, and finishing operations would still be needed to improve the hole quality. UAD could be more advantageous for drilling titanium individually than CFRP/Ti stacks.

Contents

List of Tables

List of Figures

List of Abbreviations and Symbols

2D	Two Dimensional
3D	Three Dimensional
α	Alpha
α-β	Alpha-Beta
a	Amplitude
β	Beta
φ	Point Angle
ψ	Helix Angle
κ	Half of Point Angle
σ^2	Variance
°	Degree
°C	Degree Celsius
%	Percentage
ANOVA	Analysis of Variance
BAM	Boron-Aluminium-Magnesium
BMI	Bismaleimide
CD	Conventional Drilling
cm	Centimetre
cm^3	Cubic Centimetre
CEP	Cutting Edge Preparation
CFRP	Carbon Fibre Reinforced Polymer
CFRP/Ti	Carbon Fibre Reinforced Polymer / Titanium
CMC	Ceramic Matrix Composite
Co	Cobalt
CO_2	Carbon Dioxide
D	Diameter
D_o	Nominal Diameter
f	Feed Rate
f_v	Frequency of Ultrasonic Vibration
F	Force
Fz	Thrust Force
F_A	Area-Delamination Factor
F_D	Delamination Factor

g	Gram
g/cm^3	Gram per Cubic Centimetre
GPa	Giga Pascal
H_o	Null Hypothesis
H_1	Alternative Hypothesis
HK	Knoop Hardness
HM	High Modulus
HS	High Strength
HV	Vickers Hardness
Hz	Hertz
ISO	International Organisation for Standardisation
kg/m^3	Kilogram per Cubic Metre
kHz	Kilo Hertz
K_{IC}	Strain Fracture Toughness
LFVAD	Low Frequency Vibration Assisted Drilling
LN_2	Liquid Nitrogen
m	Metre
mm	Millimetre
mm^3	Cubic Millimetre
m/min	Metre per Minute
mm/rev	Millimetre per Revolution
µm	Micrometre
µv/°C	Microvolt per Degree Celsius
MMC	Metal Matrix Composite
MPa	Mega Pascal
Mz	Torque
N	Newton
Nm	Newton Metre
PAN	Polyacrylonitrile
PMC	Polymer Matrix Composite
PCD	Poly Crystalline Diamond
RPM	Revolution per Minute
s	Second
SEM	Scanning Electron Microscopy
t_1	Un-deformed Chip Thickness
t_2	Final Chip Thickness

Tg	Glass Transition Temperature
Ti	Titanium
Ti6Al4V	Titanium Alloy (90% Titanium, 6% Aluminium, 4% Vanadium)
TiAlN	Titanium Aluminium Nitride
TiN	Titanium Nitride
UAD	Ultrasonic Assisted Drilling
UAM	Ultrasonic Assisted Machining
USB	Universal Serial Bus
V_c	Cutting Speed
V_v	Vibration Speed
WC	Tungsten Carbide
W/m.°C	Watts per Metre-Degree Celsius

Declaration

This thesis is submitted in partial fulfilment of the requirements for the degree of Doctor of Philosophy at the University of Warwick. The research was carried out at WMG, University of Warwick from October 2013 to August 2017. Unless otherwise indicated, the research described here is my own and not the product of collaboration. No part of this thesis has been submitted to any other university, or as any part of any other submission to the University of Warwick. A minor part of the practical machining work as described in Section 3.4.2 was carried out under my supervision as part of undergraduate students' final year project, although the analysis of all machinability data was performed by me. The residual stress measurement and analysis described in Section 3.3.2.4.7 were performed by Dr Darren Hughes and Conor Cafolla. The rest of experimental work and analysis of the data presented in this thesis was my original work.

Aishah Najiah Dahnel

WMG

University of Warwick

August 2017

Acknowledgement

I would like to express my deepest gratitude to my supervisors, Professor Stuart Barnes and Dr Helen Ascroft for invaluable advice and support. Their patience and continued guidance kept me going. I am very grateful to my sponsor, the Government of Malaysia (Ministry of Higher Education) and International Islamic University Malaysia (IIUM) for providing scholarship throughout my study and stay in the UK.

Thank you Austin Cook and Dave Dawson from BAE Systems for some technical advice; also, BAE Systems PLC for providing workpiece materials and cutting tools for experimental work. DMG Mori is acknowledged for the support with the machine tool.

Further thanks to Darren Grant for his assistance on practical machining work; Lewis Curry and Dr Evans Mogire for the support on sample preparation, polishing and optical microscopy using Buehler equipment; Darren Woon, Zachary Parkinson, Dave Cooper and Martyn Wilkins for their occasional help in WMG workshop.

I would like to extend my appreciation to Dr Darren Hughes and Conor Cafolla for the help with residual stress analysis, and Dr Geoff West for his advice on Scanning Electron Microscopy techniques.

Personally, thank you Fatanah, Farah and Syamra, for always offering me compassionate ears. Thanks also to all my colleagues at IDL (second floor) for keeping me motivated, and to all staffs at WMG, University of Warwick for a pleasant work environment.

To my parents and family, I am really thankful for your confidence in me, endless support, love and understanding.

Without all the support, the journey would have been much harder.

Publications

1. Dahnel, A. N., Ascroft, H., & Barnes, S. (2016). The effect of varying cutting speeds on tool wear during conventional and ultrasonic assisted drilling (UAD) of carbon fibre composite (CFC) and titanium alloy stacks. *Procedia CIRP*, *46*, 420-423.

2. Dahnel, A.N., H. Ascroft, S. Barnes, and M. Gloger. *Analysis of tool wear and hole quality during Ultrasonic Assisted Drilling (UAD) of Carbon Fibre Composite (CFC)/titanium alloy (Ti6Al4V) stacks*. in *ASME 2015 International Mechanical Engineering Congress and Exposition*. Houston, Texas, USA: 13 – 19 Nov 2015, American Society of Mechanical Engineers, pp. V02BT02A041.

3. Ascroft, H., Barnes, S., Dahnel, A. N., Gupta, A., Nor Farah Huda, A. H., & Ray, D. (2016, July). Ultrasonic assisted machining. In *UMTIK 2016 The 17th International Conference on Machine Design and Production, Conference proceedings* (Vol. 1, pp. 15-30).

4. Kourra, N., Warnett, J. M., Attridge, A., Dahnel, A., Ascroft, H., Barnes, S., & Williams, M. A. (2017). A metrological inspection method using micro-CT for the analysis of drilled holes in CFRP and titanium stacks. *The International Journal of Advanced Manufacturing Technology*, *88* (5-8), 1417-1427.

Chapter 1 Introduction

1.1 Research background

This research was conducted to replicate the hole-making process by drilling through Carbon Fibre Reinforced Polymer (CFRP) and titanium (Ti) alloy stacks for the purpose of aircraft assembly, using controlled laboratory experiments. For manufacturing military aircraft (e.g. F-35), drilling is normally performed from the CFRP outer skin through to the titanium airframe in a single continuous operation to produce aligned holes for mechanical assembly. This drilling operation involving stack materials is often termed "one-shot drilling" in the industry, hence, this term will be used throughout this thesis, for simplicity. The combination of CFRP and titanium alloy in a stack is referred to as a CFRP/Ti stack in this thesis, for simplicity.

Whilst combining the materials in a stack is seen as a resolution to meet higher service requirements by combining their exceptional properties, it has become a challenge for mechanical assembly, as drilling operations are required. A drilling operation is a relatively simple manufacturing process. However, the fact that it is often performed for mechanical assembly towards the end of a production line when manufacturing an aircraft makes the operation crucial. Damage to the parts caused by the drilling is a concern for production cost and time, as the parts can be rejected after undergoing a series of thorough, time-consuming and costly manufacturing processes. A military aircraft (e.g. F-35 Lighting) requires up to 300,000 holes to be drilled for mechanical assembly, therefore, having cutting tools that have long tool life is important [1]. Much attention and research has been devoted to improving tool life while achieving the required hole quality when drilling CFRP and titanium alloy on an individual basis. However, the lack of literature involving drilling CFRP/Ti stacks is limiting understanding of their machinability.

CFRP and titanium alloy require different drilling strategies in terms of specific cutting tools and cutting parameters, due to the distinct structures and properties of the materials. This leads to the research question of how reliable is the drilling process when uniform cutting parameters are employed for one-shot drilling of CFRP/Ti stacks? Both CFRP and titanium alloys are difficult to machine due to rapid tool wear and poor hole quality. The rapid tool wear shortens the tool life, hence necessitating frequent tool changes and increasing tooling cost. The poor hole quality requires secondary machining operations to repair the holes, which leads to additional time and cost. This raises a further question as to whether drilling the two different materials in a stack exacerbates the issues or does the interaction between the materials complement the drilling process? Therefore, this research focuses on developing an understanding of how the interaction between CFRP and titanium when drilling in a stack (in one-shot) conventionally influences the tool wear mechanisms, tool life and hole quality.

For CFRP/Ti stacks, which exhibit totally different properties, but need to be drilled together, yet the materials require different drilling strategies, it is difficult to concurrently attain tool life advantage and achieve excellent hole quality. Ultrasonic Assisted Drilling (UAD) of CFRP and titanium alloy individually has recently attracted the interest of researchers and people in the industry, as it has been shown to have potential to improve tool life and hole quality compared to conventional drilling, which further motivated this research. UAD is a hybrid machining technique in which ultrasonic vibration is superimposed on the feed direction of a conventional drill during drilling.

Research involving UAD has been focused on an individual material, specifically in terms of cutting force generation. The lack of comprehensive machinability data involving UAD, specifically for CFRP/Ti stacks, in the published literature precluded

understanding of its performance. This prompts the research question of how does the use of ultrasonic vibration on the drill when drilling CFRP/Ti stacks affect the cutting mechanism compared to conventional drilling? An understanding of this aspect is essential to explain and evaluate the performance of UAD in terms of whether a significant advantage in tool life and hole quality of CFRP/Ti stacks could be achieved.

1.2 Aims and objectives

This research aimed to develop the fundamental knowledge of machinability of CFRP/Ti stacks in terms of tool wear and hole quality when drilling conventionally (CD) and with ultrasonic assistance (UAD) using uniform cutting parameters and carbide drills. The research objectives were outlined as follow:

1) To critically review the published literature regarding drilling of CFRP-only, Ti-only and CFRP/Ti stacks.

2) To investigate tool wear mechanisms and hole quality (hole diameter, CFRP entrance delamination, CFRP pull-out and Ti burr) when drilling CFRP/Ti stacks conventionally compared to drilling CFRP and titanium alloy individually.

3) To determine the effect of cutting parameters (cutting speed and feed rate) during CD and UAD of CFRP/Ti stacks on tool wear, hole diameter consistency, CFRP damage (entrance delamination, CFRP pull-out) and machined Ti surface integrity (burr, surface roughness, hardness).

4) To examine cutting force profiles and chip formation during UAD of CFRP/Ti stacks compared to conventional drilling, in order to develop a fundamental understanding of the cutting mechanism of UAD.

Chapter 2 Literature Review

Prior to discussing drilling strategies of CFRP/Ti stacks, it is important to consider the key structures and properties of the constituent materials individually, which explains the reason for them being difficult to machine. Consequently, this chapter will also discuss conventional drilling of Carbon Fibre Reinforced Polymer (CFRP) and titanium alloy on an individual basis, highlighting the issues, and thereby, the strategies for drilling the materials in a stack will be reviewed.

2.1 Carbon fibre reinforced polymer

A composite is an engineered material exhibiting a heterogeneous structure, comprising two or more different materials with distinct properties that are combined together as a matrix and reinforcement to rectify the limitations of the individual constituents [2]. Composites can be categorised based on the nature of their matrix, such as polymer, metal and ceramic, generally denoted as Polymer Matrix Composite (PMC), Metal Matrix Composite (MMC) and Ceramic Matrix Composite (CMC), respectively [3, 4]. This research focuses on Carbon Fibre Reinforced Polymer (CFRP), a type of PMC wherein the polymer is reinforced with carbon fibres. It is well known that the high specific strength, specific stiffness, light weight and corrosion resistance are among the attractive properties of CFRP [5].

The strength and stiffness of CFRP are governed by the volume, form and orientation of the carbon fibres, as well as the bonding strength between carbon fibres and the polymer matrix. Carbon fibres in CFRP can be in the form of discontinuous (short, chopped) or continuous (uni-directional, multi-directional, woven) with diameters ranging from 10 to 20 μm [6]. CFRPs with continuous carbon fibres are preferably used in the aerospace industry. This is because continuous carbon fibres can be oriented in a

specific direction to achieve the desired strength. The continuous fibres extend for the entire CFRP, which makes the composite suitable for load-bearing applications. Whereas, discontinuous carbon fibres are much shorter, and hence often exhibiting random orientations in CFRP leading to a reduction in the composite strength [7]. Nevertheless, CFRPs with discontinuous carbon fibre reinforcement are easier, faster and less costly to manufacture, therefore, they are usually employed in the applications where cost minimisation is more important than achieving the high strength of a component.

CFRP is distinguishable from metallic alloys in such that it is anisotropic, meaning that its strength varies according to the direction of carbon fibres, which sometimes may limit its application [8, 9]. For instance, CFRP (with continuous carbon fibres) exhibits a higher tensile strength when the load is applied along the fibre direction (longitudinal direction) compared to across the fibres (transverse direction), Figure 2.1 (a). To overcome the constraint of anisotropic behaviour, CFRP is often made up by orientating the carbon fibres' plies in multi-directions, such as 0˚, 90˚, -45˚ and +45˚, Figure 2.1 (b), so that the strength is more distributed across the CFRP component.

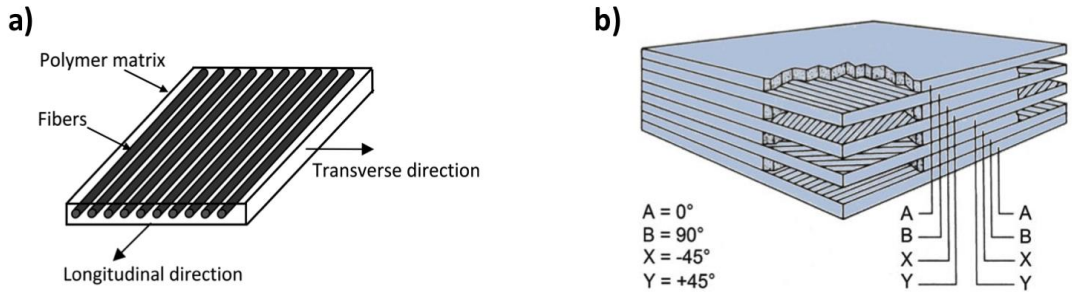

Figure 2.1: Schematic of CFRP with continuous carbon fibres, showing (a) a single ply / prepreg having uni-directional fibres [10, 11]; (b) fibre orientations in typical CFRP (0˚,90˚, -45˚ and +45˚) used in the aerospace industry [2]

The overall strength of CFRP components is influenced by the volume fraction of the carbon fibre and polymer matrix. Improvement in the strength and mechanical properties of CFRP can be achieved by having a higher volume of carbon fibres [12-14].

Increasing carbon fibre content from 50% to 70% has been reported to increase the flexural strength of the composite (with an epoxy matrix) from 1025 to 1139 MPa and the flexural modulus from 50 to 56 GPa [13]. This makes the composite stronger and stiffer. However, it is important to note that increasing the carbon fibre content also increases the weight and brittleness of the composite. From the machining point of view, higher brittleness of CFRP means a reduction in its deformation ability, which indicates a higher tendency to fracture when being machined.

For aircraft applications, CFRP typically consists of 60% to 70% continuous carbon fibres and 30% to 40% polymer matrix. The maximum practical limit of carbon fibre volume fraction in a composite is recognised to be 70% to ensure a strong interfacial bonding between the carbon fibres and polymer matrix [7]. Increasing carbon fibres content from 70% to 80% in a composite (with epoxy matrix) has been reported to reduce the flexural strength and flexural modulus of CFRP from 1139 to 1000 MPa and from 56 GPa to 28 GPa, respectively [13]. A higher percentage of carbon fibre content means little space for the polymer matrix to support the carbon fibres, preventing sufficient interfacial bonding hence causing porosity and weakening of the CFRP component [7, 13]. The key properties of carbon fibre reinforcement and polymer matrix that make the CFRP are explained in Sections 2.1.1 and 2.1.2.

2.1.1 Carbon fibre reinforcement

Most carbon fibres are produced from a polyacrylonitrile (PAN) precursor which is stretched and heated in a non-oxygen environment at temperatures above 1000 °C in order to remove all non-carbon atoms [6]. The mechanical properties of carbon fibres vary according to the grades, such as high modulus (HM) and high strength (HS) grades. Typical mechanical properties of HM and HS grades are compared in Table 2.1. As an individual material, carbon fibre is stiff with an elastic modulus of 390 – 400 GPa

for a HM grade, while a HS grade exhibits a lower value within 230 – 250 GPa, Table 2.1. The tensile strength of carbon fibres is typically in the range of 2.5 to 4.5 GPa for the HM grade, whereas the HS grade exhibits a higher value within 3.8 to 4.2 GPa. Despite the high specific strength and modulus of carbon fibres as indicated in Table 2.1, it is not practical to use carbon fibres alone to make a product due to their brittleness and low impact resistance. Thus, in order to utilise the strength of carbon fibres for high-performance components, a matrix or resin (polymer) is required to hold and support the carbon fibres.

Table 2.1: Typical mechanical properties of carbon fibre for CFRP applications [2, 6]

Properties	**PAN-based carbon fibre**	
	High Modulus (HM)	**High Strength (HS)**
Density (g/cm^3)	1.81 – 1.95	1.75 – 1.78
Elastic modulus (GPa)	390 – 400	230 – 250
Tensile strength (GPa)	2.5 – 4.5	3.8 – 4.2
Specific modulus (GPa/(g/cm^3))	200 – 220	129 – 140
Specific tensile strength (GPa/(g/cm^3))	1.28 – 2.48	2.13 – 2.40

It must be noted that carbon fibres are highly abrasive, which means that, when machining, the fine abrasive dust can damage the machine tool and endanger the operator's health if they inhale the fine particles. Therefore, a dust extractor is essential when CFRP is machined in dry condition. Otherwise, cutting fluid can be used to suppress and wash away the carbon fibre dust. Moreover, the high electrical conductivity of carbon fibre dust can damage the electrical components in the machine tool, such as causing a short circuit when the dust penetrates into the electronic machine tool.

2.1.2 Polymer matrix

Mouldability (easiness to shape), high resistance to corrosion and light weight has made polymers attractive to many industries in recent decades. Polymers, however, need reinforcement to improve their strength for aircraft application, which has led to the development of composites with the carbon fibres. The polymer resin within a CFRP also serves as to protect the brittle carbon fibres from impact and damage.

Polymers generally have low strength, thus not all polymers are suitable to be used as the matrix for CFRP intended for aircraft components. The strength and maximum service temperature of a CFRP component are normally governed by the polymer's glass transition temperature (Tg), which is described as the temperature at which it starts to soften, i.e. transitioning from the hard glassy state to the rubbery state. Therefore, it is important for CFRP to have a polymer matrix that has a high Tg. From the machining point of view, a high Tg of the polymer matrix is beneficial as it can withstand the cutting temperature, thereby keeping the carbon fibres intact.

The two types of polymers, thermoplastics and thermosets, can be differentiated based on the bonds and crosslinks between their molecular chains (of hydrogen-carbon atoms). Thermoplastic is characterised by linear molecular chains; there are no physical and chemical connection or crosslinks between the polymer chains. Instead, the chains are held and linked together by intermolecular forces known as Van der Waals bonds [6], Figure 2.2. The intermolecular force keeps the thermoplastic chains intact, preventing movements between the chains, particularly in ambient / room temperature environment. An increase in temperature above the Tg of thermoplastic weakens the intermolecular forces, which causes a reduction in its stiffness and viscosity as a result of sliding between the molecular chains, leading to melting upon reaching its melting temperature [2, 7].

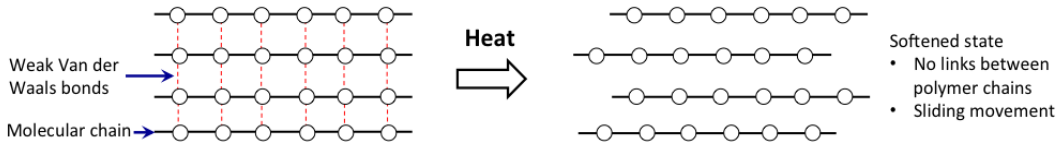

Figure 2.2: Schematic diagram of thermoplastic polymer chains and structure (adapted from [7, 15])

A notable advantage of thermoplastics over thermosets is that they can be re-processed and reshaped several times after the melting [2]. Examples of thermoplastics that are commonly used for making composites include but are not limited to, Polyamide (PA), Polyphenylenesulfide (PPS) and Polyetheretherketone (PEEK) [7, 16]; typical properties are shown in Table 2.2. These thermoplastics are increasingly used in CFRP due to their higher toughness and lower processing cost than thermosets, although the low Tg restricts their application at elevated temperature environment.

Table 2.2: Typical mechanical properties of thermoplastics used as the matrix for CFRP [6]

Properties	Polyamide (PA)	Polyphenylene sulfide (PPS)	Polyetheretherketone (PEEK)
Density (g/cm^3)	1.10	1.36	1.26 –1.32
Elastic modulus (GPa)	2.0	3.3	3.2
Tensile strength (MPa)	70 – 84	84	93
Glass transition temperature, Tg (°C)	55 – 80	85	145
Melting temperature, Tm (°C)	265	285	345

In comparison to thermoplastics, a thermoset has strong crosslinks between molecular chains, known as covalent bonds [5], Figure 2.3. The fact that physical and chemical connections exist between the polymer chains to hold them together prevents

movement, which makes a thermoset material stiffer than a thermoplastic. Thermosets generally have a higher elastic modulus, thermal stability and glass transition temperature (Tg), as indicated in Table 2.3, compared to thermoplastics, Table 2.2 [6, 17]. An increase in temperature for thermoset can reduce their stiffness and strength, however, unlike a thermoplastic, it does not eventually lead to melting. Instead, the thermoset degrades and decomposes upon exceeding its Tg [2, 5].

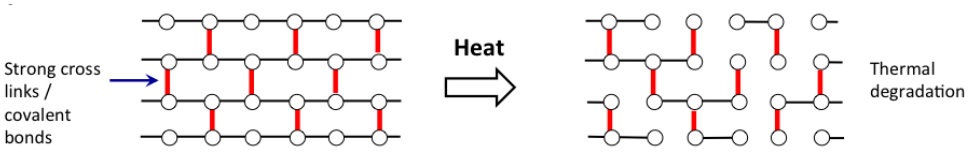

Figure 2.3: Schematic diagram of thermoset polymer chains and structure (adapted from [7, 15])

Table 2.3: Typical mechanical properties of thermosets used as the matrix for CFRP [6]

Properties	Epoxy	Bismaleimide (BMI)	Polyester
Density (g/cm^3)	1.10 – 1.20	1.20 – 1.32	1.10 – 1.23
Elastic modulus (GPa)	2.6 – 3.8	3.2 – 5.0	3.1 – 4.6
Tensile strength (MPa)	60 – 85	48 – 110	50 – 75
Glass transition temperature, Tg (°C)	65 – 175	230 – 345	70

Typical thermosets used in composites for industrial applications are epoxy, Bismaleimide (BMI) and polyimides [16, 18, 19]. Epoxy has been widely used as the matrix for CFRP, although BMI is often employed as the matrix in CFRP for manufacturing aircraft. This is due to the higher Tg of BMI, which makes it more resistant to heat compared to epoxy, Table 2.3. The polymer matrix has a significant influence on determining the weight and mechanical properties of CFRP [20]. It is

apparent in Tables 2.2 and 2.3 that the density, elastic modulus and tensile strength of polymers are much lower than the carbon fibres, Table 2.1. This indicates that the weight and strength of CFRP decrease as the volume fraction of polymer matrix increases.

2.2 Titanium alloys

Titanium (Ti) is a transition metal, grey or silver in colour and represented by atomic number 22 in the periodic table. It constitutes approximately 0.6% of the earth's crust and can be found in abundance after aluminium, iron and magnesium. Titanium is rarely found in its pure state directly from the earth's crust as the metal naturally exists in the form of mineral sands consisting of ilmenite ($FeTiO_3$) and rutile (TiO_2) [21, 22]. Therefore, an extraction process is required, and the complex process makes titanium and its alloys more expensive than other common metals. The extraction, purification and further manufacturing of titanium are costly because titanium has high reactivity with oxygen which requires processes to be carried out in a vacuum or an inert environment and it is also a labour-intensive process [23, 24].

The mechanical properties of pure titanium can be improved by the alloying process. Titanium alloys are mainly classified into three major groups which are Alpha (α) alloy, Beta (β) alloy and Alpha-Beta (α-β) alloy [25]. These different groups of titanium alloys exist due to the content and amount of elements alloyed with titanium during its manufacture. Adding a major amount of α alloying elements (stabilisers), such as aluminium, oxygen, carbon and tin to pure titanium produces an α titanium alloy. This α alloy is not heat treatable and is categorised as having low to medium strength among titanium alloys [26]. Mixing pure titanium with β elements (stabilisers) such as vanadium, chromium, molybdenum, iron and nickel transforms the metal into β titanium alloy [21]. β alloys have higher strength and good forgeability, although

higher density compared to α and α-β alloys [27, 28]. An α-β titanium alloy contains a mixture of both α and β elements. They are heat treatable, also exhibiting an excellent combination of strength, toughness and corrosion resistance [21, 29]. Common examples and application of titanium alloys are shown in Table 2.4.

Table 2.4: Examples and common application of titanium α alloy, α-β alloy and β alloy [30]

Titanium alloys	Example	Common application
α alloy	Ti3Al2.5V Ti5Al2.5Sn	Gas turbine engine casing
β alloy	Ti10V2Fe3Al Ti15V3Cr3Al3Sn	Aircraft spring
α-β alloy	Ti6Al4V Ti6Al6V2Sn	Airframe and structural aircraft components

This research focuses on Ti6Al4V, which is an α-β titanium alloy commonly used for making airframe and structural aircraft components (with 50% of usage compared to other titanium alloys) [23]. The mechanical properties of titanium alloys are significantly influenced by their microstructures in terms of the volume fraction of globular α-phase and lamellar β-phase. These two microstructural phases are formed by a recrystallisation process as a result of post-processing heat treatment and the cooling processes of the titanium alloys when they are being manufactured [22, 31]. The microstructures of Ti6Al4V are typically described as fine globular equiaxed, coarse globular equiaxed, lamellar, or bimodal [26], as shown in Figure 2.4. The equiaxed microstructure means that the grains have equal dimension throughout. The bimodal microstructure exhibits a mixture of lamellar and equiaxed grains.

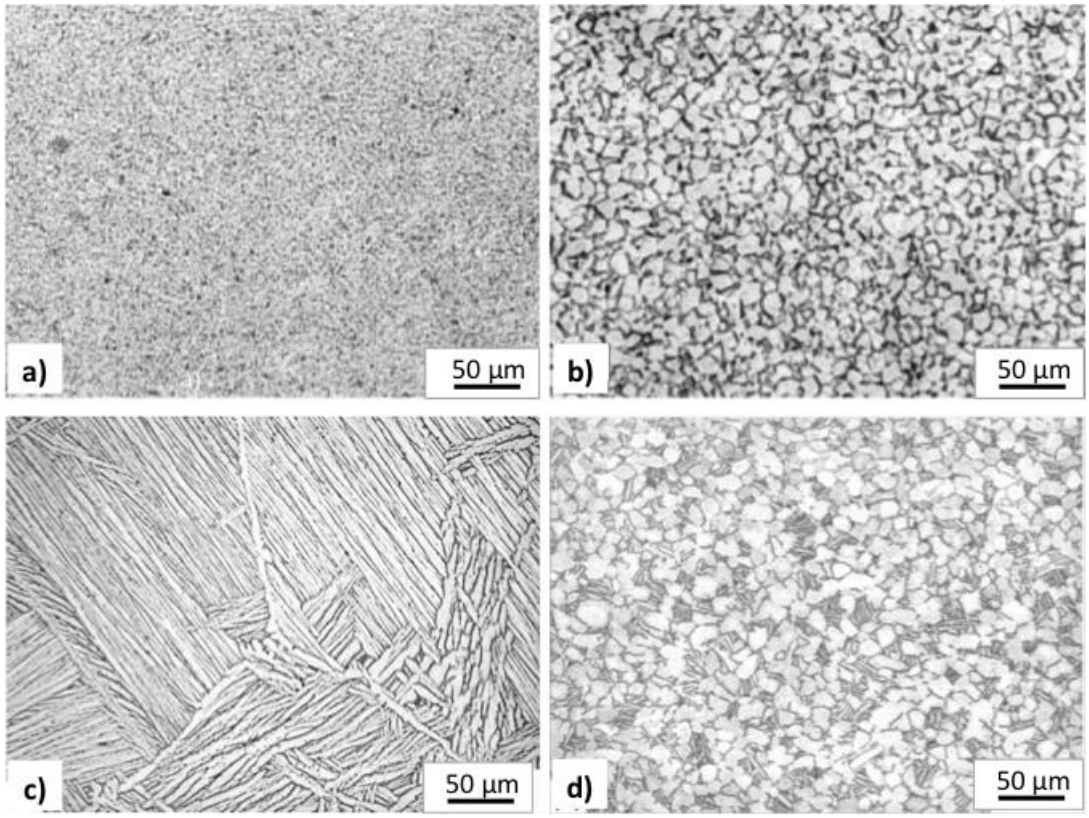

Figure 2.4: Typical microstructures of titanium alloy Ti6Al4V showing (a) fine equiaxed grains, (b) coarse equiaxed grains, (c) lamellar, (d) bimodal [21]

Compared to the globular α-phase, the β-phase exhibiting lamellar structures is relatively soft, which makes it more easily deformable, although it is more resistant to crack propagation and creep [21, 31]. The equiaxed (globular) microstructure has a balance of high strength and ductility, although the fine and smaller globular grains (e.g. less than 5 µm) are more ductile and have higher toughness compared to the coarse globular grains (e.g. 10 – 50 µm) [21]. Among all, bimodal microstructures are usually preferable in industry because they possess balanced properties of both equiaxed and lamellar structures. Some key mechanical properties of titanium alloy Ti6Al4V in comparison to pure titanium and other metals are shown in Table 2.5.

Table 2.5: Key properties of titanium in comparison to iron, nickel and aluminium [23, 32]

Materials	Pure Titanium	Ti6Al4V	Iron	Nickel	Aluminium
Density (kg/m^3)	4500	4400	7900	8900	2700
Yield strength (MPa)	430	1000	1000	1000	500
Elastic modulus (GPa)	115	115	215	200	72
Melting temperature (°C)	1670	1670	1538	1455	660
Thermal conductivity (W/m.°C)	19 - 23	15	73	90	204
Comparative corrosion resistance	Very High	Very high	Low	Medium	High

A yield strength of 1000 MPa and density of 4400 kg/m^3 indicate that titanium Ti6Al4V has a higher specific strength (ratio of strength to weight) compared to other metals, which makes the alloy advantageous for aerospace structural components. Yield strength, which is regarded as the amount of stress required to permanently deform the material is used as an indicator to determine the strength of the material, while density (kg/m^3) gives an impression of the weight of the material. In machining, the fact that titanium Ti6Al4V exhibits yield strength of 1000 MPa, which is two times higher than aluminium, Table 2.5, indicates that Ti6Al4V is more difficult to deform and hence requires a stronger cutting tool.

Compared to other metals, the low thermal conductivity of titanium Ti6Al4V (15 W/m.°C) indicates poor heat dissipation, which often renders its application as a good thermal insulator. However, when the titanium needs to be machined, its low thermal conductivity means the heat produced is hardly removed from the cutting zone (through the titanium workpiece / chip). This will cause a concentration of heat in the cutting zone, which is detrimental for the cutting tool.

At normal room temperature, titanium alloys are chemically inert, meaning that they do not react with other materials. However, it becomes highly reactive with other metals (cutting tool when machining) when the temperature increases above 500 °C [33], which is a critical issue during machining. The excellent properties of titanium alloys have made them attractive for aerospace components, however, such properties are also the reasons for them being difficult to machine.

2.3 Carbon fibre reinforced polymer/ titanium alloy stacks

A stack is made when discrete materials are piled and combined together. More complex stack configurations consist of more than two combinations of material, such as titanium, composites, and aluminium. The multi-materials stacks are typically employed in the aerospace industry, for manufacturing military aircraft and are increasingly gaining applications in commercial aircraft. The materials are combined in a stack to overcome the limitation in properties when they are used individually; this approach is also seen as a way to exploit their excellent properties. Being lightweight while maintaining the required strength and properties during flight and the aircraft's entire lifespan is crucial due to concerns over fuel saving, emission legislation and environmental awareness, which is the reason for employing both CFRP and titanium alloys. The lower weight of the aircraft means less work for the engines, which leads to less fuel consumption, less carbon dioxide (CO_2) emission per unit time and also further flying distance.

This research focuses on a stack combination of CFRP and titanium alloy Ti6Al4V. CFRP is increasingly used for making the fuselage and aircraft outer skin, whereas, the airframe is typically made of titanium alloys since it requires high metallic structural strength. Assembly of the aircraft's CFRP outer skin to the titanium Ti6Al4V airframe

leads to the formation of CFRP/Ti stacks. The detailed structures and properties of both CFRP and titanium alloys were discussed in Sections 2.1 and 2.2, respectively, which explained the reasons for their application, poor machinability and hence the on-going machining challenges. The hole making process is a crucial operation, comprising 40% to 60% of the total machining operation in order to manufacture and assemble the aircraft [20]. Hence, this research focuses on investigating and understanding machinability of CFRP/Ti stacks, subject to one-shot drilling, in terms of tool wear and hole quality.

2.4 Cutting tools

A cutting tool that is used for making holes by drilling is termed a drill. The drill performance in terms of having long tool life, producing the required machined surface finish and producing holes within tolerance, is mainly dependent on the materials from which the drill is made and its geometry [34]. Before discussing common drilling practices involving CFRP, titanium alloys and CFRP/Ti stacks, it is useful to review the key features of drill materials and nomenclature of typical drill geometry; these are outlined in Sections 2.4.1 and 2.4.2.

2.4.1 Drill materials

High speed steel (HSS), cemented carbide and polycrystalline diamond (PCD) are known to be the most common materials for drills. Their application and suitability for drilling are distinguished primarily based on their hardness, toughness and their reactivity relative to the workpiece material [25, 28]. Drill hardness is defined as the ability to maintain its shape and properties, resist indentation, deformation and wear during the drilling operation [32, 34]. Drill toughness is regarded as the ability of the drill to resist drilling impact and to absorb the stress during drilling before fracture

[20]. Figure 2.5 and Table 2.6 show a relative comparison of hardness and toughness of HSS, cemented carbide and PCD drills.

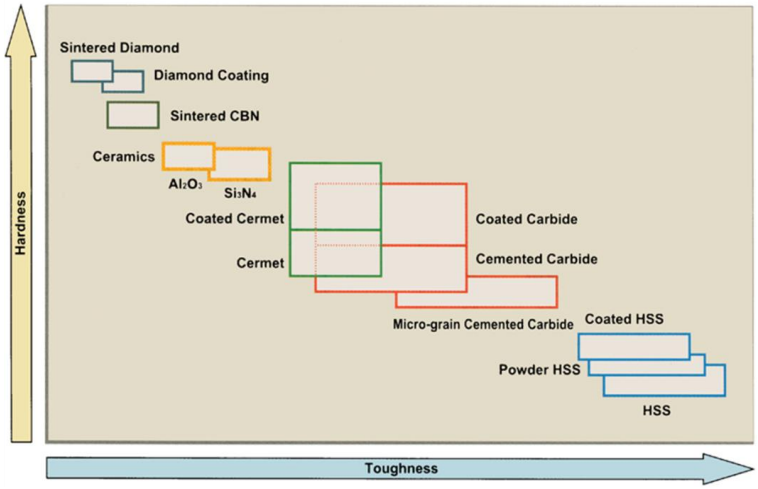

Figure 2.5: Comparison of hardness versus toughness of common cutting tool materials [34]

Table 2.6: Comparison of typical hardness and toughness of high speed steel (HSS), tungsten carbide (WC-Co) and polycrystalline diamond (PCD) drills [6, 35, 36]

Drill material	Hardness (HV)	Fracture toughness, K_{IC} ($MPa.m^{-1/2}$)
High Speed Steel (HSS)	800 – 910	10 – 18
Tungsten Carbide (WC-6%Co)	1300 – 2000	8 – 14
Polycrystalline Diamond (PCD)	7000 – 10,000	3 – 9

HSS drills are known for having high toughness (10 – 18 $MPa.m^{-1/2}$) and are normally used for roughing operations and drilling soft metals like aluminium. However, the low strength and hardness (800 – 910 HV) of HSS drills make them not practical for drilling CFRP and titanium alloys due to rapid wear and drill breakage (as early as drilling the first hole). Thus, it is not of an interest in this research, and no further details about HSS drills will be discussed.

Straight cemented carbide (WC-Co) drills have been reported as the most commonly used for drilling CFRP, titanium and CFRP/Ti stacks [27, 37-41] due to their balanced

hardness and toughness compared to other drill materials, Figure 2.5 and Table 2.6. Cemented or tungsten carbide drills are manufactured using powder metallurgy by mixing, sintering and bonding tungsten carbide (WC) grains and cobalt (Co) powders at a temperature within 1350 – 1650 °C. Despite having high hardness, an individual WC grain is brittle and it has low impact strength, therefore, cobalt is used as a binder to hold the WC grains hence improving the overall strength [32, 42]. The size of WC grains that are generally used for making carbide drills are within 0.1 – 20 μm and the typical Co proportion is normally within 4% to 30% [6, 36].

The size of WC grains and the proportion of Co binder are important in determining the hardness and toughness of carbide drills. As a general rule, a low Co binder content and smaller WC grains size are beneficial for improving the hardness of a carbide drill, although this reduces the drill's toughness. Specifically, for a carbide drill with 6% Co content, the overall hardness increases from 1400 HV to 1750 HV with a decrease in WC grain sizes from medium coarse (2.1 – 3.4 μm) to submicron (0.5 – 0.9 μm), however, the fracture toughness reduces from 12 to 10 $MPa.m^{-1/2}$ [36]. For a carbide drill with submicron WC grain sizes (0.5 – 0.9 μm), a decrease in Co binder content from 15% to 5% increases the average hardness of the drill from 1400 HV to 1800 HV, however, the fracture toughness reduces from 16 to 8 $MPa.m^{-1/2}$ [36].

PCD drills are known for having exceptional hardness (7000 – 10,000 HV) compared to other drills, Table 2.6, although PCD drills are costly as the price is normally 10 to 30 times higher than cemented carbide drills [34, 43], which limits their application. PCD drills are made by sintering diamond grains having sizes of 0.5 to 50 μm in a metallic binder, typically cobalt, at high temperature (1500 °C) and high pressure (60 GPa) [34]. The sintered PCD wafer is then cut to the required segment as a cutting edge, which is brazed onto a carbide substrate. A disadvantage in the property of PCD drills compared to cemented carbide drills is that they have lower hot hardness,

whereby they begin to lose hardness as the diamond reverts to graphite when the temperature increases higher than 500 °C [34]. Thus, a PCD drill is normally recommended when cutting temperature is lower than 500 °C, otherwise using a cemented carbide drill is regarded as a better option. PCD drills have also been recognised for having lower toughness than carbide drills, in which edges fracture and breakage have often been reported when they were used for drilling titanium alloys [32, 44-46].

2.4.2 Drill geometry

The shape and geometry of a drill have a major influence on cutting force generation, chip formation and hole quality [47]. Before discussing drilling strategies, it is useful to know the key geometry of a standard two-flute twist drill, such as the cutting lips (or cutting edges), point angle, helix angle, chisel edge, flank face and rake face; these are shown in Figure 2.6.

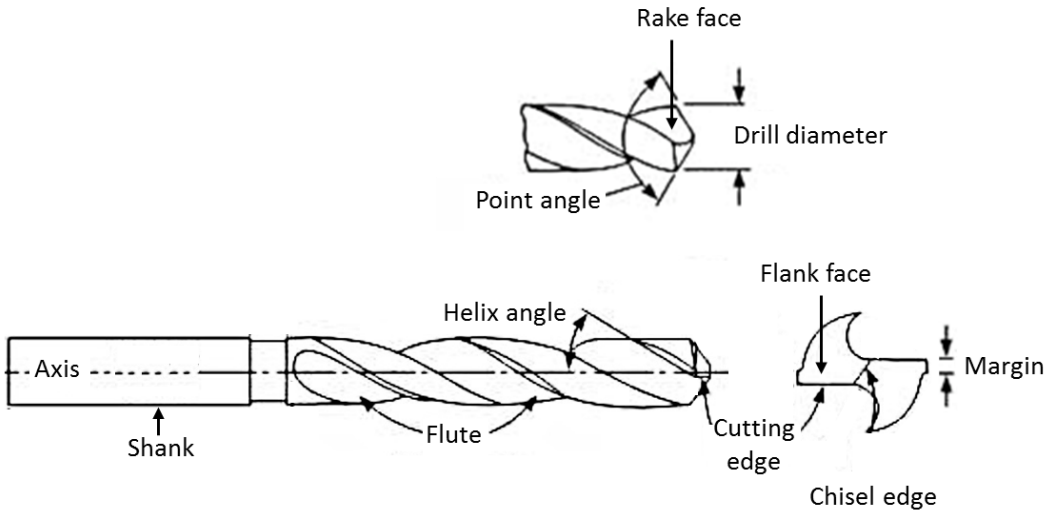

Figure 2.6: Major geometry of a standard two-flute twist drill (adapted from [48])

The point angle for a standard two-flute twist drill is the included angle that is formed between the cutting lips, Figure 2.6, which varies from 90° to 140° depending on the workpiece materials to drill. A larger point angle makes the drill stronger. The drill

helix angle for a standard two-flute twist drill is typically within 12° to 38°. The helical flutes provide a passage for chips to flow and for cutting fluid to reach the cutting zone. A larger helix angle facilitates chip removal from cutting zone [43]. The flank face of the drill is the surface which passes over the newly machined workpiece surface, while the rake face is the surface on which the chip flows [44]. The chisel edge is the edge that connects the main cutting edges together [34].

2.5 Thrust force and torque

Thrust force and torque are generated during drilling as a result of shearing workpiece material and chip formation. Thrust or axial force is denoted as Fz, which is a summation of forces acting on the chisel edge (F_{ce}), cutting lips / edges ($F_{cl,A}$), side surface (F_{ss}) and helical flutes (F_{hf}) of the drill, in the axial or feed direction during drilling [20], Figure 2.7. It has been reported that 60% of the thrust forces generated during drilling is contributed by the chisel edge action [34]. Whereas, torque (Mz) is the force applied along or at the radius of cutting edges, $F_{cl,N}$, when the drill rotates to shear the workpiece material [20], Figure 2.7.

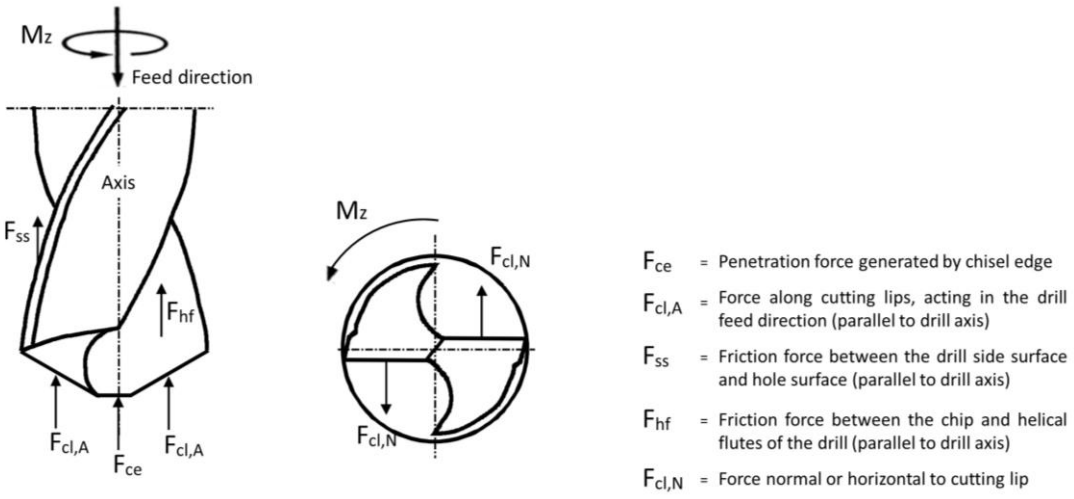

Figure 2.7: Forces acting on a drill during drilling (adapted from [20])

Thrust force and torque indicate the effort required to form chips, which are mainly dependent on the workpiece material, drill geometry, cutting parameters and wear of

cutting edges. These cutting forces are important because they affect the machined surface integrity, dimensional accuracy and the extent of workpiece damage [6, 32].

2.6 Conventional drilling of CFRP

2.6.1 Background

CFRP components are normally fabricated near-net shape, although machining operations, particularly drilling is often required to make holes for mechanical assembly. Drilling CFRP is generally difficult due to the abrasive nature of carbon fibre causing rapid tool wear and failure [49]. In addition, the heterogeneous and brittle fracture of CFRP often resolve in irregular surface finish and damage to the machined part, thereby causing a reduction in the quality of CFRP component [50]. Before further discussing the tool wear and hole quality when drilling CFRP individually, a brief explanation of the chip formation of CFRP is presented in Section 2.6.2 to provide an understanding of the cutting mechanism of the CFRP.

2.6.2 Chip formation

Machining of CFRP produces chips in the form of fine dust, due to brittle fracture of the CFRP. The mechanism of chip formation of CFRP is highly dependent on the carbon fibre orientation [6]. The fracture of carbon fibres with 0° orientation (relative to cutting direction) occurs due to the compression and micro-buckling by the cutting tool, Figure 2.8 (a). For carbon fibres having orientation 90° and -45° relative to the cutting direction, the chips are formed by cracking and fracture as a result of compression and inter-laminar induced shear by the cutting edges across the carbon fibres, Figure 2.8 (b, c). For +45° fibre orientation, the chip formation is explained as a result of extensive cracking followed by macro-fracture due to the elastic bending and

compressive force against the carbon fibres [6], Figure 2.8 (d). These multi-orientations of carbon fibres and their fracture behaviour cause difficulty in achieving a uniform machined surface finish and is the primary reason for the CFRP damage occurring during drilling, and hence poor hole quality.

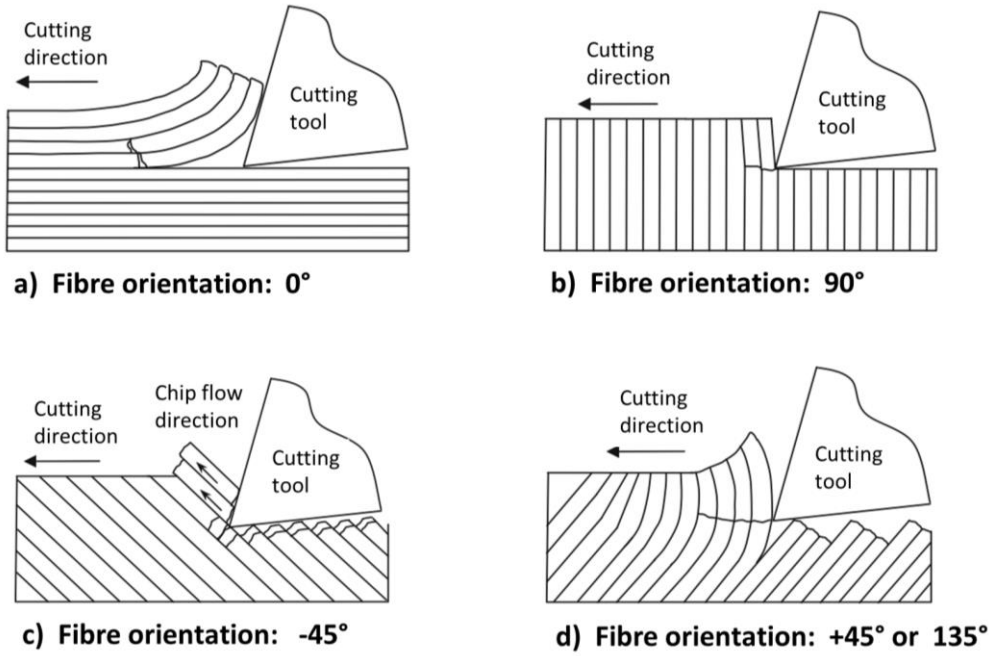

Figure 2.8: Schematic showing chip formation mechanism during conventional machining of typical uni-directional CFRP [6]

2.6.3 Tool wear / life

Tool wear is defined as "progressive loss of tool material" due to an interaction and relative motion between the tool and workpiece during machining, causing a change in geometry of cutting edges, tool flank face and rake face [35]. Abrasive wear, which is often indicated by cutting edge rounding or uniform wear along the cutting edges, Figure 2.9, are typical when drilling CFRP using carbide drills [51-54]. Abrasive wear occurs when two solid surfaces are forced and rubbed against each other, resulting in the softer material being removed mechanically by the harder material [55]. The edge rounding when drilling CFRP occurs as a result of abrasive CFRP workpiece and fine chip flowing around the cutting edges [52].

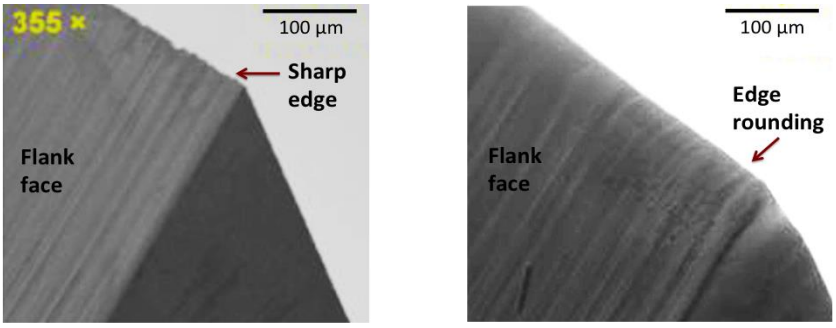

a) New drill (0 hole) **b) After 60 holes**

Figure 2.9: Edge rounding of the uncoated carbide drill when drilling CFRP [52]

Three-body abrasion has been proposed as the mechanism, which governs the abrasive wear of tungsten carbide (WC-Co) drills when drilling CFRP [6, 52, 53]. Three-body abrasion of WC-Co cutting edge is described as abrasion or removal of carbide (WC) grains by WC micro-particles that fractured due to prior removal of cobalt (Co) binder during drilling. The carbon fibres have been reported to have lower hardness (800 – 1100 HV) than WC grains (1700 – 2000 HV) [35, 48, 52]. Therefore, the carbon fibres are not able to abrade the WC grains, instead the carbon fibres abrade the cobalt (Co) binder, which is relatively soft (hardness of 400 – 1200 HV) compared to the carbon fibres [56, 57]. Consequently, the Co binder is preferentially removed, leaving voids between WC grains. Since WC grains are inherently brittle, the continuous stress and impact during drilling on the exposed WC grains (without Co binder to support them) cause micro-fragmentation and pull-out of WC grains. These WC fragments then abrade the WC grains that are still intact on the cutting edges.

Carbide drills with WC grain sizes within the range of 0.1 to 1 µm and Co binder of 5% to 13% are practically used for drilling CFRP due to high overall hardness (1500 – 2000 HV) and hence high resistance to abrasive wear [36]. The wear rate of carbide drills depends on the percentage composition of Co binder and the size of WC grains. The flank wear of a carbide drill when machining CFRP has been reported to reduce from 0.25 to 0.21 mm (cutting distance = 300 m) with decreasing Co binder content

from 10% to 5% (WC grain size = 1.5 μm) [56]. Also, flank wear of the carbide drill reduced from 0.2 to 0.18 mm (cutting distance = 300 m) with increasing WC grain size from 0.5 to 3.0 μm (5% Co binder) [56]. Therefore, when drilling CFRP, using a drill with a lower Co binder content and larger WC grain size is favourable for obtaining longer tool life. The lower Co content in a carbide drill suggests that there would be less void between WC grains when the Co binder is preferentially removed by carbon fibres during drilling, thereby reducing micro-fracture, removal and wear of the WC grains. With regards to WC grain size, despite a reduction in overall hardness with an increase in WC grain size, the improved abrasive wear resistance of the tool when machining CFRP is attributed to improved interlock between the larger WC grains [56].

The advance of coating technology for carbide drills has provided an improvement in the drills' wear resistance to abrasion. The coating type, thickness and sufficient adhesion to the drill substrate are important in determining the wear resistance, performance, and life of coated drills compared to uncoated drills [58]. The coatings that have been typically used for carbide drills when drilling CFRP include Titanium Nitride (TiN), Titanium Aluminium Nitride (TiAlN) and diamond. Several studies [52, 58-60] have shown that drilling CFRP (cutting speeds = 90 – 200 m/min, feed rates = 0.05 – 0.1 mm/rev) using carbide drills with diamond coating of 6 – 12.5 μm thick resulted in two to twelve times longer tool life than uncoated carbide drills. In contrast, TiAlN and TiN coating (3 μm thick) typically did not show marked improvement in wear resistance and tool life compared to uncoated carbide drills (WC-9%Co) when drilling CFRP (cutting speeds = 90 – 180m/min, feed rates = 0.05 – 0.08 mm/rev) [6, 52]. The substantial improvement in tool life of diamond coated drills is attributed to the exceptional hardness of diamond coating (7000 – 10,000 HV), which provides extended protection to the drill substrate from the abrasive CFRP materials during drilling, compared to TiAlN coating (hardness = 2000 – 3000 HV) [6, 32].

Despite higher wear resistance, it must be noted that a thicker coating can affect the cutting edge geometry leading to an increase in cutting force. The coating on the drills can make the cutting edges slightly rounded, reducing their sharpness compared to the uncoated drill. This is notable when higher thrust forces of 120 N and 150 N were reported [52] during drilling CFRP using TiAlN and diamond coated drills, respectively, compared to the uncoated drills which generated lower thrust force of 100 N, for the first three holes when the tool wear was negligible. Thus, although the coating can improve the abrasive wear resistance of the cutting edges, the thickness of the coating needs to be carefully observed so that it does not change the geometry and sharpness of the drills, causing an increase in thrust force, which may be detrimental to hole quality. In contrast, a coating that is too thin may not be useful in improving the drill's wear resistance, in which case it is better to use an uncoated drill since the coating only leads to an additional cost with no significant benefit in tool life.

In terms of drilling environment, dry drilling of CFRP is seen to be advantageous to reduce tool wear and hence prolong tool life compared to drilling with cutting fluid. Barnes *et al*. [61] found lower abrasive flank wear of 0.155 mm after dry drilling of 325 holes through CFRP using TiAlN coated carbide drills (cutting speed = 94 m/min, feed rate = 0.065 mm/rev) compared to when using water-based and cryogenic (liquid nitrogen, LN_2) cutting fluids, which caused a higher tool wear of 0.180 mm and 0.162 mm, respectively. The higher tool wear in the presence of cutting fluid has been reported to be due to the CFRP being able to maintain its strength as cutting temperature was kept lower than the Tg of the epoxy matrix (125 °C). In this case, the cutting edges have to work more to remove the harder and stronger CFRP material, which increases the cutting force, thereby causing more abrasion and a higher tool wear [61]. In contrast, dry drilling (absence of cutting fluid) causes an increase in cutting temperature, which softens the CFRP materials, hence making the drill easier to

remove the material causing a reduction in cutting forces and tool wear. However, it must be noted that thermal softening of CFRP material when dry drilling could be detrimental for the hole quality (this will be discussed in Section 2.6.4). This conflict makes conventional drilling of CFRP complex.

In terms of drilling parameters, cutting speed has been regarded to be a major factor, which governs tool wear, whereas feed rate typically does not influence the wear rate. Tool life of uncoated carbide drills was found to increase from 275 to 512 holes, with a reduction in cutting speed from 235 m/min to 188 m/min when dry drilling of CFRP [53]. This was reported to be due to lower abrasive wear rate of 26.30×10^{-6} m/s when using the lower cutting speed of 188 m/min compared to the higher cutting speed of 235 m/min, which exhibited a higher abrasive wear rate of 38.60×10^{-6} m/s [53]. There is general agreement that increasing cutting speed causes an increase in cutting temperature [62, 63], however, this is not regarded as the primary reason for increasing tool wear when drilling CFRP. The temperatures when dry drilling of CFRP using cutting speeds of 40 – 200 m/min have been reported to be within 120 – 280 °C (measured by thermocouples embedded on the flank face) [52, 62, 64, 65], which are not as high as when machining metals. The temperatures when drilling CFRP are not high enough to deteriorate the drill material (WC-Co) since carbide drills typically have high temperature strength up to 500 °C.

Even though reducing the cutting speed when drilling CFRP is useful to reduce the abrasion of cutting edge so that a longer tool life can be achieved, this also means longer cutting time, which reduces productivity. Thus, in the case when achieving higher productivity is more important than cost minimisation, using PCD drills is regarded as a better option. The higher hardness and abrasion resistant of PCD drill permit the use of a higher range of cutting speeds (150 – 2000 m/min) than carbide drills (cutting speed = 10 – 220 m/min) when drilling CFRP [32]. PCD drills have been

reported to exhibit 50 to 200 times longer life than carbide drills when employed for drilling CFRP [6, 34].

Cutting edge rounding of PCD drills have been commonly observed when drilling CFRP, indicative of an abrasive wear mechanism, however, the detail as to how the abrasion of PCD grains occurs has not been detailed [66, 67]. Considering that diamond is the hardest material known on earth, it is very unlikely that carbon fibres are able to abrade the PCD grains. Therefore, similar to the case of carbide drills, the wear of PCD drill is also regarded to be due to three-body abrasion, caused by micro-fragmentation of the diamond grains. Due to the established performance of PCD drills and that they are expensive, research involving the wear of PCD drills is little and hence much research in the literature has focussed more on improving the life of cemented carbide drills.

2.6.4 Hole quality

2.6.4.1 CFRP delamination

Delamination of CFRP materials is described as a separation of plies due to drilling, which is one of the reasons for the deterioration of hole quality [49]. The fact that CFRP is heterogeneous and made up by a layup process of prepreg plies makes it prone to being delaminated during drilling when subjected to cutting forces higher than the bonding strength between the plies [49]. Delamination of CFRP during drilling is commonly measured and evaluated based on the ratio of the extent of delamination occurring around the hole relative to the diameter or area of the hole [51, 58, 68, 69], as illustrated in Figure 2.10. It is denoted as delamination factor (F_D) when the extent of delamination is calculated in reference to the hole diameter, whereas it is denoted as regional delamination factor (F_A) when the area of delamination is considered relative to the area of the hole [6], Figure 2.10.

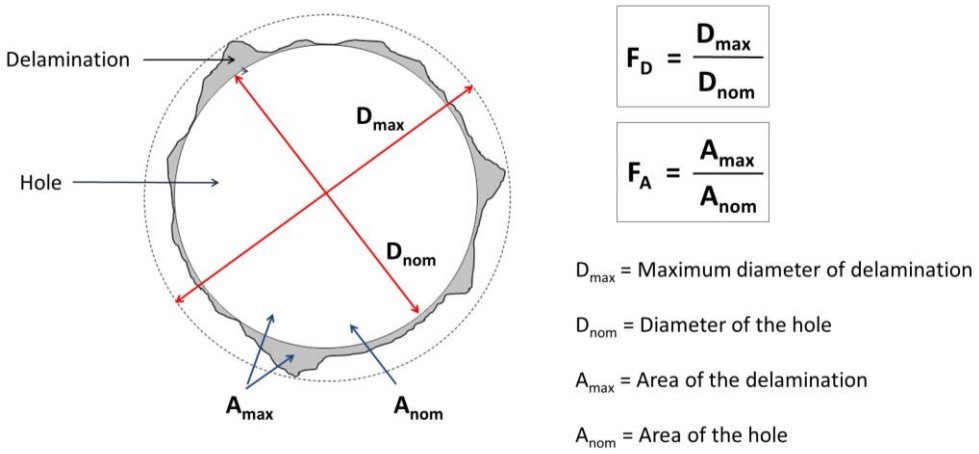

Figure 2.10: Schematic showing the measurement of delamination ratio in terms of delamination factor (F_D) and regional delamination factor (F_A) at the entry and exit of the hole produced when drilling CFRP

CFRP delamination is normally observed at the hole entry due to materials being pulled up, Figure 2.11 (a), and at the hole exit due to materials being pushed out, Figure 2.11 (b). The hole exit normally exhibits larger extent of delamination (F_D = 1.3 – 2.2) than entrance delamination (F_D = 1.0 – 1.3) when drilling using cutting speeds of 94 – 220 m/min and feed rates of 0.02 – 0.07 mm/rev [49, 58, 70, 71]. Exit delamination is more difficult to control due to the reduction of the number of plies to withstand the cutting force as the drill approaches the few final uncut plies of CFRP workpiece.

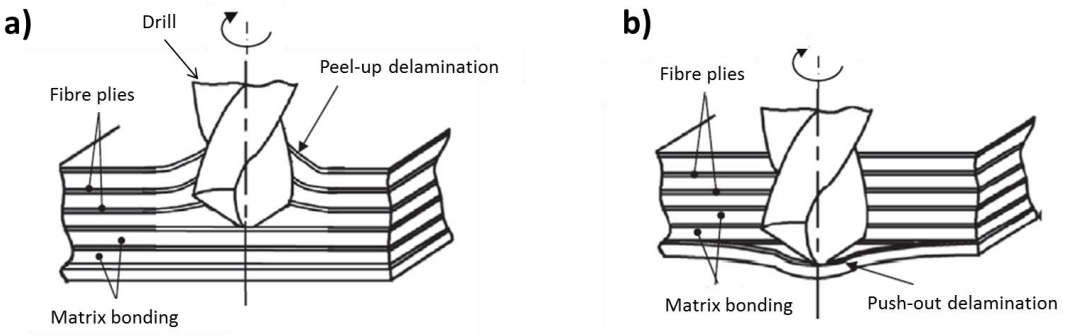

Figure 2.11: Schematic showing the occurrence of delamination at (a) hole entrance, (b) hole exit [72]

Providing a backing plate at the bottom of CFRP plaque to be drilled is useful to reduce the exit delamination [73]. However, this is often not the ideal solution in industry, as

the components are not always horizontally positioned, making it difficult to provide support at the hole exit. Therefore, researchers have constantly investigated cutting tools, cutting parameters and drilling techniques, which can reduce the CFRP damage during drilling.

In terms of drill geometry, cemented carbide twist drills having point angles of 90° – 130° have been typically employed when drilling CFRP, and there is general agreement that a lower point angle is favourable for producing lower delamination due to lower thrust forces [74-77]. This is due to the fact that a lower point angle makes the drill more pointed, thereby improving penetration of the drill and less pressure being induced onto CFRP plies.

There is a consensus in the literature that tool wear has a significant positive correlation with CFRP delamination. Numerous studies [11, 49, 51, 58, 69, 72, 73] have shown that CFRP delamination increased with an increase in tool wear due to increased thrust forces. Therefore, having a drill that has a lower tool wear rate is important to minimise the delamination occurring during drilling. Exit delamination has been reported to reduce by 85% when drilling using a diamond coated carbide drill (6 mm diameter), which was attributed to 78% lower tool wear compared to the uncoated carbide drill, up to 248 holes [58]. This means that more holes can be drilled with less delamination when the drill has a higher wear resistance or when the cutting edge sharpness is maintained and cutting force is lowered. This is the reason why diamond coated carbide drills and PCD drills are often preferable when drilling CFRP, in spite of being more costly than the uncoated carbide drills.

With regards to cutting parameters, there has been little agreement on the influence of cutting speed on CFRP delamination. It has been reported that CFRP delamination increased with increasing cutting speeds (30 – 100 m/min) due to higher thrust force

as a result of higher tool wear when using higher cutting speeds [62, 78, 79]. However, others [76, 80, 81] argued that CFRP delamination reduced with increasing cutting speeds (60 – 200 m/min) because of a reduction in thrust force, which was explained to be due to softening of CFRP materials. This is because of more heat being generated at higher cutting speeds, although in the studies, the temperature that caused softening of CFRP materials was not reported. Softening of CFRP material, caused by increasing cutting speed during drilling is seen as favourable for reducing cutting force and hence delamination. However, it is important to note that the studies [76, 80, 81] did not take into account the influence of tool wear. As more holes are drilled with higher cutting speeds, the tool wear could be dominating, and the combination of higher tool wear and more heat generation can be more damaging for CFRP. In addition, more damage to CFRP could occur if cutting temperature caused by higher cutting speeds, is higher than the Tg of the polymer matrix.

In comparison to cutting speed, the influence of feed rate on the occurrence of delamination of CFRP materials is dominant. There is a general agreement in the literature that CFRP delamination reduces with reducing feed rate (within 0.01 – 0.1 mm/rev) [67, 68, 73]. Regardless of drill geometry, drill material (carbide or PCD) and CFRP structure (woven or uni-directional), the use of a lower feed rate when drilling CFRP has been reported to be essential for generating lower thrust force, thereby reducing CFRP delamination. A lower feed rate indicates less material is removed per unit time causing lower load and cutting forces being exerted on the CFRP plies. Therefore, less CFRP plies being delaminated when a lower feed rate is used, compared to the case of using a higher feed rate (which would cause a higher cutting force and more delamination).

Although numerous studies [11, 68, 69, 76] have shown that lower cutting forces when drilling CFRP are important in producing less delamination and improved machined

surfaces, several studies [61, 82] have found that this case is not necessarily true when various cutting environments are introduced. It was found that the use of both flood water-based and LN_2 cutting fluid when drilling CFRP (cutting speed = 94 m/min and feed rate = 0.065 mm/rev) produced 25% – 40% lower exit delamination despite exhibiting higher thrust force and tool wear, compared to dry drilling [61]. The lower delamination when drilling CFRP with cutting fluid has been reported to be due to the reduction in cutting temperature (although not specified in the study) which helps to sustain the inter-laminar strength of CFRP, thus withstanding the thrust forces [61]. The larger delamination during dry drilling was attributed to the effect of more heat in the cutting zone to cause softening and weakening of the CFRP material [61]. Dry drilling of CFRP requires the use of a lower cutting speed compared to the case when cutting fluid / coolant is employed to reduce heat generation and hence maintaining the strength of CFRP materials.

2.6.4.2 CFRP pull-out

Hole quality is also deteriorated due to CFRP pull-out and fibre breakout during drilling. The extent of fibre breakout and pull-out from the machined surface is typically influenced by the orientation of the carbon fibres, which are complex and continually changing during drilling. For instance, as shown schematically in Figure 2.12, during drilling of CFRP, the fibres' orientation is 0° when they are parallel to the direction of cutting edge, while 90° when they are perpendicular to the cutting edge direction [6]. Carbon fibres with +45° (or also referred as 135°) orientation have been reported to suffer the most severe pull-out or loss of carbon fibres and polymer matrix, indicated by cavities on the machined surface, compared to those of 0°, 90° and -45° [83]. As shown previously in Figure 2.8 (c, d), it is more difficult to achieve a smooth machined surface finish with carbon fibres that have +/-45° fibre orientation since they are more susceptible to macro-fracture caused by the combination of

extensive elastic bending, micro-buckling and compression as the cutting tool moves against the carbon fibres' direction [6].

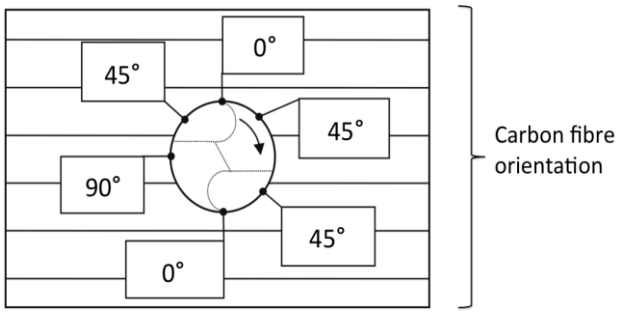

Figure 2.12: Description of carbon fibre orientation relative to cutting direction and rotation of the drill (adapted from [6])

The fibre pull-out from the machined surface is commonly assessed and described subjectively through microscopy, as seen in Figure 2.13. To date, there has been too little quantitative analysis of CFRP pull-out. Compared to delamination at the hole entrance and exit, researchers have not treated the measurement of fibre pull-out from the bore surface in much detail due to the difficulty in quantifying them.

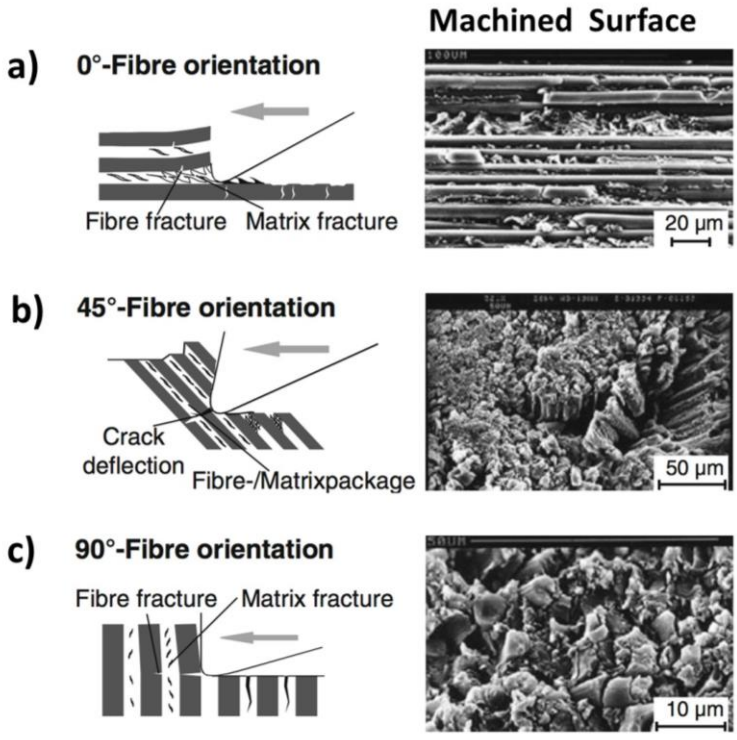

Figure 2.13: Typical machined surface of CFRP with respect to carbon fibre orientation [31]

There have been several attempts to quantify the CFRP pull-out by cross-sectioning the holes, polishing and measuring the cavity along the edges [61], Figure 2.14. However, the problem with this technique is that it does not consider the whole machined surface and the measurement is usually random and limited, since only the cross-sectional part is assessed.

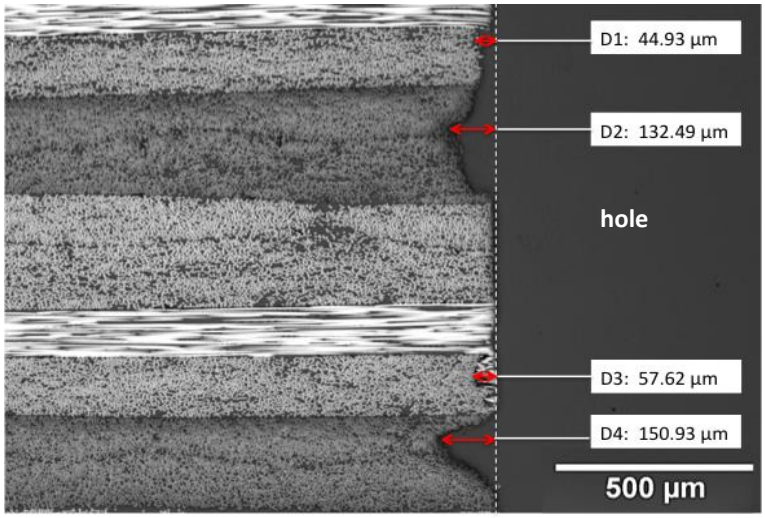

Figure 2.14: Quantifying fibre pull-out from a CFRP machined surface by cross-sectioning the hole

Investigating and quantifying CFRP pull-out considering a larger area or the whole machined surface can provide a better insight of the extent of material being pulled out due to drilling operation. Recent developments of three-dimensional (3D) surface profilometer (e.g. Alicona Infinite Focus), which is capable of scanning a machined surface in X, Y, and Z directions, and hence quantifying the volume of cavities (or materials being pulled-out) has offered an improvement in the quantitative analysis of the CFRP pull-out. Yet, no published study incorporating the technique for quantifying the amount of CFRP materials being pull-out has been found. A more comprehensive study would include the volume measurement of CFRP being pulled out due to drilling to provide a better insight of the machined surface condition and hence hole quality.

2.6.4.4 Hole diameter

Hole diameter is usually measured in industry to evaluate drilled hole quality. The accuracy or deviation of hole diameter in CFRP is affected by tool wear, cutting temperature and damage to the bore machined surface [6]. Undersized holes in CFRP, which are smaller than the nominal diameter of the drill has been reported, which was attributed to drilling with increasingly worn drills [53, 84]. The increase in wear reduces the drill's performance to shear the carbon fibres, causing more uncut carbon fibres stuck out from the surface, and hence resulting in undersized holes [53, 84].

Oversized holes in CFRP in which the average diameters increased from 5.18 to 5.35 to 5.55 mm have been reported to occur with increasing cutting speeds from 188 to 250 to 315 m/min (feed rate = 0.05 mm/rev) when dry drilling of CFRP using 5 mm diameter carbide drills [70]. The study [70] did not consider the holes tolerance, nevertheless, if H7 tolerance (-0.00/+0.015 mm) is considered, the holes were oversized by 0.17 – 0.54 mm. The larger holes in CFRP produced by the higher cutting speeds were explained due to more heat generation, causing an increase in cutting temperature to degrade the polymer matrix, although evidence was not provided [70]. In addition, a larger variation in hole diameter and hole distortion in CFRP may occur due to high cutting temperature during drilling, causing complex thermal expansion between carbon fibres having multi-orientations and polymer matrix [6, 70].

Whilst the undersized holes can be repaired by a secondary drilling operation to enlarge the holes, the oversized holes that are larger than the required tolerance are more difficult to repair which often leads to the parts being rejected. Therefore, having a drill that has lower tool wear rate and employing a drilling strategy which generates lower cutting temperature is important to produce more holes in CFRP having an accurate and consistent diameter within the required tolerance.

2.7 Conventional drilling of titanium alloy

2.7.1 Background

The main issue when drilling titanium alloy (Ti6Al4V) is high cutting temperature concentrating at the cutting interface (cutting edges, flank face/workpiece and rake face/chip), which has been reported to exceed 500 °C and can reach 1000 °C particularly in the absence of cutting fluid / coolant [24, 85]. Since a tungsten carbide (WC-Co) drill exhibits higher thermal conductivity (110 W/m.°C) than titanium alloy Ti6Al4V (15 W/m.°C), 90% of the heat dissipates through the drill, which is the reason for weakening and rapid wear of the drill [29, 85, 86]. Moreover, at high cutting temperature, titanium alloy becomes highly reactive with the drill materials (e.g. WC-Co) causing issues such as adhesion and diffusion between the materials, hence deteriorating the drilling performance.

In order to reduce heat generation hence cutting temperature, titanium alloys are often drilled with low cutting speeds within the range of 20 to 60 m/min. The temperature measured by thermocouples embedded at the flank face of the drill has been reported to reduce from 1060 to 480 °C as cutting speed reduced from 73 to 24 m/min (constant feed rate = 0.05 mm/rev) when dry drilling of titanium Ti6Al4V using carbide drills [85]. The use of lower cutting speed requires less energy and power because of slower tool rotation, which in turn generates less heat compared to the higher cutting speed that requires more energy. In addition, the use of cutting fluid / coolant is highly recommended when drilling titanium alloys to dissipate the heat.

It must be noted that using lower cutting speeds when drilling titanium alloys also means longer cutting time, hence reducing productivity. Therefore, titanium is usually drilled using high feed rates (0.1 – 0.3 mm/rev, i.e. higher than those used for drilling CFRP) to improve productivity. The use of high feed rate when drilling titanium is also

important to avoid rubbing of the drill against the workpiece (often occurs when using lower feed rates). Rubbing of the drill against the workpiece causes more plastic deformation and workpiece hardening, consequently higher cutting forces and can cause rapid drill breakage.

2.7.2 Chip formation

Previous studies involving drilling of titanium alloys have not dealt with the chip formation in much detail. Nevertheless, in the case of turning and milling of titanium alloys, continuous chips exhibiting segmentation or serration, which is also termed as shear localised chips has typically been reported [87-90]. The chip segmentation normally is not apparent macroscopically, however, cross sectioning the chip, polishing and etching can reveal the segments. The segmentation occurs due to the formation of narrow bands as indicated by the red arrows in Figure 2.15 (a). The narrow bands between the chip segments represent the shear plane when forming the chip, Figure 2.15 (b).

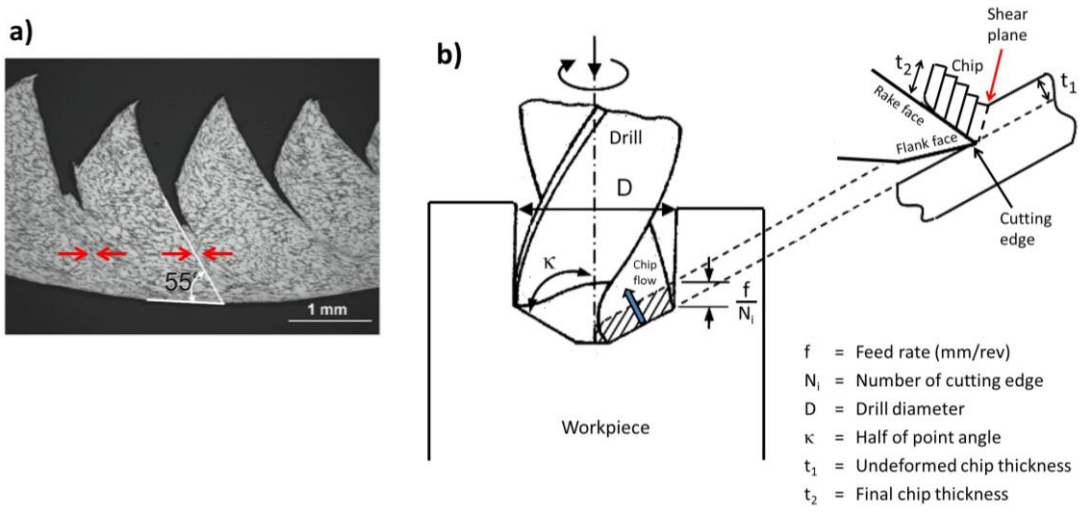

Figure 2.15: (a) Cross section of Ti6Al4V chip showing segmentation; red arrows show heavily deformed shear bands between segments [91], (b) schematic showing chip formation when drilling titanium alloy (adapted from [6])

There are two theories regarding the mechanism of segmented chip formation when machining metallic materials, which are:

(i) localisation of thermal softening in the shear region causing more intense grain deformation in the region / plane, typically the case of machining metallic materials having low thermal conductivity [87, 92, 93].

(ii) cyclic cracking initiates and occurs along the shear plane typically when machining metallic materials having low ductility (brittle) or metals having hard inclusions [94].

Since titanium alloy is typically not brittle and it has low thermal conductivity, the first theory is more relevant to explain the chip segmentation when drilling titanium alloy. The low thermal conductivity of titanium (15 W/m.°C) causes the heat to localise in the shear plane when forming a chip, thereby causing localised softening of the shear region. The thermally softened region thus is heavily deformed compared to the surrounding colder region (which tends to work harden), resulting in the apparent shear bands, and hence chip segmentation [32, 92]. For comparison, machining metallic materials having high thermal conductivity such as aluminium (204 W/m.°C) normally does not form a segmented chip [32]. Instead, a continuous chip exhibiting homogeneous grain deformation is formed since the heat does not concentrate in the shear region; rather the heat is easily dissipated through the chip.

It is difficult to measure the exact cutting temperature in the shear region during drilling. Since the formation of the segmented chip is closely related to heat generation, the more apparent shear band and chip segmentation when drilling titanium can be used as an indicator to describe that more heat is generated in the shear region. It is suggested that during drilling of titanium alloy, when cutting temperature is minimum, less or no apparent chip segmentation would occur. The work of Sun *et al.* [91]

involving turning of Ti6Al4V chips has shown that chips became more segmented as cutting speed increases from 16 to 75 m/min due to increased cutting temperature, although temperature measurement was not reported. It is generally known that more heat is generated with increasing cutting speed, thus causing more thermal softening at the shear region, hence apparent chip segmentation. For drilling titanium alloy, more work is needed to establish the correlation between cutting parameters and chip formation, and importantly, its relation to the quality of the machined surface.

2.7.3 Tool wear / life

Adhesive wear is typical when drilling titanium alloys using tungsten carbide drills [24, 41, 95, 96]. Adhesive wear is described as the occurrence of a strong bonding and adhesion of the materials in contact, followed by tearing of the weaker material [55]. During drilling of titanium alloys, the chips adhere on the cutting edge because of the high chemical affinity between the two, which is highly governed by the high contact pressure (over 1000 MPa) and high localised temperature (over 500 °C) at the cutting interface [34]. The adhesion between titanium chip and cutting edge is characterised by a strong metallic bond causing micro-welds at the seized interface [48, 97]. This leads to chipping of the cutting edge when the tool substrates (e.g. WC grains and Co binder) are torn away by the adherent titanium, which has been reported as the primary reason for the tool failure during drilling of titanium alloys [32, 44, 88].

Tool wear when drilling titanium alloys can be reduced, hence tool life is improved by reducing cutting temperature during drilling through the use of cutting fluid / coolant, and the technique in which the cutting fluid is supplied is important [98-100]. Using high-pressure flood coolant is generally recommended to provide better cooling in the cutting zone [98-100], although there are concerns over additional cost and environmental pollution for using, handling, and disposal of the fluid. This has driven

people in the industry to pursue dry drilling, near dry (e.g. spray mist) drilling and drilling with cryogenic cutting fluid (e.g. liquid nitrogen (LN_2) and carbon dioxide (CO_2)). Less cutting edge chipping and 28% improvement in tool life has been reported when drilling Ti6Al4V with water-oil spray mist that was supplied through a nozzle compared to dry drilling (cutting speed = 40 m/min, feed rate = 0.06 mm/rev) [101]. Bermingham *et al*. [98] investigated tool life when dry machining of Ti6Al4V, and machining with flood conventional water-based and LN_2 cutting fluids using uncoated carbide tools (cutting speed = 85 m/min, feed rate = 0.15 mm/rev). The tool life when using flood water-based and LN_2 cutting fluids were respectively 182% and 63% longer than dry machining. Thus, the application of flood water-based cutting fluid is still more advantageous for drilling titanium alloys as it outperformed the case of when using LN_2 cutting fluid. Quick evaporation of LN_2 is regarded as the reason for less effective cooling in the cutting zone compared to the water-based cutting fluid [98].

Although cutting fluid is employed, the use of a lower cutting speed is still important when drilling titanium alloy to minimise heat generation, hence prolonging the tool life. Costa *et al.* [100] reported that tool life improved by 104% with a reduction in cutting speed from 60 m/min (tool life = 134 holes) to 45 m/min (tool life = 273 holes) when drilling Ti6Al4V using 10 mm diameter TiAlN coated carbide drill with flood cutting fluid (semi-synthetic oil). A limitation of the study [100] is that there is no information on tool wear measurement, which ended the drill life, and also the mechanisms in which the drill failed were not included.

The effect of feed rate on tool wear when drilling titanium alloy did not receive much interest in the literature, although it is important to note that feed rates of 0.05 to 0.25 mm/rev have been typically employed in numerous studies [40, 102-105] when drilling titanium alloys. The selection of feed rate typically does not affect the heat

generation as much as the cutting speed, however, it can affect the cutting forces because the higher feed rate means more amount of material is removed per unit time, hence causing higher cutting forces which may break the cutting edges. Li *et al*. [96] found that increasing the feed rate by 100% (from 0.05 to 0.1 mm/rev) increases the thrust force by 30% (from 200 to 260 N), when drilling Ti6Al4V with new carbide drills, while cutting speeds has been reported as not affecting the thrust forces. However, tool wear when drilling the Ti6Al4V with the different feed rates was not reported in the study [96]. The feed rate when drilling titanium alloy has to be carefully observed so that it does not increase the cutting force up to the point that it deteriorates the drill performance causing cutting edge fracture and drill breakage.

Using a drill with a coating that has less reactivity with the titanium workpiece is beneficial to hinder Ti adhesion on the cutting edges during drilling [24]. Several studies [40, 41, 106] have shown that carbide drills with TiAlN and TiN coating (3 μm thick) generally have 25% – 30% longer tool life compared to the uncoated carbide drill when drilling Ti6Al4V using cutting speeds of 15 – 45 m/min and feed rates of 0.05 – 0.06 mm/rev. Sharif and Rahim [40] however suggest that there is a limitation in cutting speed, in which the coated carbide drill performs better than the uncoated carbide drill. The life of TiAlN coated drills has been reported to reduce from 7.5 minutes to 2 minutes and become similar to the uncoated drills with increasing cutting speeds from 25 to 55 m/min at a constant feed rate of 0.05 mm/rev [40]. This was due to the accelerated removal of the TiAlN coating by flaking with increasing cutting speed due to faster chip flow over the cutting edge and rake face. The carbide substrate of the drill was exposed rapidly, resulting in the increase in Ti adhesion, edge fragmentation and wear progression similar to the uncoated drill.

Edge chipping and tool breakage when drilling titanium alloys can also occur without titanium chip initially adhering to the cutting edges [40, 41]. In this case, the wear

mechanism is referred to as attrition [107]. Attrition wear when drilling Ti6Al4V is described as a loss of drill material due to disintegration when the cutting edges are not strong enough to withstand the force during drilling [55]. An extremely sharp cutting edge is generally prone to chipping. Thus, instead of extremely sharp cutting edges, having cutting edge preparation (CEP), which is typically done either by chamfering or honing of the cutting edges, is beneficial to strengthen the cutting edge and to avoid rapid edge chipping [108]. In addition, a drill having a large point angle of 130° – 140° is suggested to be more resistant to breakage, and is favourable to prolong the tool life when drilling titanium alloy [40, 109].

Diffusion wear, which is indicated by the formation of craters on the drill face, has also been reported when drilling titanium alloys because of the high chemical reactivity of the tool material with titanium [32, 95, 110, 111]. It often occurs on the drill rake face as the chip flows causing the drill materials being diffused into the chip and vice versa. Diffusion wear involves the depletion of material at an atomic level [111]. The diffusion wear / crater on the rake face has been reported to be prevalent when using cutting speeds higher than 100 m/min but not when the cutting speed was lower [111]. Increasing the cutting speeds from 100 to 120 m/min increased the crater depth from 6.85 μm to 50.99 μm, which was attributed to the high cutting temperature of 790 °C and 869 °C, respectively, accelerating the diffusion of the tool materials [111]. This signifies the importance of using lower cutting speed when drilling titanium alloy in order to extend the tool life. Although the diffusion wear and crater typically occur on the rake face rather than the cutting edges, the crater on the rake face still needs to be considered. The fracture on the rake face has been reported to initiate from the crater's location [95], which can be the reason for drill weakening, consequently leading to drill fracture and failure.

2.7.4 Hole quality

2.7.4.1 Burr

Burr formation is one of the reasons for the deterioration of hole quality when drilling titanium alloys. The burr is defined as a partially formed chip that leaves a sharp protrusion at the edge of the machined surface due to incomplete shearing [32], Figure 2.16. This is typical when machining ductile metals and alloys because of their plastic flow, which is described as the ability to deform up to high strain before breaking [32, 112]. The burr at the exit of drilled holes is highly unfavourable because it makes assembly with other parts difficult. A sudden breakage of the burr due to the unstable bonding between the burr and the parent material can lead to failure in the assembly [113]. The presence of micro-cracks in the burr can further propagate into the parent material, causing further deterioration of the whole part. In addition, the burr is sharp, hence, it can cause injury to people who handle the part. Therefore, a de-burring process is necessary, and this means additional cost and time for production [114, 115].

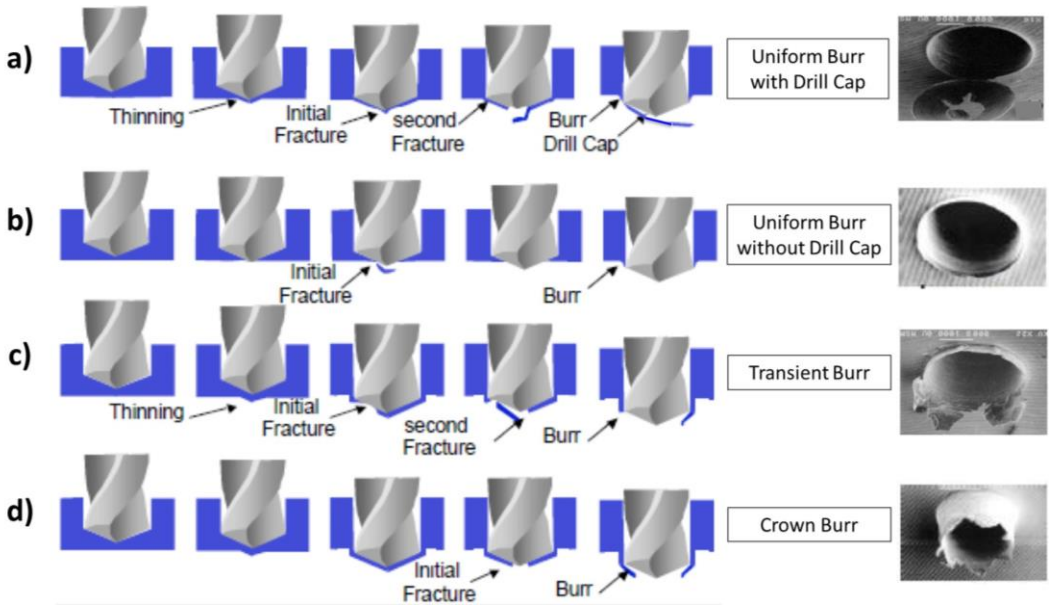

Figure 2.16: Schematic of burr formation mechanisms when drilling – (a) uniform burr with drill cap, (b) uniform burr without drill cap, (c) transient burr, (d) crown burr [116, 117]

With regards to cutting parameters, the effect of cutting speed on the burr formation when drilling TI6Al4V using carbide drills has been a controversial subject. Several studies [105, 114] found that the burr height increased with an increase in cutting speed (within the range of 6 – 20 m/min). This was explained due to an increase in heat generation, causing a reduction in the strength and an increase in the ductility and more plastic flow of the workpiece, which consequently leaving more burr at the hole exit [114]. However, Percin *et al*. [118] reported otherwise, as they found a linearly negative correlation between burr height and cutting speed (5 – 18 m/min), which is supported by Isbilir and Ghassemieh [37] although employing a higher range of cutting speeds (of 25 – 45 m/min) than the work of Percin *et al*. [118]. The reduction in the burr height with increasing cutting speed has been reported to be due to a reduction in thrust force that induces less pressure on the workpiece. It is possible that the reduction in cutting force was due to the effect of more heat generation at higher cutting speed, which softens the material. However, the previous work [105, 114] which showed a linearly positive correlation between cutting speed and the burr height did not provide the result of cutting force, hence a comparison cannot be made.

Furthermore, no definite trend in the burr height (varies from 20 – 48 μm) when drilling titanium Ti6Al4V with the change in cutting speed from 10 to 30 m/min has also been reported, however further explanation was not provided [104]. The main weakness of all these studies [37, 104, 105, 114, 118] is that the effect of tool wear due to drilling with various cutting speeds on the burr formation was not considered and included. It appears that the studies failed to draw a distinction between whether the burr height is caused by the particular cutting speed or drilling with a worn drill. These studies would have been more convincing if the results of cutting forces and tool wear for drilling with respective cutting speeds, in addition to the number of holes at which the burr measurement was done, were included.

In terms of feed rate, there is general agreement [37, 105, 114, 118] that the burr height increases with increasing feed rate when drilling titanium alloys, which has been explained due to an increase in thrust force, although the aspect of tool wear was not included. It must be noted that the thrust forces can also increase as the tool wear increases, however it is not clear in the previous studies [37, 105, 114, 118] whether the burr increment was due to the higher cutting forces caused by the higher feed rate, higher tool wear or combination of both. Therefore, further work is required considering the influence of tool wear, to establish factors, which govern the burr formation. By establishing a distinction between the effect of respective cutting parameters on tool wear and the burr when drilling titanium alloy, it would be more convincing on which factors need to be controlled to reduce the burr formation.

2.7.4.2 Surface roughness

Surface roughness is usually measured in terms of R_a (average roughness), R_z (mean distance between peaks to valleys) and R_t (distance between the highest peak and the deepest valley) [32] using stylus-type profilometers, to evaluate the quality of machined surfaces. The higher value of R_a, R_z and R_t indicates that the surface is rougher. The surface roughness of titanium is influenced by the amount of irregularities such as material adhesion, feed marks, grooves or valleys on the surface. Among the roughness parameters, R_a measurement is commonly recognised. Conventional drilling of titanium alloys using standard twist drills generally produces surface roughness, R_a within the range of 0.8 to 6.5 µm, depending on cutting parameters and drilling environment [119, 120]. An increase in feed rate has been reported to be the most influential factor for increasing surface roughness values when drilling titanium [37, 121]. The use of a higher feed rate causes more intense and larger separation between feed marks on the surface, thereby is regarded as a major reason for higher values of surface roughness [119].

Increasing cutting speed from 12.5 to 25 m/min when dry drilling of Ti6Al4V has been reported to reduce the R_a from 1.80 to 1.62 μm due to increasing cutting temperature from 356 to 429 °C [121], which caused softening of the workpiece hence fewer grooves on the machined surface. In addition, the use of cutting fluid when drilling titanium is important to act as a lubricant and hence improving machined surface finish as the R_a of the first three holes has been reported to be lower (0.5 – 1.5 μm) than those produced by dry drilling (1.0 – 2.4 μm) [96]. Holes that require finer surface finish (e.g. less than 0.5 μm) usually need to undergo a secondary machining operation (e.g. reaming) to remove or burnish the irregularities (e.g. feed marks and material adhesion) on the surface [32].

2.7.4.3 Surface hardness and residual stress

Hardness and residual stress are important criteria that describe the machined surface integrity and hence functional performance and fatigue strength of a part. The machined surface of Ti6Al4V (up to 300 μm beneath the surface) has been reported to exhibit 15% – 24% higher hardness than the parent workpiece [95, 122, 123]. Hardening of the machined surfaces is typically attributed to grain deformation as a result of plastic deformation during drilling [95, 124].

Residual stress within the machined surface after drilling can be compressive as a result of mechanical load or tensile which is typically due to thermal factor [119]. Compressive residual stress is indicated mathematically by negative values, whereas, tensile residual stress is indicated by positive values. Compressive residual stress is generally favourable as it strengthens the machined surface hence improving the fatigue life. In contrast, tensile residual stress is highly undesirable as it causes weakening of a part [119].

Several researchers [124-126] found that there is a positive correlation between hardness and compressive residual stress within the machined surfaces of Ti6Al4V subject to various machining operations (milling, turning and grinding). For drilling of Ti6Al4V, Paulsen *et al*. [127] reported tensile residual stress of 100 to 550 MPa up to 70 μm beneath the machined surface when tool wear was negligible, although residual stress became compressive (-180 to -450 MPa) when tool wear reached 200 μm. The compressive residual stress was attributed to increased cutting forces as tool wear increased [128]. Nevertheless, the machined Ti surfaces (up to 250 μm) exhibited higher hardness (430 – 520 HV) than the bulk workpiece (350 HV) regardless of tensile or compressive residual stress, hence no definite correlation between compressive residual stress and hardness can be deduced in the study [127].

2.7.4.3 Hole diameter

Hole diameter measurement is not the subject of interest in the literature concerning drilling of titanium Ti6Al4V individually. However, in industry, hole diameters are usually measured and checked for controlling quality. Producing holes that have accurate and consistent diameters within tolerance is important. Inaccuracy and deviation in hole diameter in Ti6Al4V may occur due to drill wandering during drilling, increased tool wear and adhered material on cutting edges. The diameter of five holes drilled in Ti6Al4V has been reported to be not significantly affected by either cutting speed (10 – 30 m/min) or feed rate (0.1 – 0.2 mm/rev) when drilling using 6.35 mm diameter TiAlN coated carbide drills with flood cutting fluid [104]. Nevertheless, all holes were oversized by 20 – 40 μm from the drill nominal diameter [104]. Due to the small sample size (5 holes) and the aspect of tool wear (and cutting edge condition) was not considered in the previous work [104], it is difficult to establish any discernible correlation between the hole diameter accuracy and the cutting parameters.

2.8 Conventional drilling of CFRP/Ti stacks

2.8.1 Background

Drilling CFRP and titanium alloy in a stack is relatively a new practice compared to drilling the materials individually. Thus, literature involving drilling of CFRP/Ti stacks is limited. Research involving one-shot drilling of CFRP/Ti stacks in the literature has often been conducted by treating the materials as a separate entity. This means that the CFRP/Ti stacks are drilled using variable cutting parameters (cutting speeds and feed rates), which are suitable for the respective materials in the stacks, although the same drill is employed. Specifically, the cutting parameters were changed alternately and accordingly when drilling different materials of the stacks.

The reason for using variable cutting parameters through the stacks is because the practical cutting parameters when drilling CFRP contrast significantly those of titanium alloys. For instance, employing cemented carbide drills, CFRPs are preferably drilled using high cutting speeds of 80 – 200 m/min and low feed rates of 0.01 – 0.05 mm/rev (as discussed in Section 2.6). In contrast, TiAl4V are practically drilled using low cutting speeds of 20 – 60 m/min and high feed rates of 0.1 – 0.3 mm/rev (as discussed in Section 2.7).

Although employing variable cutting parameters is feasible on Computer Numerical Control (CNC) machine tools as they can be pre-programmed, manual drilling operations are sometimes required, in which changing the cutting parameters while drilling the stack materials continuously is not practical. In addition, the use of variable cutting parameters is impractical in the industry when the materials in stacks have inconsistent thickness. This requires changing the drilling program constantly to meet the requirement of different materials and stacks configuration, which is time-consuming, incurs additional costs and hence not practical.

Nevertheless, there is a consensus in practice when drilling CFRP and titanium alloy in terms of the drill material, in which both materials have been appropriately drilled using cemented carbide drills. Yet, the materials require different drill geometry. For instance, when drilling CFRP, drills with point angles of 90° – 120° are often used to generate low thrust forces hence reducing delamination [58, 68, 80, 129]. In contrast, drilling of titanium alloys requires drills with a larger point angle within 130° – 140° since it makes the drill stronger and more resistant to fracture [40, 85, 130, 131]. The helix angles of 25° – 30° are typical when drilling both CFRP and titanium alloys to facilitate chip removal through the flutes [40, 85, 131]. The different requirements in cutting parameter and drill geometry when drilling CFRP and titanium alloy individually is the main challenge for drilling CFRP/Ti stacks in one-shot.

A uniform set of cutting parameters (cutting speed and feed rate) when drilling through CFRP/Ti stacks is favourable in industry, hence is the focus of this research. Uniform cutting parameters for drilling the stack materials are a compromise between those that are practical for drilling CFRP and titanium. This has raised a research question of what are the compromised cutting parameters and drill geometry, which are appropriate for drilling CFRP/Ti stacks? Several studies [102, 103, 132, 133] have been reported in the literature, which employed a uniform set of cutting parameters during conventional drilling of CFRP/Ti stacks; the details of drill geometry and drilling environment are presented in Table 2.7. In summary, for drilling CFRP/Ti stacks using uniform cutting parameters through the stacks, previous studies have employed:

- cutting speeds of 6 – 60 m/min, which is practical for drilling titanium alloys to minimise the heat generation.
- feed rates of 0.03 – 0.25 mm/rev, the ranges typically used for drilling both CFRP and titanium individually.
- uncoated and coated tungsten carbide (WC-Co drill) twist drills.

Since research concerning drilling of CFRP/Ti stacks using uniform cutting parameters is limited, the following Sections 2.8.2 and 2.8.3 will discuss tool wear and hole quality of CFRP/Ti stacks, taking into consideration literature [37, 41, 45, 134-137] which employed variable cutting parameters as presented in Table 2.8. Tables 2.7 and 2.8 will be referred in the discussion (Sections 2.8.2 and 2.8.3).

Table 2.7: Detailed drill, cutting parameters and drilling environment involving conventional drilling of CFRP/Ti stacks using uniform cutting parameters in the literature, (D = diameter, φ = point angle, ψ = helix angle, Vc = cutting speed, f = feed rate)

References	CFRP/Ti stacks thickness	Drill	Cutting parameters	Drilling environment
Kim and Ramulu, [103]	**CFRP** = 7.6 mm **Ti6Al4V** = 3.1 mm	Uncoated WC-Co twist drill D = 6 mm φ = not specified ψ = not specified	Vc = 12, 21, 33 m/min f = 0.08, 0.13, 0.20, 0.25 mm/rev	Flood water-based cutting fluid
Ramulu *et al*., [132]	**CFRP** = 7.6 mm **Ti6Al4V** = 3.1 mm	Uncoated WC-Co twist drill D = 6 mm φ = not specified ψ = not specified	Vc = 6, 12, 21, 33, 52 m/min f = 0.03, 0.08, 0.13, 0.20, 0.25 mm/rev	Flood water-based cutting fluid
Senthilkumar *et al*. [133]	**CFRP** = not specified **Ti6Al4V** = not specified	TiAlN coated WC-Co twist drills D = 6 mm φ = 118, 130° ψ = 20°, 30°	Vc = 16 m/min f = 0.05 mm/rev	Not specified
Xu and Mansori, [102]	**CFRP** = 7.5 mm **Ti6Al4V** = 6.7 mm	Uncoated WC-Co twist drills D = 6.35 mm φ = 135° ψ = 20° TiAlN coated WC-Co twist drills D = 6.35 mm φ = 140° ψ = 27°	Vc = 15, 30, 45, 60 m/min f = 0.03, 0.06, 0.09, 0.12, 0.15 mm/rev	Dry

Table 2.8: Detailed drill, cutting parameters and drilling environment involving conventional drilling of CFRP/Ti stacks using variable cutting parameters in the literature, (D = diameter, φ = point angle, ψ = helix angle, Vc = cutting speed, f = feed rate)

References	CFRP/Ti stacks thickness	Drill	Cutting parameters	Drilling environment
Beal *et al.* [134]	**CFRP** = 7.5 mm **Ti6Al4V** = 6.7 mm	Uncoated WC-Co twist drills D = 9.5 mm φ = 135° ψ = 28°	**CFRP** Vc = 60, 180 m/min f = 0.08 mm/rev **Ti6Al4V** Vc = 12, 24 m/min f = 0.05 mm/rev	Spray mist water-based cutting fluid
Isbilir and Ghassemieh [37]	**CFRP** = 20 mm **Ti6Al4V** = 20 mm	TiAlN coated WC-Co twist drill D = 8 mm φ = 140° ψ = 45°	**CFRP** Vc = 113 m/min f = 0.025 mm/rev **Ti6Al4V** Vc = 35 m/min f = 0.3 mm/rev	Through tool water-based cutting fluid
Park *et al.* [45]	**CFRP** = 7.5 mm **Ti6Al4V** = 6.7 mm	Uncoated WC-Co and PCD twist drills D = 9.5 mm φ = 135° ψ = 28°	**CFRP** Vc = 60, 180 m/min f = 0.07 mm/rev **Ti6Al4V** Vc = 12, 24 m/min f = 0.05 mm/rev	Spray mist water-based cutting fluid
Park *et al.* [135]	**CFRP** = 7.5 mm **Ti6Al4V** = 6.7 mm	Uncoated and BAM (boron, aluminum, magnesium) coated WC-Co twist drills D = 9.5 mm φ = not specified ψ = not specified	**CFRP** Vc = 60, 180 m/min f = 0.05 mm/rev **Ti6Al4V** Vc = 12, 24 m/min f = 0.05 mm/rev	Spray mist water-based cutting fluid
Park *et al.* [136]	**CFRP** = 7.5 mm **Ti6Al4V** = 6.7 mm	Uncoated WC-Co twist drills D = 9.5 mm φ = 135° ψ = 28°	**CFRP** Vc = 60, 180 m/min f = 0.07 mm/rev **Ti6Al4V** Vc = 12, 24 m/min f = 0.05 mm/rev	Spray mist water-based cutting fluid
Poutord *et al.* [137]	**CFRP** = 20.7 mm **Ti6Al4V** = 25.5 mm	Uncoated WC-Co twist drills D = 12 mm φ = 140° ψ = 30°	**CFRP** Vc = 100 m/min f = 0.05 mm/rev **Ti6Al4V** Vc = 10 m/min f = 0.2 mm/rev	Dry
Wang *et al.* [41]	**CFRP** = 7.5 mm **Ti6Al4V** = 6.7 mm	Uncoated, TiAlN and nanocomposite coated WC-9%Co twist drills D = 9.5 mm φ = 135° ψ = 25°	**CFRP** Vc = 180 m/min f = 0.07 mm/rev **Ti6Al4V** Vc = 15 m/min f = 0.05 mm/rev	Dry, spray mist

2.8.2 Tool wear / life

Cutting speed, feed rate and drilling environment (dry or with cutting fluid/coolant) are major factors which influence tool wear and tool life when drilling CFRP/Ti stacks. When drilling CFRP/Ti stacks using uniform cutting parameters, the flank wear has been reported to increase with increasing cutting speed and feed rate [103, 132] (detailed drilling parameters in Table 2.7). The flank wear accelerates with increasing cutting speed due to the effect of more heat being generated causing weakening of the cutting edges [103]. Whereas, the flank wear accelerates with increasing feed rate due to increased mechanical load being exerted on the cutting edges [103, 132]. However, the information of wear mechanisms which govern the wear rate and drill failure when drilling CFRP/Ti stacks conventionally using uniform cutting parameters was not included in the literature. Therefore, it is unclear which wear mechanisms are dominant, whether cutting edge rounding (abrasive wear), material adhesion followed by edge chipping (adhesive wear), merely edge fracture (attrition wear), a combination of all, or other types of wear occur.

The knowledge of wear mechanisms which govern the tool failure is important so that tool life can be controlled. Since drilling CFRP and titanium alloy on an individual basis exhibit different tool wear mechanisms, as discussed previously in Sections 2.6.3 and 2.7.3, it is useful to know the factors which influence the dominant wear mechanism and their relationship to the change in wear rate hence drill failure (from gradual to rapid or sudden). A more comprehensive study would include detailed information of tool wear mechanisms and how they affect the rate of tool wear and tool life (in the experimental work chapters).

Nevertheless, in the case of drilling CFRP/Ti stacks with a change in cutting parameters between CFRP and titanium using carbide drills, Wang *et al*. [41] (drilling parameters

in Table 2.8) reported that abrasive wear which was indicated by cutting edge rounding was dominant, similar to the case of drilling CFRP-only. The flank wear after drilling 80 holes through CFRP/Ti stacks were 90 – 120 μm, which resembled those of drilling CFRP-only (90 – 120 μm after 80 holes), notably, lower than drilling Ti-only in which the drill failed after 46 holes due to substantial cutting edge chipping [41]. However, it is unclear how the longer tool life was achieved when drilling CFRP/Ti stacks compared to drilling Ti-only. The effect of cutting speed and feed rate on tool wear mechanisms was not investigated in their work [41].

In contrast, Isbilir and Ghassemieh [37] (drilling parameters shown in Table 2.8) argued that drilling CFRP/Ti stacks using carbide drills causes more rapid tool wear and a shorter tool life of 15 holes, compared to drilling CFRP-only (tool life of 56 holes) and Ti-only (tool life of 32 holes). The rapid drill failure when drilling CFRP/Ti stacks compared to drilling CFRP-only and Ti-only was attributed to the combination of multiple wear mechanisms [37], however, the detailed mode of tool wear mechanisms was not given.

The various cutting parameters, drills and workpiece materials specification employed in the previous studies [37, 41] make it difficult to resolve which major factors contribute to the conflicting information of tool wear when comparing drilling CFRP/Ti stacks to those of drilling CFRP-only and Ti-only. Therefore, further work investigating the interaction between the multiple wear mechanisms when drilling CFRP/Ti stacks using uniform cutting parameters is required.

A PCD drill is not favourable for drilling CFRP/Ti stacks as it has been reported to break and fail after 76 holes, compared to a carbide drill (WC-9%Co) which exhibited lower flank wear of 180 μm after 80 holes [45] (Table 2.8). The uncoated carbide drill has been shown to exhibit lower tool wear rate than TiAlN and nanocomposite

(nanocrystalline TiAlN grains surrounded by Si_3N_4 matrix) coated carbide drills, Figure 2.17 [41] (drilling parameters in Table 2.8). However, the authors [41] did not explain further the reason for the uncoated carbide drill outperforming both coated drills when drilling CFRP/Ti stacks. Similarly, a BAM coated carbide drill has been found to not exhibit marked improvement in tool life when drilling CFRP/Ti stacks compared to an uncoated carbide drill [135] (drilling parameters in Table 2.8), since the coating flaked from the carbide substrate after 40 holes. It is possible that the coated carbide drills have different carbide grades to allow adhesion with the coating, in which they are less hard and hence less wear resistant than the uncoated carbide drills.

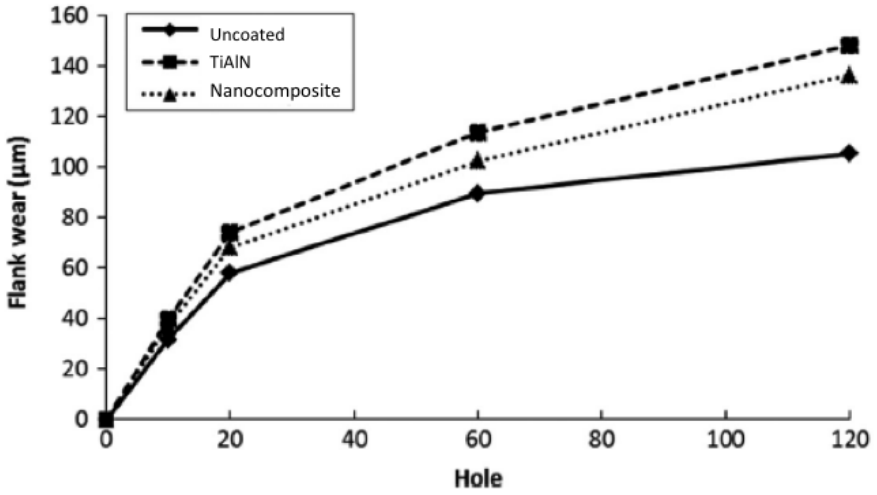

Figure 2.17: Comparison of flank wear of uncoated and coated carbide drills when drilling CFRP/Ti stacks [41] (detailed drilling parameters are in Table 2.8)

2.8.3 Hole quality

Similar to drilling CFRP and titanium alloy individually, CFRP delamination, CFRP pull-out and titanium burr (as explained in Sections 2.6.4 and 2.7.4) occur when the materials are drilled together in a stack, Figure 2.18, which affect the hole quality. The combination of damage occurring to both materials makes controlling the hole quality in CFRP/Ti stacks more difficult.

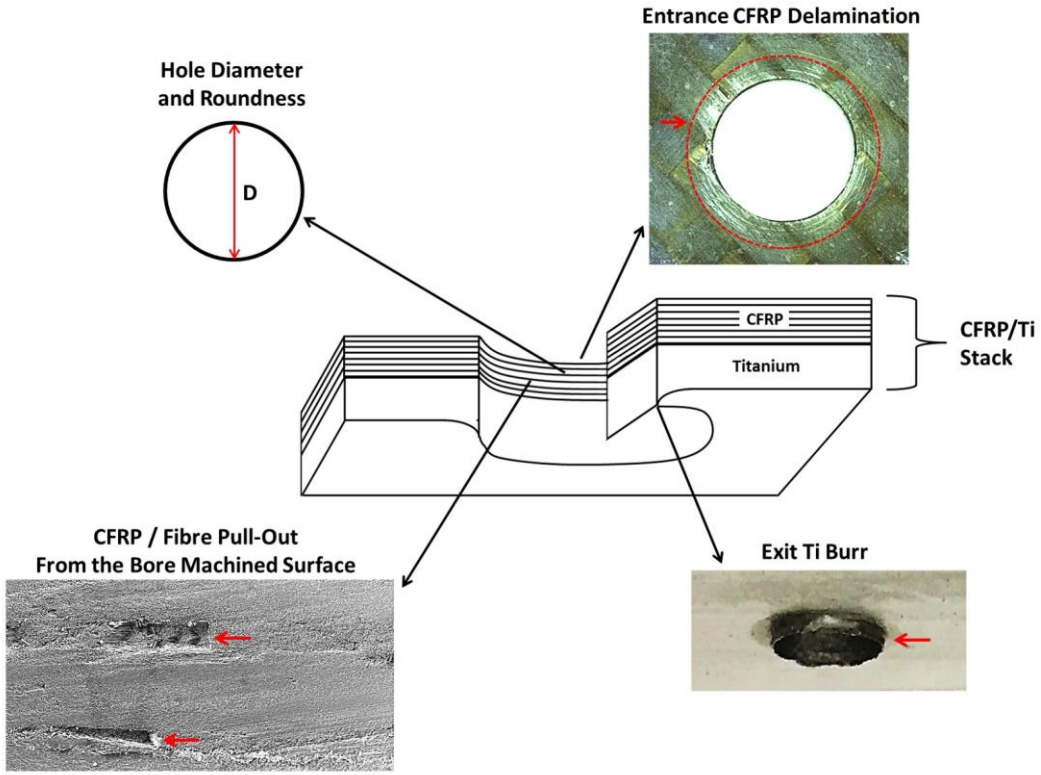

Figure 2.18: Schematic and diagrams showing key features for determining the drilled hole quality in a CFRP/Ti stack

2.8.3.1 CFRP delamination

CFRP delamination at the hole entrance when drilling CFRP/Ti stacks has been reported to be mainly influenced by the use of feed rate [102], which is similar to the case when drilling CFRP-only as discussed in Section 2.6.4.1. The entrance delamination increased (F_D = 1.01 – 1.15) with increasing feed rate from 0.03 to 0.15 mm/rev, due to an increase in thrust forces, regardless of cutting speeds (15 – 60 m/min), whereas no distinctive trend has been deduced regarding the effect of cutting speed [102].

However, it is unclear whether the CFRP entrance delamination when drilling in a stack with titanium is equal, more or less than the case of drilling CFRP-only since it has not been directly compared in a single study. Even though there are extensive studies on CFRP delamination when drilling individually, it is difficult to directly compare with the

studies involving drilling of CFRP/Ti stacks in the literature because of the use of a different range of cutting parameters, drill geometry and drilling environment.

2.8.3.2 CFRP pull-out

Quantitative analysis of the amount of CFRP pull out from the machined surface when drilling CFRP/Ti stacks has not been reported in the literature. Nevertheless, several studies [103, 132] have described the fibre pull-out subjectively, and several authors [37, 39] have measured the surface roughness (R_a) of the machined CFRP as a way to describe its surface topography when drilling in a stack with titanium. Isbilir and Ghassemieh [37] reported that the machined surface roughness of CFRP when drilling CFRP/Ti stacks were 15% – 70% higher compared to the surface roughness of CFRP that was drilled individually, however, no further explanation was provided. The fibre breakout and pull-out from the machined surface of CFRP, and hence the surface roughness, is expected to be higher when drilling CFRP/Ti stacks due to the influence of the hot and work hardened titanium chips as they evacuate from the holes, although further work is needed for confirmation.

Similar to the case of drilling CFRP individually, high cutting force is also regarded as a factor that causes fibre pull-out when drilling CFRP/Ti stacks [132]. The machined surface of CFRP has been observed to exhibit more severe fibre pull-out and fractured (visually) when CFRP/Ti stacks were drilled using a higher feed rate of 0.25 mm/rev due to higher thrust forces of 200 – 300 N compared to when using a lower feed rate of 0.03 mm/rev which generated lower thrust forces of 40 – 100 N [132]. In contrast, the effect of cutting speed on the fibre pull-out is unclear in the literature, hence further investigation is required.

2.8.3.3 Titanium burr

Several researchers [37, 39, 132] have investigated the factors that govern titanium burr formation when drilling CFRP/Ti stacks. In terms of cutting parameters, Ramulu *et al*. [132] found that the burr was influenced by cutting speed (6 – 52 m/min), while feed rate (0.03 – 0.25 mm/rev) was not a major factor for burr formation. The titanium burr height at the hole exit increased from 0.1 to 0.8 mm as cutting speed increased from 6 to 52 m/min at a constant feed rate of 0.08 mm/rev when drilling CFRP/Ti stacks with an uncoated carbide drill [132]. However, the study [132] failed to acknowledge the significant influence of tool wear, caused by drilling with various cutting parameters which can also affect the burr formation. It would have been more useful if the information on the number of holes drilled and at which hole number the burr measurement was performed was included. Nevertheless, others [37, 39] have shown that titanium burr height increased with increasing hole number, which is expected, due to increasing tool wear.

2.8.3.4 Hole diameter

In addition to the unique machining-induced damage of the individual materials, the main important characteristic that describes the hole quality in CFRP/Ti stacks is the consistency in diameter between the holes in CFRP and titanium. The different structure and properties between CFRP and titanium alloys lead to complex cutting mechanisms, tool wear mechanisms, chips morphology, cutting forces and heat generation, which result in the difficulty in achieving dimensional accuracy and consistency in holes produced in CFRP and titanium panels.

Several studies on drilling CFRP/Ti stacks have included the analysis of hole diameters in CFRP and titanium [39, 102, 103], however, the consistency between the holes in CFRP and titanium with respect to cutting parameters and tool wear has not been

explained. It has been shown that the diameter of holes in CFRP was equivalent to the nominal diameter of the drill (6.35 mm) when drilling with flood cutting fluid [39]. Drilling CFRP/Ti stacks using spray mist cutting fluid however produced larger holes in CFRP (6.42 – 6.44 mm), which was attributed to insufficient cooling in the cutting zone, hence the hot titanium chips removed more CFRP material as they evacuated through CFRP holes [39]. In contrast, the hole diameter in titanium has been reported to be not affected by the use of either flood or spray mist cutting fluid [39].

In terms of cutting parameters, Xu and Mansori [102] (drilling parameters in Table 2.7) found no significant trend in hole diameter in both CFRP and titanium in a stack with increasing cutting speed and feed rate. In contrast, Kim and Ramulu [103] (drilling parameters in Table 2.7) reported that the deviation in hole diameter increased (10 – 40 μm) with increasing cutting speed and feed rate when drilling with a 6 mm diameter carbide drill. However, it is unclear if the tool wear is a dominant factor contributing to the deviation in the hole diameter. The main weaknesses of these studies were that they considered a small sample size (5 holes for each cutting parameter [102]) and the effect of tool wear was overlooked. This causes difficulty to deduce the results and make a distinction in the contribution of cutting speed, feed rate and tool wear on the hole quality. Therefore, a more comprehensive study on the effect of cutting parameters on the damage of the drilled materials and hole diameter, considering the factors of tool wear and cutting forces, including a larger sample size is required.

2.9 An overview of ultrasonic assisted drilling

Ultrasonic Assisted Drilling (UAD) is a hybrid drilling process referring to the combination of conventional drilling and ultrasonic vibration applied to the drill. This means that the workpiece material is removed by forming a chip in a conventional mode, which involves physical contact between the workpiece and the drill that is vibrated ultrasonically. During UAD, the ultrasonic vibration (oscillation) is normally superimposed on the drill's feed, which is in an axial direction (parallel to the axis of drill's rotation). As illustrated in Figure 2.19, UAD is conducted by transmitting an electrical signal by induction from the transmitter segment at the tool spindle to the receiver coil of the tool holder (or ultrasonic actuator), which contains piezoelectric crystals [138]. The voltage makes the piezoelectric crystals vibrated. The mechanical vibration is then transferred to the drill to vibrate it in an axial direction.

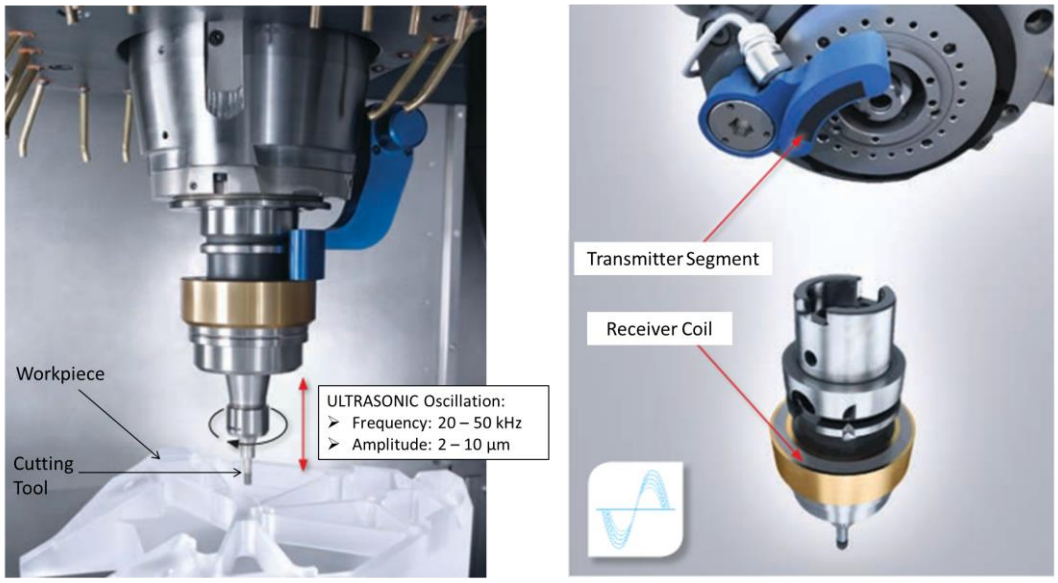

Figure 2.19: Ultrasonic Assisted Drilling [138]

Henceforth in this thesis, conventional drilling will be termed as CD, for comparison with UAD. Compared to CD, the main parameters that govern the UAD are the frequency (f_v) and amplitude (a) of the ultrasonic vibration. The frequency of ultrasonic

vibration that has been used during UAD in the literature is within the range of 20 to 50 kHz, and the amplitude is between 2 to 20 μm [138-142].

UAD should not be confused with Low Frequency Vibration Assisted Drilling (LFVAD). LFVAD involves a similar concept to UAD, in that it is also a hybrid drilling operation, combining drilling by conventional mode and vibration of the drill. However, the main difference between UAD and LFVAD is that LFVAD employs much lower frequency (usually less than 200 Hz) and much higher amplitude (usually higher than 100 μm); these are far beyond the range of amplitude and frequency of ultrasonic vibration. The main aim of LFVAD is to improve metallic chip evacuation by breaking the long chips and forming shorter chips as the drill oscillates during drilling. This is achieved by periodically disengaging the cutting edges from the workpiece, which prevents continuous cutting, thereby restricting the formation of long and continuous chips. This means that intermittent cutting occurs during LFVAD, thereby forming shorter and broken chips.

LFVAD has been successfully applied on CFRP/Ti stacks as it has been shown that the attainable smaller and broken Ti chips in LFVAD do improve the machined surface finish of CFRP, which is attributed to the improved evacuation of the chips compared to the long chip produced by conventional drilling [143-145]. However, to date, the possibility of improving chip evacuation, machined surface finish and tool wear during UAD of CFRP/Ti stacks remains unanswered, despite the growing availability of machine tools equipped with UAD, which has thus triggered this research. Since there is limited literature involving UAD of CFRP/Ti stacks, the following Sections 2.9.1, 2.9.2, and 2.9.3 will review previous studies involving UAD of CFRP and titanium alloy individually, while also considering LFVAD of CFRP/Ti stacks. UAD of CFRP/Ti stacks will be investigated and discussed in the Chapters of Experimental Work.

2.9.1 Cutting force

Previous studies involving UAD of CFRP-only [140-142, 146] and titanium-only [141, 147, 148] focused on cutting forces, while little attention was given to the study of tool wear and hole quality compared to CD. The use of a higher value of ultrasonic amplitude and lower cutting speed has been recognised as the factors that cause a reduction in cutting force during UAD compared to CD. Pujana *et al*. [147] have shown that the thrust force during UAD of titanium Ti6Al4V reduced from 400 to 380 to 200 N with the increase in the ultrasonic peak-to-peak amplitude from 2 to 5 to 9 µm at a frequency of 17.7 kHz, compared to CD, which generated a higher thrust force of 400 N (cutting speed = 25 m/min, feed rate = 0.1 mm/rev). The higher vibration amplitude indicates that the drill feeds further and oscillates backward more, alternately, in one cycle of the drill oscillation, Figure 2.20.

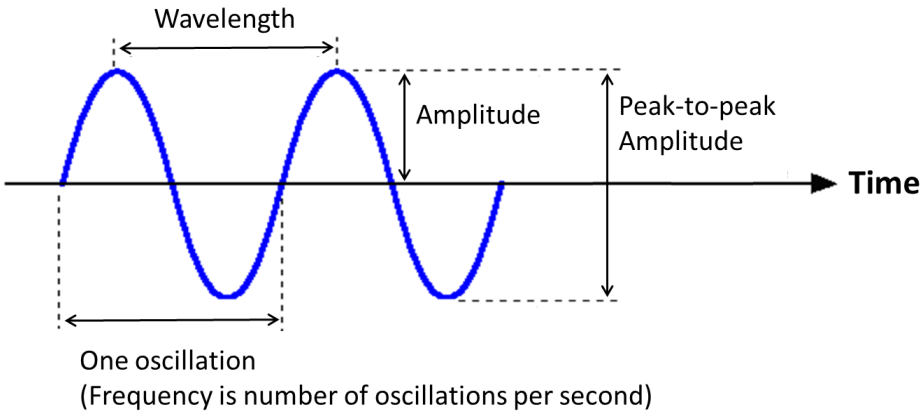

Figure 2.20: Schematic of amplitude and frequency of the ultrasonic vibration / oscillation

The effect of greater drill oscillation has been suggested to improve the drill's penetration and might intermittently disengage the cutting edges from the workpiece, which was considered as the reason for cutting force reduction in UAD [140, 148]. Maximising the amplitude of ultrasonic vibration at a resonant frequency has been recommended to cause a greater reduction in cutting force during UAD compared to CD [147].

With regard to cutting speed, it has been suggested that using a cutting speed that is lower than the vibration speed of the drill is important for cutting force reduction, otherwise the cutting force in UAD is similar to the case of CD [149]. The vibration speed (V_v) of the drill during UAD, which is how fast the drill oscillates back and forth per unit time, is influenced by the amplitude and frequency of the ultrasonic vibration, which can be calculated using the formula:

$$V_v = 2\pi \,.\, f_v \,.\, a \quad \text{……………………………………………………………(1)}$$

Where, V_v = vibration speed, a = amplitude of the ultrasonic vibration (in μm), f_v = frequency of the vibration (in kHz), and π = 3.142 (constant). Multiplying the amplitude (in μm) and frequency (in kHz) results in the vibration speed (in mm/s). Due to the rotation of the drill during drilling, angular frequency has to be considered in calculating the vibration speed. It is established that one revolution of the cutting tool is equal to 2π radians (hence the frequency has to be multiplied by the constant 2π radians) [150].

It has been shown that the average thrust force generated during UAD of CFRP-only and titanium alloy-only is 4% to 90% lower than CD of the materials [140-142, 147, 148]. The highest percentage reduction by 90% in cutting forces during UAD (peak-to-peak amplitude = 12 μm, frequency = 28 kHz) of CFRP compared to CD has been reported by Makhdum *et al.* [140], which employed a cutting speed of 0.38 m/min and feed rates of 0.1 – 0.4 mm/rev using a carbide drill. The vibration speed of the drill was calculated using the equation (1), which is 127 m/min that is 334 times higher than the cutting speed. However, the cutting speed (0.38 m/min) employed in their work [140] is not practical and too slow for industrial application. Using a more practical cutting speed of 28 m/min and a feed rate of 0.05 mm/rev during UAD of CFRP (ultrasonic peak-to-peak amplitude = 15 μm, frequency = 26 kHz), Sanda *et al.* [141] found that the

average thrust force was 26% lower than CD. The vibration speed of the drill was 147 m/min, which was calculated using equation (1). The percentage of force reduction reduced to 12% and 7% with the increase in cutting speeds of 34 and 40 m/min, respectively.

In the same paper, Sanda *et al*. [141] also reported that thrust force during UAD of titanium Ti6Al4V individually was 16% lower than CD when using a cutting speed of 12 m/min and feed rate of 0.03 mm/rev. However, the authors [141] found higher percentages of force reduction by 32% and 27% during UAD compared to CD, when the cutting speed was increased to 19 and 25 m/min, respectively. This finding suggests that a reduction in cutting speed does not necessarily result in greater force reduction in UAD compared to CD. The main weakness of the study is that the contribution of tool wear on the cutting force is unknown. It is possible that the factor of increased tool wear influences the result of thrust force. It would have been more convincing if they had included the information on the number of holes drilled and tool wear, so that it would be clear whether the thrust force is affected by tool wear or solely attributed to the application of UAD.

The reason for lower cutting forces in UAD compared to CD that has been reported in the literature is not convincing. Despite several studies [140, 141] which have claimed that the lower cutting force in UAD than CD is due to intermittent disengagement of the cutting edges from the workpiece, no evidence has been provided to show that this takes place. Nevertheless, the occurrence of cutting edges disengagement from the workpiece and intermittent cutting has been demonstrated during LFVAD of CFRP/Ti stacks. The disengagement of the cutting edges from the workpiece means that the cutting edges are not in contact with the workpiece, hence no workpiece material is removed at that time. Lonfier *et al*. [145] investigated the thrust force profiles and demonstrated that the value reduced to 0 N from 1100 N, at a regular

interval (every 0.05 seconds) during LFVAD of titanium Ti6Al4V, Figure 2.21 (a). The vibration frequency used was 28 Hz, although the amplitude was not specified.

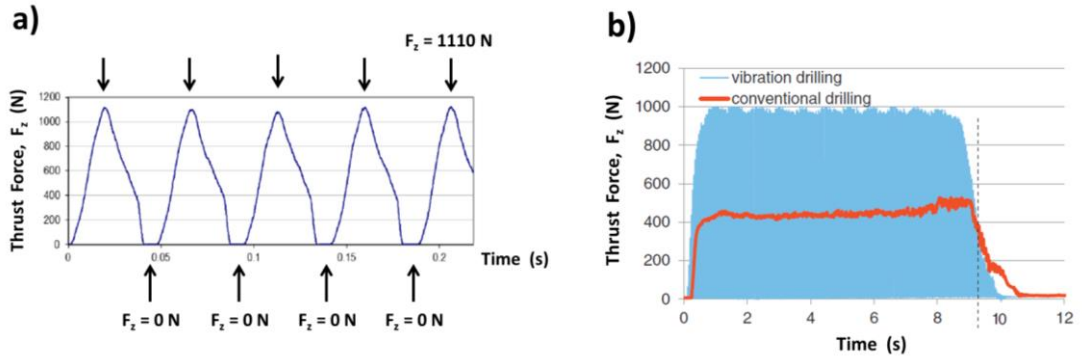

Figure 2.21: (a) Thrust force profile during LFVAD of Ti6Al4V using a cutting speed of 27 m/min and feed rate of 0.06 mm/rev [145], (b) comparison of thrust force profiles during CD and LFVAD of Ti6Al4V using a cutting speed of 15 m/min and feed rate of 0.075 mm/rev [143]

The observation of thrust forces approaching 0 N periodically during LFVAD supports the claim that the cutting edges are disengaged periodically causing intermittent cutting. In the paper [145] however, it is unknown how the thrust force profile during LFVAD differs from CD, since the thrust force profile of CD was not included. Referring to Figure 2.21 (a), it is reasonable to assume that the thrust force during CD of Ti6Al4V in the study [145] was constantly at 1110 N as the cutting was continuous. When evaluating a relatively new drilling operation such as LFVAD and UAD, it is important that the machining data (e.g. thrust force profile) is compared against those of CD. Otherwise, it is unclear whether any improvement has been made.

To justify the continuous cutting in CD and intermittent cutting in LFVAD, Pecat and Brinksmeier [143] compared the thrust force profiles during LFVAD (amplitude = 115 µm, frequency = 25 Hz) of Ti6Al4V against CD. As seen in Figure 2.21 (b), it is apparent that the thrust force during LFVAD were within 0 – 1000 N, which indicated that the cutting edges disengaged from the workpiece intermittently and the drill fed further into the workpiece during LFVAD, whereas the thrust force during CD was constantly at 420 N. It would be useful to investigate if the same case would occur

during UAD of CFRP/Ti stacks since UAD relies on the same concept of drill oscillation (although UAD uses 10 times lower amplitude and 1000 times higher frequency than LFVAD), to show that whether cutting edges disengage and intermittent cutting occurs during UAD as claimed by many researchers.

2.9.2 Tool wear

The tool wear and tool life during UAD of CFRP and titanium alloy compared to CD are unclear due to the lack of studies reporting the aspect of tool wear during UAD in the literature. Makhdum *et al*. [140] reported that the flank wear of a TiN coated carbide drill after UAD (peak-to-peak amplitude = 12μm, frequency = 28 kHz) of 50 holes through 10 mm-thick CFRP using a cutting speed of 0.4 m/min and 0.2 mm/rev, was 4.5 μm, while CD exhibited a flank wear of 5.1 μm. This information however is not very useful in determining whether the drill performance and tool life in UAD were better than CD, since the tool wear mechanism was not included. In addition, the reported flank wear of 4.5 μm for UAD and 5.1 μm for CD are regarded as negligible since the standard maximum flank wear before the end of tool life is 300 μm, following ISO 3685:1993 [151]. It is also important to note that the cutting speed used in the study [140] was too low (0.4 m/min) and not practical for industrial application.

A more comprehensive study on tool wear during UAD of CFRP/Ti stacks in comparison to CD using more practical cutting speeds is required. Nevertheless, it has been shown that LFVAD of CFRP/Ti stacks caused cutting edge rounding with less titanium adhesion on the cutting edges [143]. This was associated to less contact between the cutting edges and workpiece during LFVAD due to intermittent disengagement of the cutting edges, compared to continuous cutting in CD which exhibited more titanium adhesion and edge chipping [143]. The experimental work in this thesis focused on the application of UAD of CFRP/Ti stacks. LFVAD is not the

interest, although a relevant study in the literature on LFVAD of CFRP/Ti stacks [143] is included here due to the similarity in the concept and very limited previous studies on UAD of CFRP/Ti stacks.

2.9.3 Hole quality

The use of UAD for making holes in CFRP individually has been reported to result in 20% – 40% lower entrance delamination, exit delamination and surface roughness (R_a), which were attributed to the lower cutting forces compared to CD [140, 141]. With regard to the machined surface roughness of holes in CFRP, it has been suggested that the lower R_a caused by UAD was due to the polishing effect on the machined surface as the drill oscillated back and forth, compared to the continuous feed in CD [141] although no evidence was provided. Determining the machined surface quality of CFRP based on R_a measurement only is not sufficient. It would have been more convincing if the authors [140, 141] had provided the images of the machined surfaces to resolve whether UAD produced less fibre breakage and pull-out compared to CD. As for titanium alloy, it has been reported that the burr height of 75 holes produced by UAD and CD exhibits no significant difference (similar range of 60 – 120 μm) when using a cutting speed of 8.8 m/min and feed rate of 0.02 mm/rev [141]. No other work involving UAD which investigates the titanium burr formation has been found. Also, the machined surface finish of titanium and the consistency of the hole diameter in CFRP/Ti stacks produced by UAD compared to CD has not been reported.

Another important aspect which must be considered during UAD of CFRP/Ti stacks is the influence of titanium chip on CFRP damage, yet this has not been shown in the literature. Previous studies of LFVAD of titanium individually [152] and CFRP/Ti stacks [144] suggested that intermittent cutting produces discontinuous titanium chip, which improves the chip evacuation, hence improving the machined surface finish of CFRP. In

comparison to LFVAD, CD produces long chips, leading to chip clogging in the flutes, hence damaging the machined surface [144]. The impact of the drill vibration during drilling has been reported to cause pulverisation of titanium chips, which results in broken chips. For this to occur, it has been suggested that the amplitude of the drill vibration must be high enough (e.g. higher than the feed rate) [152, 153]. This is unlikely to occur in UAD, since the amplitude of ultrasonic vibration is too low (typically less than 10 μm) and it is uncommon to use a very low feed rate (less than 0.01 mm/rev) due to concern over productivity. However, further investigation regarding UAD of CFRP/Ti stacks is required to investigate the cutting mechanism and to establish whether the process can improve the hole quality of CFRP/Ti stacks compared to CD.

2.10 Summary of literature review

Despite extensive research involving CFRP and titanium alloy Ti6Al4V individually, little is reported about the machinability of the materials when drilling together in a stack. The knowledge gap and some areas that require further investigation are summarised as follow:

- There has been limited literature to understand the machinability of CFRP/Ti stacks in terms of tool wear and hole quality when drilling using uniform cutting parameters. Thus, drilling of CFRP/Ti stacks using a set of uniform cutting parameters was pursued in the experimental work due to practicality for industrial application, instead of using variable cutting parameters through the CFRP and titanium layers of the stack.

- A comprehensive study comparing drilling of CFRP/Ti stacks with drilling of CFRP and titanium individually is required to understand how the interaction

between different wear mechanisms affects the tool life. The knowledge of the wear mechanisms and the way the tool would fail is useful as a basis to control the tool life.

- Hole quality in CFRP/Ti stacks is affected by inconsistency in hole diameter and damage to the holes (e.g. CFRP delamination, CFRP pull-out, titanium burr). The majority of previous studies involving drilling of CFRP/Ti stacks, which investigated how hole quality was affected by the change in cutting speed and feed rate, paid little attention to the factor of tool wear. A distinction between the effect of using the cutting parameters on tool wear considering a larger sample size, and how does it affect the hole quality needs to be drawn.

- UAD has been emphasised as a promising machining technique to reduce cutting forces when drilling materials on an individual basis (not in stacks), however, limited information of tool wear and hole quality has been given. Specifically, limited research has been published to understand the UAD application on CFRP/Ti stacks. Investigation of how UAD of CFRP/Ti stacks affects the tool wear, the accuracy and consistency of hole diameter, and the extent of damage to the drilled holes compared to conventional drilling need to be established.

- Previous studies have claimed that intermittent cutting (periodic disengagement between the cutting edges and the workpiece) occurs during UAD, which is likely the reason for lower cutting forces compared to CD, however, evidence has not been provided. Further work investigating the thrust force profile and chip morphology during UAD in comparison to CD is required to show whether intermittent cutting occurs as shown in the case of LFVAD in the literature.

Chapter 3 Experimental Methodology

3.1 Workpiece materials

3.1.1 Carbon fibre reinforced polymer

The CFRP used throughout this research was 4 mm thick CFRP 5250-4 BMI panels supplied by BAE Systems. The typical mechanical properties of CFRP 5250-4 BMI, obtained from the Cytec material data sheet [154] are shown in Table 3.1. The CFRP panels comprised 28 plies of uni-directional carbon fibres bonded with bismaleimide (BMI) resin matrix. A cross-section of a CFRP panel showing the microstructure and fibre orientation of each ply (0°, 45°, 90°) is shown in Table 3.2. Each ply thickness was within the range of 130 to 155 μm.

Table 3.1: Typical mechanical properties and glass transition temperature of CFRP 5250-4 BMI [154]

Specification	Value
Density	1.25 g/cm^3
Tensile strength	103 MPa
Tensile modulus	4.6 GPa
Flexural strength	163 MPa
Glass transition temperature, Tg	270 °C
Carbon fibre volume fraction	60%
BMI matrix volume fraction	40%

Table 3.2: Orientation of carbon fibres within CFRP 5250-4 BMI (sectioned parallel to 0°)

Ply Number	Carbon Fibre Orientation	*Carbon Fibre Diameter: 2 – 3 µm
1	45°	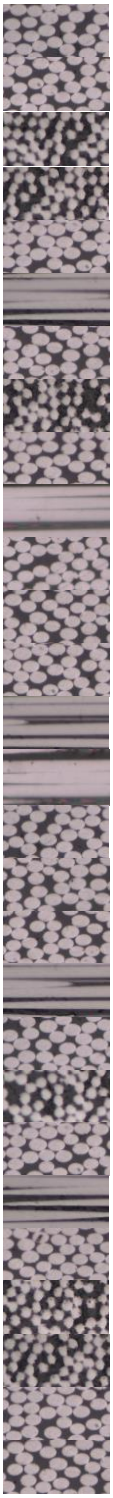
2	45°	
3	90°	
4	90°	
5	45°	
6	0°	
7	45°	
8	90°	
9	45°	
10	0°	
11	45°	
12	45°	
13	45°	
14	0°	
15	0°	
16	45°	
17	45°	
18	45°	
19	0°	
20	45°	
21	90°	
22	45°	
23	0°	
24	45°	
25	90°	
26	90°	
27	45°	
28	45°	

3.1.2 Titanium alloy

The titanium alloy used in all drilling trials was Ti6Al4V (also known as Ti64 or grade 5), and was supplied by BAE Systems. Typical composition and mechanical properties of Ti6Al4V are summarised in Tables 3.3 and 3.4. The hardness of the Ti6Al4V workpiece was measured to be 346 HV. Figure 3.1 (a) shows that the Ti6Al4V in this work has fine grains comprising a mixture of globular α-phase and lamellar β-phase. The uniform direction of the grains was due to rolling process used to produce the 4 mm thick sheet. The workpiece material was verified as Ti6Al4V by Energy Dispersive X-ray Spectroscopy (EDS) analysis, Figure 3.1 (b). For simplicity, henceforth, Ti6Al4V will be referred as Ti, throughout the experimental work in this thesis.

Table 3.3: Typical composition of technical grade titanium alloy Ti6Al4V [30]

Chemical Composition	Weight %
Titanium, Ti	Remainder (~90)
Aluminium, Al	5.5 – 6.75
Vanadium, V	3.5 – 4.5
Oxygen, O	0.20
Iron, Fe	0.03
Carbon, C	0.08
Molybdenum, Mo	<0.01
Manganese, Mn	<0.01
Silicon, Si	<0.01

Table 3.4: Typical mechanical properties of Ti6Al4V [30]

Specification	Value
Density	4500 kg/m^3
Tensile strength	1170 MPa
Modulus of elasticity	114 GPa
Thermal conductivity	15 W/m.°C

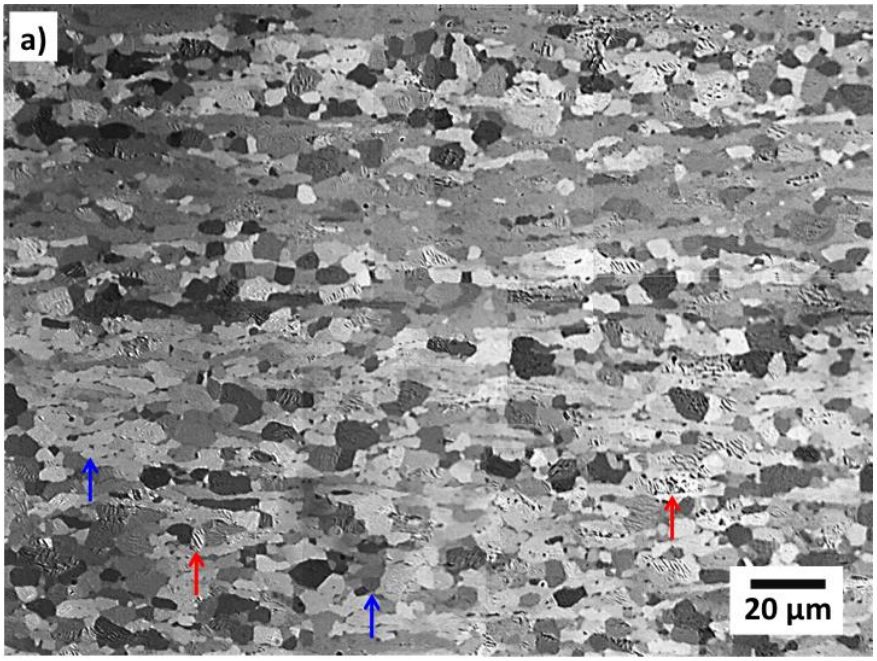

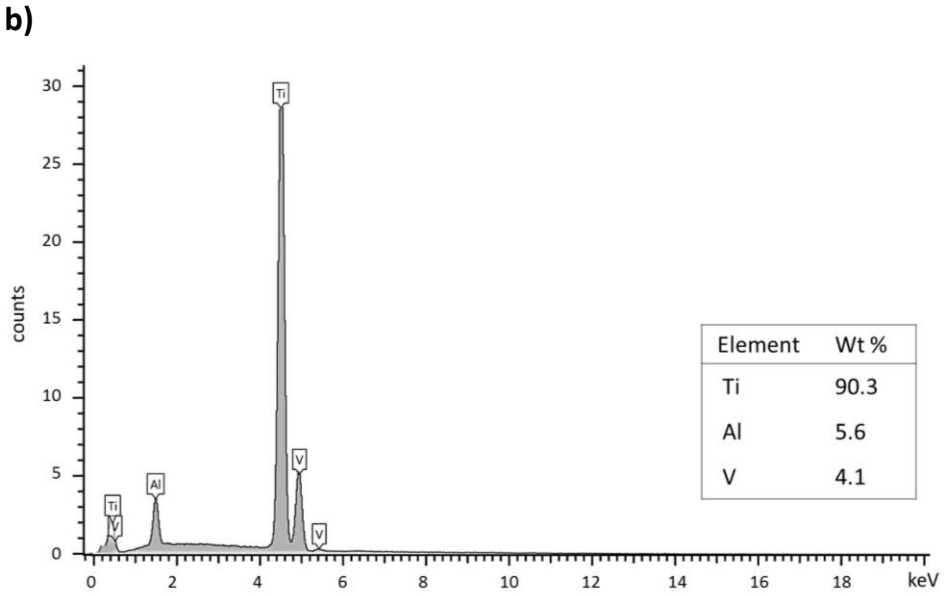

Figure 3.1: (a) Microstructure (cross section) of the Ti6Al4V workpiece used in all experimental work; blue arrows show the α-phase, and red arrows show the lamellar β-phase, (b) EDS analysis of the Ti6Al4V workpiece

3.1.3 CFRP/Ti stacks

The CFRP/Ti stacks were made by adhesive joining the CFRP and Ti panels. The adhesive used was Epoxy Loctite Hysol 9492 (supplied by Henkel). A uniform thickness of the adhesive was maintained at 0.3 mm by spreading a limited and small amount of 0.3 mm-diameter glass beads within the adhesive. The stacks were then clamped in a fixture, Figure 3.2, and left for five days at room temperature (22 °C) for the adhesive to fully cure. The CFRP/Ti stacks had an overall size of 8.3 mm. Figure 3.3 shows a finished CFRP/Ti stack, ready for drilling trials. All drilling trials were conducted by drilling from CFRP side of the stack. The effect of adhesive on tool wear and hole quality was assumed to be negligible.

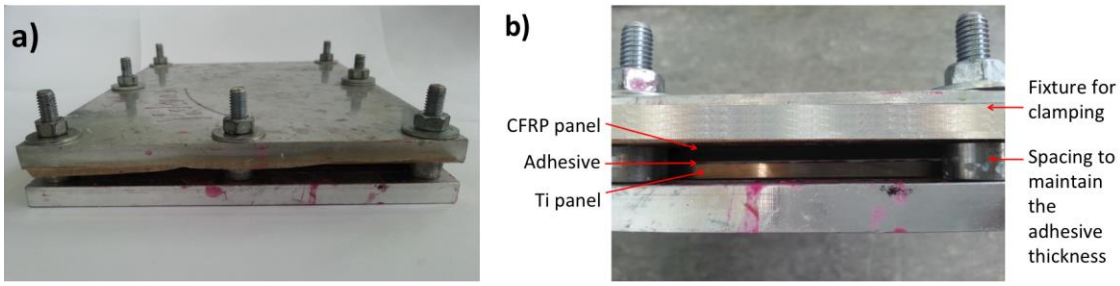

Figure 3.2: Setup for making CFRP/Ti stacks

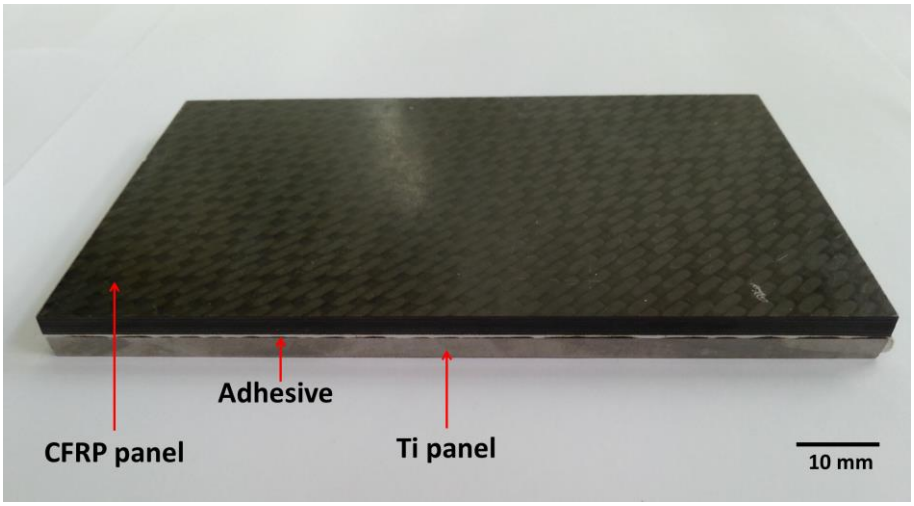

Figure 3.3: A CFRP/Ti stack for drilling work

3.2 Drills

The drill (geometry and material) was kept constant throughout experimental work. All drills employed were Sandvik Corodrill R840-0610-30-A0A, which were two-flute tungsten carbide twist drills, having a diameter of 6.1 mm with point and helix angles of 140° and 35°, respectively. This drill has been specifically employed by BAE systems for drilling CFRP/Ti stacks. The details of the drills are indicated in Figure 3.4 and Table 3.5. Based on the literature [45, 133], a tungsten carbide drill appears the most practical for drilling both CFRP and titanium alloys due to the balanced toughness and hardness, which is appropriate for both materials in the stack. In addition, the 140° point angle assists in achieving reliable tool life when drilling CFRP/Ti stacks. The large helix angle of 35° is required to allow the flow of the Ti chips through the flutes.

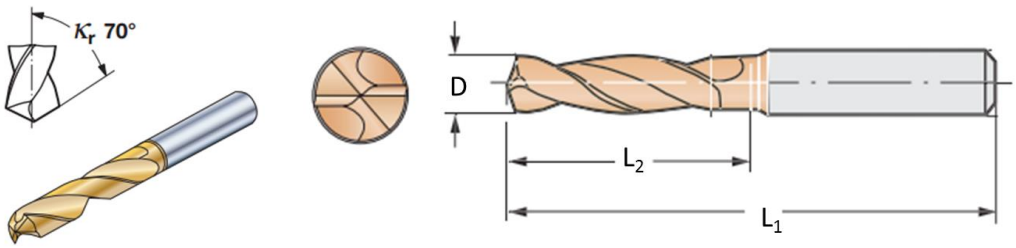

Figure 3.4: Schematic of Sandvik Corodrill R840-0610-30-A0A [155]

Table 3.5: Detail of Sandvik Corodrill R840-0610-30-A0A [155]

Specification	Detail
Tool material	Straight tungsten carbide (WC-9% Co)
Drill diameter, D	6.1 mm
Overall length, L_1	82 mm
Cutting length, L_2	44 mm
Point angle	140°
Helix angle	35°
Clearance angle	10°
Number of flutes	2

At BAE Systems, a drill is typically re-ground up to three times in order to minimize tooling costs. Therefore, reground drills were supplied by BAE Systems and employed for this research instead of new ones, since reground drills represent actual production conditions and typical practice in the industry. Hence, the data and finding from this work will be representative of actual production. All reground drills were thoroughly inspected via optical and Scanning Electron Microscopy (SEM) prior to performing drilling tests. The geometry of the drills was confirmed to be consistent, although the coating condition was different from new drills. There was no coating at the cutting edges and the flank faces of the drill as it was removed during the regrinding process. However, the TiAlN coating was fully intact at the rake faces and flutes of the drills, Figure 3.5.

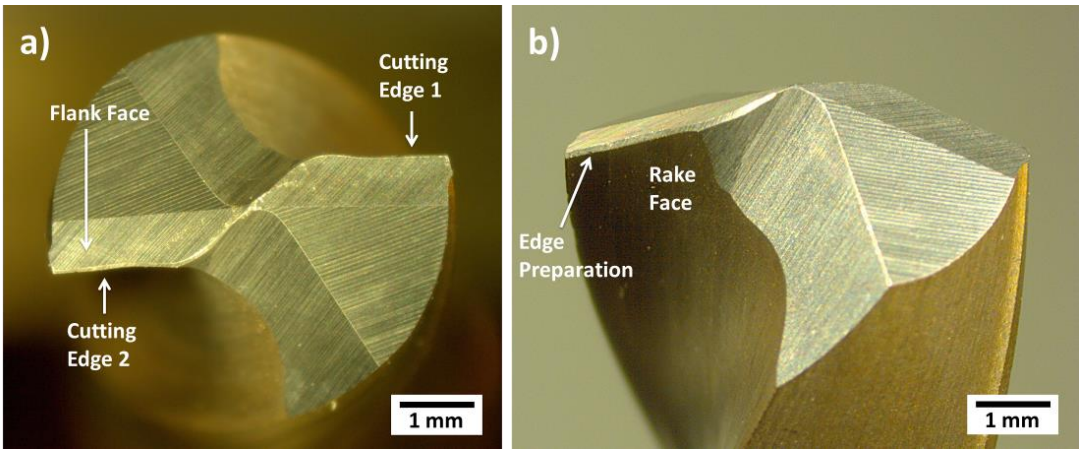

Figure 3.5: Reground, Sandvik Corodrill R840-0610-30-A0A, provided by BAE Systems

The drills also underwent cutting edge preparation (CEP) or chamfering to produce a radius of 70 µm to strengthen the cutting edges, Figures 3.5 (b) and 3.6 (a). Chamfered cutting edges are stronger and are recommended for drilling titanium alloy, compared to extremely sharp cutting edges which are more prone to being fractured [108]. Figure 3.6 (b) is a high magnification SEM image, showing the condition of the tungsten carbide (WC) grains and cobalt (Co) binder at the cutting edge prior to drilling. The material of the drill (at the cutting edge) was confirmed to be purely WC and Co by EDS analysis, Figure 3.7.

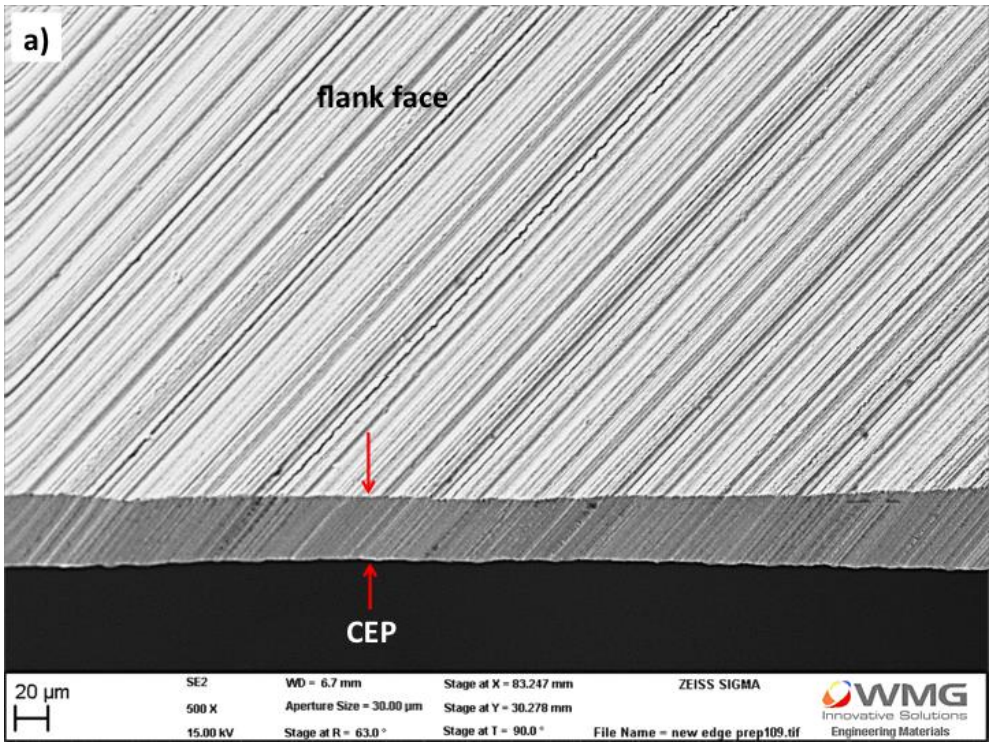

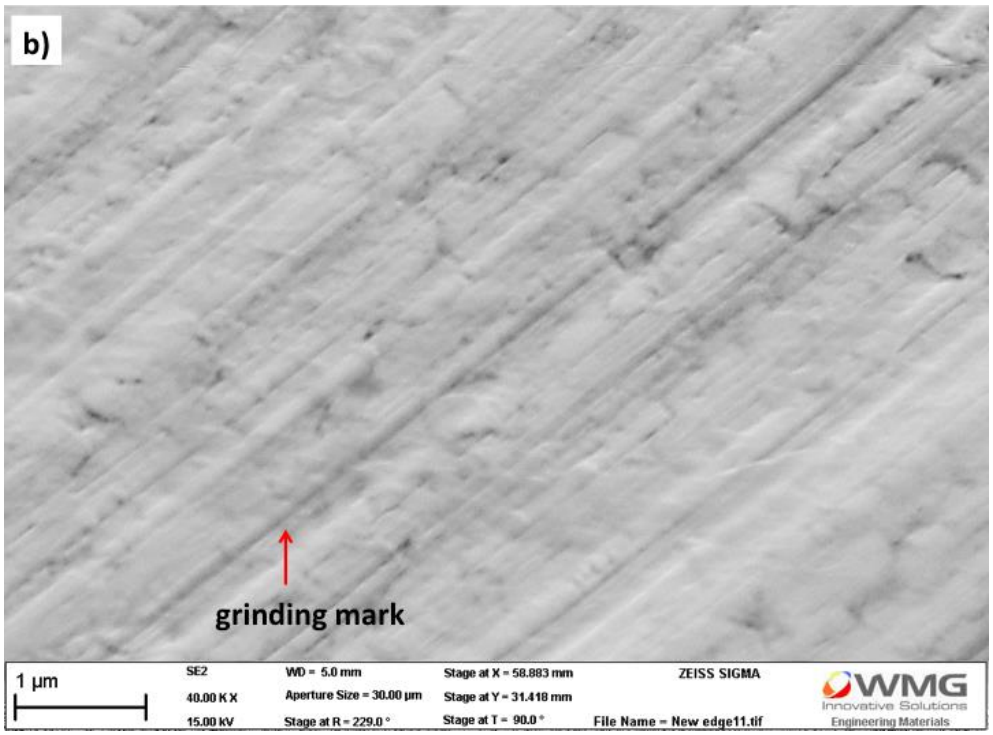

Figure 3.6: SEM micrographs showing (a) cutting edge preparation (CEP) and (b) condition of tungsten carbide grains (WC) and cobalt (Co) binder at the cutting edge prior to drilling operations

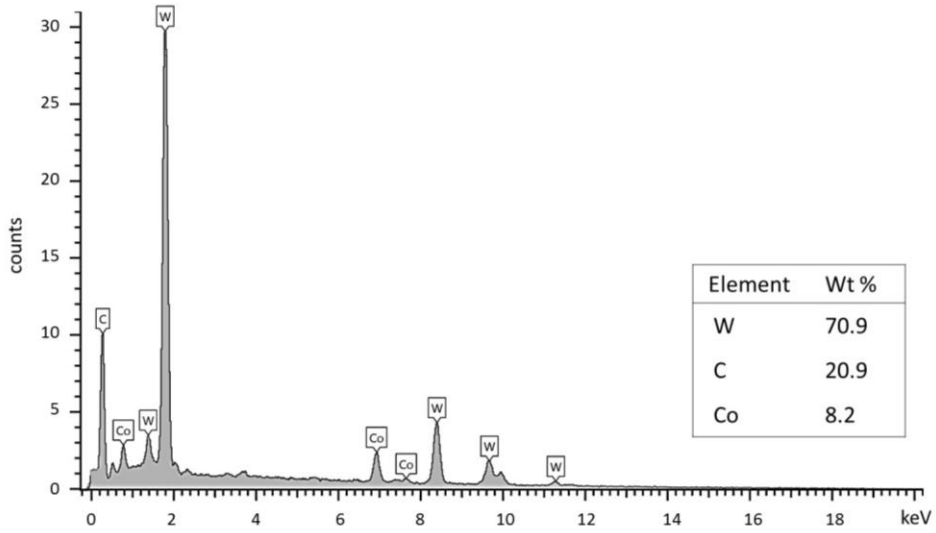

Figure 3.7: EDS analysis of drill substrate at the cutting edge, indicating tungsten carbide (WC) and cobalt (Co) elements

3.3 Experimental equipment and methodology

3.3.1 Machine tool

A DMG MORI Ultrasonic 65 was used for all drilling operations, Figure 3.8. It is a commercially available 5-axis machining centre, with a continuously variable spindle speed up to 18,000 rpm and feed capability up to 40 m/min, and equipped with ultrasonic assisted machining capability.

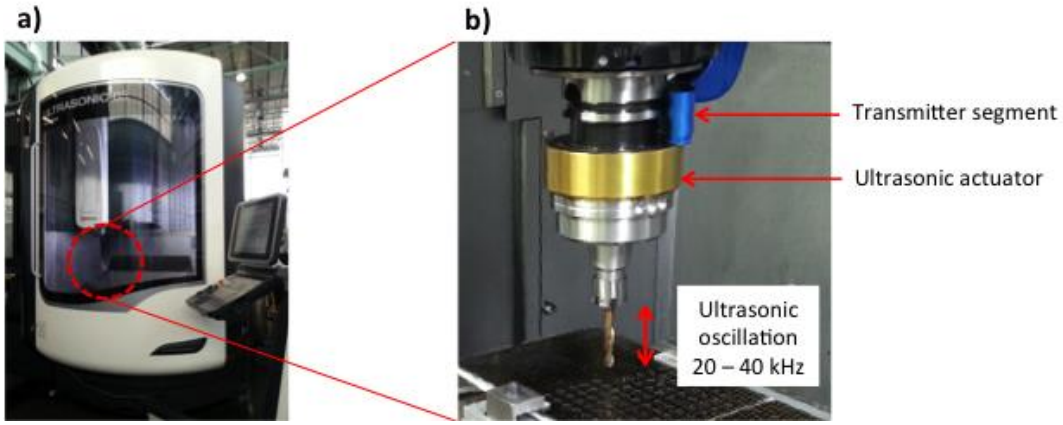

Figure 3.8: (a) DMG MORI Ultrasonic 65 machine tool, (b) Ultrasonic actuator for drilling

The working principle of transferring the ultrasonic vibration to the cutting tool on this machine tool was explained previously in Section 2.9. The machine determines the ultrasonic frequency to give the optimal ultrasonic amplitude at the resonant frequency for the particular drill. The frequency and amplitude of the ultrasonic vibration determine the vibration speed of the drill during UAD, as detailed in Section 2.9.1. Whilst the exact value of the ultrasonic frequency (in Hz) is displayed on the machine controller screen, the exact value of the ultrasonic amplitude is not. Therefore, an external laser sensor device was used for measuring the ultrasonic amplitude, Section 3.3.1.1.

3.3.1.1 Ultrasonic amplitude measurement

The ultrasonic amplitude of the cutting tool was measured using a Keyence laser sensor device (repeatability of 0.02 µm) [156], Figure 3.9, connected to a computer equipped with LK-Navigator software for analysing the ultrasonic vibration signals. The laser beam was set up straight, perpendicular to the flat surface (flank) of the cutting edges to reflect the laser, and the signal was processed by the LK-Navigator software.

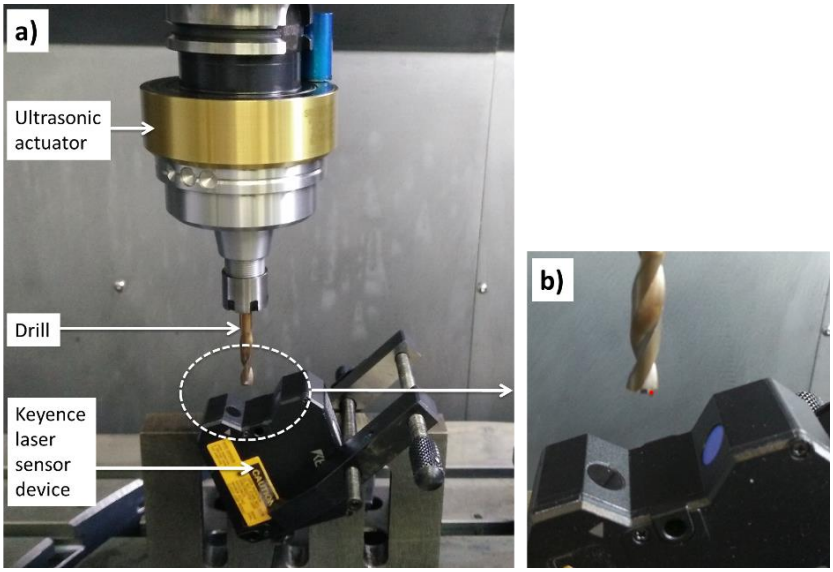

Figure 3.9: Ultrasonic vibration measurement setup, (a) the overview (b) the red light on the cutting edge is the laser which read ultrasonic signals

Figure 3.10 (a) shows the vibration waves displayed as detected by the laser, indicating (i) the natural vibration of the machine tool when the ultrasonic was turned off, and (ii) the ultrasonic vibration of the cutting tool when the ultrasonic actuator was turned on. Figure 3.10 (b) shows a magnified view of the ultrasonic oscillation. The peak-to-peak amplitude of the drill oscillation (during UAD) was determined by measuring the difference between the highest and the lowest peaks, Figure 3.10 (b).

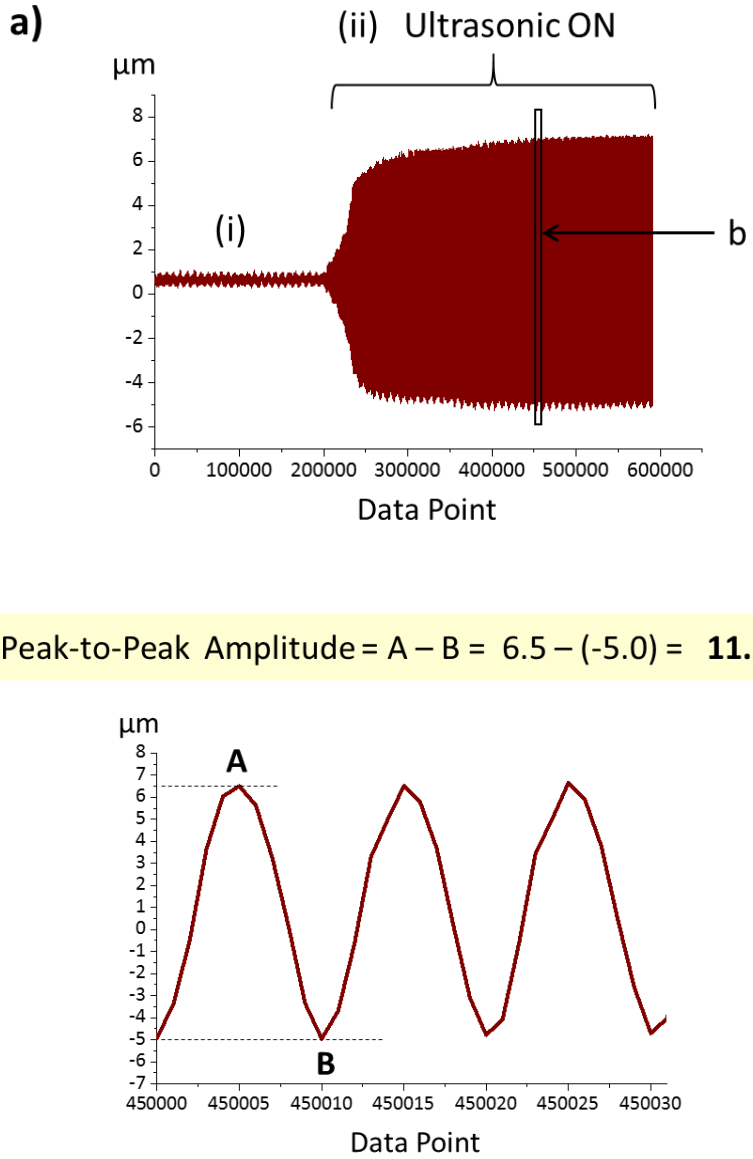

Figure 3.10: (a) Ultrasonic vibration profile, (b) measurement of peak-to-peak ultrasonic amplitude

3.3.2 Data acquisition equipment and procedure

3.3.2.1 Cutting force and torque

Thrust force and torque during drilling were measured using Kistler piezo-electric dynamometer Type 9257B, Figure 3.11 (a). This dynamometer was connected to a data acquisition system consisting of a multi-channel charge amplifier and data acquisition box, Figure 3.11 (b), which was connected to a computer equipped with Dynoware software. The dynamometer consists of built-in force sensors, which detect the force exerted in the X, Y and Z directions. The workpiece was clamped on top of the dynamometer. The signals from the dynamometer were converted into the respective forces, and torque was calculated by the Dynoware software. For drilling, only thrust force (Fz) and torque (Mz) were considered since the direction of the drilling and feed was in the Z direction. Forces were measured when drilling the 1st, 2nd, 3rd and every 10th holes.

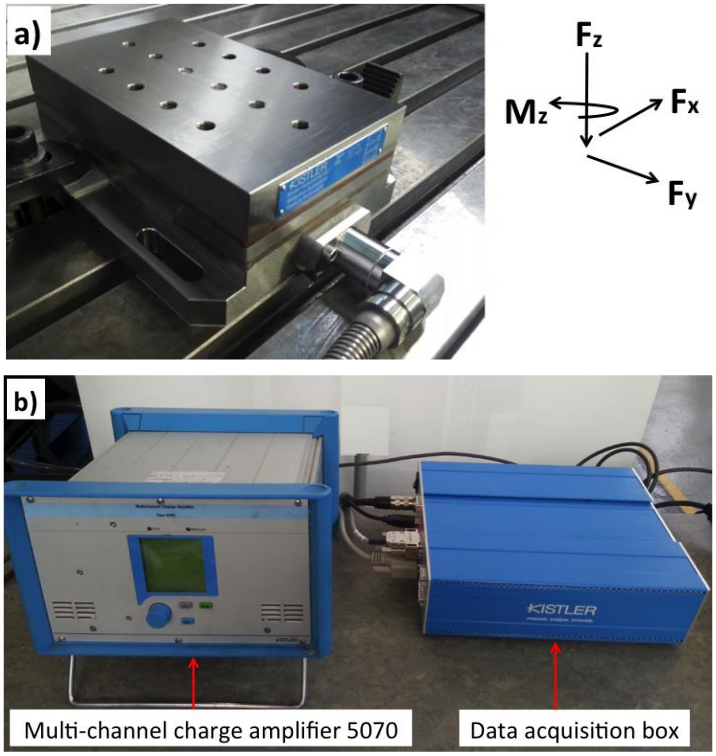

Figure 3.11: Kistler dynamometer 9257B used for measuring cutting force during drilling

3.3.2.2 Tool wear

Tool wear was examined and quantified using Nikon SMZ 74 ST optical microscope, Figure 3.12, connected to a computer with Carl Zeiss image analysis software. Drills were examined after drilling the 1st, 2nd, 3rd and each subsequent 10th holes until the end of drilling trials. The drill (attached to the tool holder) was taken out from the machine tool and placed under the optical microscope, Figure 3.12, and tool wear was photographed and recorded using the Carl Zeiss software.

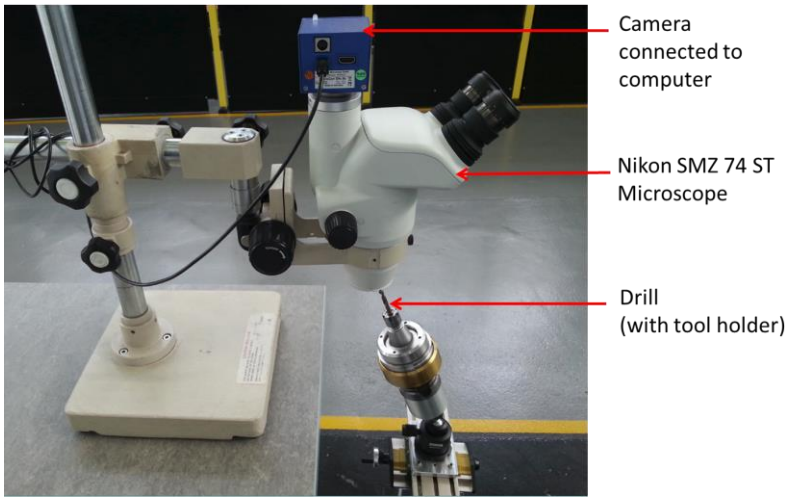

Figure 3.12: Nikon SMZ 74 ST optical microscope for measuring tool wear

In some instances when drilling CFRP/Ti stacks, the adherent titanium on the cutting edges masked the worn cutting edges and made it difficult to measure the wear. Taking advantage of the abrasive CFRP, which alternately removed the adhering titanium during drilling the stacks and revealing the worn cutting edges, the flank wear was measured after drilling CFRP and before drilling Ti. Figure 3.13 details the measurement of the flank wear. The wear was the difference between the original lengths, Figure 3.13 (a), and the length of the cutting edge after drilling, Figure 3.13 (b), in which the maximum was considered as in equation (2) for evaluation:

$$\text{Flank wear} = \text{Maximum of } [(A0 - A10), (B0 - B10), (C0 - C10)] \quad \ldots\ldots\ldots\ldots (2)$$

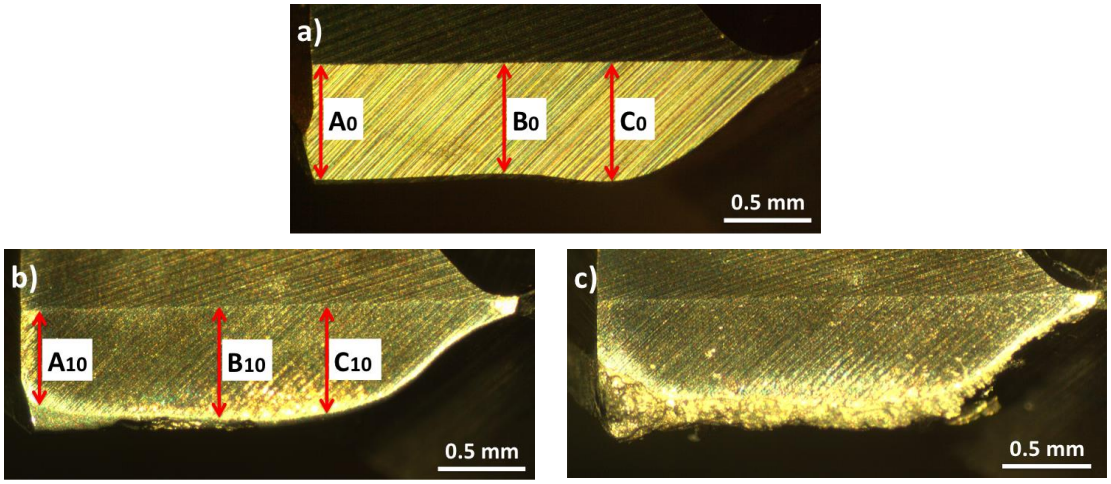

Figure 3.13: Measurement of flank wear; (a) new cutting edge, (b) clean cutting edge showing the worn surface after drilling CFRP; A_{10}, B_{10} and C_{10} indicate 10 holes, (c) titanium adhesion on the cutting edge after drilling through Ti layer of the stack

Flank wear was measured until the end of tool life or up to 80 holes (due to the limitation of workpiece material) in the case when the tool life was above 80 holes. According to ISO 3685:1993 (E) standard [151], tool life ends when maximum flank wear reaches 300 µm. In this experimental work, however, end of tool life was regarded as when the wear reached 200 µm, in accordance with BAE Systems end of tool life. Further investigation of tool wear mechanisms at higher magnification was carried out using Scanning Electron Microscopy (SEM) (Model: Carl Zeiss Σigma), integrated with SmartSEM (image navigation software), Figure 3.14.

Figure 3.14: Carl Zeiss Scanning Electron Microscope (SEM)

Further examination, measurement and analysis of the volume of titanium adhered on the cutting edges after drilling tests were performed using a 3D micro-coordinate measuring microscope, Alicona Infinite Focus G5, Figure 3.15. The drill was scanned optically to generate 3D images, and the volume of adhered material on the cutting edges was measured in the Alicona software based on the 3D images.

Figure 3.15: Alicona surface profilometer

3.3.2.3 Temperature during drilling

Omega Type-K thermocouples, Figure 3.16 (a), comprising thermocouple wires having a diameter of 0.30 mm were used because of instantaneous response times (0.2 – 0.6 seconds). The thermocouple had a thermal sensitivity of 41μv/°C and able to measure temperature in the range of -100 to 600 °C. The limit of error for the Type K thermocouples was 2.2 °C. The thermocouples measurement were checked by measuring temperatures of boiling water which were confirmed to be 98 – 100 °C. For measuring temperatures during drilling, the thermocouple conductors were attached to the workpiece and positioned 1 mm from where the hole was to be drilled, Figure 3.17. The connector of the thermocouples was connected to the thermocouple data logger, Picolog TC-08, Figure 3.16 (b). The data logger was then connected to the

USB port of a computer, which was equipped with Picolog Data Acquisition software whereby the recorded temperature was displayed and analysed.

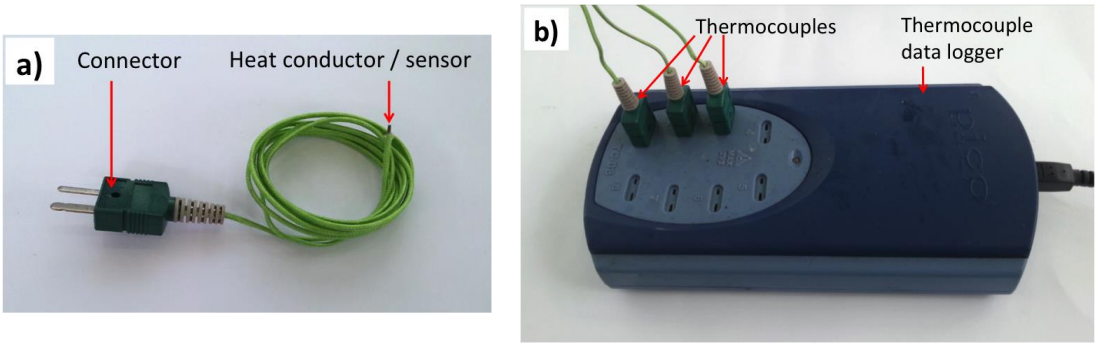

Figure 3.16: (a) Omega Type-K thermocouple for measuring cutting temperature (diameter of the heat conductor / sensor = 1 mm), (b) thermocouple data logger, Picolog TC08

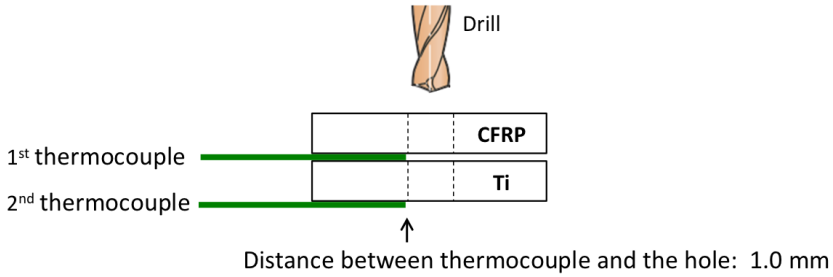

Figure 3.17: Thermocouples' positions for measuring temperatures when drilling CFRP/Ti stacks

3.3.2.4 Hole quality measurement

3.3.2.4.1 Hole diameter

The diameter of holes drilled in CFRP and Ti was measured using a three-points Bowers analogue hole micrometer, Figure 3.18. A setting ring was used to check the micrometer's reading before performing the measurement of the drilled hole diameters. For each hole, measurements were performed three times and averaged.

Figure 3.18: Bowers hole micrometer for measuring 6 – 8 mm hole diameter, with a setting ring (diameter = 7.995 mm) for calibration

3.3.2.4.2 CFRP delamination

A Nikon SMZ18 optical microscope was used to photograph the CFRP entrance delamination. Measurement of the CFRP delamination around the entrance of the hole was conducted considering the ratio of the extent of delamination in reference to the hole diameter (F_D), as discussed in Section 2.6.4.1 (Figure 2.10), using Buehler OmniMet Image Analysis software. For each hole, measurements were performed three times and averaged.

3.3.2.4.3 CFRP pull-out

Selected holes were sectioned into half, Figure 3.19 (a), to investigate the condition and topography of the machined surfaces via SEM, and Alicona Infinite Focus. The volume of CFRP pulled out from the bore machined surface was measured based on three-dimensional (3D) images generated through the Alicona software. As demonstrated in Figure 3.19 (b), the blue regions indicate the pull-out of material, below the reference machined surface, which is shown in green. The red regions indicate materials above the machined / reference surface (e.g. carbon fibres stuck out).

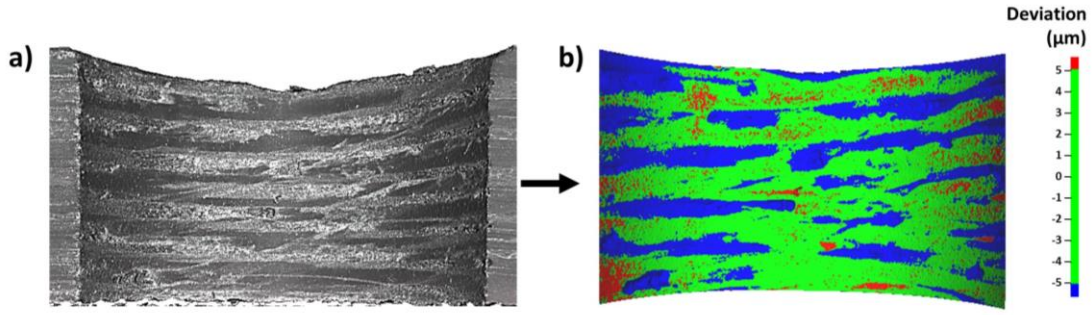

Figure 3.19: (a) Cross section of hole / machined surface of CFRP scanned by Alicona Infinite Focus, (b) surface topography generated by the Alicona software for measuring the pull out of material

3.3.2.4.4 Titanium machined surface

The condition and topography of machined Ti surfaces were examined using SEM. The machined surface roughness of Ti in terms of R_a and R_z (linear roughness), and S_a (area

roughness) were measured, Figure 3.20 using the Alicona Infinite Focus. The machine has the capability of measuring the roughness of cylindrical shape (of the hole) and performing both linear and area surface roughness (X and Y directions). Using a form removal tool in the Alicona software, the cylindrical shape of the machined surface was translated into a flat surface, and the area surface roughness, S_a was measured.

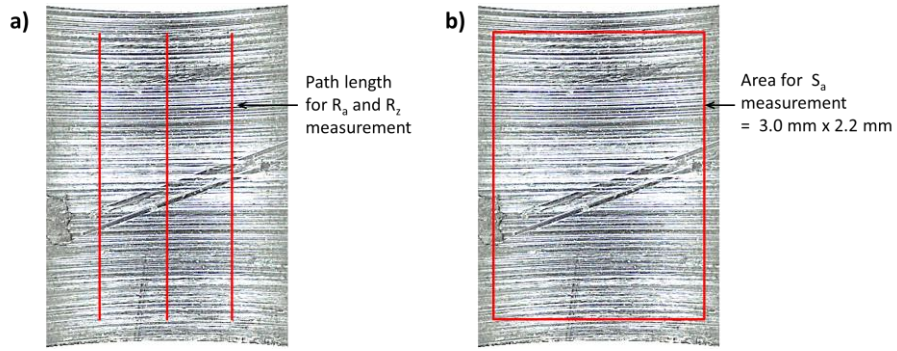

Figure 3.20: Machined surface roughness of Ti employing Alicona Infinite Focus, (a) path length for Ra and Rz measurement, (b) area surface roughness, S_a measurement

3.3.2.4.5 Titanium burr (hole exit)

The burr height at the exit of the holes in titanium was measured using a digital micrometer, Figure 3.21 (a). The thickness of the CFRP/Ti stacks was measured, followed by the total thickness of both burr and the stacks, Figure 3.21 (b, c). The burr height was the difference between the two measurements. For each hole, three measurements were conducted and averaged.

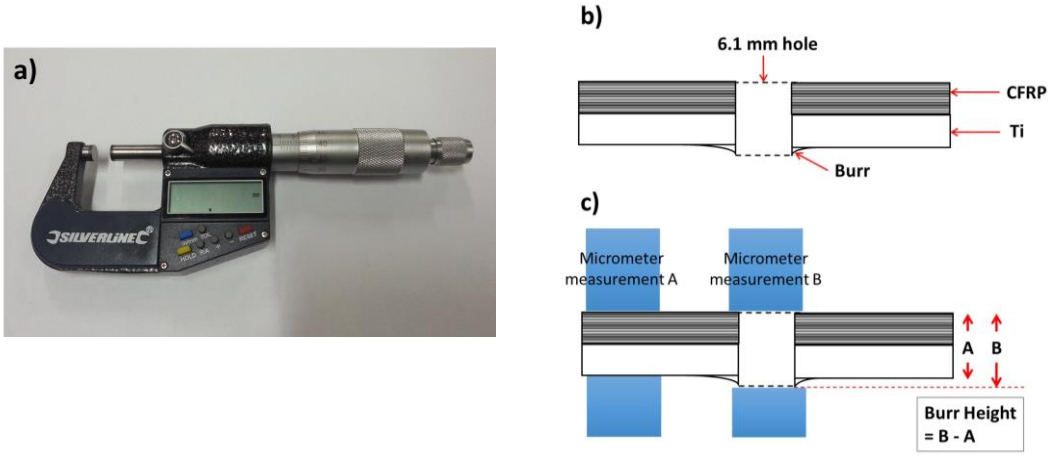

Figure 3.21: (a) Micrometer, (b) measurement of the burr height using a micrometer

In addition, the burr was also examined under an optical microscope Nikon Eclipse MA200. In order to do this, selected holes were firstly sectioned, mounted in epoxy resin and polished (using 9 µm and 3 µm MetaDi supreme diamond liquid, and 0.06 µm MasterMet Colloidal silica liquid + 30% hydrogen peroxide), Figure 3.22.

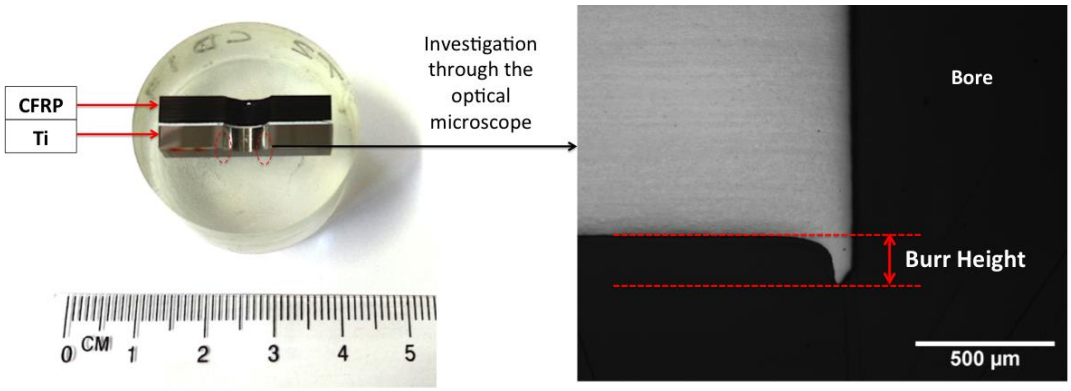

Figure 3.22: Measurement of burr height using the optical microscope

3.3.2.4.6 Titanium hardness

The hardness of sub-machined surfaces were measured using Buehler Wilson hardness automated tester, Figure 3.23, and analysed using Diamet hardness automation software. Prior to performing the hardness measurement, selected holes were sectioned, mounted in epoxy resin, ground and polished.

Figure 3.23: Buehler Wilson Knoop and Vickers hardness tester

The Knoop indenter was used as measurements were needed close to the machined surface, Figure 3.24. The shape of the Knoop indentation (which take the form of elongated diamond, Figure 3.24) provided consistent hardness measurement for the near edge. The unit of the hardness for the Knoop hardness test is HK. A recommended minimum spacing between indentations was three times the size of the indentation. Indentations that are too close to each other would result in inaccurate hardness measurement as it is affected by plastic deformation of the material when being indented. Following trials at various loads (e.g. 10, 25, 50, 100, 500 and 1000 g), a load of 25 g was determined to be optimum in terms of repeatability, hence was used for all hardness measurements in this work. Using loads more than 100 g to make indentations resulted in total damage extending to the edge of the machined surface.

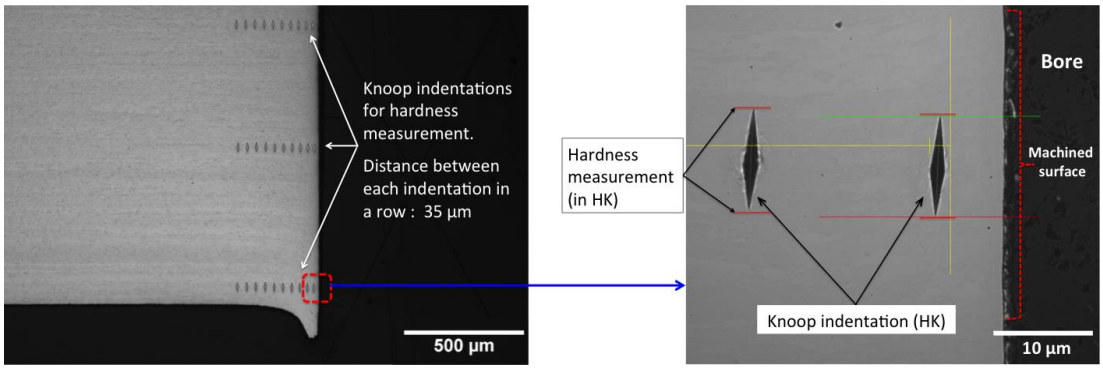

Figure 3.24: Knoop indentation for hardness measurement on the polished Ti

3.3.2.4.7 Residual strain / stress

A limited residual strain measurement of the holes drilled in the Ti workpiece was conducted using non-destructive x-tray diffraction at SALSA (Strain Analyzer for Large-Scale Applications) beam line at Institut Laue Langevin (ILL), Grenoble, France [157]. The limited access to the facility did not permit measurement of more than two samples. The strain measurement was performed at a depth of 2 mm from the Ti surface, along the radial direction, at 0.5 mm intervals as shown in Figure 3.25. The residual strain measurement at ILL, analysis of the data using LAMP (Large Array

Manipulation Program) software [158], and calculation of residual stress were conducted by Dr Darren Hughes and Conor Cafolla. The interpretation of the obtained data (plotted in a graph) was conducted by the author.

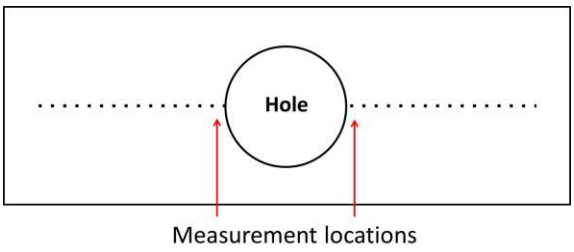

Figure 3.25: Schematic showing strain measurement along radial direction around a 6.1 mm diameter drilled hole in Ti

3.3.2.5 Chip morphology

Titanium chips were collected after drilling, Figure 3.26, and studied in terms of shape, thickness and segmentation. Images of the chips were captured using a digital camera and optical microscope, Nikon SMZ18.

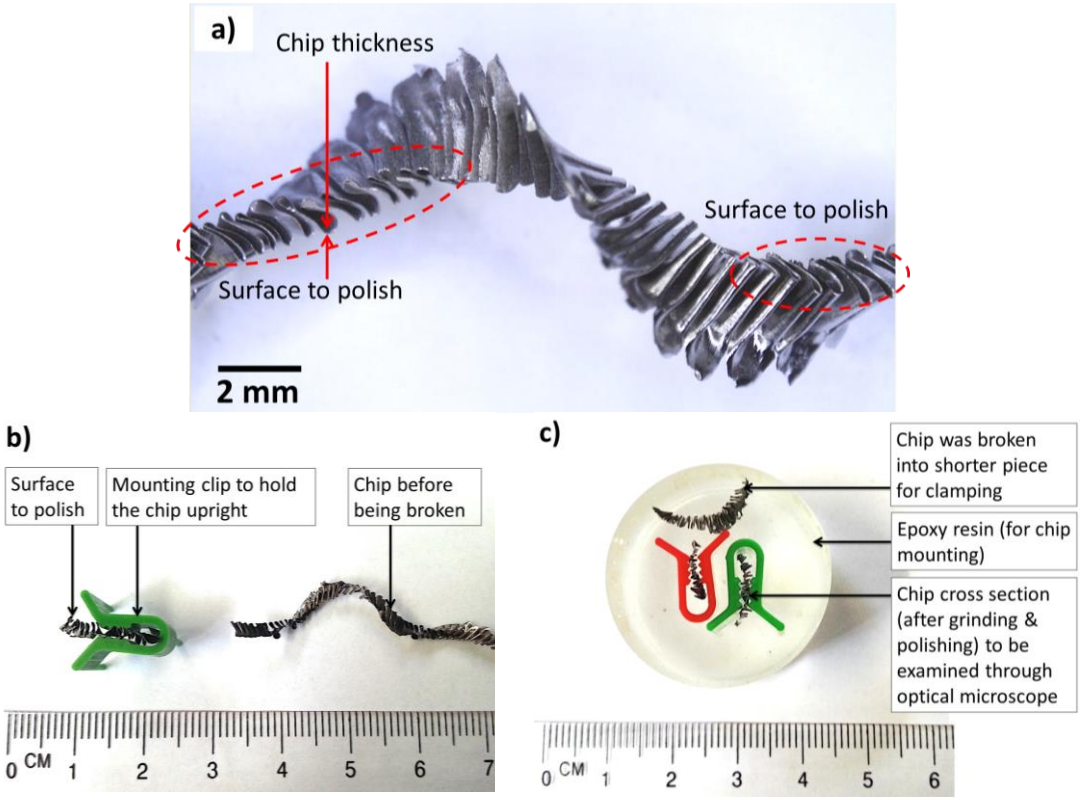

Figure 3.26: Preparation, clamping and mounting of Ti chip for polishing and investigating through the optical microscope (measurement of chip thickness)

For other alloys such as aluminium and steels where the chips are continuous and uniform, it is possible to measure the chip thickness using a micrometer. In the case of drilling titanium alloy however, where the chips were mostly spiral, folded and serrated, Figure 3.26 (a), using a micrometer to measure the thickness was not possible. Therefore, chip thickness was measured on mounted and polished sections under optical microscope Nikon Eclipse MA200 using Buehler OmniMet Image Analysis software. In doing so, the chip was first clamped upright, Figure 3.26 (b), mounted in epoxy resin, then ground and polished, Figure 3.26 (c). The measurement of thickness and shear band angle on the polished Ti chip is shown in Figure 3.27.

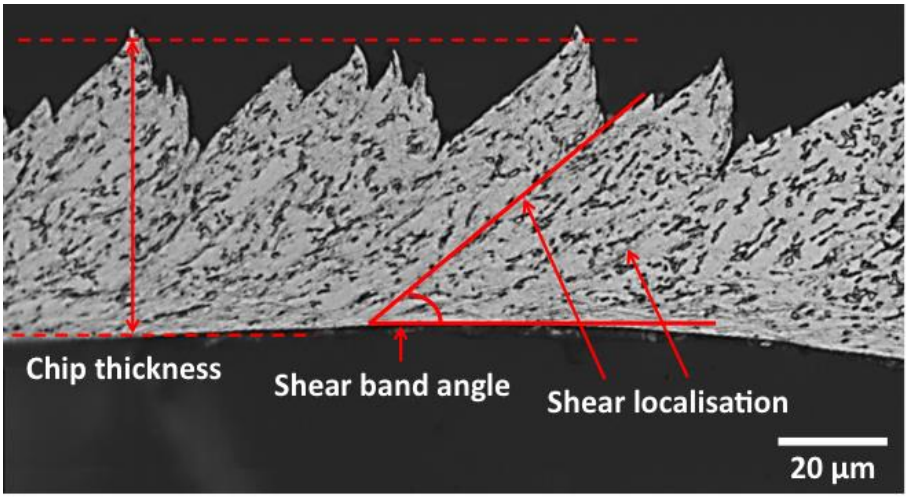

Figure 3.27: Measurement of Ti chip thickness and shear band angle on polished cross-section (Ti was polished using 9 µm and 3 µm MetaDi supreme diamond liquid, and 0.06 µm MasterMet Colloidal silica liquid + 30% hydrogen peroxide)

As much as CFRP chip formation was equally important, the involvement of cutting fluid by flood application during drilling prohibited the collection of the fine CFRP dust as it was washed away by the cutting fluid during drilling. Therefore it was difficult to engage the study of CFRP "chips" in this work. The work of previous researchers in the machining group at WMG involving dry drilling of CFRP-only has shown that interpretation of fine dust of CFRP was in fact challenging, and often did not provide useful information. Therefore, this research focuses on Ti chips only.

3.4 Experimental study: Design and procedures

3.4.1 Study 1: Conventional drilling employing constant cutting parameters

The purpose of this study was to investigate the tool wear mechanisms when drilling CFRP/Ti stacks. Specifically, the interaction between the CFRP and Ti and the cutting edges was studied. Understanding the interaction of tool wear mechanisms is useful in determining how to prolong tool life when drilling CFRP/Ti stacks. Furthermore, the effect of cutting mechanisms and tool wear on the hole quality was investigated. To understand the interaction between the drilling of different materials, conventional drilling of the materials in five different approaches was conducted, Table 3.6. The total drilling distance for each test was similar, which was 640 mm and equivalent to 80 holes.

Table 3.6: Description of drilling tests for Study 1

Materials	Description
a) CFRP-only	The materials were drilled individually.
b) Ti-only	
c) CFRP/Ti stacks (in one-shot)	The CFRP/Ti stacks were drilled continuously from CFRP through Ti in a single operation, as shown in Figure 3.28 (a).
d) CFRP and Ti separately and alternately	The CFRP panel and Ti panel were drilled as a separate entity but alternately one after another using the same drill, starting with drilling CFRP, Figure 3.28 (b (i)), followed by drilling Ti, Figure 3.28 (b (ii)).
e) CFRP/Ti stacks (in two-shots)	As schematically shown in Figure 3.28 (c): (i) The CFRP/Ti stack was drilled from and through the CFRP, (ii) The drill was retracted from the stack once it finished drilling the CFRP, and was exposed to the air (for 3 seconds), (iii) Then proceed with drilling the Ti component of the stack.

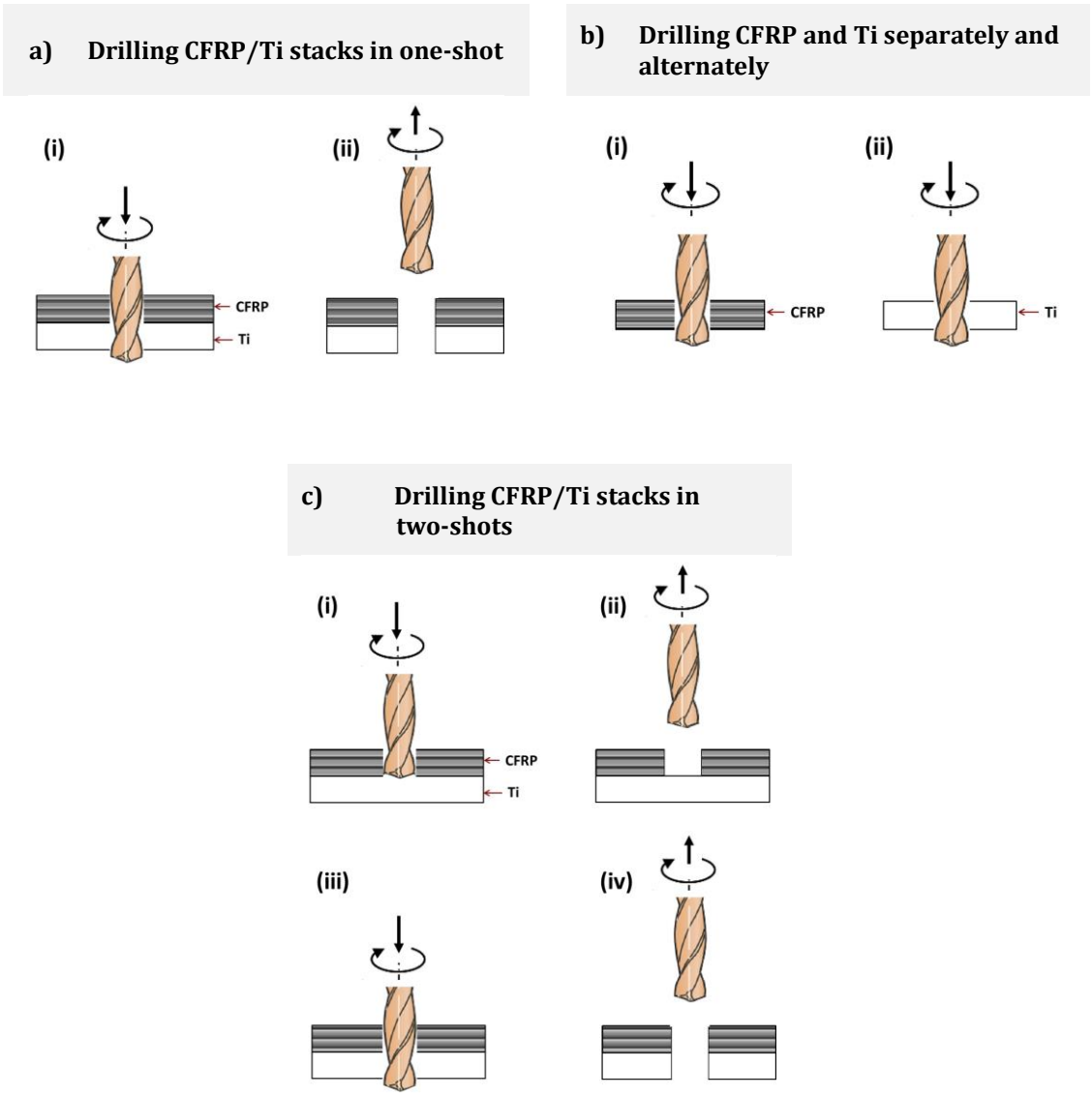

Figure 3.28: Schematic of (a) one-shot drilling of CFRP/Ti stacks, (b) drilling CFRP and Ti separately but alternately, and (c) two-shots drilling of CFRP/Ti stacks

A uniform set of cutting parameters, which were compromised cutting parameters between those for CFRP and Ti, were employed for drilling through CFRP/Ti stacks. Specifically, a cutting speed that is practical for drilling Ti (50 m/min), and a feed rate that is practical for CFRP (0.05 mm/rev), were employed, following BAE Systems recommendation [159]. This was based on the fact that Ti is more sensitive to the change in cutting speed, whereas CFRP is more sensitive to the change in feed rate. The cutting parameters, drilling condition (cutting fluid application) and drills used for drilling all materials combinations (as described in Table 3.6) were constant and

detailed in Table 3.7. A new but reground drill was used for each drilling test. All drilling trials were carried out with conventional water-based cutting fluid by flood application, supplied through nozzles around the machine tool spindle, Figure 3.29.

Table 3.7: Constant drilling parameters for Study 1

Variables	Details
Workpiece Material	CFRP-only, Ti-only, and CFRP/Ti stacks (Section 3.1)
Drill	Reground Sandvik Corodrill R840-0610-30-A0A (Section 3.2)
Cutting Speed (m/min)	50
Feed Rate (mm/rev)	0.05
Cutting Fluid	Water-based, Blasocut by Blaser Swisslube, 7% concentration
Total drilling distance for each test	640 mm = 80 holes

Figure 3.29: Flood cutting fluid application during all drilling trials

The setup of the drilling trials is shown in Figure 3.30. The 1st, 2nd, 3rd and every consecutive 10th holes, were drilled in a 25 mm-width workpiece clamped onto the dynamometer for measuring cutting forces. The remainder of the holes were drilled in

a larger workpiece (130 mm width), Figure 3.30. The detailed methodology for measuring cutting forces, tool wear and hole quality was described in Section 3.3.2. The whole drilling tests of (a) CFRP-only, (b) Ti-only, (c) CFRP/Ti stacks in one-shot, (d) CFRP and Ti separately, and (e) CFRP/Ti stacks in two-shots, were replicated or repeated two times. A new drill (reground) was used for each drilling trial.

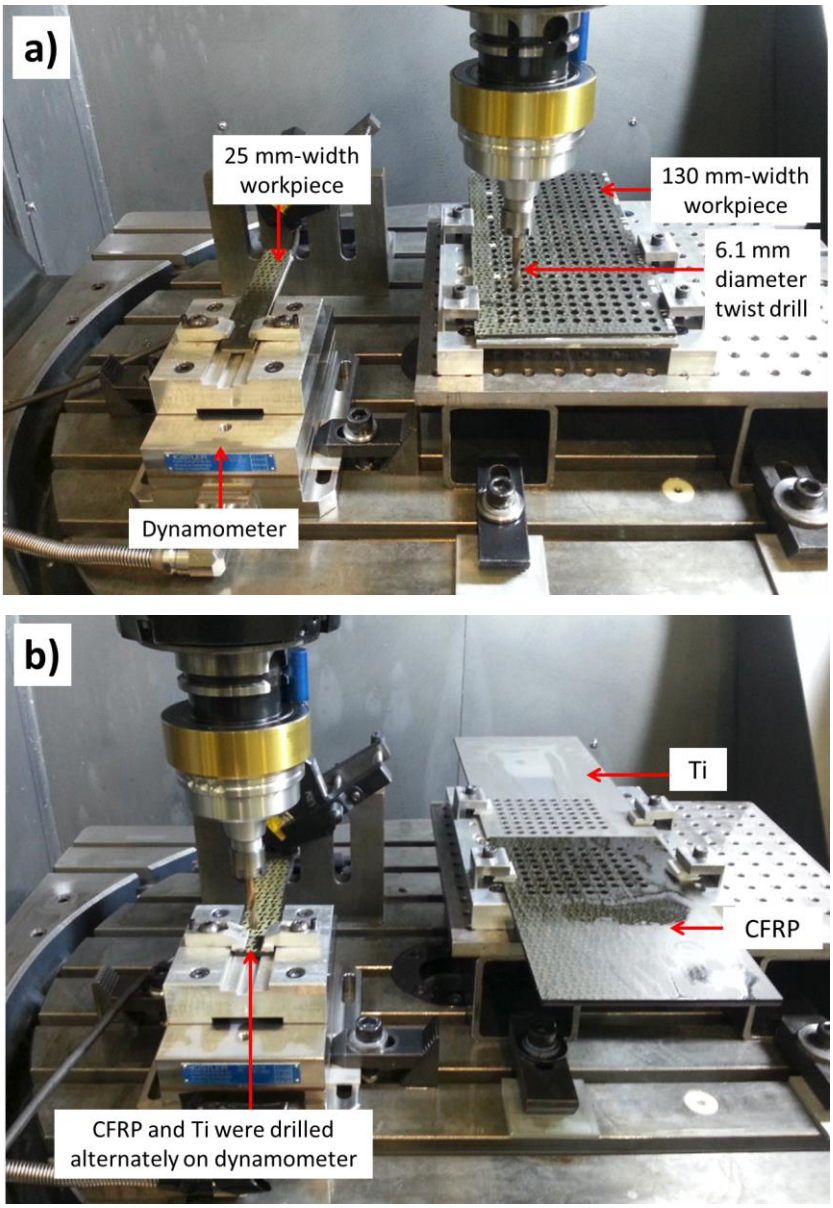

Figure 3.30: Experimental setups when drilling (a) CFRP-only, Ti-only, and CFRP/Ti stacks in one-shot and two-shots, (b) CFRP and Ti separately

3.4.2 Study 2: The effect of cutting speed during CD and UAD of CFRP/Ti stacks

The purpose of this experimental work was to study the effect of varying cutting speeds during conventional drilling (CD) and Ultrasonic Assisted Drilling (UAD) of CFRP/Ti stacks in one-shot on tool wear and hole quality. Cutting speeds were varied at 50% lower (25 min/min) and 50% higher (75 m/min) compared to the cutting speed used in Study 1 (50 m/min), as described in Section 3.4.1. All other parameters were fixed; details are presented in Table 3.8. The experimental setup was shown in Figure 3.30 (a), with cutting fluid application as in Figure 3.29. The data collected were cutting forces, tool wear, hole diameter, CFRP entrance delamination, CFRP pull out, Ti burr, Ti surface roughness, Ti micro-hardness, residual stress and Ti chip morphology; the detailed methodology for measurement was explained in Section 3.3.

Table 3.8: Drilling parameters and variables for Study 2

Variables		Test 1		Test 2		Test 3	
		CD	UAD	CD	UAD	CD	UAD
Workpiece Material		CFRP/Ti stacks (Section 3.1)					
Drill		Reground Sandvik Corodrill R840-0610-30-A0A (Section 3.2)					
Cutting Speed (m/min)		25	25	50	50	75	75
Feed Rate (mm/rev)		0.05					
Cutting Fluid		Water-based; Blasocut by Blaser Swisslube, 7% concentration					
Ultrasonic Function	Amplitude	Off	Peak-to-peak 11 µm	Off	Peak-to-peak 11 µm	Off	Peak-to-peak 11 µm
	Frequency	Off	40 kHz	Off	40 kHz	Off	40 kHz
	* Vibration Speed	Off	165 m/min	Off	165 m/min	Off	165 m/min

*** Vibration speed was calculated using equation 1 as in Section 2.9.1.**

3.4.3 Study 3: The effect of feed rate during CD and UAD of CFRP/Ti stacks

The purpose of doing this experimental work was to study the effect of varying feed rates during CD and UAD of CFRP/Ti stacks in one-shot on tool wear and hole quality. Feed rates were varied at 50% lower (0.025 mm/rev) and 50% higher (0.075 mm/rev) than the one used in Study 1 (0.05 mm/rev), as described in Section 3.4.1. All other parameters were kept constant; the detailed parameters were presented in Table 3.9. The drilling setup, methodology and drilling data collection during this work were similar to Study 2, as described in Section 3.4.2.

Table 3.9: Drilling parameters and variables for Study 3

Variables		**Test 1**		**Test 2**		**Test 3**	
		CD	**UAD**	**CD**	**UAD**	**CD**	**UAD**
Workpiece Material		CFRP/Ti stacks (Section 3.1)					
Drill		Reground Sandvik Corodrill R840-0610-30-A0A (Section 3.2)					
Cutting Speed (m/min)		50					
Feed Rate (mm/rev)		0.025		0.05		0.075	
Cutting Fluid		Water-based; Blasocut by Blaser Swisslube, 7% concentration					
Ultrasonic Function	Amplitude	Off	Peak-to-peak 11 µm	Off	Peak-to-peak 11 µm	Off	Peak-to-peak 11 µm
	Frequency	Off	40 kHz	Off	40 kHz	Off	40 kHz
	* Vibration Speed	Off	165 m/min	Off	165 m/min	Off	165 m/min

*** Vibration speed was calculated using equation 1 as in Section 2.9.1.**

3.5 Statistical analysis

For Study 2 and Study 3, to evaluate the drilling performance, it was essential to ascertain whether the results obtained (tool wear, cutting forces and relevant hole quality criteria) were statistically significant or not, in terms of:

- the difference between data / results generated by different cutting speeds (25, 50 and 75 m/min).
- the difference between data / results generated by different feed rates (0.025, 0.05 and 0.075 mm/rev).
- the difference between data / results generated by CD and UAD.

The standard method to confirm any significant difference between the data is by performing an analysis of variance (ANOVA). Two-way ANOVA tests were performed on the data to establish an understanding of any significant effect of the independent variables (cutting speeds and feed rates) and drilling processes (CD and UAD) on the dependent variables (tool wear and hole quality).

The null hypothesis and alternative hypothesis of the study were firstly set, in which one was accepted (and the other was rejected). This is summarised in equations (3) and (4). The null hypothesis is that the mean or variance (σ^2) between generated data were equivalent, which indicated that there was no significant difference between the data, i.e. the effect of cutting speed, feed rate or CD / UAD was not significant. The alternative hypothesis is that the variances (σ^2) between generated data were not similar, which indicated that there was a significant difference between the data, i.e. the effect of cutting speed, feed rate or CD / UAD was significant.

Null hypothesis, $H_0 : \sigma^2_A = \sigma^2_B$ ……(3)

Alternative hypothesis, $H_1 : \sigma^2_A \neq \sigma^2_B$ ……(4)

In order for the difference between the groups and variables to be statistically significant, the null hypothesis must be rejected, so that the alternative hypothesis is true [160]. This was done by calculating and comparing the variance ratio, F_{ratio} and $F_{critical}$ of the tested data (tool wear, thrust forces, torque and hole quality).

The level of significance or confidence used was 0.05. This indicates that in the case when the null hypothesis is true, there is 5% chance that it can be rejected. If the calculated F_{ratio} is higher than $F_{critical}$, the null hypothesis is rejected, and the alternative hypothesis is accepted, which confirms that there is a significant difference between the data / results [160]. The ANOVA is only valid when the data is normally distributed. Statistical analysis software, Minitab was used to check the normality of the data and the applicability for the ANOVA. The ANOVA was conducted using Minitab software and was also confirmed by Microsoft Excel Data Analysis Pack software.

Chapter 4 Results and Analysis

4.1 Study 1: Conventional drilling employing constant cutting parameters

The purpose of this study was to investigate the machinability of CFRP/Ti stacks, in terms of tool wear and hole quality, when drilling conventionally using a uniform cutting speed of 50 m/min and feed rate of 0.05 mm/rev. In order to establish the factors that govern tool wear and hole quality when drilling CFRP/Ti stacks, it is important to understand how the results are different or similar to the case when drilling the materials individually and separately. To summarise, this section presents, compares and discusses the tool wear and hole quality during conventional drilling of:

(a) CFRP-only,

(b) Ti-only,

(c) CFRP/Ti stacks in one-shot,

(d) CFRP and Ti together but separately (alternately),

(e) CFRP/Ti stacks in two-shots.

4.1.1 Tool wear mechanisms

CFRP and Ti are two different materials that exhibit different wear mechanisms during drilling. By taking into consideration the case of drilling the materials individually and separately, this study was designed to assess the effect of interaction between two different wear mechanisms; abrasive and adhesive wears during one-shot drilling of CFRP/Ti stacks.

Figure 4.1 shows a comparison of flank wear when drilling the various materials combinations. One-shot drilling of CFRP/Ti stacks resulted in the highest tool wear rate, hence the shortest tool life (62 holes). This was followed by two-shots drilling of

CFRP/Ti stacks, drilling CFRP-only, drilling CFRP and Ti separately, and the least wear when drilling Ti-only. The maximum flank wear at the end of drilling trials (80 holes) and the percentage increase in flank wear when one-shot drilling of CFRP/Ti stacks compared to the other drilling tests are compared and summarised in Table 4.1.

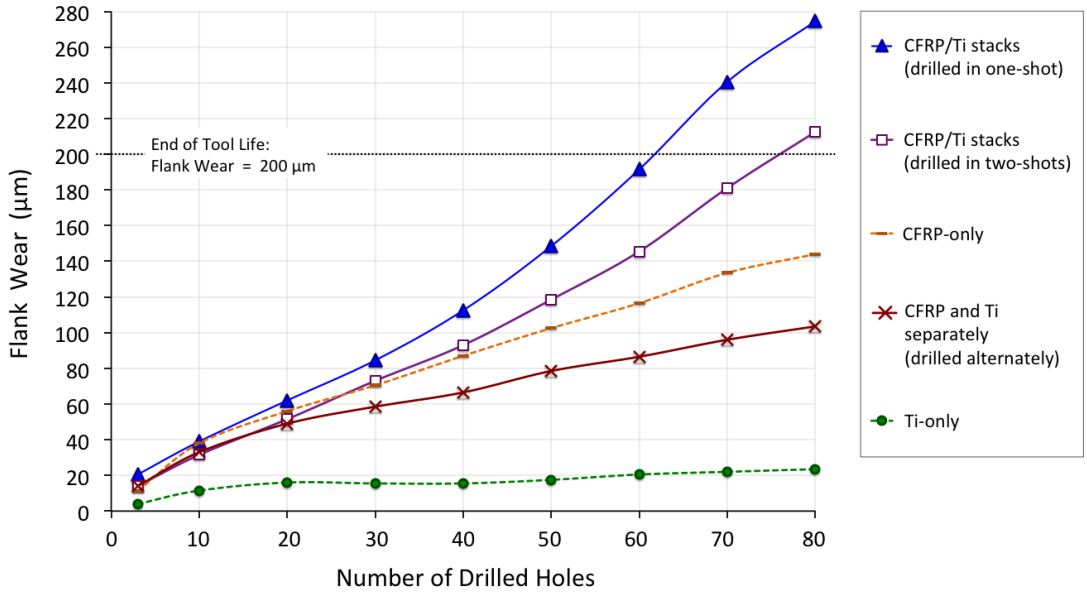

Figure 4.1: Flank wear during conventional drilling of (a) CFRP-only, (b) Ti-only, (c) CFRP/Ti stacks in one-shot, (d) CFRP and Ti separately, and (e) CFRP/Ti stacks in two-shots using a cutting speed of 50 m/min and feed rate of 0.05 mm/rev

Table 4.1: Comparison of maximum flank wear at the end of drilling trials (after 80 holes) of (a) CFRP-only, (b) Ti-only, (c) CFRP/Ti stacks in one-shot, (d) CFRP and Ti separately, and (e) CFRP/Ti stacks in two-shots

Drilling of	Flank wear (µm)	Percentage increase in flank wear when one-shot drilling of CFRP/Ti stacks compared to other drilling tests
a) CFRP-only	144	90%
b) Ti-only	24	1038%
c) CFRP/Ti stacks in one-shot	273	-
d) CFRP and Ti separately	105	160%
e) CFRP/Ti in two-shots	213	28%

Referring to Figure 4.1 and Table 4.1, it is interesting to note that one-shot drilling of CFRP/Ti stacks resulted in 160% and 28% higher flank wear than drilling CFRP and Ti separately, and two-shots drilling of CFRP/Ti stacks, respectively (after 80 holes). These results indicated that despite employing a similar materials combination (CFRP and Ti), the way that the materials were drilled influenced the wear of the drills. This is an important finding that has not been previously reported and will be discussed throughout this section (sub-sections 4.1.1.1, 4.1.1.2, 4.1.1.3 and 4.1.1.4).

To understand the wear mechanisms, the cutting edges condition at the end of drilling trials (after 80 holes) are compared in Figure 4.2, showing the wear and adhered material on the cutting edges. The three-dimensional (3D) images of the cutting edges highlight the wear in blue colour, and the adhered material on the cutting edge is in red colour, Figure 4.2 (b, d, f, h, j). When drilling CFRP-only, material adhered to the cutting edges was not evident, Figures 4.2 (a, b) and 4.3. Minor adhered material (volume = 0.002 mm^3) was observed when drilling Ti-only, Figures 4.2 (c, d) and 4.3. Whereas, there was a substantial amount of adhered material after one-shot drilling of CFRP/Ti stacks (volume = 0.063 mm^3), two-shots drilling of CFRP/Ti stacks (volume = 0.010 mm^3) and drilling CFRP and Ti separately (volume = 0.013 mm^3), Figures 4.2 (e, f, g, h, i, j) and 4.3. The adhered material on the cutting edges was confirmed to be titanium Ti6Al4V by Energy Dispersive X-ray Spectroscopy (EDS) analysis, Figure 4.4.

In summary, at the end of the tests (80 holes), one-shot drilling of CFRP/Ti stacks caused:

- 385% more Ti adhesion than drilling CFRP and Ti separately
- 530% more Ti adhesion than two-shots drilling of CFRP/Ti stacks
- 3050% more Ti adhesion than drilling Ti-only

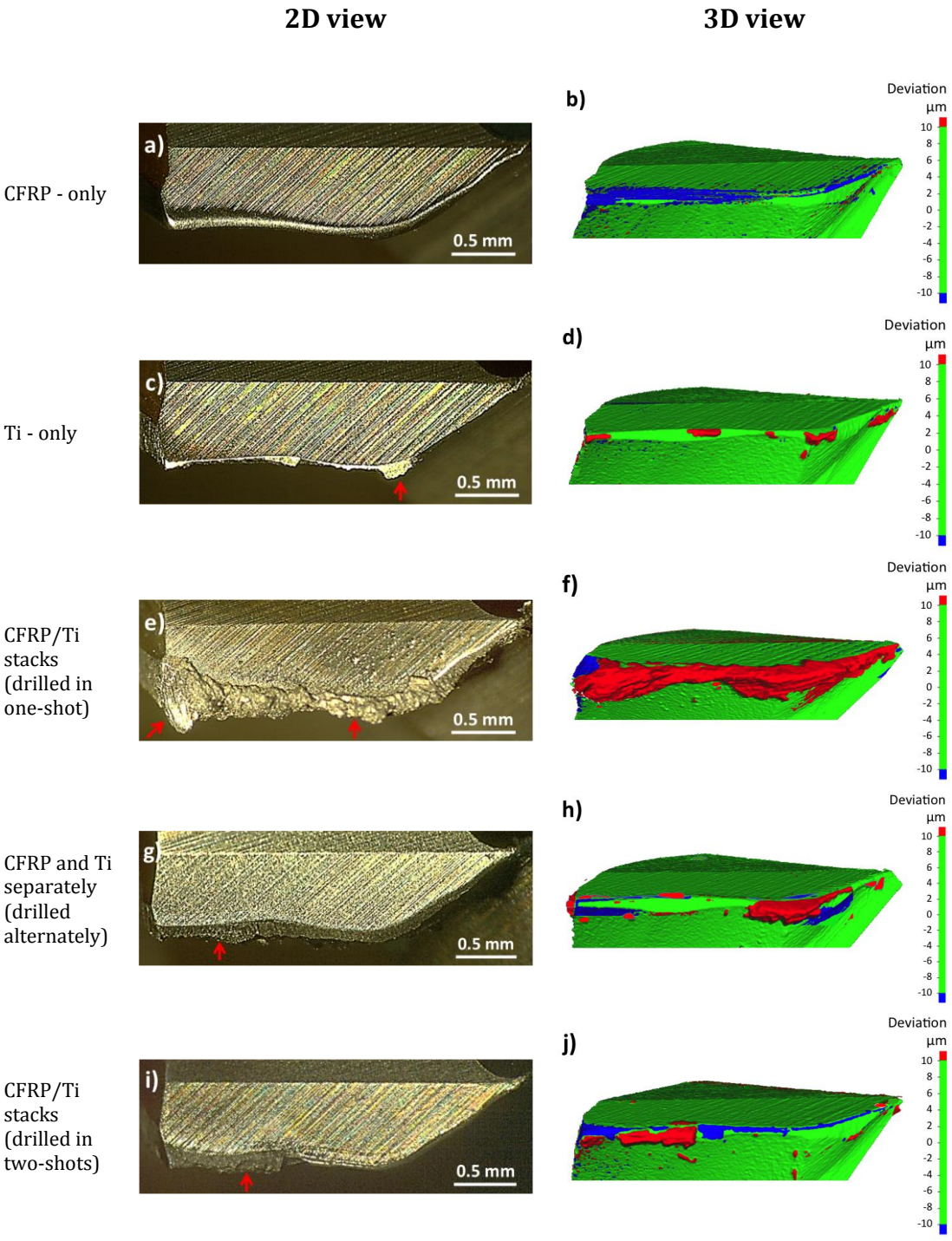

Figure 4.2: Condition of the cutting edges of the drills at the end of drilling trials of (a, b) CFRP-only, (c, d) Ti-only, (e, f) CFRP/Ti stacks (one-shot), (g, h) CFRP and Ti separately (alternately), and (i, j) CFRP/Ti stacks (two-shots). Red arrows in 2D images and red regions in 3D images show Ti adhesion

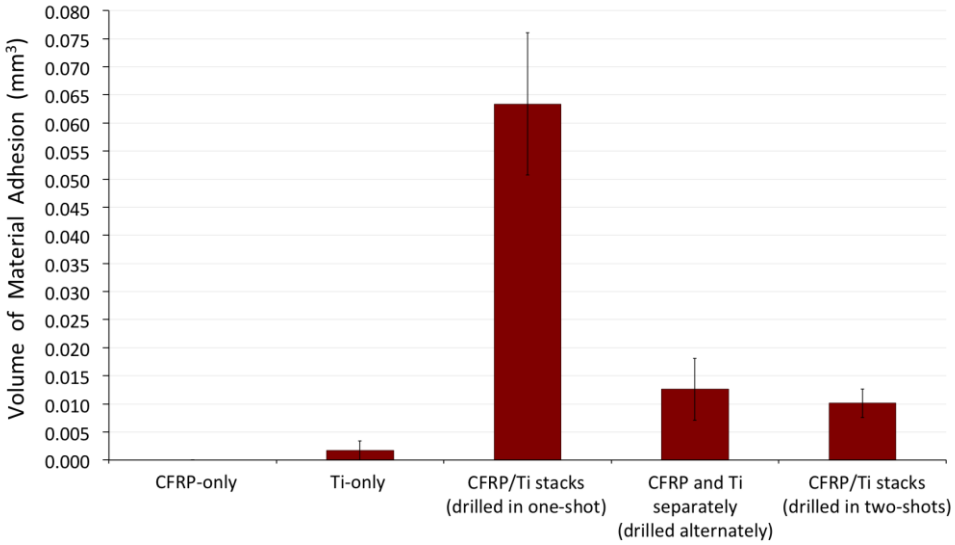

Figure 4.3: Comparison of volume of material adhesion on cutting edges after drilling 80 holes through (a) CFRP-only, (b) Ti-only, (c) CFRP/Ti stacks in one-shot, (d) CFRP and Ti separately, and (e) CFRP/Ti stacks in two-shots using a cutting speed of 50 m/min and feed rate of 0.05 mm/rev

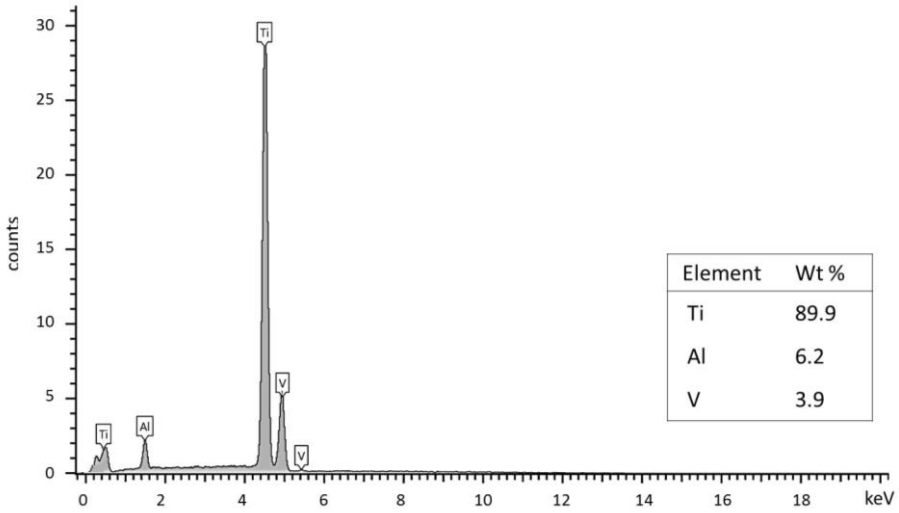

Figure 4.4: EDS analysis of adhered material on the cutting edges after one-shot drilling of CFRP/Ti stacks

The Ti was strongly bonded to the cutting edges, as it could not be removed manually, indicating a strong metallic bonding. It must be noted that in some instances, the adherent Ti totally masked the worn cutting edges and made it difficult to measure the wear. For plotting the graph in Figure 4.1, in the case of drilling CFRP and Ti together, the flank wear was measured after drilling CFRP and before drilling Ti, taking advantage of the abrasive CFRP, which alternately removed the adhered Ti and revealed the worn cutting edges.

The fact that one-shot drilling of CFRP/Ti stacks caused the largest amount of Ti adhesion and hence the highest tool wear indicated that there was a strong correlation between Ti adhesion and the wear rate of the cutting edges. These results suggest that the interaction between the abrasion of the cutting edge when drilling CFRP, followed by drilling the Ti immediately, caused the Ti chips to adhere strongly to the cutting edges, and hence leading to more rapid tool wear as the adherent Ti detached. Whereas, less Ti chips adhered to the cutting edges when there was a delay in between drilling the materials (this will be discussed in Section 4.1.1.4). Since the interaction of the abrasion of the cutting edges and Ti adhesion when drilling CFRP and Ti together is more complex than having solely abrasive or adhesive wear, it is worth discussing the wear mechanisms when drilling CFRP-only and Ti-only first.

4.1.1.1 Drilling CFRP-only

When drilling CFRP-only, wear of the cutting edges was by an abrasive wear mechanism. This was evident from cutting edge rounding and fine scratch pattern along the cutting edge after drilling 80 holes, Figure 4.5 (a) (a magnified view of the image shown in Figure 4.2 (a)). Figure 4.5 (b) shows that there were voids having widths of smaller than 0.5 μm between carbide (WC) grains at the worn cutting edge, which was not observed at the new / unworn cutting edge before drilling, Figure 3.6 (b). The sizes of the voids were smaller than the size of the WC grains (0.5 – 1.5 μm). Therefore, the voids indicated the removal of cobalt (Co) binder due to abrasion by the abrasive carbon fibres of CFRP during the drilling. Compared to WC grains, which have a reported hardness within 1700 – 2000 HV, the lower hardness of Co binder (400 – 1200 HV) makes it more susceptible to being abraded and removed by the carbon fibres (hardness = 800 – 1100 HV) during drilling [35, 48, 52].

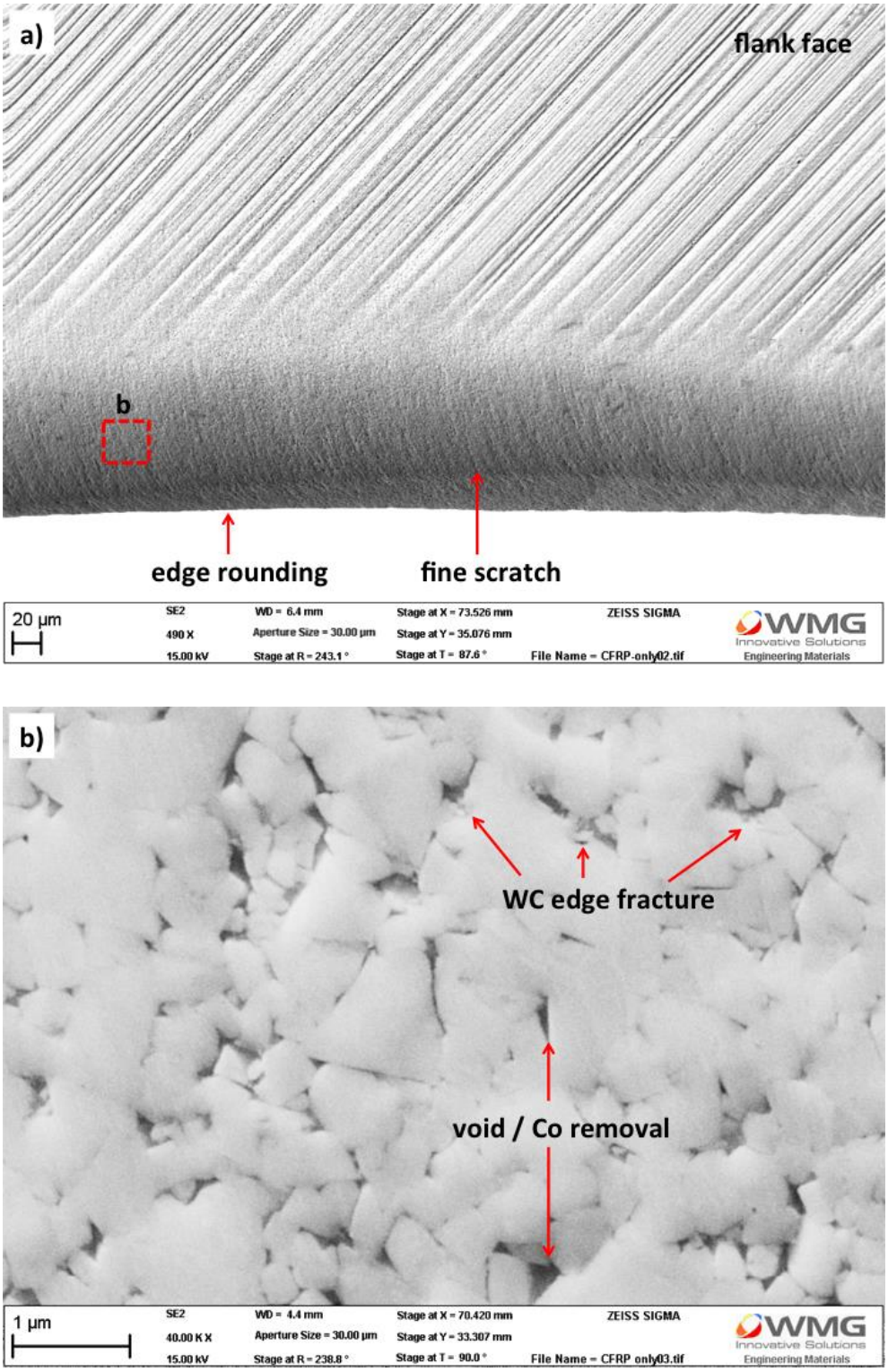

Figure 4.5: SEM micrographs showing condition of the cutting edge at the end of drilling trial (80 holes) of CFRP-only, which details (a) cutting edge rounding / worn area, (b) removal of Co binder and edge fracture of WC grains at the worn cutting edge (cutting speed = 50 m/min, feed rate = 0.05 mm/rev)

The removal of Co binder makes the WC grains prone to micro-fracture, as they are inherently brittle. In addition, the WC grains exhibit angular morphology, which makes the sharp edge of the WC grains prone to being fractured, Figure 4.5 (b), to produce WC particles. These micro wear particles of WC then abraded the WC grains that were still intact on the cutting edges as drilling progressed. The observed wear mechanism when drilling CFRP-only in the current study is similar to that described in previous work [56, 161] involving dry machining (drilling and turning) of CFRP-only.

4.1.1.2 Drilling Ti-only

In contrast, Figures 4.2 (c, d) and 4.6 show that the cutting edge used for drilling Ti-only (after 80 holes) exhibited no marked difference in geometry and sharpness compared to the new drill, Figure 3.6 (a), although a limited amount of Ti adhesion was observed. Previous studies [41, 96] which reported substantial Ti adhesion and edge chipping indicative of a severe adhesive wear mechanism as early as drilling 10 holes in Ti-only either did not use cutting fluid or employed spray mist cutting fluid.

The strong adhesion and metallic bonds between Ti chip and WC-Co cutting edge typically occur when drilling at high cutting temperatures and pressure, in the absence of a protective layer (lubricant or oxide film) on the contacting surfaces [55]. The current study shows that using cutting fluid is important when drilling titanium alloy to lessen tool wear, which is in agreement with previous studies [98-100]. The cutting fluid helps to remove the heat from the cutting zone, consequently contributed to the least adhered Ti chips (volume = 0.002 mm^3) to the cutting edge, which helped to prolong the drill life.

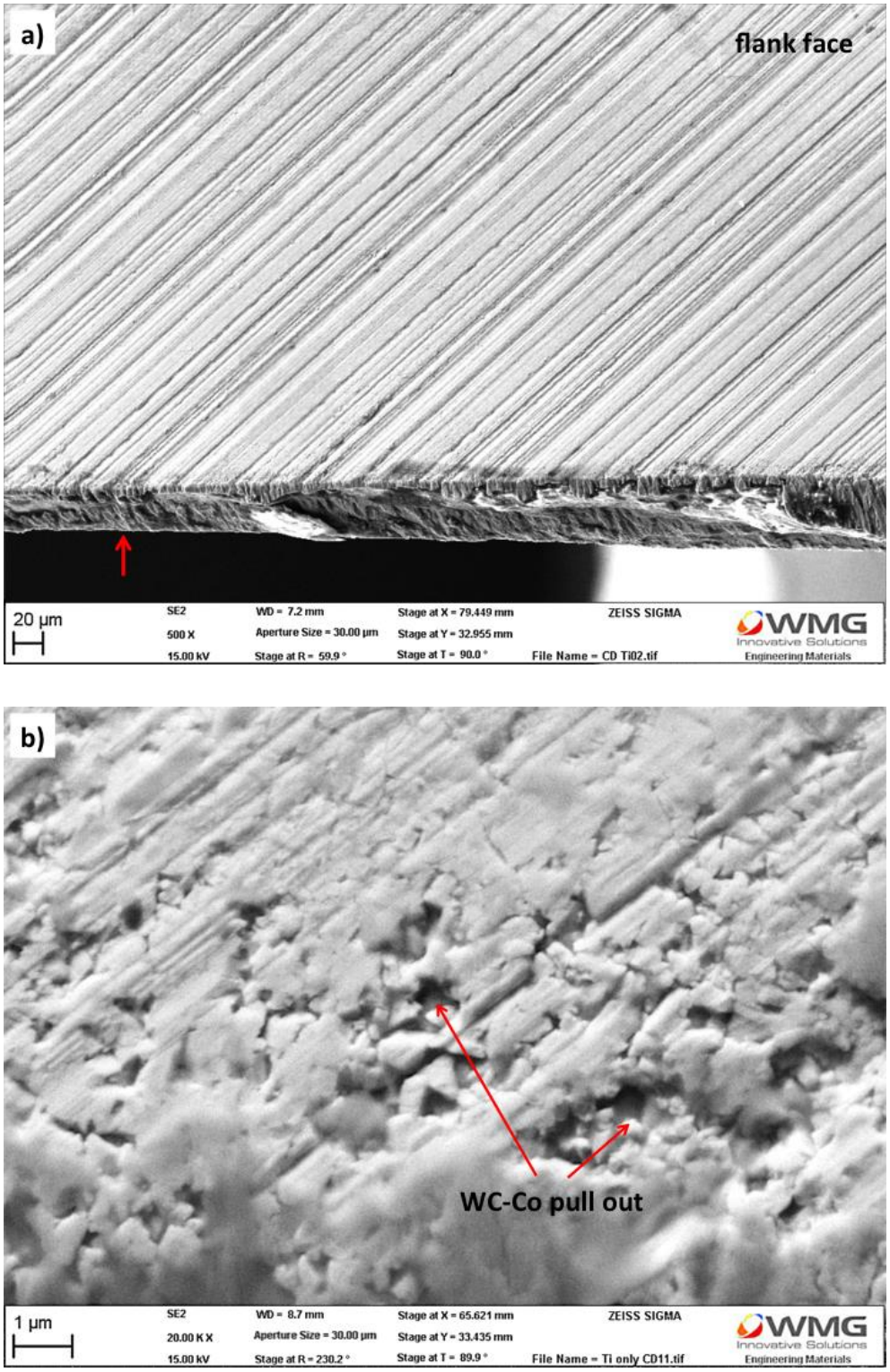

Figure 4.6: SEM micrographs showing condition of the cutting edge at the end of drilling trial (80 holes) of Ti-only, which details (a) no significant change in the geometry; the cutting edge is indicated by the red arrow, (b) WC-Co pull out from the cutting edges (cutting speed = 50 m/min, feed rate = 0.05 mm/rev)

When drilling Ti-only, there was no evidence that the cutting edges and WC grains were being abraded. Ti alloy by nature is not abrasive, and the measured hardness of Ti workpiece and work-hardened Ti chips which are 346 HV and 455 HV, respectively, were not hard enough to abrade the Co binder of the tool compared to the case of drilling CFRP-only. However, as seen in Figure 4.6 (b), there was evidence of small voids (0.2 – 1 μm) on the cutting edge used for drilling Ti-only. The size of the voids is equivalent to the size of WC grains (0.5 – 1.5 μm), which indicated that both WC grains and Co binder were pulled out when the adhered Ti chip detached as the newly formed chip flowed over it. This wear condition when drilling Ti-only (up to 80 holes) did not significantly change the geometry of cutting edges. However, it must be noted that if the drilling trial continues and with further increase in hole number, the voids (pull-out of WC-Co) would eventually increase leading to weakening of the cutting edges and hence drill failure / breakage.

4.1.1.3 Drilling CFRP/Ti stacks in one-shot

Figure 4.7 (a) shows the condition of the cutting edge after one-shot drilling of 80 holes through CFRP/Ti stacks. Substantial adhered Ti on the cutting edge exhibiting irregular and uneven surface finish is evident. Further SEM investigation of the cutting edge after removal of the adhered Ti chips (by drilling through a hole in CFRP) revealed worn, substantial cutting edge fracture and cracking, Figure 4.7 (b). Figure 4.8 (a) shows a magnified view of the worn cutting edge, confirming that there were voids (width of 0.1 – 0.8 μm) between WC grains, which indicated preferential removal of Co binder due to abrasion by CFRP. Fractured WC grains are also evident, Figure 4.8 (a). Figure 4.8 (b) shows a magnified view of the cutting edge fracture (of Figure 4.7 (b)), which revealed uneven and substantial fractured WC grains as well as pull-out of the WC grains.

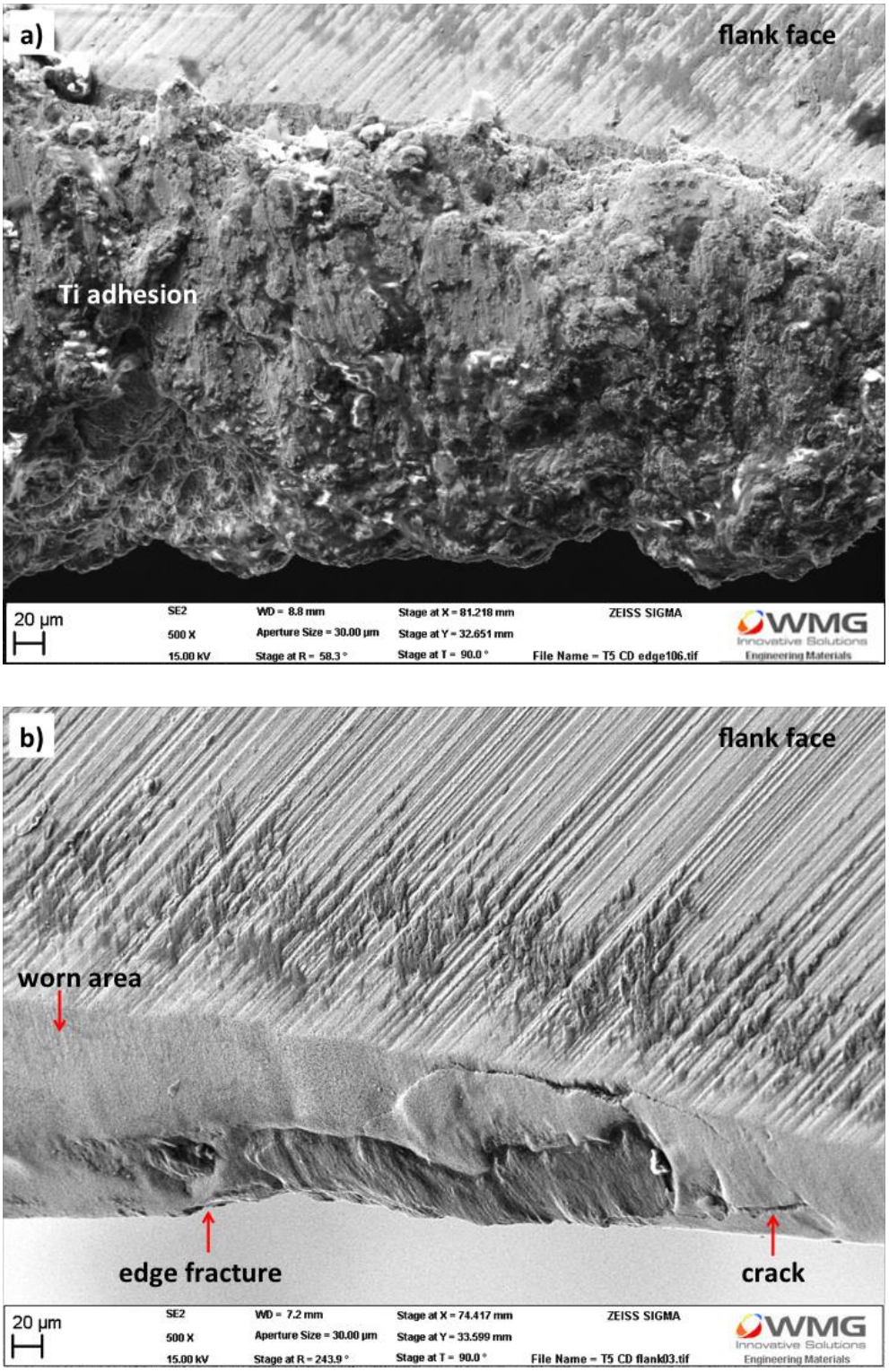

Figure 4.7: SEM micrographs showing (a) adhered Ti on the cutting edge after one-shot drilling of 80 holes in CFRP/Ti stacks using a cutting speed of 50 m/min and feed rate of 0.05 mm/rev, (b) condition of the cutting edge after removal of the adherent Ti by drilling through a hole in CFRP

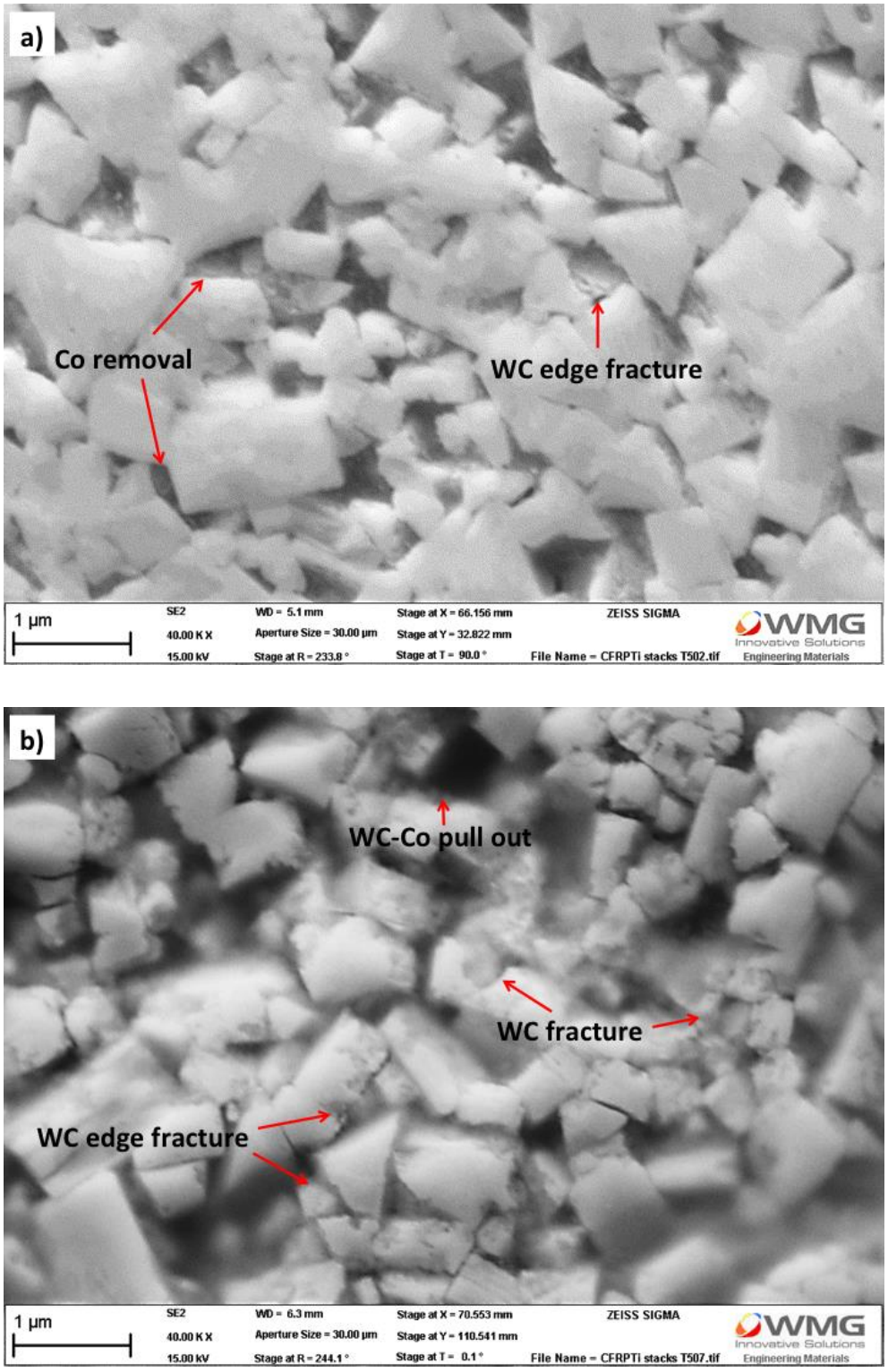

Figure 4.8: SEM micrographs of (a) the worn cutting edge showing Co binder removal and WC edge fracture (b) the fractured cutting edge showing fractured WC grains and pull-out of WC-Co, due to one-shot drilling of CFRP/Ti stacks (80 holes) using a cutting speed of 50 m/min and feed rate of 0.05 mm/rev

Previous studies [37, 41, 45, 137], which investigated tool wear when drilling CFRP/Ti stacks in one-shot did not use uniform cutting parameters, instead, the cutting speed and feed rate were changed accordingly when drilling CFRP and Ti of the stacks. Also, no previous work has reported if one-shot drilling of CFRP/Ti stacks using uniform / compromised cutting parameters would cause more rapid tool failure than drilling the materials individually. The current study has highlighted that the rapid wear and failure of reground / uncoated cutting edges of carbide (WC-Co) drills when one-shot drilling of CFRP/Ti stacks compared to drilling CFRP-only and Ti-only was due to the combination of abrasive wear and severe Ti adhesion on the cutting edges (as observed in Figures 4.7 and 4.8, and explained in the previous paragraph, page 107).

Abrasion and adhesion are regarded as two opposing mechanisms, in which abrasive wear means the tool materials are scrapped and removed. Whereas, adhesion between the cutting edge and Ti chip means an additional volume of material on the cutting edge. The adherent Ti was not considered as tool wear, however, it was the reason for cutting edge fragmentation when the strongly adhered Ti on the tool substrate (WC-Co) detached.

Whilst drilling Ti-only caused the least Ti chips adhesion, one-shot drilling of CFRP/Ti stacks resulted in the largest volume of Ti chip adhesion along the whole cutting edges, due to the fact that Ti workpiece was drilled instantaneously after the cutting edges being abraded by drilling CFRP. It is possible that the carbon fibres abraded the cutting edges and removed the oxide layer and the adhered Ti chips, exposing the nascent and clean surface of the tool substrate, which was the reason for strong Ti adhesion as there was no barrier between the contact surfaces.

4.1.1.4 Drilling CFRP and Ti separately and drilling CFRP/Ti stacks in two-shots

To confirm that the substantial Ti chip adhesion occurred during one-shot drilling of CFRP/Ti stacks was due to the abrasion / removal of the oxide layer on the cutting edges by carbon fibres, experiments involving drilling of CFRP and Ti separately and alternately were conducted. Drilling the CFRP and Ti alternately in this way exposed the cutting edges to oxygen in the air between drilling CFRP and Ti, allowing the formation of the oxide film which has been reported to be 1 – 10 nm thick [55], on the abraded tool surface. The oxide film forms instantaneously (within microseconds) on all metallic surfaces except noble metals and acts as a protective layer that restricts true contact and hence adhesion between surfaces [55, 162].

Figure 4.9 shows cutting edge condition at the end of drilling trials of CFRP and Ti separately and alternately. The adhered Ti on the cutting edges after drilling CFRP and Ti separately was significantly reduced compared to the case of one-shot drilling of CFRP/Ti stacks, Figures 4.3 and 4.9 (a). In addition, the adhered Ti on the cutting edges exhibited a uniform surface finish, Figure 4.9 (a).

Following removal of the adhered Ti, no visible cutting edge fracture was found, Figure 4.9 (b), unlike the case of drilling CFRP/Ti in one-shot. This may suggest that the Ti adhesion was not strong enough to cause cutting edge fracture as the adhered Ti detached. Instead, cutting edge rounding and uniform wear is apparent, Figure 4.9 (b), indicative of a gradual wear rate by an abrasive wear mechanism, which was the reason for observing lower flank wear than the case of one-shot drilling of CFRP/Ti stacks, Figure 4.1 and Table 4.1.

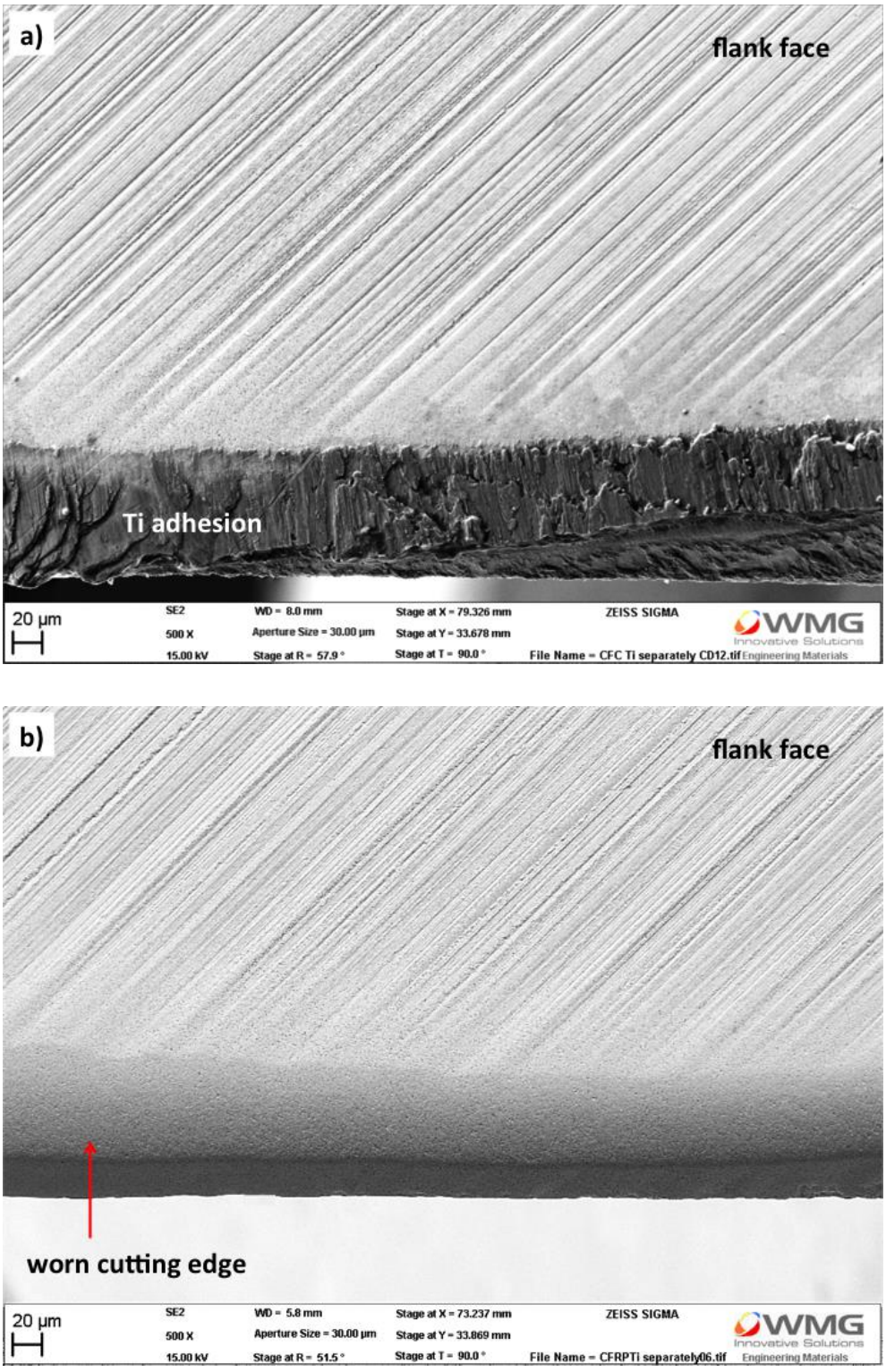

Figure 4.9: SEM micrographs of cutting edge condition at the end of drilling trials of CFRP and Ti separately and alternately using a cutting speed of 50 m/min and feed rate of 0.05 mm/rev, showing (a) uniform surface finish of adhered Ti on the cutting edges (b) worn cutting edge after removal of the adhered Ti

Further SEM investigation on the worn cutting edges revealed voids (width of 0.1 – 0.5 µm) between WC grains indicative of removal of Co binder, Figure 4.10, which resembled the wear mechanism of drilling CFRP-only. The micro-fracture of the exposed WC grains was also observed.

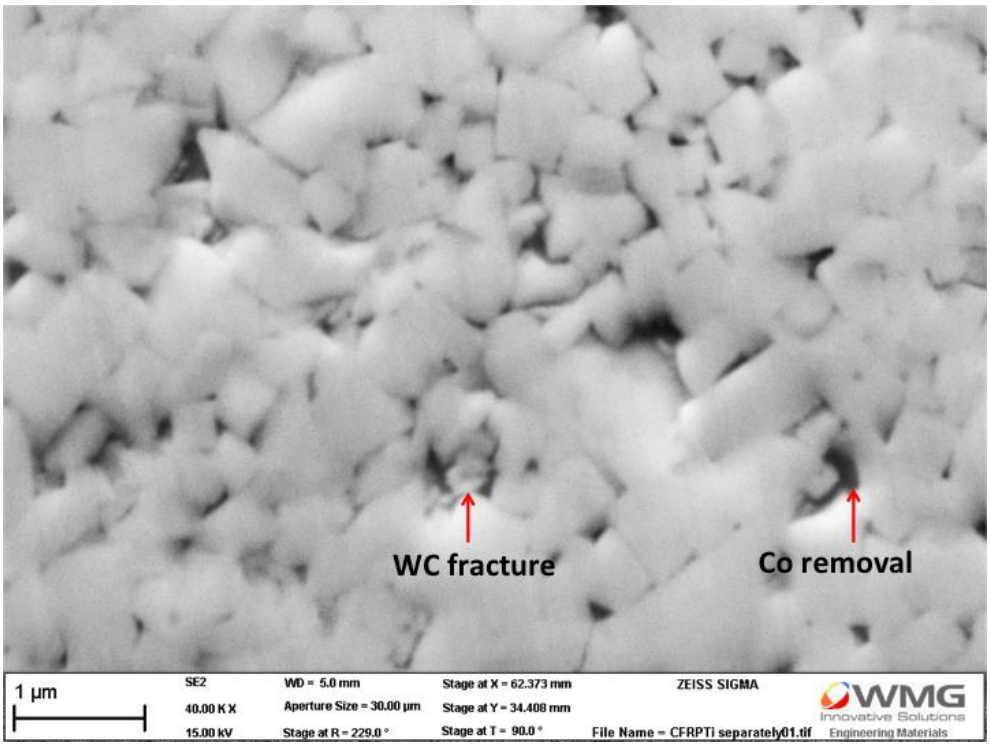

Figure 4.10: SEM micrograph of the cutting edge after drilling through CFRP and Ti separately and alternately, which details removal of the cobalt and fractured carbide grains

An interesting finding is that the tool wear at the end of drilling trials (after 80 holes) of CFRP and Ti separately was 27% lower than the case of drilling CFRP-only, Figure 4.1. The minimal adhered Ti chip observed when drilling CFRP and Ti separately was regarded to be beneficial to protect the cutting edges. This was due to the fact that the CFRP abraded and removed the adhered Ti first before abrading the cutting edges, hence causing less wear, compared to the case of drilling CFRP-only (where there was no adhered Ti to protect the cutting edge).

Since all materials, cutting parameters and cutting tool were fixed, the less Ti adhesion and wear when drilling the CFRP and Ti separately was attributed to the separation of

the drill from the workpiece after drilling the CFRP, before rapidly proceeding with drilling Ti. This allowed the formation of oxide film on the cutting edge after drilling CFRP and before drilling Ti. Hence, the results suggest that Ti adhesion and adhesive wear during drilling CFRP/Ti stacks using uncoated cutting edges can be reduced when the drill is disengaged or separated from the workpiece between drilling the CFRP and Ti. To confirm this, two-shots drilling of CFRP/Ti stacks was conducted. This was done by rapidly retreating the drill out of the hole and into the atmospheric air once the CFRP was drilled, before rapidly proceeding with drilling the Ti, Figure 3.28 (c). Earlier tribology studies [163] reported that the oxide film on the metallic surfaces forms instantly (microseconds, less than 1 second) in the presence of oxygen. Hence, rapidly retracting the drill (3 seconds) between drilling CFRP and Ti was sufficient to assure the formation of the oxide film on the cutting edges.

Figure 4.11 (a) shows the adhered Ti on the cutting edges at the end of two-shots drilling of CFRP/Ti stacks (after 80 holes), which exhibited a more uniform surface finish compared to the case of one-shot drilling of CFRP/Ti stacks, Figure 4.7 (a). At the end of the tests, the volume of the adherent Ti on the cutting edges used for two-shots drilling of CFRP/Ti stacks was significantly reduced (Figure 4.3), and the flank wear was 28% lower than the case of one-shot drilling of CFRP/Ti stacks, Figure 4.1 and Table 4.1. Nevertheless, further SEM investigation of the cutting edges used for two-shots drilling of CFRP/Ti stacks after removal of the adhered Ti revealed cutting edge fracture, Figure 4.11 (b). Figure 4.12 (a) shows evidence of Co binder removal between WC grains as well as fractured edge of WC grains at the worn cutting edge. Figure 4.12 (b) is a magnified view of the cutting edge fracture, which revealed uneven surface finish of WC grains exhibiting fracture. These observations (Figures 4.11 and 4.12) indicated a combination of abrasive and adhesive wear mechanisms during two-shots drilling of CFRP/Ti stacks.

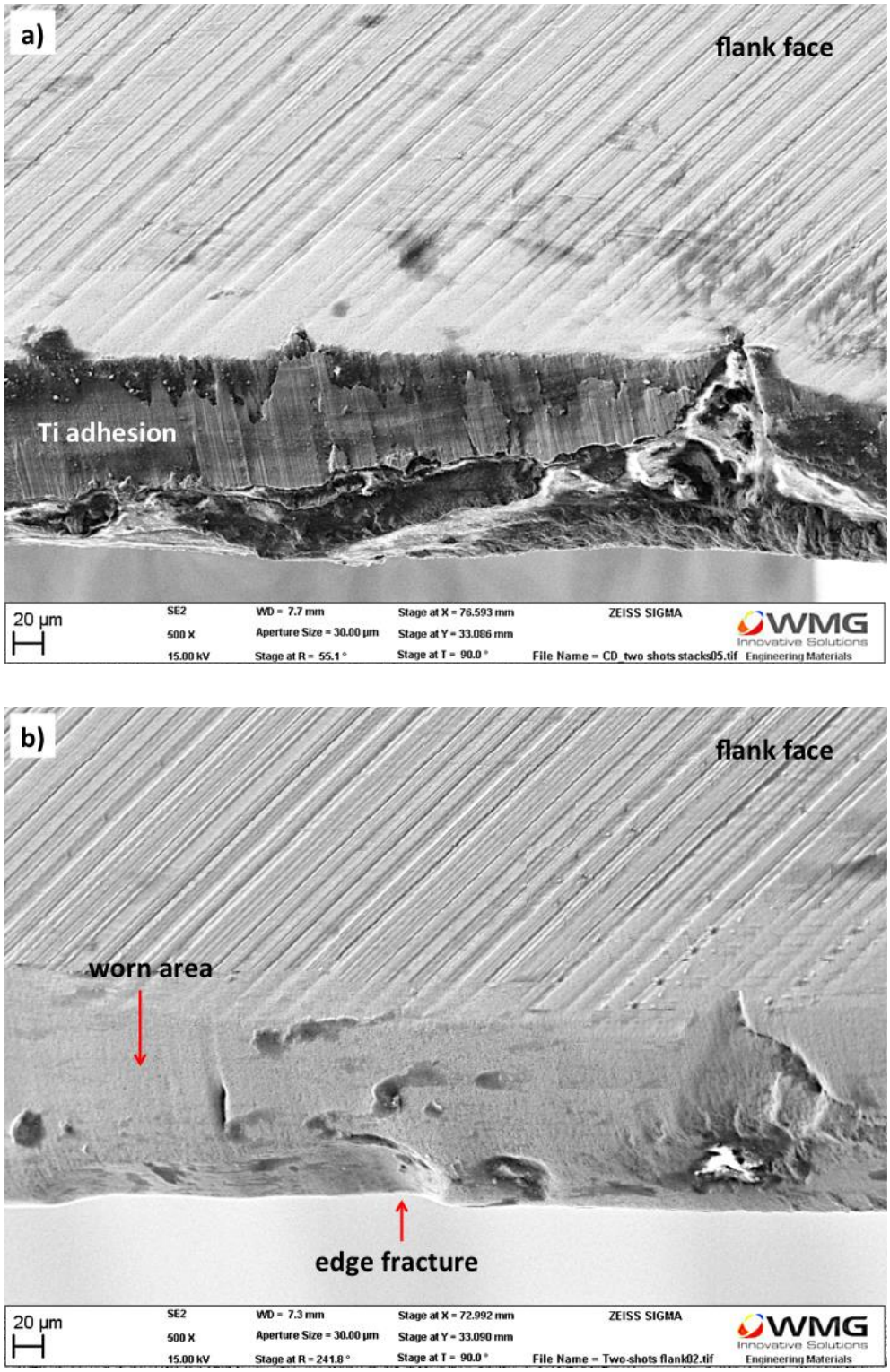

Figure 4.11: SEM micrographs showing (a) adhered Ti on the cutting edge after two-shots drilling of 80 holes in CFRP/Ti stacks using a cutting speed of 50 m/min and feed rate of 0.05 mm/rev, and (b) condition of the cutting edge after removal of the adherent Ti by drilling through a hole in CFRP

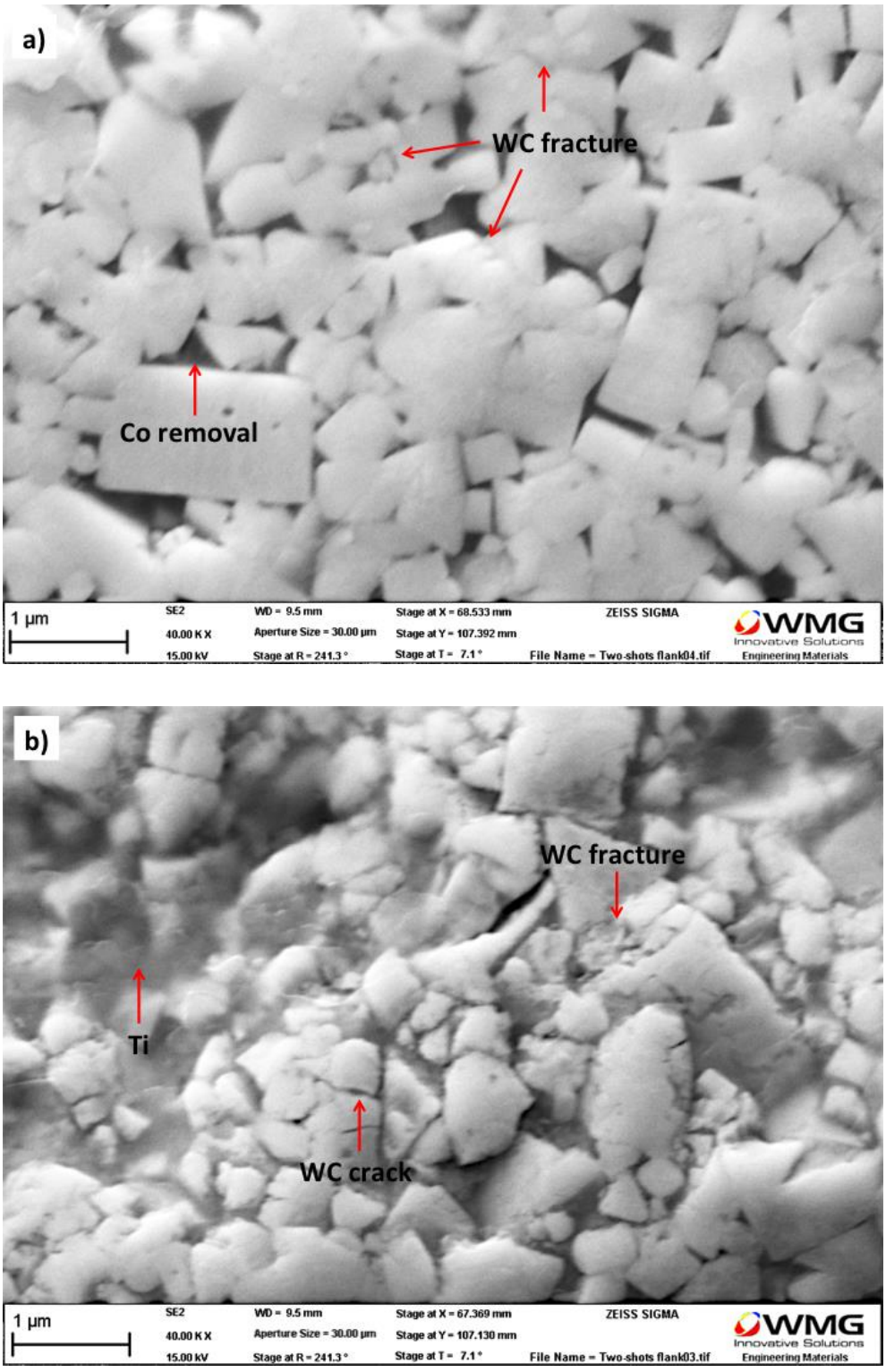

Figure 4.12: SEM micrographs showing condition of the cutting edge after drilling through CFRP/Ti stacks in two-shots, following removal of adhered Ti, which details (a) Co removal and fractured WC grains at the worn area (b) crack and fractured WC grains at the fractured cutting edge

Despite employing similar CFRP and Ti configurations, cutting parameters, and cutting fluid, it is interesting to note that the way the materials were drilled is important in determining the amount of Ti chips adhering to the cutting edges and tool wear. This is a novel finding which has not been previously reported in the literature. It was demonstrated that the Co binder of the tool was more susceptible to abrasion by the CFRP. Also, the cobalt is more likely to adhere with the titanium chip, which resulted in its removal from the cutting edges.

A cemented carbide drill with a lower cobalt content is recommended when drilling CFRP and Ti6Al4V to reduce the tendency of having large voids between WC grains (due to Co binder removal), and hence reducing fracture of the exposed WC grains. Even though two-shots drilling of CFRP/Ti stacks was found to cause less Ti chips adhering on the cutting edges and longer tool life compared to the one-shot drilling of CFRP/Ti stacks, it must be noted that the technique required three times longer drilling time, which leads to a reduction in productivity.

4.1.2 Thrust force

Figure 4.13 shows that for all tests, thrust forces generated when drilling CFRP were within 120 to 430 N, which is three to five times lower than the thrust forces generated when drilling Ti (within the range of 550 to 1330 N). The observation of three to five times lower thrust forces when drilling CFRP compared to those of drilling Ti is consistent with the previous finding [37], which was attributed to the difference in the cutting mechanisms of the materials. CFRP was deformed by brittle fracture, hence required lower forces compared to plastic deformation when drilling Ti [6, 32].

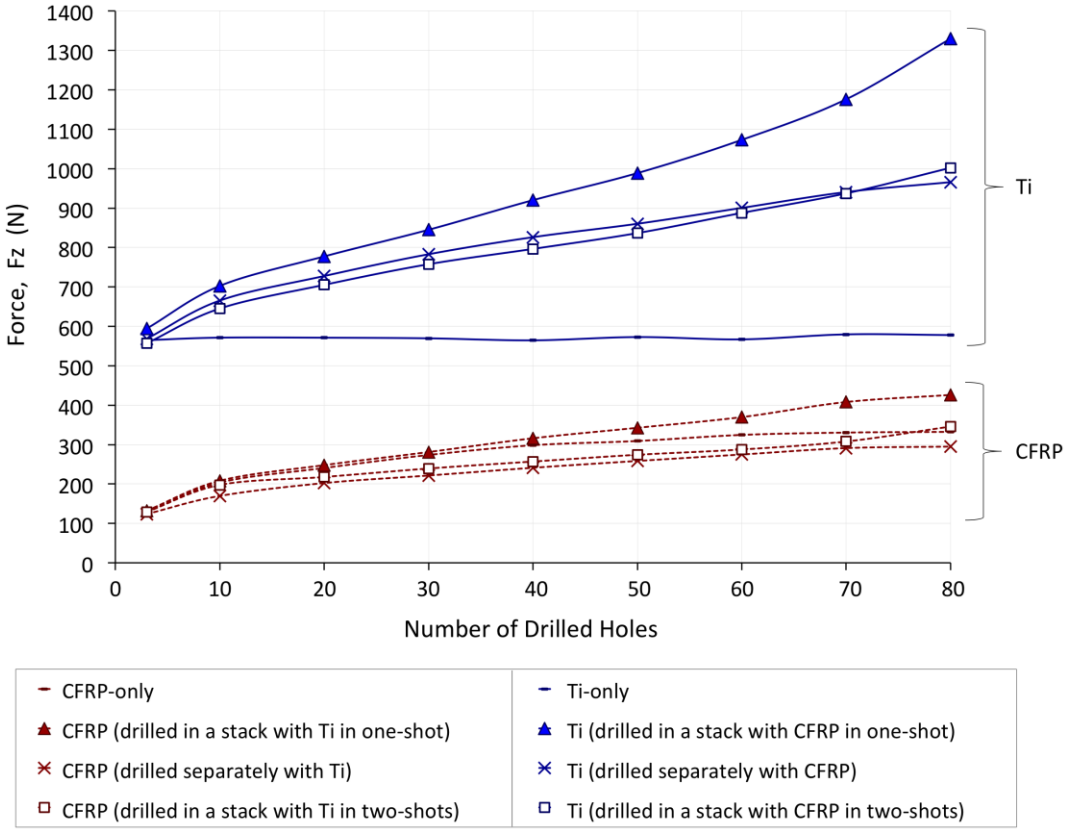

Figure 4.13: Comparison of average thrust forces when drilling (a) CFRP-only, (b) Ti-only, (c) CFRP/Ti stacks in one-shot, (d) CFRP and Ti separately, and (e) CFRP/Ti stacks in two-shots

The trend in thrust forces was observed to correspond to the trend observed in flank wear. For the 80th holes, drilling CFRP in a stack with Ti in one-shot generated the highest thrust force of 430 N, Figure 4.13, which is:

- 20% higher than drilling CFRP in the stack with Ti in two-shots,
- 26% higher than drilling CFRP-only,
- 44% higher than drilling CFRP separately with Ti.

Similarly, drilling Ti in a stack with CFRP in one-shot also generated the highest thrust forces of 1330 N, Figure 4.13, which is:

- 33% higher than drilling Ti in the stack with CFRP in two-shots,
- 38% higher than drilling Ti separately with CFRP,
- 130% higher than drilling Ti-only.

4.1.3 Hole quality

The hole quality in CFRP/Ti stacks produced by one-shot drilling was analysed with respect to how it related to the case of drilling the materials individually, drilling CFRP and Ti together but separately, and two-shots drilling of CFRP/Ti stacks, based on following criteria:

(i) accuracy and consistency of diameter between the holes in CFRP and Ti in stacks

(ii) the extent of CFRP entrance delamination

(iii) fibre pull-out from the bore machined surface of CFRP

(iv) Ti burr height

4.1.3.1 Hole diameter

A comparison of hole diameter in CFRP and Ti when drilled in stacks, individually and together (but separately) is shown in Figures 4.14 and 4.15. For one-shot drilling of CFRP/Ti stacks, initially (holes 1 – 10), the hole diameters in both CFRP and Ti were closer to the drill nominal diameter (6.100 mm) within 6.103 – 6.107 mm. However, as the hole number increased (holes 20 – 80), the hole diameters increased to 6.107 – 6.114 mm. This observation is consistent with the observation of increasing tool wear and Ti chips adhering on the cutting edges as the number of holes increased during one shot drilling of CFRP/Ti stacks. This indicated that the Ti chips adhering on the cutting edges contributed to removing of more material than what was intended, hence causing oversized holes and inconsistent hole diameter. In contrast, consistent hole diameters from the beginning until the end of drilling tests were observed when drilling Ti-only and drilling Ti separately with CFRP, Figure 4.15, where the drills exhibited the least adhered Ti on the cutting edges.

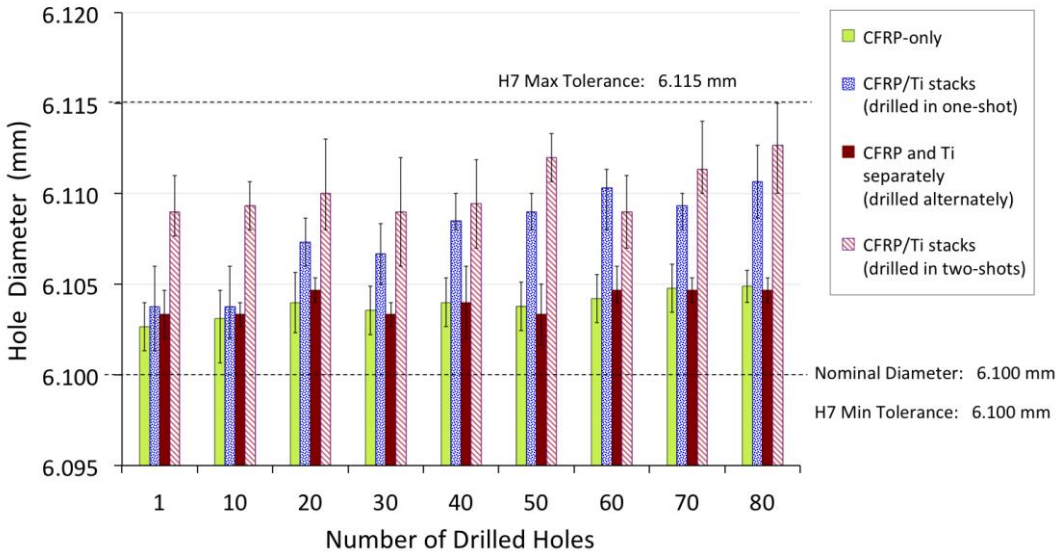

Figure 4.14: Comparison of the diameter of holes in CFRP produced when drilling CFRP-only, CFRP/Ti stacks in one-shot, CFRP and Ti separately, and CFRP/Ti stacks in two-shots

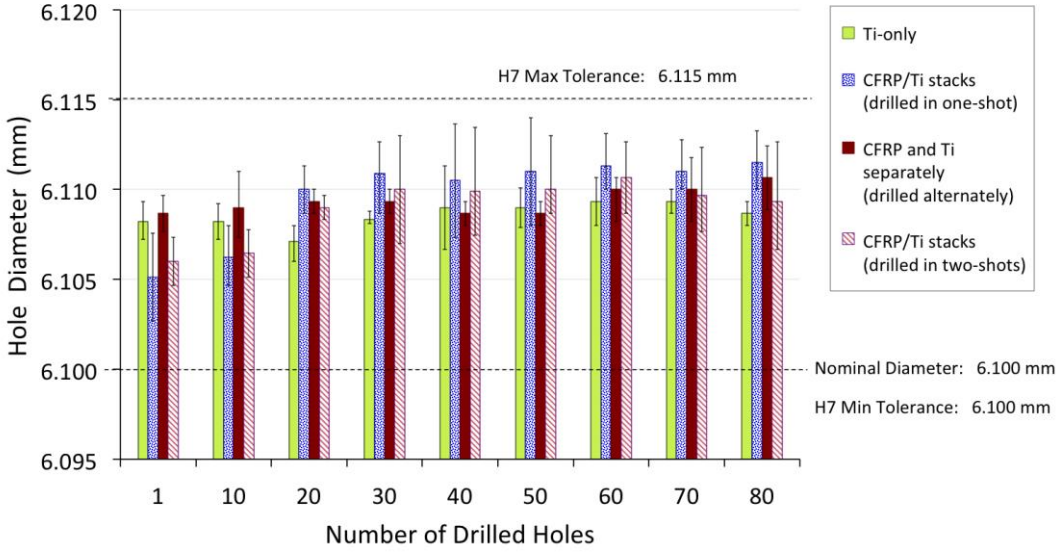

Figure 4.15: Comparison of the diameter of holes in Ti produced when drilling Ti-only, CFRP/Ti stacks in one-shot, CFRP and Ti separately, and CFRP/Ti stacks in two-shots

Interestingly for one-shot and two-shots drilling of CFRP/Ti stacks, when tool wear and Ti adhesion were minimal (holes 1 – 10), the diameters of the holes in Ti were 3 – 6 µm smaller than the case of drilling Ti individually and separately with CFRP, Figure 4.15. Previous work in the literature [104] also reported oversized holes when drilling Ti individually. The result in the current study suggests that when drilling CFRP/Ti stacks (one-shot and two-shots), the presence of CFRP assisted in guiding the drill, which

reduced drill wandering when drilling the Ti component. As a result, more accurate hole diameters in Ti that was closer to the drill nominal diameter were produced due to the drills being supported by the CFRP workpiece when drilling the Ti workpiece.

With regards to two-shots drilling of CFRP/Ti stacks, despite exhibiting less tool wear and less Ti adhesion, the holes in CFRP were 2 – 6 µm larger than those of one-shot drilling of CFRP/Ti stacks, Figure 4.14. This indicated that the way that the CFRP was drilled has a major influence in hole diameter. Nevertheless, the hole diameters in CFRP (for both two-shots and one-shot drilling of CFRP/Ti stacks) were still within the H7 tolerance (-0.000/+0.015 mm) up to 80 holes.

4.1.3.2 CFRP delamination (hole entrance)

Figure 4.16 compares CFRP delamination, measured at the hole entrance, for all drilling tests.

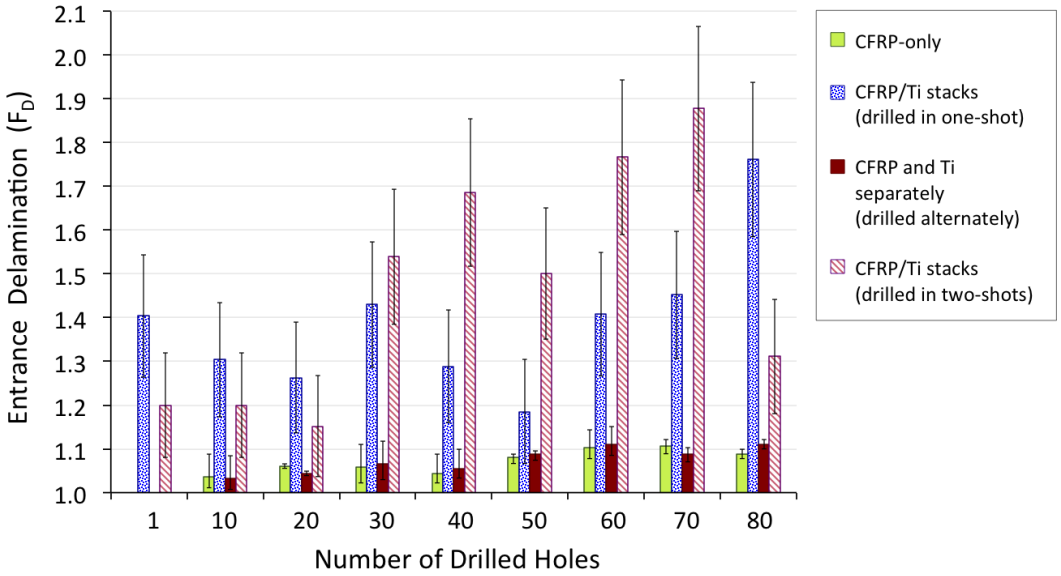

Figure 4.16: Comparison of CFRP delamination at hole entrance when drilling CFRP-only, CFRP/Ti stacks in one-shot, CFRP and Ti separately, and CFRP/Ti stacks in two-shots

When drilling CFRP-only and drilling CFRP separately with Ti, the delamination at the hole entrance increased gradually with increased hole number, tool wear and thrust force. This indicated that when drilling CFRP-only, having a drill that has a higher wear

resistance and longer tool life is important for producing more holes with less delamination. In contrast, for one shot and two-shots drilling of CFRP/Ti stacks, no distinctive trend can be deduced with respect to increasing hole number and tool wear since the CFRP entrance delamination was observed to fluctuate unpredictably from the first until 80th holes, Figure 4.16.

One-shot and two-shots drilling of CFRP/Ti stacks resulted in 22% – 62% larger CFRP entrance delamination than the case of drilling CFRP-only and drilling CFRP and Ti separately, from the beginning until the end of test. The observation of CFRP entrance delamination when drilling CFRP/Ti stacks did not correlate with the observation of tool wear and thrust force. This suggests that CFRP entrance delamination during drilling CFRP/Ti stacks was not mainly governed by tool wear and thrust force. Thus, the results indicated that CFRP delamination when drilling CFRP/Ti stacks could not be reduced simply by using a drill that has a higher wear resistance and longer tool life.

A possible explanation for fluctuation and larger CFRP entrance delamination when drilling CFRP/Ti stacks was due to Ti chips evacuating through the CFRP workpiece and whirling (entangling and moving around the drill) on the CFRP surface. It may be argued that drilling CFRP/Ti stacks with the cutting edges having adherent Ti was the reason for damaging the CFRP layers. However, as shown in Figure 4.16, for one-shot and two-shots drilling of CFRP/Ti stacks, there were substantial CFRP entrance delamination (F_D = 1.4 and F_D = 1.2) as early as the first holes. In contrast, no CFRP entrance delamination (F_D = 1.0) was observed when drilling the first holes in CFRP-only and when drilling CFRP and Ti separately (where there was no Ti chip evacuating through the CFRP); and the CFRP entrance delamination were minimal (less than F_D 1.15) until 80th holes, Figure 4.16. Both one shot and two-shots drilling of CFRP/Ti stacks produced no distinctive difference in the amount of CFRP entrance delamination since both drilling techniques were affected by the Ti chips. The Ti chips

entangling around the drill after drilling CFRP/Ti stacks is shown in Figure 4.17, which damaging the CFRP as it rotated (together with the drill) on the surface. It is difficult to predict and control the whirling of the entangled Ti chips.

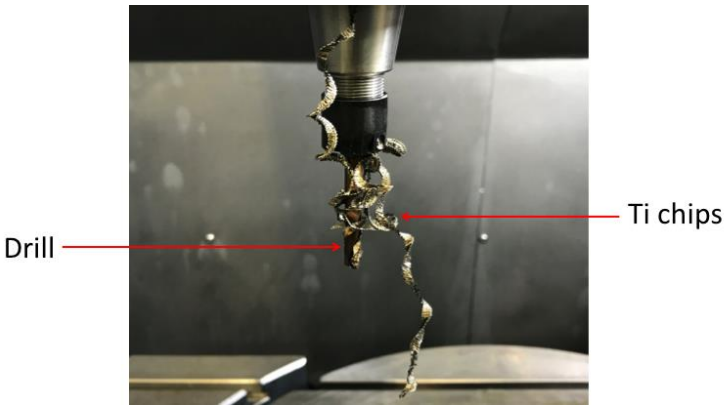

Figure 4.17: Ti chip entangling around the drill (diameter = 6.1 mm) when drilling CFRP/Ti stacks

In any drilling operation involving metallic materials, smooth chip evacuation is important since the metallic chips jamming inside the holes could cause drill breakage [159]. In the case of drilling CFRP/Ti stacks, this work provided evidence that the Ti chip was more detrimental to the CFRP counterpart in stacks after the Ti chips evacuating from the holes. It could be suggested that instead of drilling the stacks from CFRP to Ti, the stacks should be drilled from Ti to CFRP to avoid Ti chips evacuating through the CFRP layers, which may reduce the tendency of Ti chips damaging the CFRP. This means making the Ti workpiece as the hole entrance, and CFRP as the hole exit. However, this approach could actually cause more CFRP delamination (at the hole exit), not due to Ti chips but due to there is no backing support to withstand the thrust forces. Xu *et al*. [102] have shown that drilling CFRP/Ti stacks from Ti to CFRP caused 8% more CFRP delamination (hole exit) compared to the case of drilling from CFRP to Ti (when using a similar range of cutting parameter as in the current study). Hence, drilling the stacks from CFRP to Ti is regarded as a better approach as the Ti workpiece can act as a support for the CFRP workpiece. Furthermore, in practice, when manufacturing an aircraft, it is difficult to drill from the Ti airframe to the CFRP outer skin (which is from the inside out).

4.1.3.3 CFRP pull-out from machined surface

Figures 4.18 and 4.19 show the cross sections of the 1st holes (minimal tool wear) and 20th holes (increased tool wear) in CFRP, revealing the morphology and topography of the machined CFRP surfaces when drilled (a, b) individually, (c, d) in a stack with Ti in one-shot, (e, f) separately with Ti, and (g, h) in a stack with Ti in two-shots. The regions below the machined surface (or reference surface: green zone) are indicated by the blue colour, and represent voids and cavities as a result of the CFRP materials being pulled-out from the surface during the drilling.

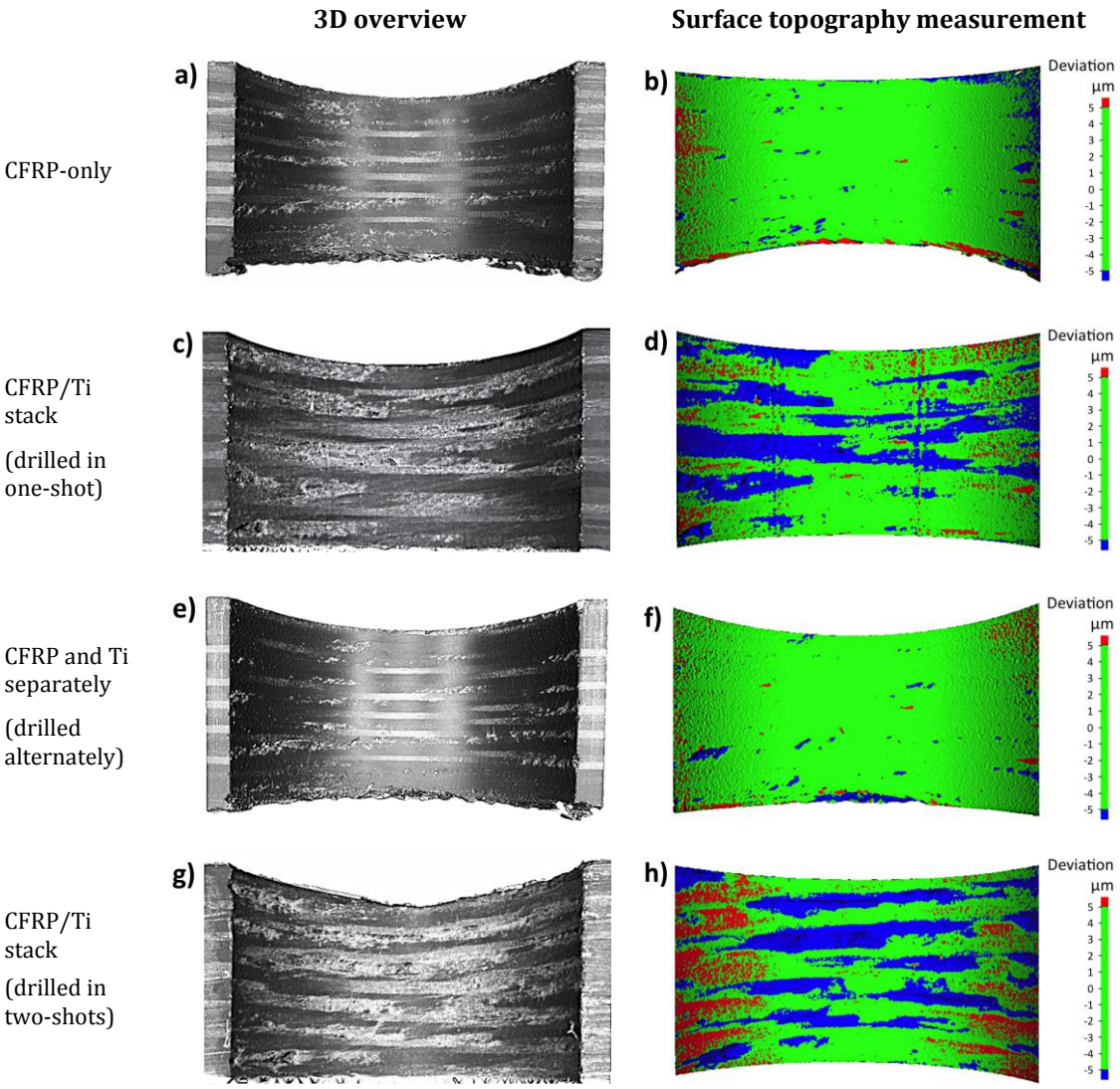

Figure 4.18: Topography of the machined CFRP surfaces when drilling (a, b) CFRP-only, (c, d) CFRP/Ti stacks in one-shot, (e, f) CFRP and Ti separately, (g, h) CFRP/Ti stacks in two-shots – cross section of the 1st holes scanned by 3D microscope Alicona

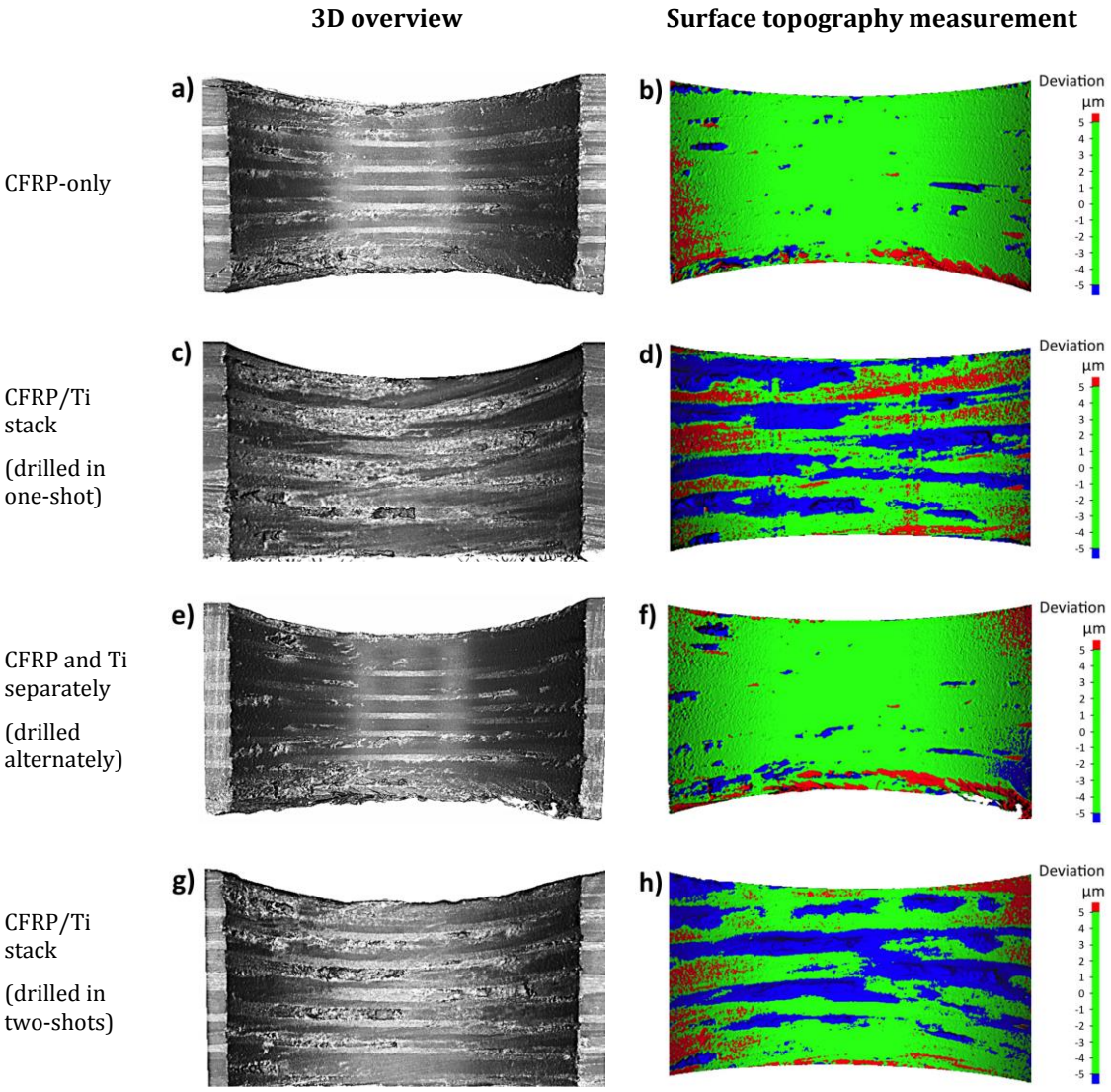

Figure 4.19: Topography of the machined CFRP surfaces when drilling (a, b) CFRP-only, (c, d) CFRP/Ti stacks in one-shot, (e, f) CFRP and Ti separately, (g, h) CFRP/Ti stacks in two-shots – cross section of the 20th holes scanned by 3D microscope Alicona

The volume of CFRP pull-out from the machined surfaces was measured using 3D image analysis software (Alicona) and compared in Figure 4.20. Comparison between the machined surface finish of CFRP and carbon fibre being pulled-out when drilled individually and in stacks with Ti has not been shown in the previous literature. In this research, by quantifying the volume of carbon fibre pull-out, it was shown that drilling CFRP/Ti stacks (in one-shot and two-shots) caused 170% – 530% more CFRP pull-out compared to the case of drilling CFRP-only and drilling CFRP and Ti separately, Figures 4.18, 4.19 and 4.20.

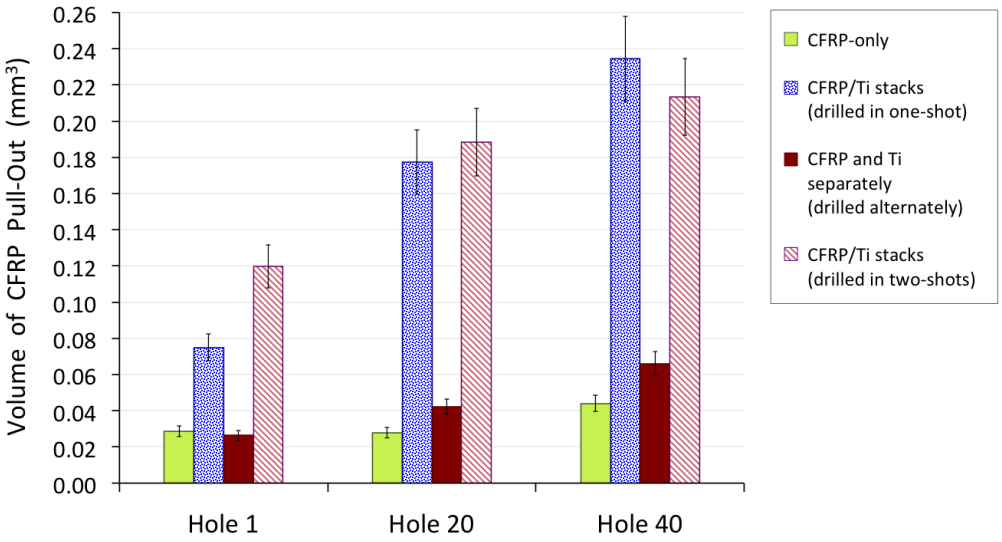

Figure 4.20: Comparison of the volume of CFRP pull-out from the machined surfaces when drilling CFRP-only, CFRP/Ti stacks in one-shot, CFRP and Ti separately, and CFRP/Ti stacks in two-shots

It is reasonable that the substantial CFRP pull-out when drilling CFRP/Ti stacks was predominantly affected by Ti chips that flowed against and rubbed the machined surface of CFRP. When drilling CFRP and Ti separately, the CFRP machined surface morphology resembled the case of drilling CFRP-only, Figures 4.18 (a, b, e, f) and 4.19 (a, b, e, f). This was due to the fact that when drilling CFRP and Ti separately, the CFRP machined surfaces were not affected by the Ti chip evacuation since the Ti chips did not flow through the CFRP workpiece.

When tool wear was minimal (hole 1) and in the absence of Ti chip flowed through the CFRP workpiece as in the case of drilling CFRP-only and drilling CFRP and Ti separately, the volume of CFRP pull out was minimal (0.021 – 0.025 mm^3), Figures 4.18 (a, b, e, f) and 4.20. With increasing tool wear (holes 20 and 40), minimal CFRP pull out was consistently observed when drilling CFRP-only and CFRP and Ti separately, Figures 4.19 (a, b, e, f), and 4.20, due to the absence of Ti chip, compared to the case of drilling CFRP/Ti stacks, Figures 4.19 (c, d, g, h) and 4.20. Both one-shot and two-shots drilling of CFRP/Ti stacks exhibited no marked difference in the volume of CFRP

pull-out as seen in Figures 4.18 (c, d, g, h), 4.19 (c, d, g, h) and 4.20, which were attributed to the Ti chips flowing through the CFRP workpiece.

4.1.3.4 Titanium burr (hole exit)

Figure 4.21 compares the Ti burr height caused by all drilling tests. One-shot drilling of CFRP/Ti stacks produced the highest Ti burr. At the end of drilling tests (holes 80), the Ti burr height caused by one-shot drilling of CFRP/Ti stacks was 30%, 220% and 720% respectively higher than those of two-shots drilling of CFRP/Ti stacks, drilling CFRP and Ti separately, and drilling Ti-only.

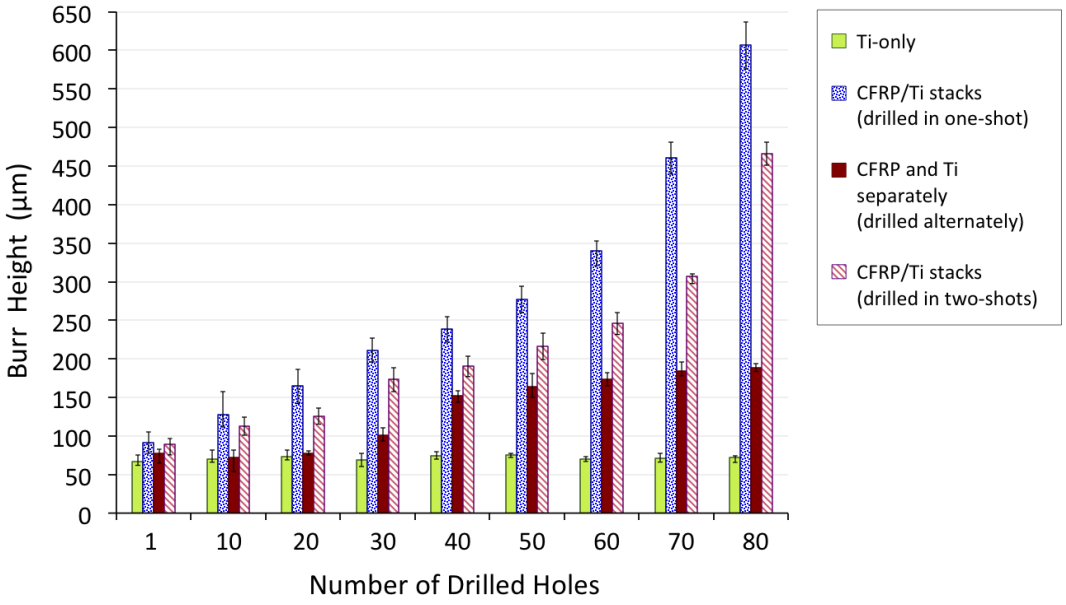

Figure 4.21: Comparison of Ti burr height produced when drilling Ti-only, CFRP/Ti stacks in one-shot, CFRP and Ti separately and CFRP/Ti stacks in two-shots

The result of Ti burr height progression, Figure 4.21, is consistent with the result of tool wear, Figure 4.1. This indicated that the increase in Ti burr height at hole exit was affected by the increase in tool wear. The least and consistently minimal Ti burr height (65 – 70 µm) was observed when drilling Ti-only, which is in agreement with the observation of the minimal tool wear from the beginning until the end of the drilling tests, Figure 4.21. It is suggested that using a drill that has a higher wear resistance and longer tool life is important to minimise the Ti burr height. However, in this study, the

fact that there were Ti burr with the height of 65 – 90 µm at as early as the first 10 holes (when tool wear was minimal) suggests that the drilling strategy and the cutting parameters employed was not optimum for resisting burr formation. In order to achieve a good quality of drilled holes in CFRP/Ti stacks, eliminating Ti burr is important. Therefore, following studies (Sections 4.2.4.5 and 4.3.4.5) investigated the influence of cutting parameters and drilling operations (CD or UAD) on the burr formation.

4.1.4 Conclusions from Study 1

In summary, the interaction of wear mechanisms and hole quality when drilling CFRP/Ti stacks were studied referring to the case of drilling the constituent materials individually and drilling the materials separately to determine the factors which govern tool wear and hole quality in CFRP/Ti stacks. With regard to one-shot drilling of CFRP/Ti stacks, no reported work in the literature was found on the association of cutting edges condition and hole quality. Previous studies involving drilling CFRP/Ti stacks often reported the aspects of tool wear and hole quality separately.

It was established in this study that the interaction between two different wear mechanisms (abrasive and adhesive) during one-shot drilling of CFRP/Ti stacks caused strong Ti chip adhesion on the cutting edges. This is because Ti chips adhere strongly to the nascent and abraded surface compared to a non-abraded surface. Consequently, the drill used for drilling CFRP/Ti stacks failed rapidly due to substantial cutting edge fracture as the adhered Ti detached. Tool wear when one-shot drilling of CFRP/Ti stacks was 90% and 1038% higher than the case of drilling CFRP-only and Ti-only, respectively. This indicates less productivity when drilling CFRP/Ti stacks compared to drilling CFRP-only and Ti-only.

The severe Ti adhesion on the cutting edges when drilling CFRP/Ti stacks produced oversized holes. Drilling CFRP/Ti stacks (both in one-shot and two-shots) caused 22% – 62% more CFRP delamination, and 170% – 530% more CFRP pull-out from the machined surfaces compared to the case of drilling CFRP individually. The CFRP damage when drilling CFRP/Ti stacks was found to be mainly caused by Ti chips evacuating through the CFRP workpiece, rather than by tool wear. Whereas, Ti burr formation was found to be largely affected by tool wear, i.e. Ti burr height increases with an increase in tool wear.

This study has shown that the key to achieving long tool life and improved hole quality when drilling CFRP/Ti stacks is minimising the Ti adhesion on the cutting edges and improving Ti chips evacuation. Titanium chip adhesion on the cutting edges was reduced, and the drill wore gradually and uniformly by abrasive wear when drilling CFRP and Ti separately, however, this is not the solution as the materials need to be drilled in stacks for the purpose of mechanical assembly.

Even though two-shots drilling of CFRP/Ti stacks was found to cause less Ti adhesion on the cutting edges and longer tool life, the technique produced oversized holes in CFRP and did not substantially improve the hole quality. In addition, it required three times longer drilling time compared to one-shot drilling, which would lead to a reduction in productivity. Nevertheless, the result confirmed that a separation or disengagement between the cutting edges and the workpiece when drilling CFRP/Ti stacks can reduce Ti chip adhesion and hence reduce tool wear.

Further understanding to reduce Ti adhesion and tool wear during one-shot drilling of CFRP/Ti stacks is necessary. Hence, the following studies, Sections 4.2 and 4.3 investigated the effect of cutting parameters (cutting speed and feed rate) and drilling operations (Conventional Drilling (CD) and Ultrasonic Assisted Drilling (UAD)) on tool

wear, Ti chip formation, thereby their influence on hole quality. It was reported in the literature that UAD might cause disengagement and separation between the cutting edges and the workpiece, which may be favourable for reducing Ti chip adhesion to the cutting edges and improving Ti chip evacuation. However, research has not been reported for UAD of CFRP/Ti stacks (except the author's publications).

4.2 Study 2: The effect of cutting speed during CD and UAD of CFRP/Ti stacks

This study was designed to investigate the effect of varying cutting speed (25, 50 and 75 m/min) at a constant feed rate of 0.05 mm/rev using reground cemented carbide (WC-Co) drills during Conventional Drilling (CD) and Ultrasonic Assisted Drilling (UAD) of CFRP/Ti stacks in one-shot on tool wear and hole quality. This study aimed to provide an understanding of the correlation between drilling operations (CD or UAD), cutting speeds, tool wear mechanisms, tool life and hole quality.

4.2.1 Tool wear mechanisms

Figure 4.22 shows that CD and UAD of CFRP/Ti stacks using the slowest cutting speed of 25 m/min resulted in the lowest flank wear, hence the longest tool life of 160 holes (extrapolated). Whereas, using the highest cutting speed of 75 m/min resulted in the highest flank wear, hence the shortest tool life of 35 holes.

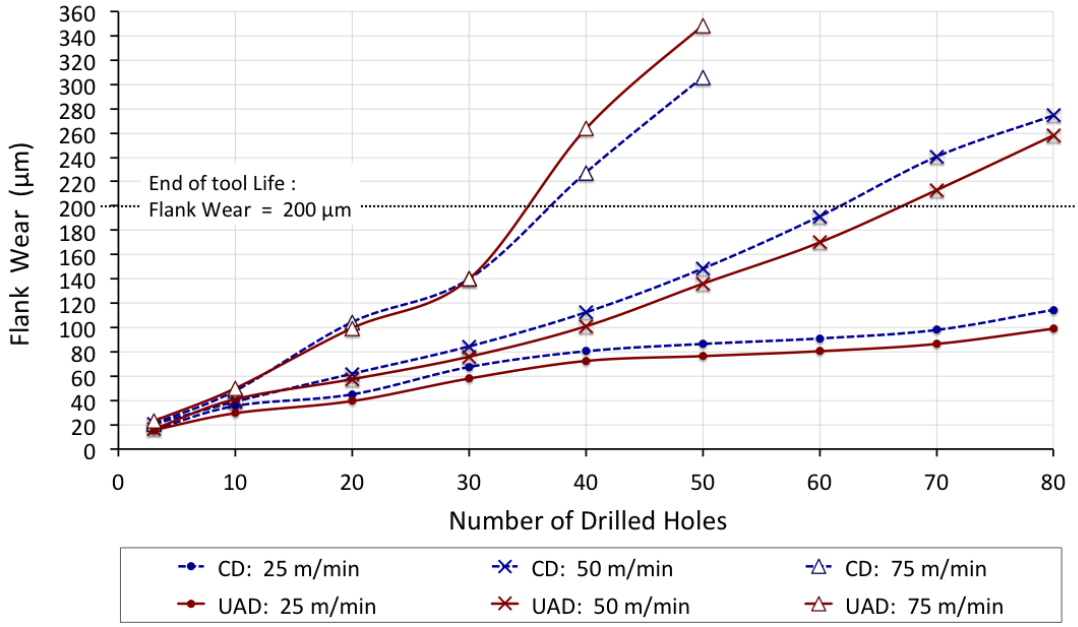

Figure 4.22: Comparison of flank wear during CD and UAD of CFRP/Ti stacks using cutting speeds of 25, 50 and 75 m/min at a constant feed rate of 0.05 mm/rev

Statistical analysis using a two-way ANOVA confirmed that the difference between the flank wear data generated by drilling with different cutting speeds of 25, 50 and 75 m/min was statistically significant, Appendix A, Table A.1. This indicated that flank wear was significantly reduced and longer tool life was obtained by reducing cutting speed, i.e. tool wear accelerated when cutting speed was increased. This result is typical of most machining operations. Specifically, for drilling CFRP and Ti in a stack, the result is consistent with previous studies [103, 132] employing a similar range of cutting speeds despite much higher feed rates (0.1 – 0.25 mm/rev), compared to the current study which employed a lower feed rate of 0.05 mm/rev.

However, it was found that within the range of cutting parameters and drills employed, the use of UAD on CFRP/Ti stacks did not provide a significant advantage in tool life. The flank wear results during UAD at each cutting speed of 25, 50 and 75 m/min were observed to replicate those of CD, Figure 4.22. Although visual examination of the graph in Figure 4.22 suggests that UAD at 25 and 50 m/min produced slightly (8%) lower wear than CD, ANOVA confirmed that the difference in the flank wear observed during CD and UAD was not statistically significant, Appendix A, Table A.1.

A comparison of cutting edge condition after CD and UAD of CFRP/Ti stacks using cutting speeds of 25, 50 and 75 m/min is shown in Figures 4.23, 4.24 and 4.25. The cutting edges of the drills used for drilling at higher cutting speeds of 50 m/min, Figure 4.24, and 75 m/min, Figure 4.25, exhibited substantial amount of Ti adhesion (the adhered material was confirmed to be Ti by EDS analysis), compared to the lower cutting speed of 25 m/min, Figure 4.23. The Ti adhesion affected the drill's wear rate (which will be discussed throughout this section). However, no marked difference in the cutting edge condition of UAD compared to CD was observed.

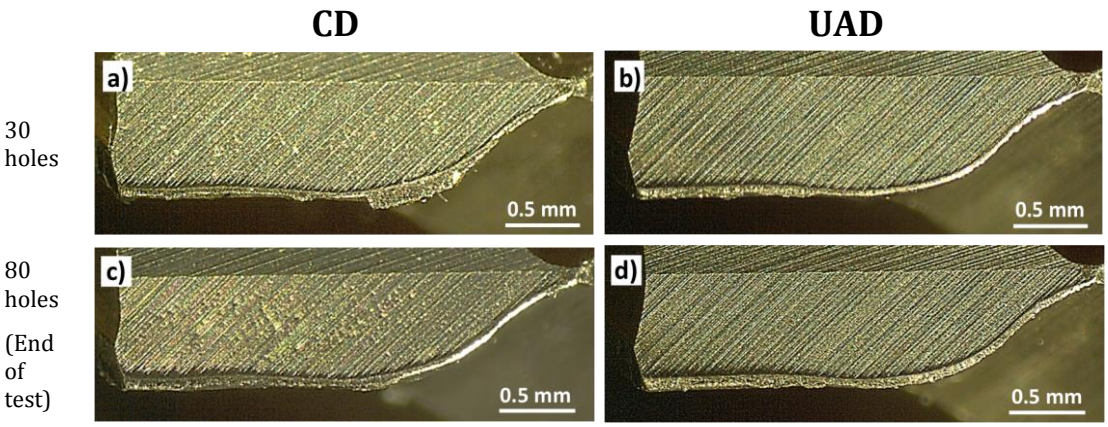

Figure 4.23: Cutting edge condition after CD and UAD of (a, b) 30 holes and (c, d) 80 holes through CFRP/Ti stacks using a cutting speed of 25 m/min and feed rate of 0.05 mm/rev

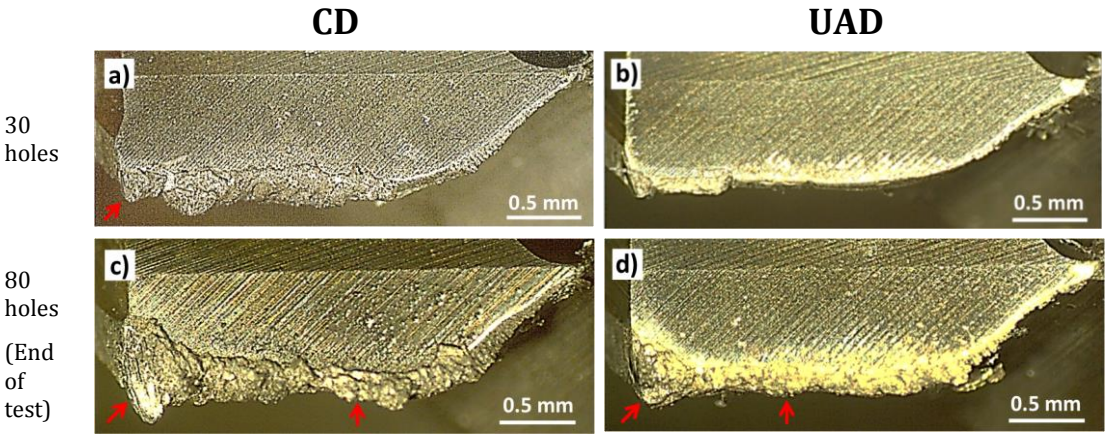

Figure 4.24: Cutting edge condition after CD and UAD of (a, b) 30 holes, and (c, d) 80 holes through CFRP/Ti stacks using a cutting speed of 50 m/min and feed rate of 0.05 mm/rev. Red arrows show Ti adhesion on the cutting edge

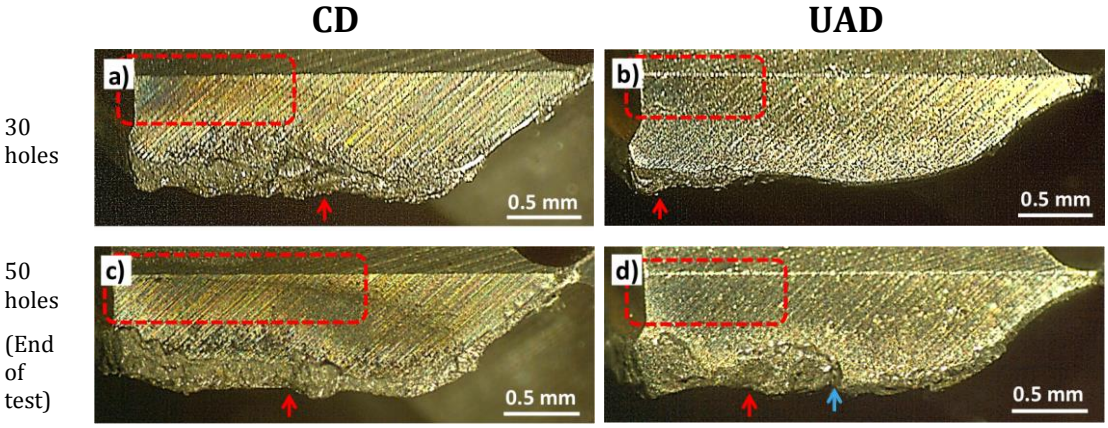

Figure 4.25: Cutting edge condition after CD and UAD after of (a, b) 30 holes, and (c, d) 50 holes through CFRP/Ti stacks using a cutting speed of 75 m/min and feed rate of 0.05 mm/rev. Red arrows show Ti adhesion on the cutting edge; blue arrows show cutting edge chipping. Dashed rectangles show discolouration of flank faces

The main factor that caused substantial adhered Ti chips and weakening of the cutting edges, thereby earlier drill failure with increasing cutting speed was greater heat generation [32]. The heat in cutting zone is generated by plastic deformation during the chip formation, at the interface of rake face/chip and flank face/machined surface. A higher cutting speed means faster tool rotation per unit time (25 m/min = 1300 RPM, 50 m/min = 2600 RPM, and 75 m/min = 3900 RPM). The amount of deformation per unit time increases as the cutting speed increases, hence causing higher temperatures as more mechanical energy is converted to heat [32].

As shown in Figure 4.25, the flank faces of drills used for CD and UAD at the highest cutting speed of 75 m/min exhibited some discolouration (as denoted by the darker colour, brownish-bluish colour in the red boxes). The discolouration was not seen on the drills used during CD and UAD with the lowest cutting speed of 25 m/min, Figure 4.23. Hence, this observation confirmed that despite employing flood coolant during drilling of CFRP/Ti stacks, increasing cutting speeds generated more heat, thereby increasing cutting temperature. This led to substantial Ti chip adhesion on the cutting edges, increased tool wear by edge chipping as the cutting edge weakened, and hence shortened tool life.

Attempts at measuring cutting temperatures during drilling CFRP/Ti stacks in this study were conducted using thermocouples that were fixed in the stacks (between CFRP and Ti panels) and at the drill exit (Figure 3.17). However, all attempts failed as the recorded temperatures were within the range of 25 – 33 °C for all cutting speeds used, which was no difference compared to the ambient or initial temperature of 22 °C before drilling. This was due to the fact that flood coolant / cutting fluid was employed when drilling CFRP/Ti stacks, which caused difficulty in assessing the actual temperature in the cutting zone. It is possible that the thermocouples measured the temperature of the cutting fluid instead of the actual cutting temperature.

Measuring the cutting temperature during drilling by attaching thermocouples to the cutting edges, rake and flank faces has been reported to give better results [62, 85]. This technique required the drill to be stationary to avoid entangling and cutting the thermocouples, while the workpiece was rotating for drilling. Most cutting temperature measurement was performed on a lathe machine (the workpiece was fixed in the spindle). However, this was not possible in the current study due to the limitation of the machine tool, which required the drills to be in the spindle to use the ultrasonic actuator and rotate for drilling.

Nevertheless, previous work [62, 85] employing a similar range of cutting parameters as in the current study, which focused on measuring cutting temperatures by embedding thermocouples on the flank faces and cutting edges during dry drilling of CFRP and Ti have provided some temperature data. It has been shown that drilling of CFRP with cutting speeds of 40 to 100 m/min increased the cutting temperature from 120 to 207 °C [62]. Whereas, drilling Ti with increasing cutting speeds from 24 to 73 m/min (with a fixed feed rate of 0.05 mm/rev) resulted in an increase in cutting temperature from 480 to 1060 °C [85]. The temperature generated when drilling Ti particularly at the higher cutting speed is high enough to enhance the affinity and adhesion of Ti chip to the cutting edges (WC-Co) and also weakening the cutting edges as it has been reported that carbide drill started to lose its strength as the temperature increases above 500 °C [24].

To further understand how the drill wore when using the cutting speed of 25 m/min that contributed to the longest tool life, a SEM investigation of the cutting edges after CD and UAD of 80 holes through CFRP/Ti stacks was conducted, Figure 4.26. The adhered Ti on the cutting edges when drilling with 25 m/min was uniform, although no marked difference was observed between CD, Figure 4.26 (a) and UAD, Figure 4.26 (b). The flank face of the drills exhibited clean surface with no visible adhered Ti.

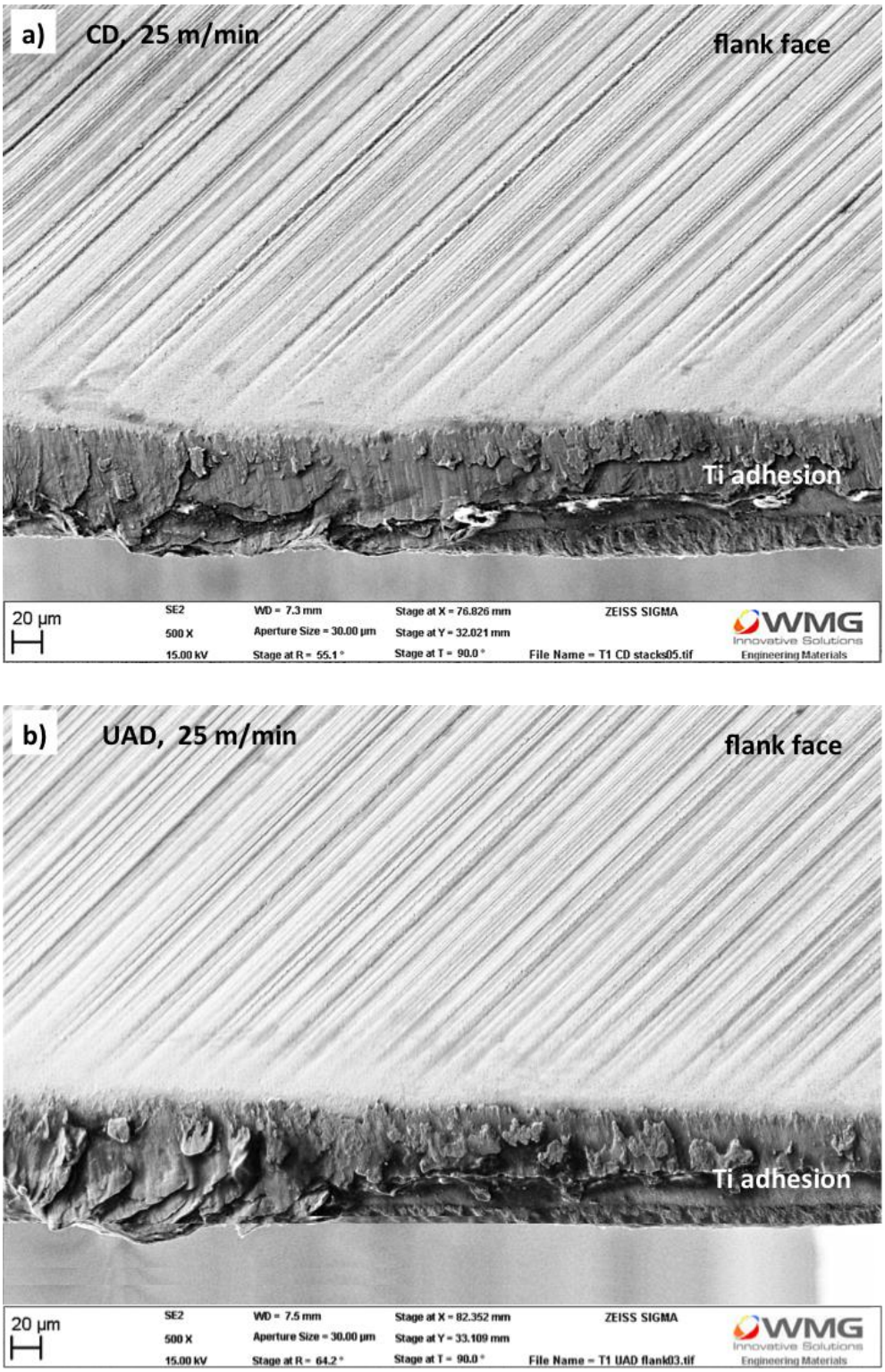

Figure 4.26: SEM micrographs showing morphology of adhered Ti on the cutting edge, and flank face condition after (a) CD and (b) UAD, of 80 holes through CFRP/Ti stacks using a cutting speed of 25 m/min and feed rate of 0.05 mm/rev

Following removal of the adhered Ti by drilling through a hole in CFRP (4 mm thick), it is evident that the cutting edges used for both CD and UAD of CFRP/Ti stacks at 25 m/min wore uniformly by abrasive wear mechanism, which was indicated by cutting edge rounding, Figures 4.27 (a) and 4.28 (a). The uniform wear is preferable for a longer tool life, rather than cutting edge chipping. Magnified views of the cutting edges revealed the removal of Co binder between WC grains, Figures 4.27 (b) and 4.28 (b). The wear condition during CD and UAD of CFRP/Ti stacks at 25 m/min was observed to resemble the case of drilling CFRP-only (as discussed in Study 1). The wear mechanism was detailed in Section 4.1.1.1. It was shown previously in Section 4.1.1.2 that Ti alloy was not hard enough to abrade the WC-Co of the cutting edges and in most cases as reported in the literature, drilling of Ti-only did not cause edge rounding. Therefore, the edge rounding when drilling CFRP/Ti stacks with 25 m/min was attributed to drilling CFRP layer of the stacks. There was no evidence of edge chipping and fracture at any other part of the drills during CD and UAD using the lowest cutting speed of 25 m/min, up to 80 holes.

As described in Section 3.2, all drills were reground, which means that the cutting edges and flank faces were WC grains with Co binder without coating, but the rake face of the drills still has TiAlN coating. Further SEM investigation revealed that the TiAlN coating was still fully intact on the rake face of the drills at the end of CD, Figure 4.29 (a), and UAD, Figure 4.29 (b), of CFRP/Ti stacks using the cutting speed of 25 m/min. Nevertheless, limited adhered Ti was observed on the rake face of the drills, which was expected as the Ti chip flowed over it during drilling.

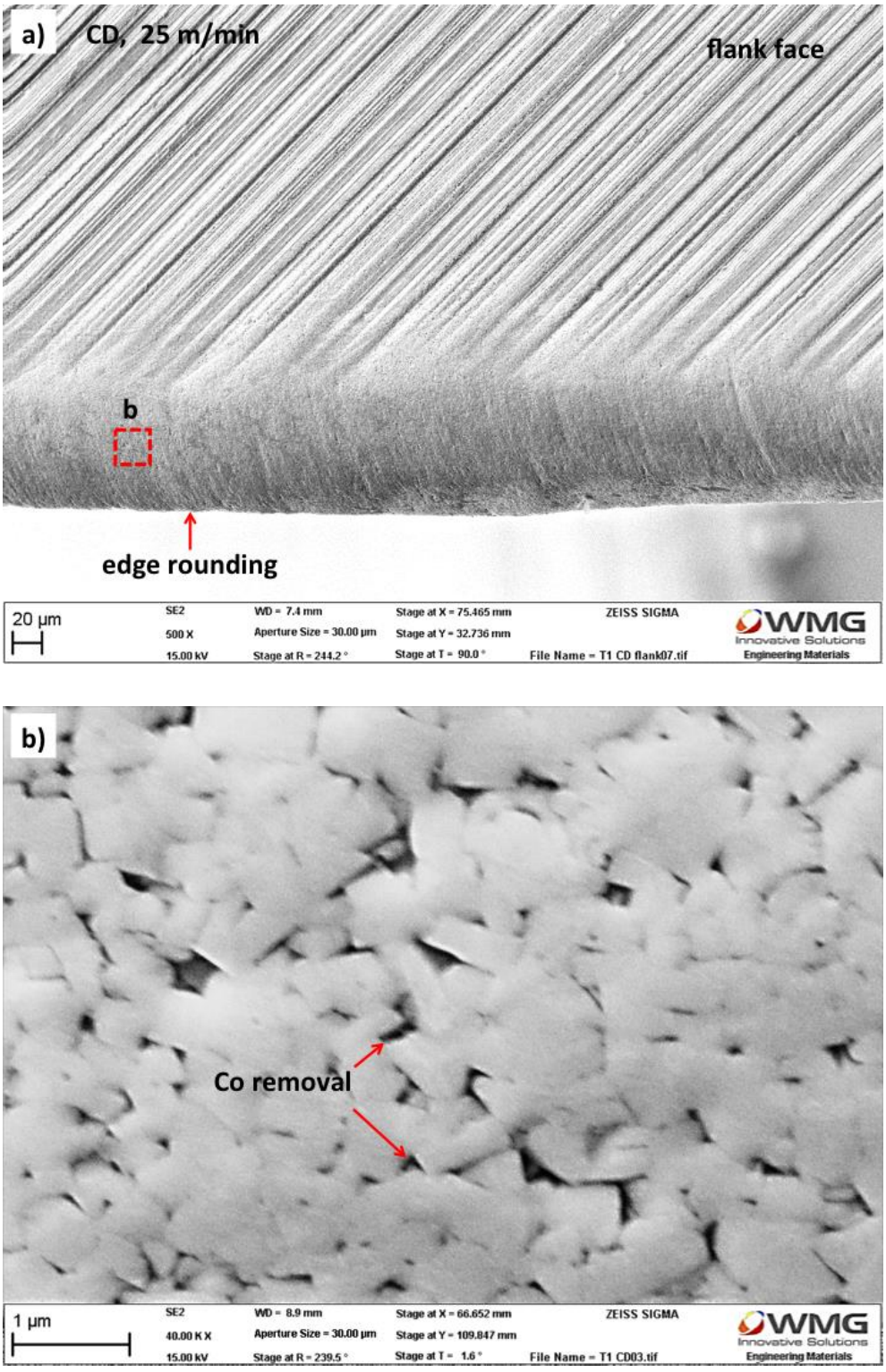

Figure 4.27: SEM micrographs showing cutting edge and flank face condition after CD of 80 holes through CFRP/Ti stacks using a cutting speed of 25 m/min and feed rate of 0.05 mm/rev; following removal of the adhered Ti

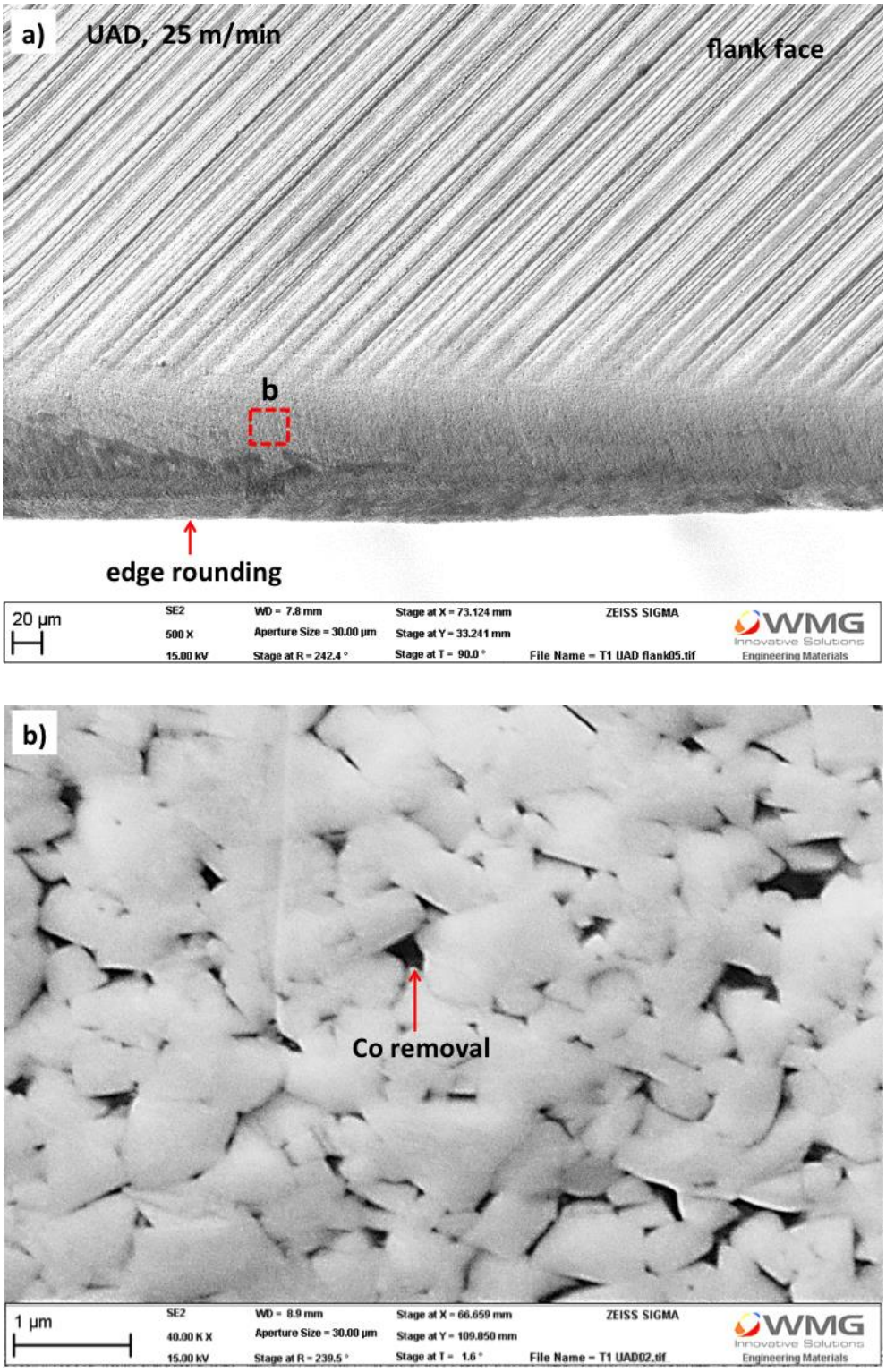

Figure 4.28: SEM micrographs showing cutting edge and flank face condition after UAD of 80 holes through CFRP/Ti stacks using a cutting speed of 25 m/min and feed rate of 0.05 mm/rev; following removal of the adhered Ti

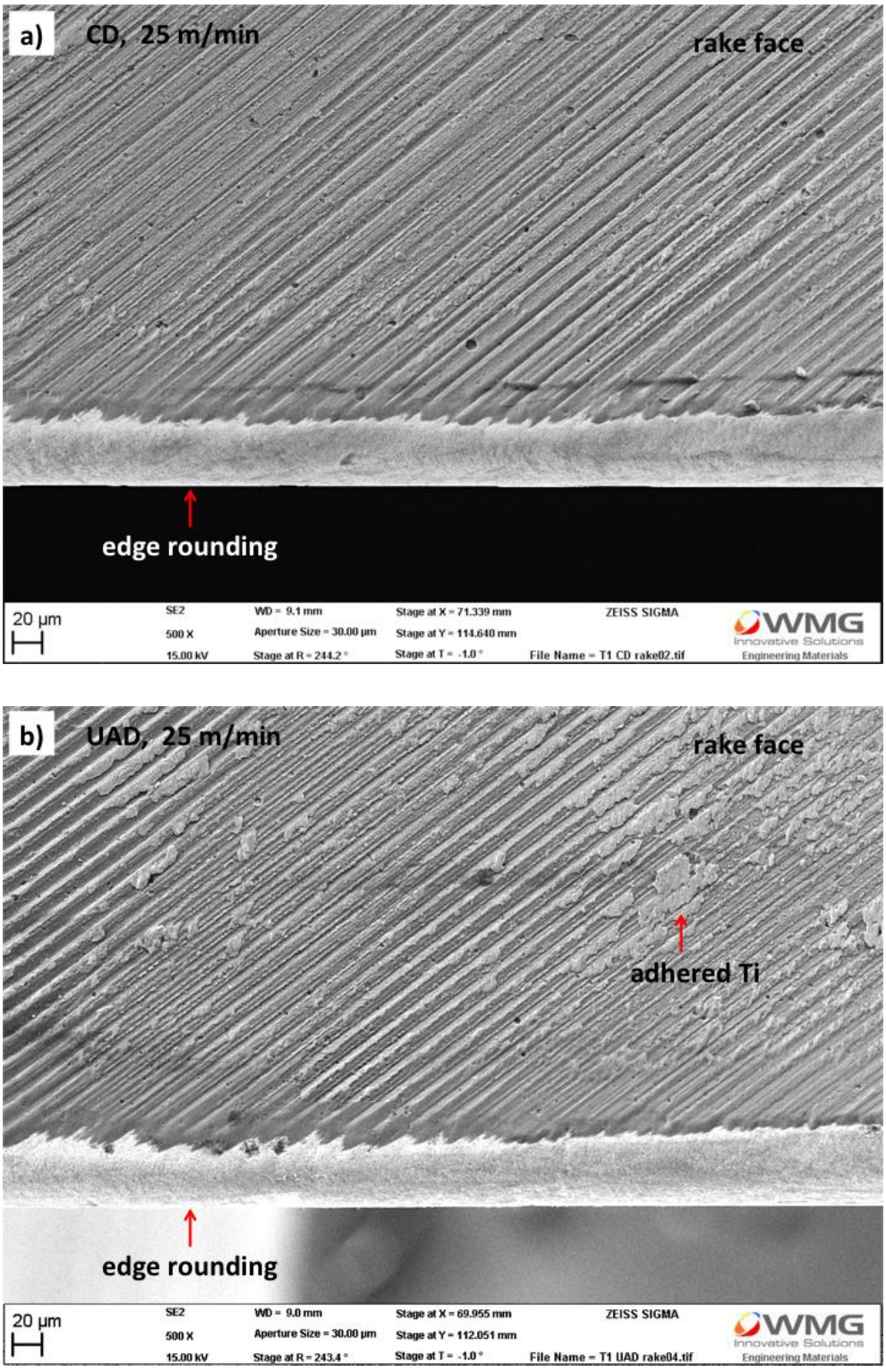

Figure 4.29: SEM micrographs showing rake face condition after (a) CD, and (b) UAD of 80 holes through CFRP/Ti stacks using a cutting speed of 25 m/min and feed rate of 0.05 mm/rev

In contrast, severe adhesive wear occurred when CD and UAD of CFRP/Ti stacks using higher cutting speeds of 50 and 75 m/min, which rendered faster drill failure. Figure 4.30 shows SEM micrographs of the cutting edges at the end of CD and UAD of CFRP/Ti stacks using the highest cutting speed of 75 m/min (after 50 holes). SEM micrographs of cutting edges used for CD and UAD of CFRP/Ti stacks at 50 m/min are attached in Appendix B, Figure B.1. The adhered Ti exhibited irregular morphology and it attached strongly to the cutting edges as it was not able to be removed manually. Following removal of the adhered Ti (by drilling through CFRP), cutting edge fracture is evident as shown in Figures 4.31 (a), 4.32 (a), and Appendix B, Figures B.2, B.3, which was the reason for rapid drill failure for CD and UAD at high cutting speeds of 50 and 75 m/min. Further SEM investigation of the edge fracture revealed fractured WC grains and pull-out of the WC-Co, Figures 4.31 (b) and 4.32 (b). This condition makes Ti prone to adhere as drilling progressed, and hence, edge fracture occurred consecutively.

Notably, UAD of CFRP/Ti stacks using the highest cutting speed of 75 m/min was observed to cause larger cutting edge fracture, Figure 4.32 (a), compared to CD, Figure 4.31 (a). The rake face of the drill used for UAD at the highest cutting speed of 75 m/min also exhibited larger fracture of 185 µm from the cutting edge, Figure 4.33 (b), compared to CD which exhibited smaller fracture of 120 µm, Figure 4.33 (a). This suggests more weakening of the cutting edges during UAD at higher cutting speed, which was attributed to the drill oscillation, compared to CD. As discussed in the literature review [95, 111], diffusion wear or crater on the drill's rake face is common when drilling Ti alloy at high cutting speeds using uncoated carbide drills. Whereas, in this study, no evidence of crater or diffusion wear on the rake face was found (for both 50 and 75 m/min). It is possible that the presence of cutting fluid and coating (on the rake face) was helpful to resist diffusion of WC-Co when Ti chips flowed over the rake face during drilling.

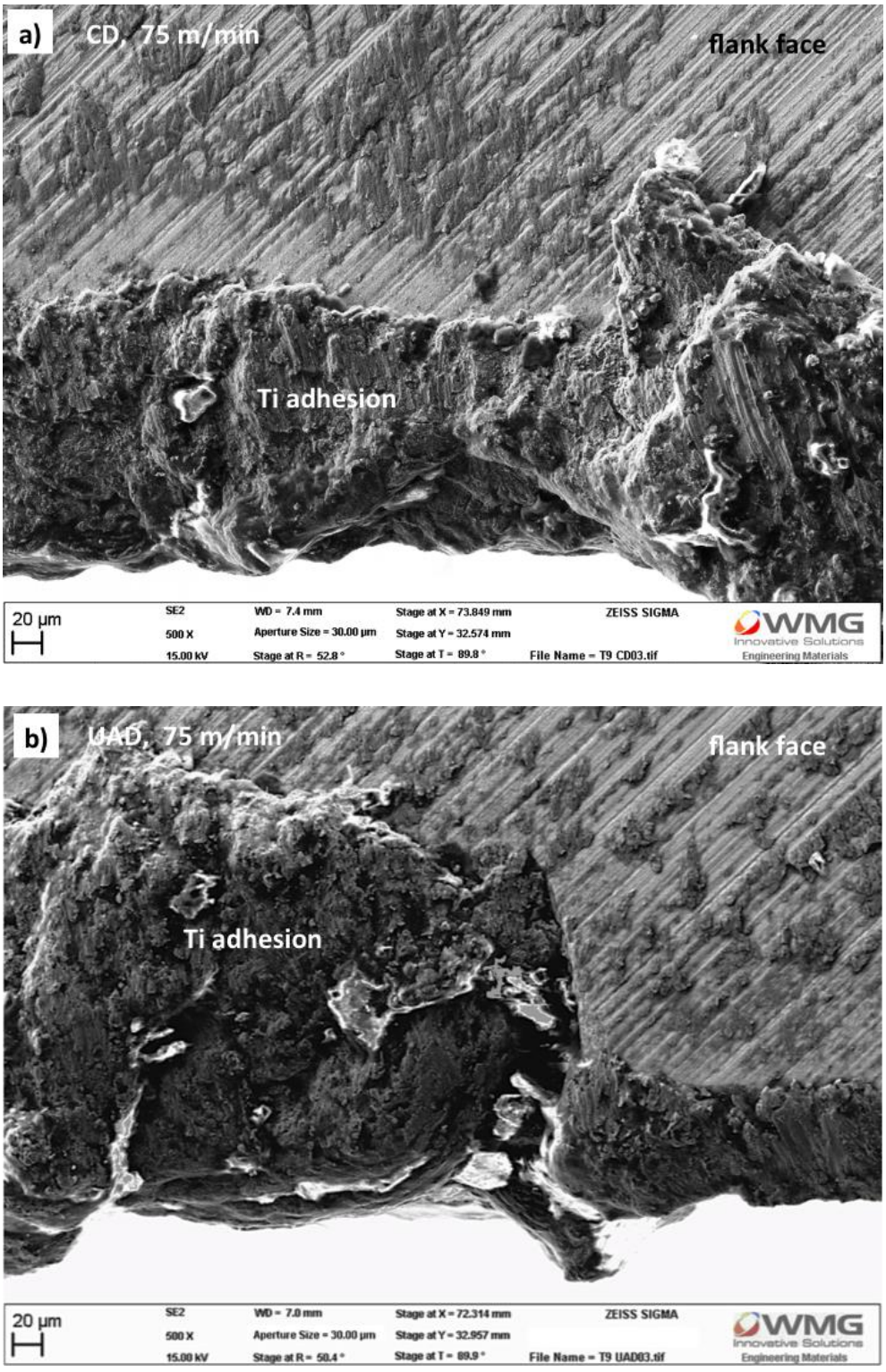

Figure 4.30: SEM micrographs showing morphology of adhered Ti on the cutting edge and flank face condition after (a) CD and (b) UAD, of 50 holes through CFRP/Ti stacks using a cutting speed of 75 m/min and feed rate of 0.05 mm/rev

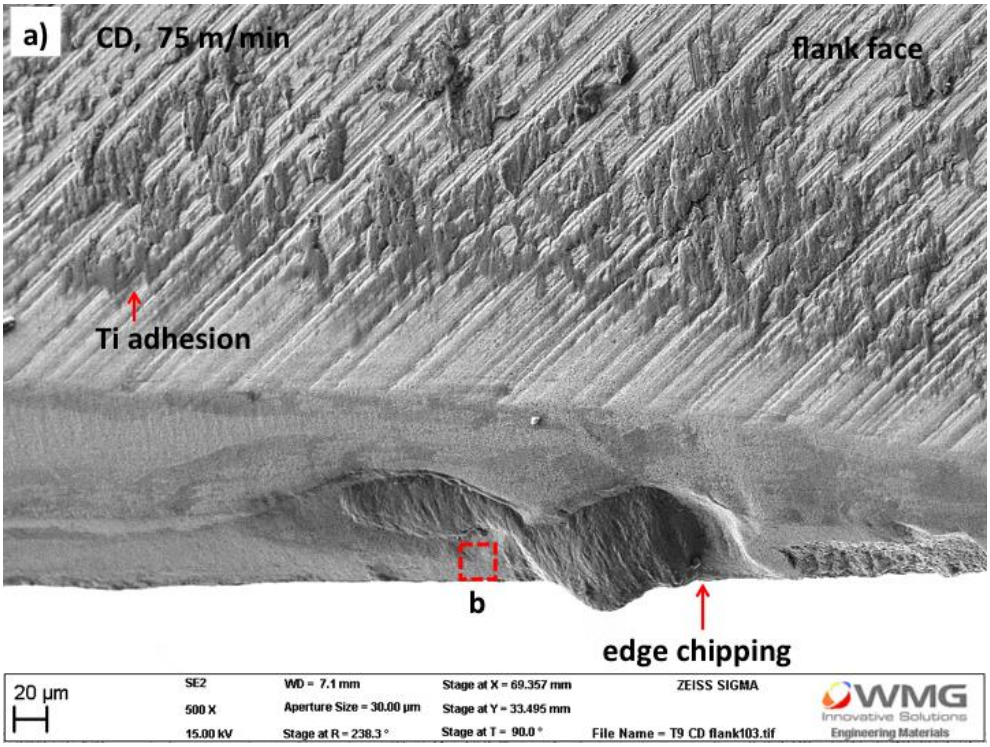

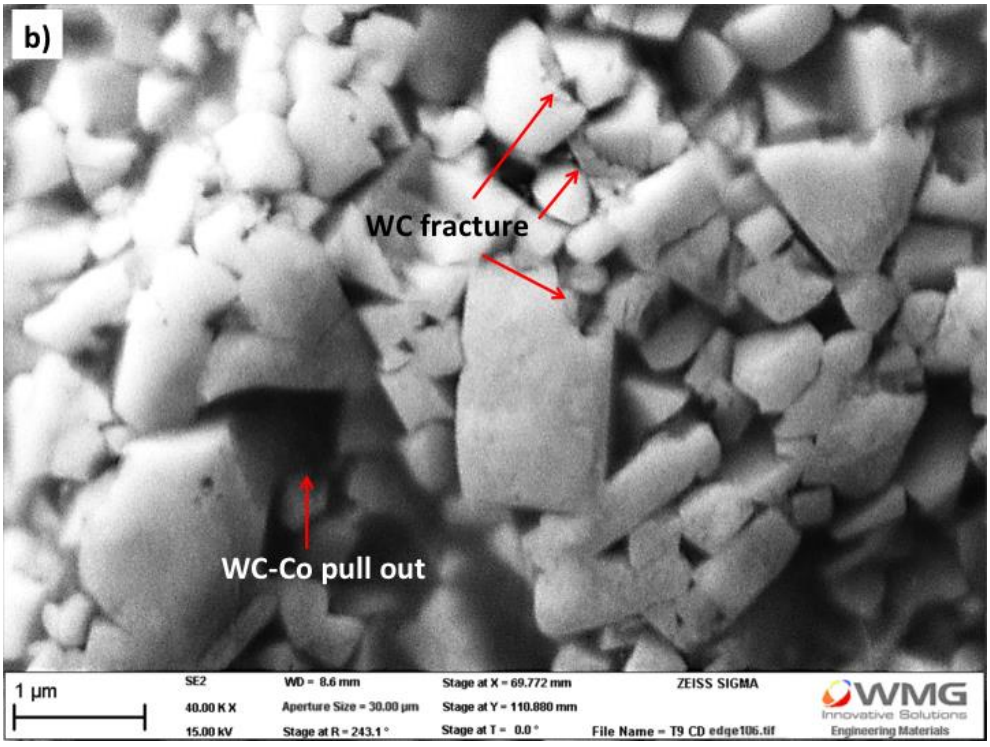

Figure 4.31: SEM micrographs showing cutting edge and flank face condition after CD of 50 holes through CFRP/Ti stacks using a cutting speed of 75 m/min and feed rate of 0.05 mm/rev; following removal of the adhered Ti

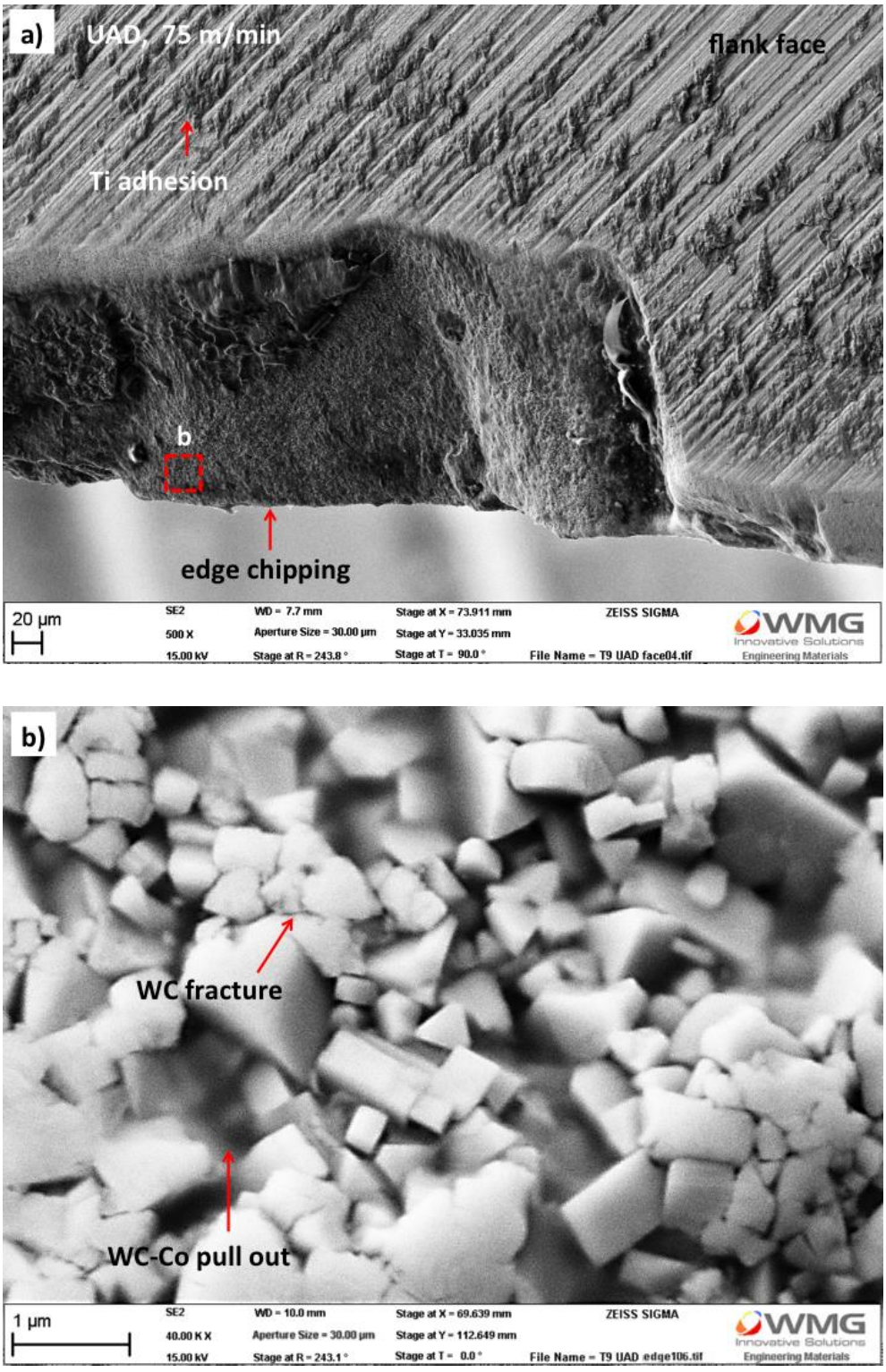

Figure 4.32: SEM micrographs showing cutting edge and flank face condition after UAD of 50 holes through CFRP/Ti stacks using a cutting speed of 75 m/min and feed rate of 0.05 mm/rev; following removal of the adhered Ti

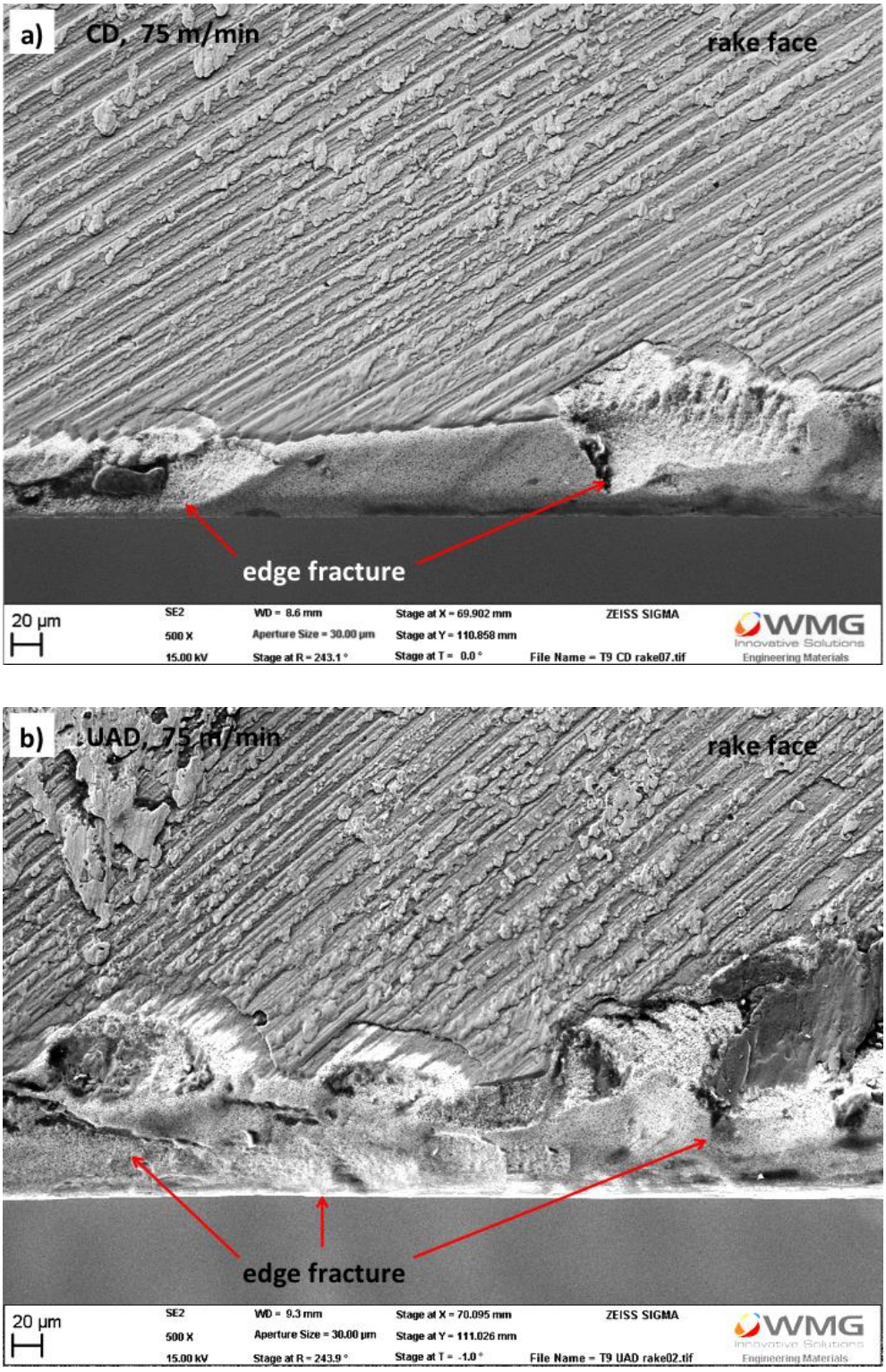

Figure 4.33: SEM micrograph showing rake face condition after (a) CD, and (b) UAD of 50 holes through CFRP/Ti stacks using a cutting speed of 75 m/min and feed rate of 0.05 mm/rev

In summary, the results established that the tool wear mechanisms, which governed the tool failure rate when drilling CFRP/Ti stacks, were significantly influenced by cutting speed. The drill wore gradually by abrasive wear mechanism when drilling CFRP/Ti stacks using a low cutting speed (25 m/min). The limited and uniform Ti that masked the cutting edges was beneficial as it protected the cutting edges from severe wear and can be easily abraded when drilling CFRP, leading to cutting edge rounding. In contrast, at higher cutting speeds of 50 and 75 m/min, which generated more heat, the cutting edges failed earlier by severe adhesive wear mechanism due to severe Ti adhesion and build up, leading to WC-Co fragmentation and cutting edge chipping as the adhered Ti detached.

The fact that there was no significant difference in tool wear / life between UAD and CD of CFRP/Ti stacks in this study may suggest that the drills did not oscillate sufficiently during UAD to induce intermittent cutting. Previous work [143] suggested that intermittent cutting during drilling may reduce the workpiece material adhering at the cutting edges hence reducing tool wear compared to continuous cutting. To confirm the cutting mechanism during UAD compared to CD, it is important to investigate the cutting force profile, chip morphology and the machined surface finish; the results will be discussed in the following Sections 4.2.2, 4.2.3 and 4.2.4.4.

4.2.2 Thrust force and torque

Thrust force profiles during one cycle of CD and UAD through CFRP/Ti stacks were examined to determine how UAD affects the cutting mechanism, whether periodic disengagement between the cutting edges and the workpiece, or continuous cutting occurred as in the case of CD. The results are presented in Figure 4.34, showing the whole thrust forces profiles, also, the minimum and maximum forces throughout the drilling cycles of the respective materials (CFRP and Ti).

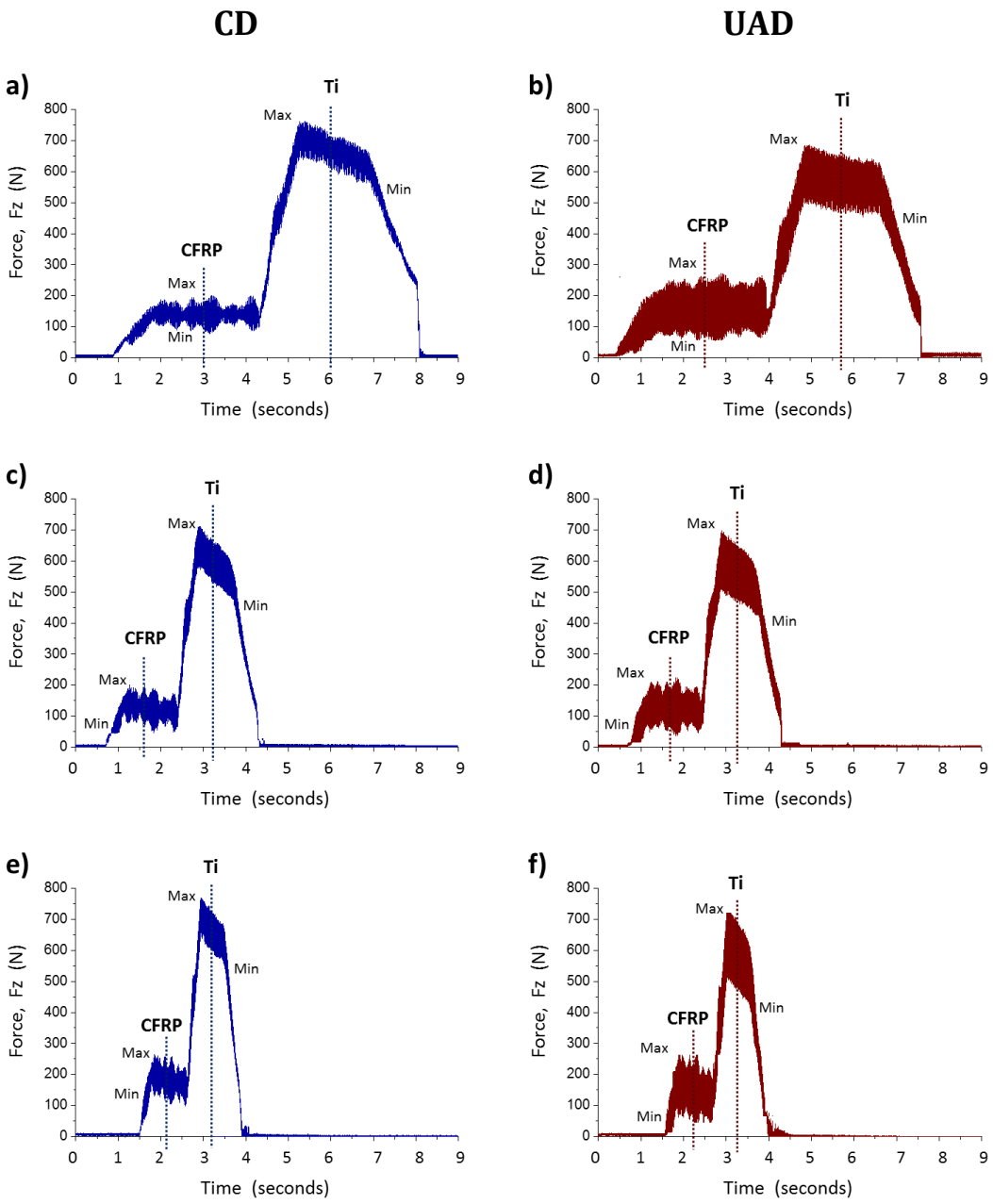

Figure 4.34: Thrust force profiles during CD and UAD of the 1st holes in CFRP/Ti stacks using cutting speeds of (a, b) 25 m/min, (c, d) 50 m/min and (e, f) 75 m/min at a constant feed rate of 0.05 mm/rev (sampling rate = 80,000 Hz)

At all cutting speeds, UAD, Figure 4.34 (b, d, f) exhibited larger difference between the minimum and maximum thrust forces, compared to CD, Figure 4.34 (a, c, e). Table 4.2 summarises and compares the difference between the minimum and maximum thrust forces during CD and UAD of the stacks. It was confirmed that in one drilling cycle, UAD exhibited 24% – 43% larger forces variation compared to CD (as highlighted in

Table 4.2). The larger fluctuation in thrust force during UAD was attributed to the oscillation of the drills back and forth (peak-to-peak amplitude = 11 μm) causing a variation in the feed rate. It is evident that the thrust forces generated during UAD at all cutting speeds never reached 0 N, Figure 4.34 (b, d, f) indicative of continuous cutting as the cutting edges did not disengage from the workpiece throughout the drilling process, similar to the case of CD, Figure 4.34 (a, c, e). This finding does not support the assertion of intermittent cutting during UAD by previous studies [140, 141]. The intermittent cutting means that the cutting is not continuous since cutting edges disengage from the workpiece (not in contact) periodically during a drilling cycle. As demonstrated previously in work involving low-frequency vibration assisted drilling (LVFAD) [143, 145, 152, 153], the forces would reach 0 N (intermittently) if a separation between the cutting edges and the workpiece occurred during drilling. This is not apparent in the case of UAD of CFRP/Ti stacks in the current study.

Table 4.2: Difference between minimum and maximum thrust forces during CD and UAD of CFRP/Ti stacks using cutting speeds of 25, 50 and 75 m/min at a feed rate of 0.05 mm/rev – 1st holes

Cutting Speed (m/min)	CFRP			Ti (N)		
	CD (N)	UAD (N)	* UAD – CD	CD (N)	UAD (N)	* UAD – CD
25	115	164	**43%**	185	251	**36%**
50	138	188	**36%**	220	273	**24%**
75	147	205	**39%**	220	305	**39%**

*** Indicates that UAD exhibited a larger force variation compared to CD, by the percentage shown.**

As the oscillation amplitude was measured prior to drilling (before contact with the workpiece), it is important to ensure that drill oscillation continued during drilling. Previous studies have not provided any evidence whether a drill remained oscillated throughout a UAD process. In the current study, further examination of the thrust forces profiles (at the dashed lines in Figure 4.34) revealed that UAD of CFRP, Figure 4.35 (b, d, f) and UAD of Ti, Figure 4.36 (b, d, f) exhibited "beat" patterns due to

constructive and destructive interference of waves, as opposed to the case of CD showing constant forces, Figures 4.35 (a, c, e) and 4.36 (a, c, e). Interference wave patterns only occur when two vibration systems interfere with each other [164]. In the case of UAD, the ultrasonic vibration of the drill interfered with the natural vibration of the machine tool, hence generating forces in the form of beat patterns. This observation indicated that the drills oscillated or vibrated continuously during UAD in the current work.

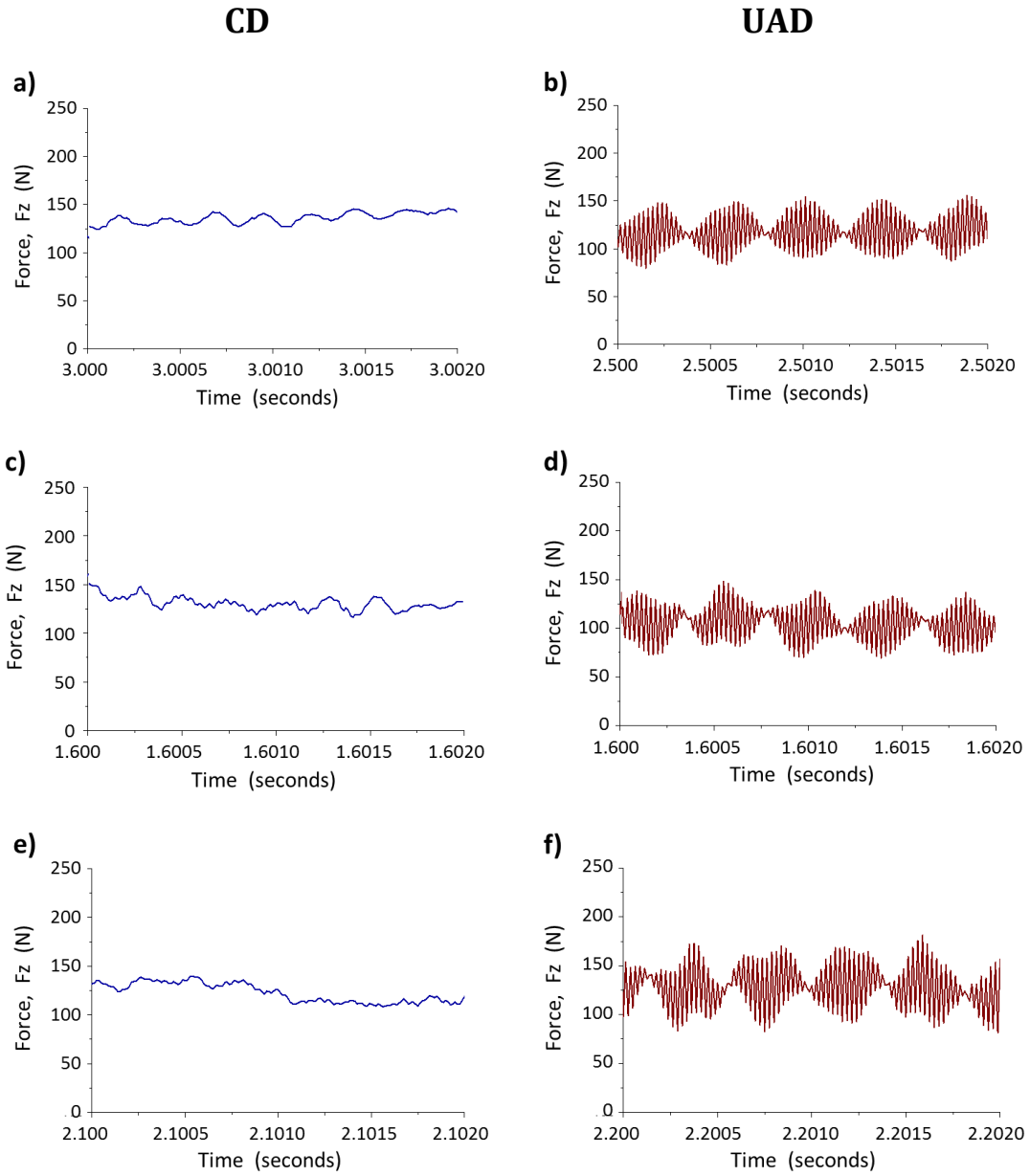

Figure 4.35: Thrust force profiles during CD and UAD of the 1st holes through CFRP component of the stack using cutting speeds of (a, b) 25 m/min, (c, d) 50 m/min and (e, f) 75 m/min at a constant feed rate of 0.05 mm/rev (sampling rate = 80,000 Hz)

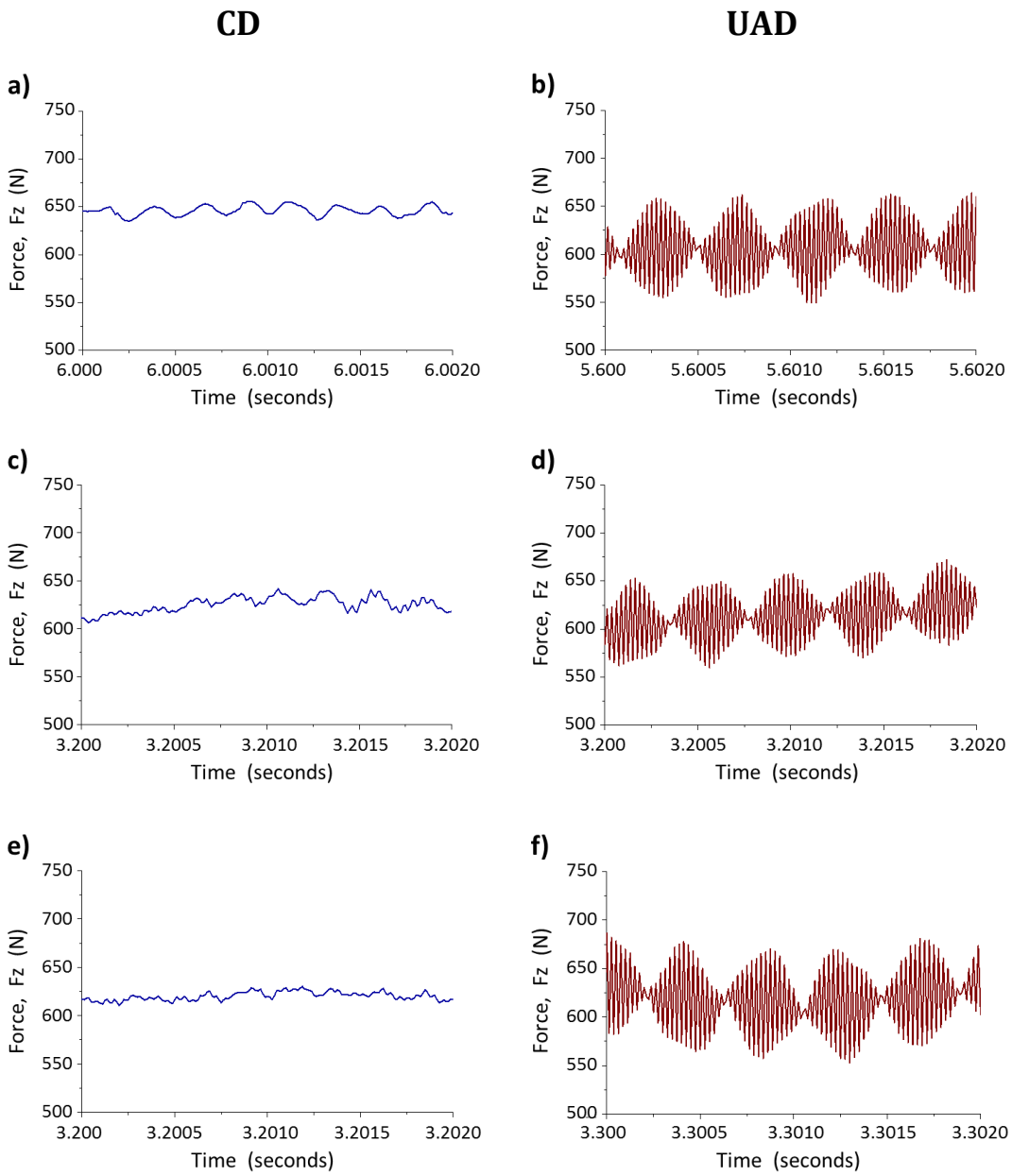

Figure 4.36: Thrust force profiles during CD and UAD of the 1st holes through Ti component of the stack using cutting speeds of (a, b) 25 m/min, (c, d) 50 m/min and (e, f) 75 m/min at a constant feed rate of 0.05 mm/rev (sampling rate = 80,000 Hz)

Figures 4.37 and 4.38 show a comparison of average thrust force throughout CD and UAD of CFRP/Ti stacks (when the cutting edges are in full engagement with the workpiece) at cutting speeds of 25, 50 and 75 m/min with increasing hole number. The average thrust forces during CD and UAD of both CFRP and Ti components of the stacks at all cutting speeds were shown to increase as the number of holes increased (from 1st to 80th holes), due to the effect of increasing tool wear.

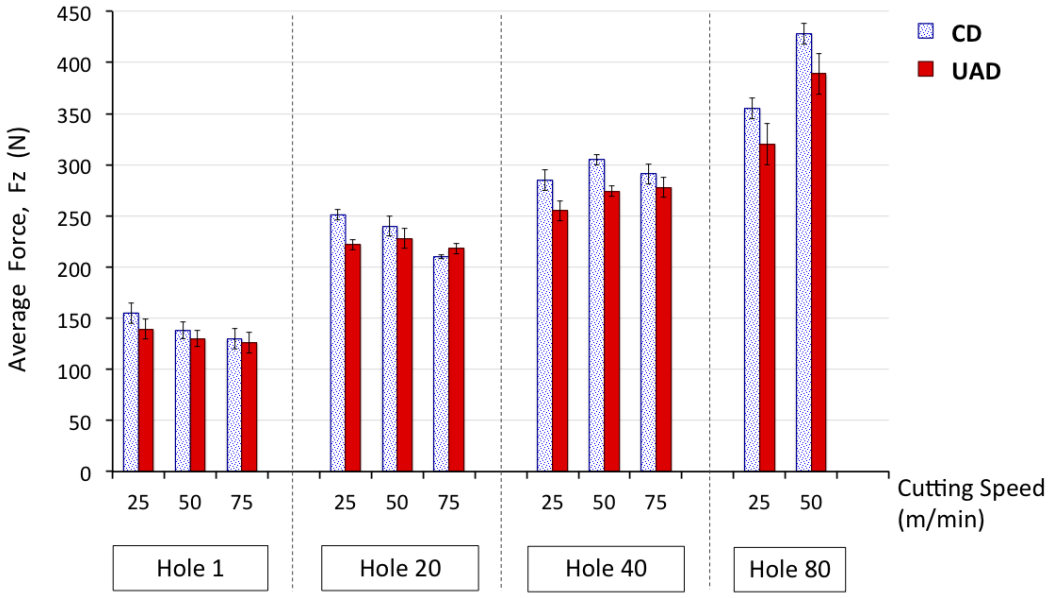

Figure 4.37: Comparison of average thrust forces during CD and UAD of CFRP component of the stacks using cutting speeds of 25, 50 and 75 m/min at a constant feed rate of 0.05 mm/rev. Range bars indicate variation for three consecutive holes (e.g. hole 1-3, hole 19-21, hole 39-41)

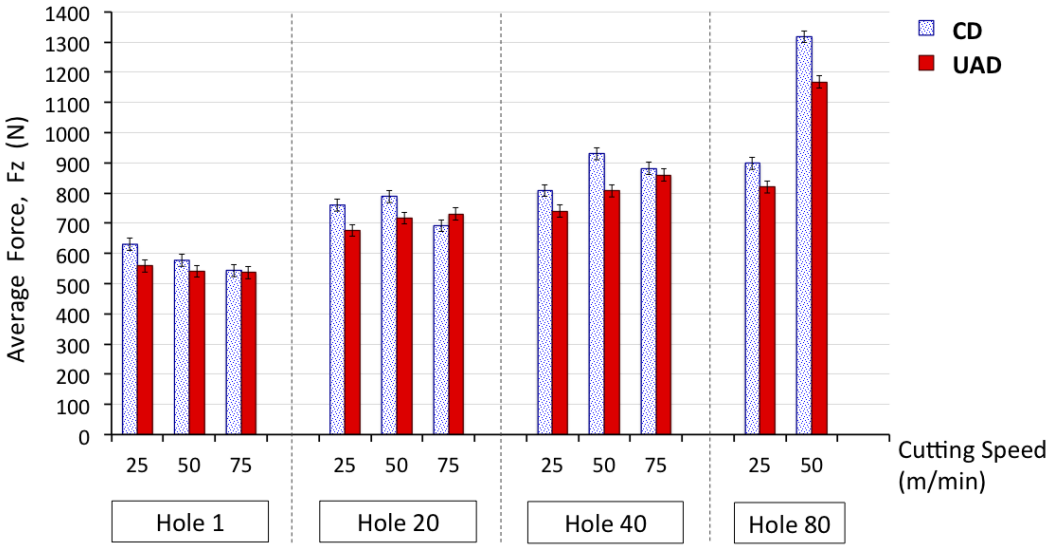

Figure 4.38: Comparison of average thrust forces during CD and UAD of Ti component of the stacks using cutting speeds of 25, 50 and 75 m/min at a constant feed rate of 0.05 mm/rev. Range bars indicate variation for three consecutive holes (e.g. hole 1-3, hole 19-21, hole 39-41)

For the first holes, with increasing cutting speed from 25 to 75 m/min, the average thrust forces was observed to reduce by 10 – 25 N for CFRP, Figure 4.37, and reduced by 20 – 85 N for Ti, Figure 4.38. The difference in tool wear when drilling the first holes with different cutting speeds was negligible, Figure 4.22. Therefore, the observation of

decreasing thrust force with increasing cutting speed suggests thermal softening of the workpiece material in the cutting zone due to increased heat generation at higher cutting speeds. Workpiece softening required less effort to shear, hence lower thrust force. However, as the number of holes increased (holes 40 and 80), average thrust forces generated when drilling at 50 and 75 m/min increased by 10 – 73 N for CFRP, Figure 4.37, and increased by 75 – 410 N for Ti, Figure 4.38, higher than those of 25 m/min, due to the dominating influence of increasing tool wear. The average thrust forces during UAD of CFRP particularly at 25 and 50 m/min was observed to be on average 10% (25 N) lower than those of CD, Figure 4.37. For UAD of Ti at 25 and 50 m/min, the average thrust forces were 9% (85 N) lower than those of CD. The reduction in thrust forces during UAD compared to CD is consistent with the literature. However, it must be noted that it was not due to intermittent cutting, rather it was due to oscillation of the drills that caused larger variation in feed rate and forces.

Torque profiles during CD and UAD of CFRP/Ti stacks are compared in Figure 4.39. Similar to the case of thrust forces, larger torque variation (by 20% – 34%) was observed during UAD compared to CD. A closer examination of the torque (at the dashed lines in Figure 4.39) revealed that the torque generated during UAD of both CFRP and Ti exhibited interference wave patterns, Figures 4.40 (b, d, f) and 4.41 (b, d, f) confirming that the drills were vibrated continuously throughout the drilling process, as opposed to the case of CD, Figures 4.40 (a, c, e) and 4.41 (a, c, e).

Notably, in the case of CD of CFRP at all cutting speeds, Figure 4.40 (a, c, e), it is evident that the torque fluctuated (increased to 200 Nmm and decreased to 0 Nmm) regularly over times throughout the drilling. This was attributed to the heterogeneous structure and brittle fracture of CFRP when drilling. In contrast, for CD of Ti, there were less fluctuation in torque (as the torque was observed to be more consistent at 1400 Nmm,

1250 Nmm and 1200 Nmm for CD using 25, 50 and 75 m/min, respectively), Figure 4.41 (a, c, e). This was expected as Ti exhibited homogenous structure.

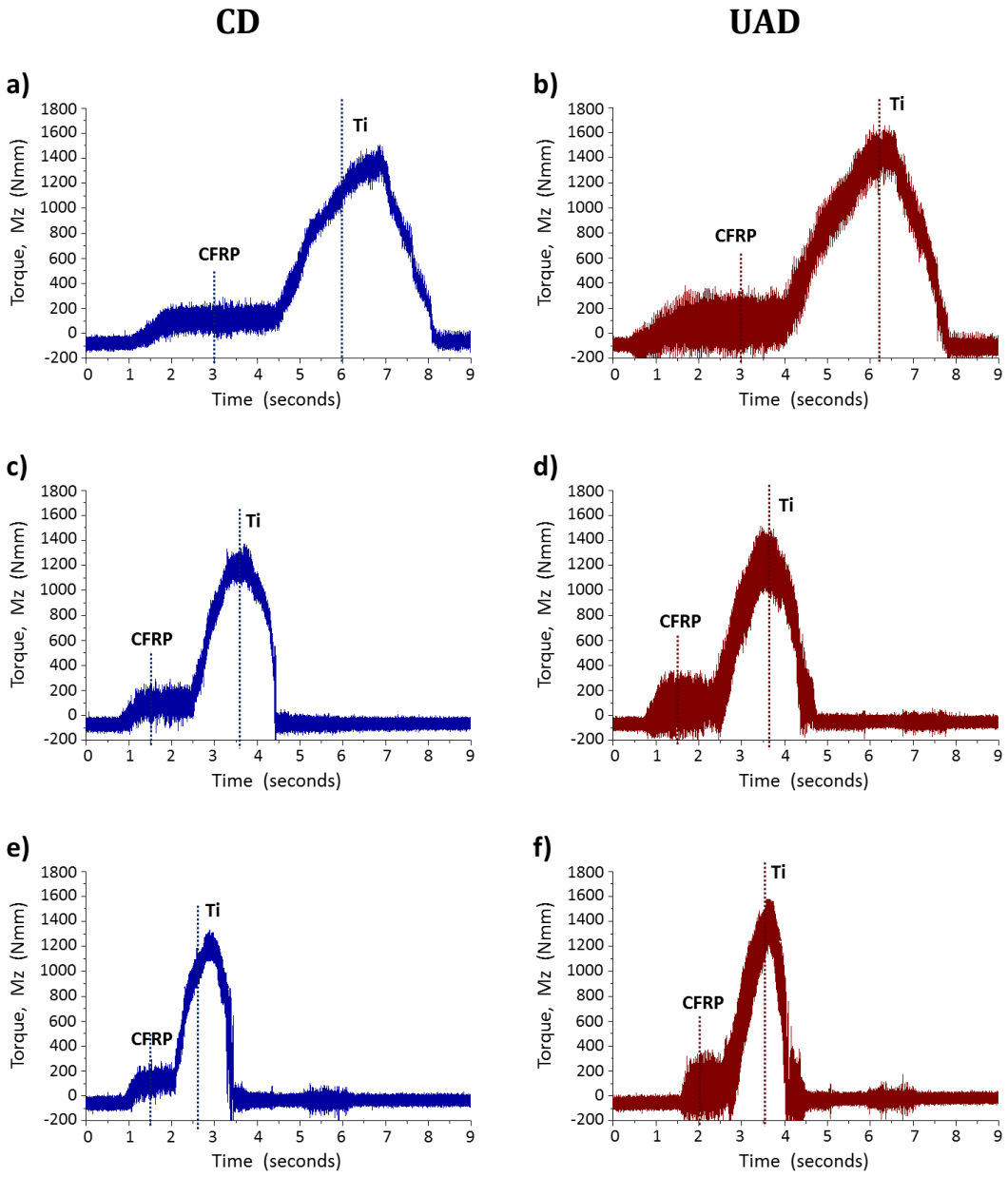

Figure 4.39: Torque profiles during CD and UAD of the 1st holes in CFRP/Ti stacks using cutting speeds of (a, b) 25 m/min, (c, d) 50 m/min and (e, f) 75 m/min at a constant feed rate of 0.05 mm/rev (sampling rate = 80,000 Hz)

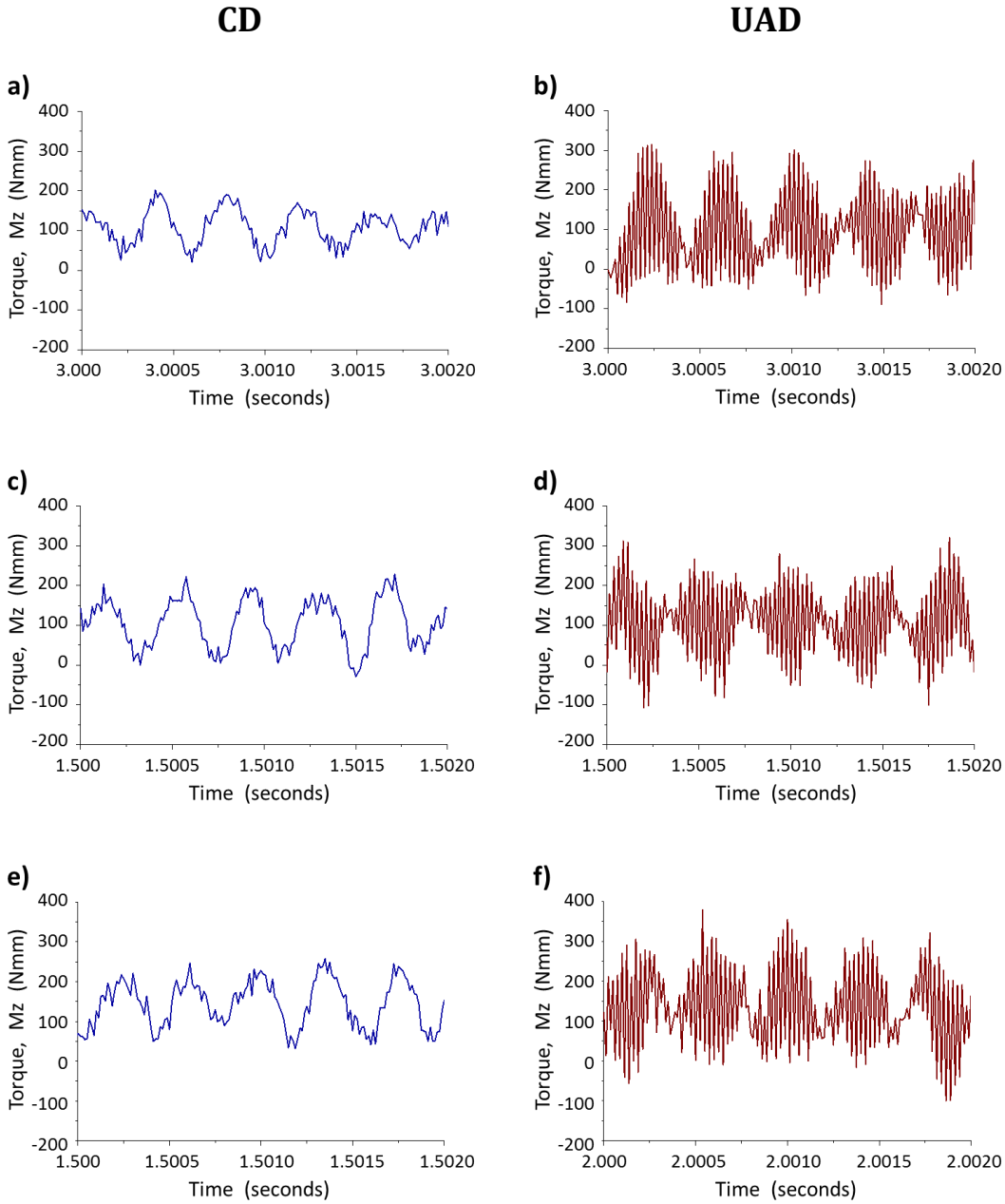

Figure 4.40: Torque profiles during CD and UAD of the 1st holes through CFRP component of the stack using cutting speeds of (a, b) 25 m/min, (c, d) 50 m/min and (e, f) 75 m/min at a constant feed rate of 0.05 mm/rev (sampling rate = 80,000 Hz)

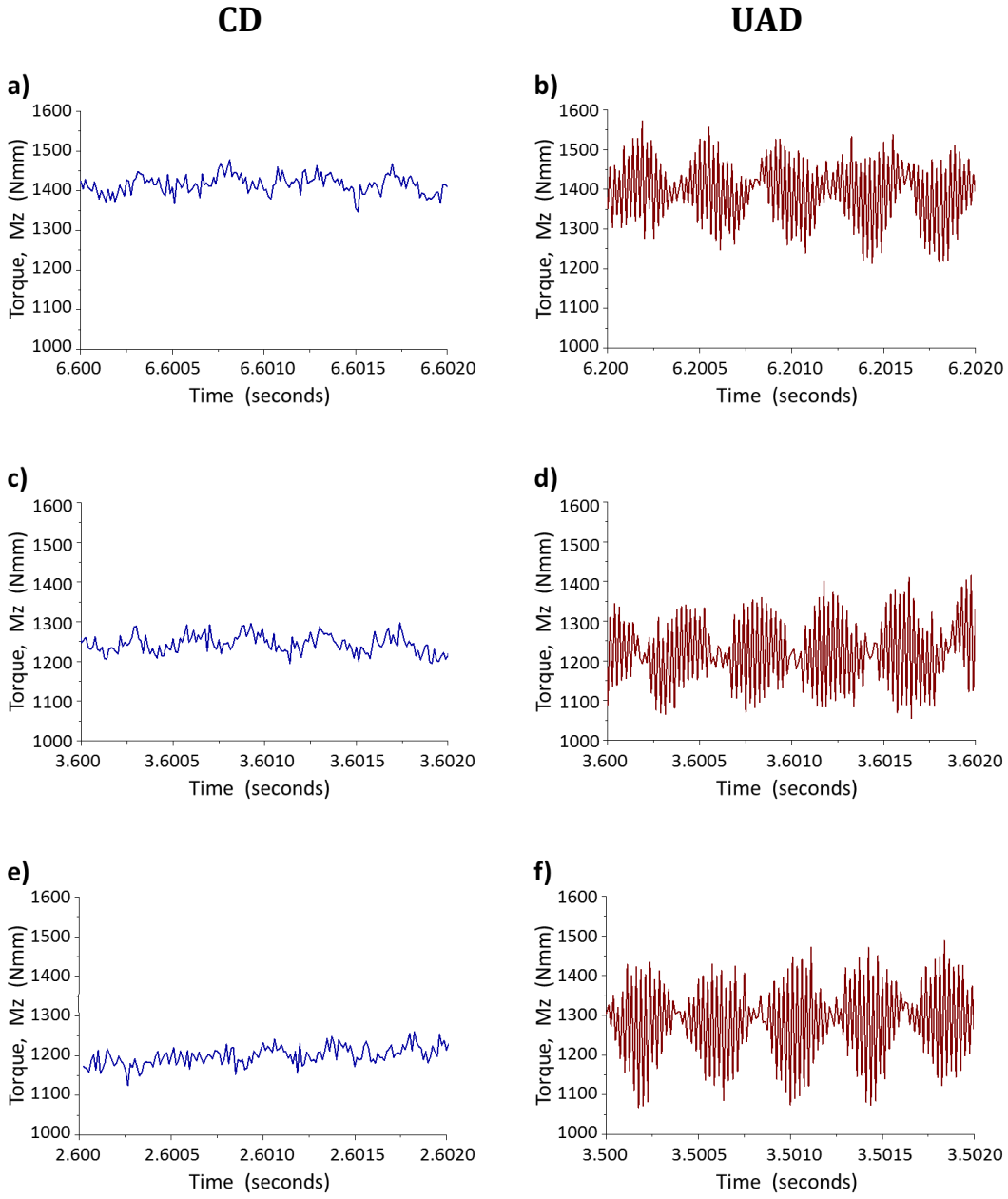

Figure 4.41: Torque profiles during CD and UAD of the 1st holes through Ti component of the stack using cutting speeds of (a, b) 25 m/min, (c, d) 50 m/min and (e, f) 75 m/min at a constant feed rate of 0.05 mm/rev (sampling rate = 80,000 Hz)

Figures 4.42 and 4.43 compare average torques (when the drills were in full engagement with the workpiece) during CD and UAD of both CFRP and Ti at all cutting speeds.

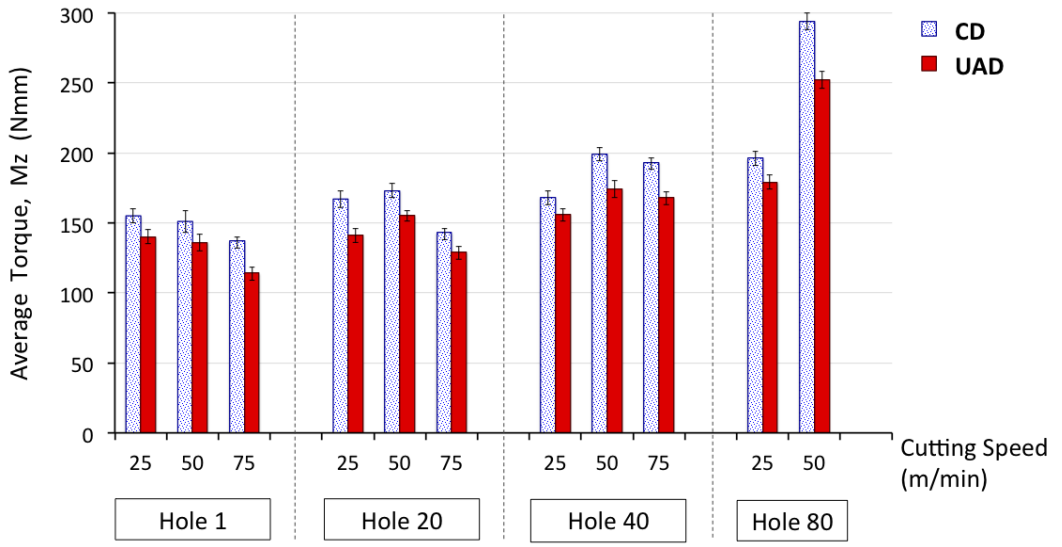

Figure 4.42: Comparison of average torque during CD and UAD of CFRP component of the stacks using cutting speeds of 25, 50 and 75 m/min at a constant feed rate of 0.05 mm/rev. Range bars indicate variation for three consecutive holes (e.g. hole 1-3, hole 19-21, hole 39-41)

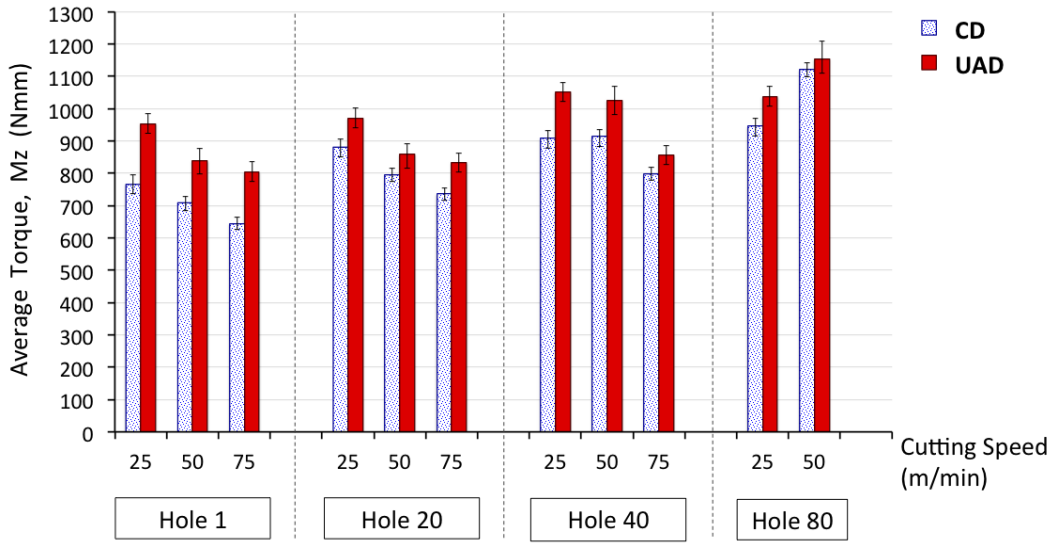

Figure 4.43: Comparison of average torque during CD and UAD of Ti component of the stacks using cutting speeds of 25, 50 and 75 m/min at a constant feed rate of 0.05 mm/rev. Range bars indicate variation for three consecutive holes (e.g. hole 1-3, hole 19-21, hole 39-41)

Similar to the case of average thrust force, the average torque was observed to decrease with increasing cutting speed, particularly for the first and 20th holes,

indicative of increasing heat generation due to faster tool rotation, thereby softening the workpiece materials and less effort to shear the workpiece. For the 80th holes, the average torque when drilling CFRP and Ti at 50 m/min increased, 45% and 15% higher, respectively, than those of 25 m/min due to increased tool wear. UAD of CFRP at all cutting speeds generated 12% lower torque (on average) compared to CD of CFRP, Figure 4.42, similar to the observation of thrust forces. However, interestingly, UAD of Ti at all cutting speeds caused on average 14% higher torque than CD of Ti, Figure 4.43. A possible explanation for the higher torque during UAD of Ti compared to CD was due to hardening of Ti workpiece caused by the drill's vibration against the workpiece. Therefore, higher forces were required to shear the work-hardened material. This will be discussed in detail in Section 4.2.4.4.

4.2.3 Titanium chip morphology

The Ti chips produced by CD and UAD of CRP/Ti stacks at all cutting speeds of 25, 50 and 75 m/min were in the form of a long spiral, ribbon, and folded chips, Figure 4.44. At all cutting speeds, there was no discernible difference in terms of the shape and length of the chips produced by CD, Figure 4.44 (a, c, e) and UAD, Figure 4.44 (b, d, f). In general, the measured lengths of the Ti chip were within the range of 4 to 12 cm. Previous studies have speculated that UAD could produce smaller and broken metallic chip compared to those of CD, however, this was not observed in the current study. Broken metallic chip may be produced if the cutting is not continuous in the case when the cutting edges were disengaged intermittently throughout the drilling as shown by LFVAD [145, 152]. The resemblance of the continuous and long Ti chips produced by UAD to those of CD suggests that the chips were formed continuously during UAD, similar to the case of CD. This observation supports the force data, which suggested that UAD operation with an ultrasonic frequency of 40 kHz and a peak-to-peak amplitude of 11 μm, was continuous.

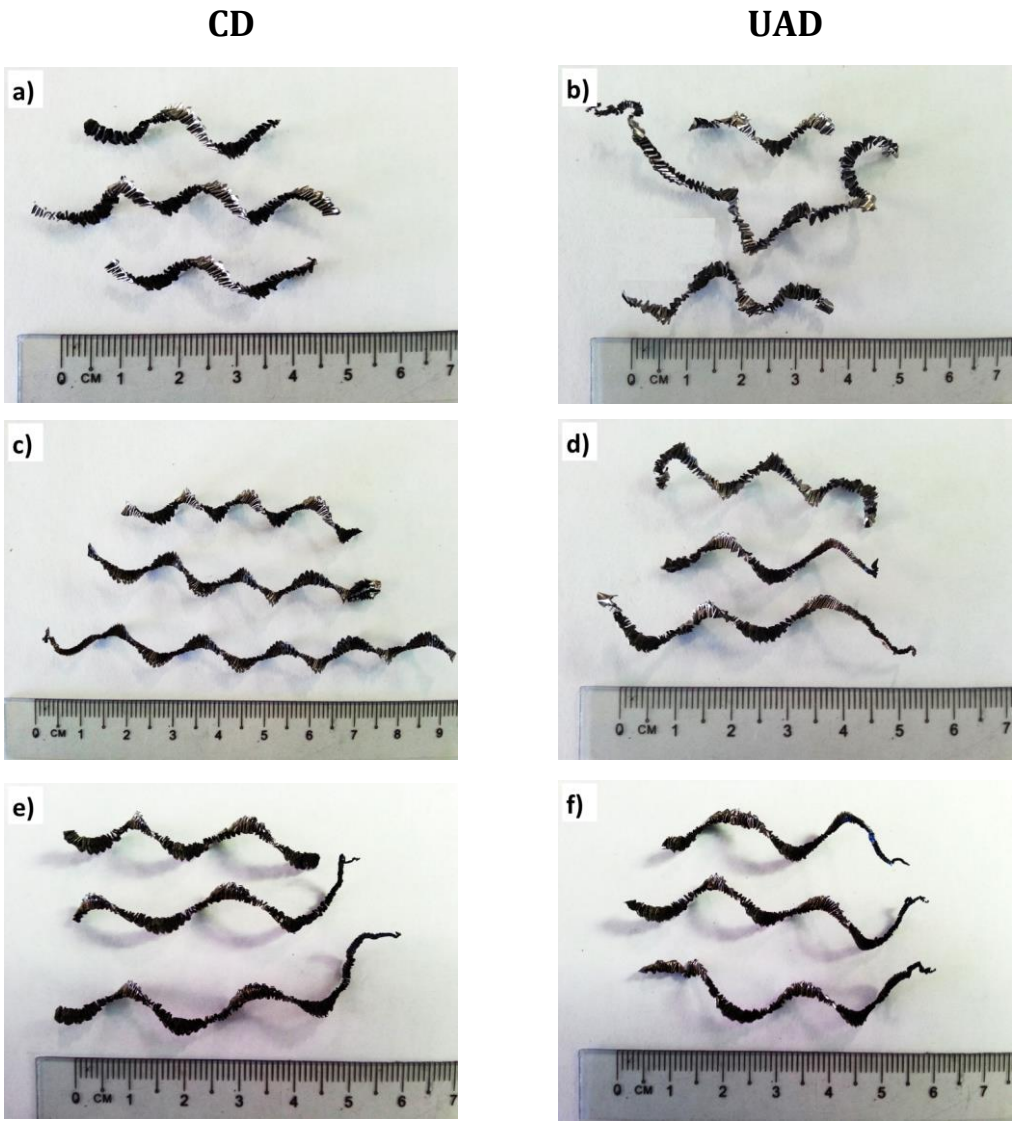

Figure 4.44: Morphology of Ti chips produced by CD and UAD of CFRP/Ti stacks using cutting speeds of (a, b) 25 m/min, (c, d) 50 m/min and (e, f) 75 m/min at a constant feed rate of 0.05 mm/rev

To further understand the chip formation mechanism, the Ti chips produced by CD and UAD of CFRP/Ti stacks were cross-sectioned, polished and compared, Figure 4.45. The Ti chips became more segmented showing apparent shear bands with increasing cutting speed due to more heat was generated and localised in the shear plane. This caused the grains within the heat localisation area to be softened and heavily deformed. The narrow shear bands that exhibited more intense microstructural deformation between the chip segments was a direct representation of the shear plane when forming the chip. Previous studies involving drilling of Ti did not detail the chip

formation. However, the work of Sun *et al*. [91] involving conventional turning of Ti (a different machining operation compared to the current study) reported a similar observation of Ti chip became more segmented with increasing cutting speed. This indicated that regardless of machining operations, the use of cutting speed has a significant influence on producing Ti chip segmentation and shear bands.

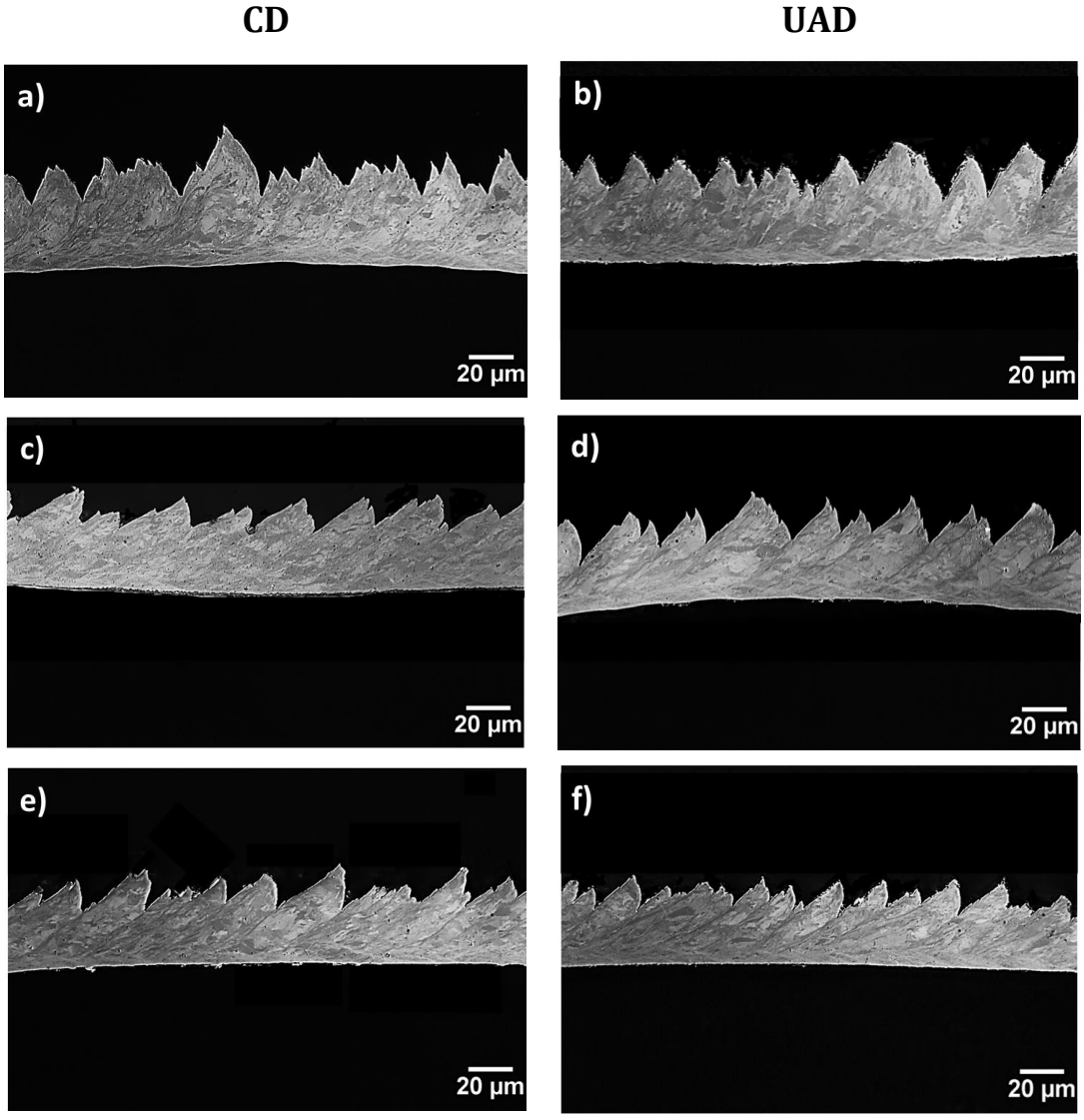

Figure 4.45: Cross section of Ti chips produced by CD and UAD of CFRP/Ti stacks using cutting speeds of (a, b) 25 m/min, (c, d) 50 m/min and (e, f) 75 m/min at a constant feed rate of 0.05 mm/rev

Ti6Al4V has been reported to start softening at a temperature of 350 °C [165], although the actual temperature at the shear plane in the current study was unknown due to the

limitation and difficulty in measuring the temperature as explained previously (page 135). Nevertheless, Li *et al*. [85] reported a temperature of 1060 °C when drilling Ti6Al4V at 73 m/min, which was measured using thermocouples attached at flank faces (2 mm from cutting edges), and a temperature of 480 °C when using a lower cutting speed of 24 m/min. Even though the reported temperatures were not the exact temperature at the shear plane, they were measured close enough to the shear plane. Therefore, it is plausible to assume that the temperature generated at the shear plane, particularly, when using the highest cutting speed of 75 m/min in the current study would exceed 350 °C. Consequently, more thermal softening and more intense grain deformation in the shear region occurred, hence causing apparent shear bands and chip segmentation, Figure 4.45 (e, f). At the lowest cutting speed of 25 m/min, the shear bands and segmentation were less apparent, Figure 4.45 (a, b), indicating that heat generation at this cutting speed was not sufficient to cause softening and severe grain deformation at the shear plane when shearing the Ti workpiece. When comparing the Ti chips produced by CD and UAD of CFRP/Ti stacks, no marked difference in the morphology and segmentation was observed at all cutting speeds, Figure 4.45, which suggests a similarity in the cutting mechanism and heat generation at shear planes between the two operations.

On average, the shear band angle (measured as in Figure 3.27) was observed to decrease from 56° to 48° and to 35° as cutting speed increased from 25 to 50 to 75 m/min (for both CD and UAD), Figure 4.46. The average thickness of the Ti chip also decreased from 53 to 51 to 44 µm with increasing cutting speed from 25 to 50 to 75 m/min, Figure 4.47. Even though on average, no marked difference was observed between CD and UAD, it is important to note that the chips produced by UAD exhibited on average 42% larger variation in the shear band angle and thickness as indicated by larger range bars, compared to those of CD, Figures 4.46 and 4.47.

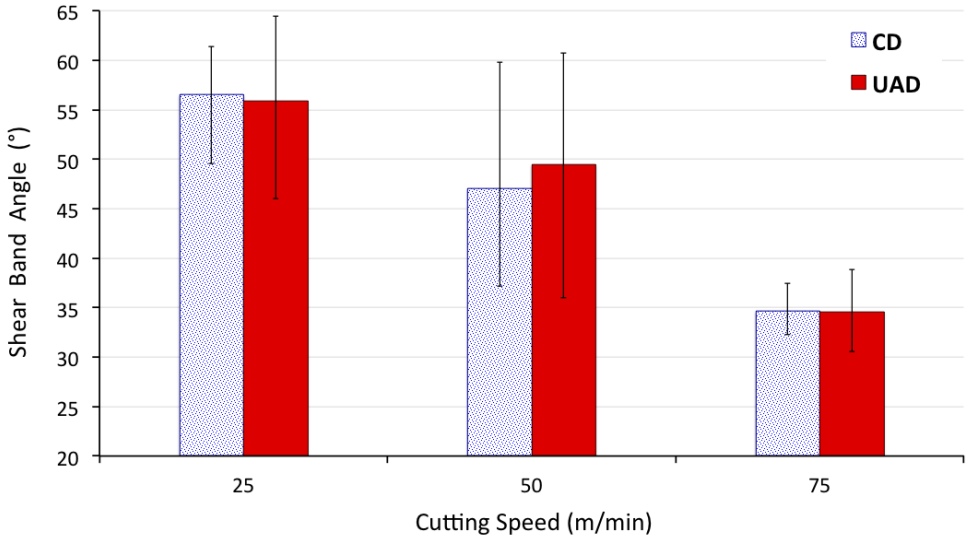

Figure 4.46: Comparison of average shear band angles of Ti chips produced by CD and UAD of CFRP/Ti stacks using cutting speeds of 25, 50 and 75 m/min at a constant feed rate of 0.05 mm/rev

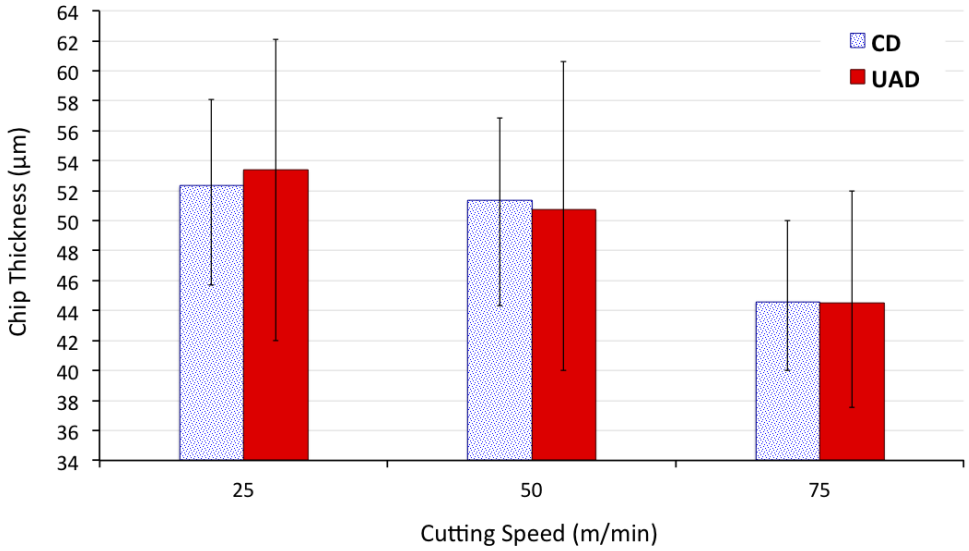

Figure 4.47: Comparison of average thickness of Ti chips produced by CD and UAD of CFRP/Ti stacks using cutting speeds of 25, 50 and 75 m/min at a constant feed rate of 0.05 mm/rev

ANOVA established that the difference between the Ti chip thickness data produced by different cutting speeds, also by CD and UAD were statistically significant, Appendix A, Table A.2. This means increasing cutting speed significantly reduced Ti chips thickness, and UAD produced significantly larger variation in the chip thickness compared to CD. Although continuous cutting was demonstrated during UAD, the larger variation of Ti

chip thickness would be related to the variation in feed rate due to drill's oscillation in the feed direction. In contrast, the feed rate is constant during CD.

4.2.4 Hole quality

The hole quality in CFRP/Ti stacks produced by CD and UAD with respect to the change in cutting speed, 25, 50 and 75 m/min, at a constant feed rate of 0.05 mm/rev were compared and evaluated in terms of:

- accuracy and consistency of hole diameter in the CFRP and Ti of the stacks
- the extent of CFRP entrance delamination
- fibre pull-out from the machined surface of CFRP
- topography, roughness and sub-surface hardness of machined Ti
- Ti burr height

4.2.4.1 Hole diameter

Figure 4.48 compares hole diameter in CFRP/Ti stacks produced by CD and UAD using cutting speeds of 25, 50 and 75 m/min at a constant feed rate of 0.05 mm/rev. Drilling of CFRP/Ti stacks using the lowest cutting speed of 25 m/min was found to be advantageous in producing holes that were consistent in diameter (CD: 6.102 – 6.108 mm, UAD: 6.103 – 6.108 mm), within H7 tolerance limit (-0.00/+0.015 mm) and closer to the drill nominal diameter of 6.100 mm, from the beginning until the end of drilling tests, Figure 4.48 (a). This was attributed to the drills exhibiting uniform and low tool wear with the least adherent Ti on the cutting edges. Increasing the cutting speed to 50 m/min during both CD and UAD of CFRP/Ti stacks produced holes having 2 – 7 µm larger diameter, Figure 4.48 (b), than those produced by the lower cutting speed of 25 m/min, Figure 4.48 (a). Nevertheless, all holes produced at 50 m/min were still within the tolerance limit (CD: 6.102 – 6.114 mm, UAD: 6.103 – 6.115 mm).

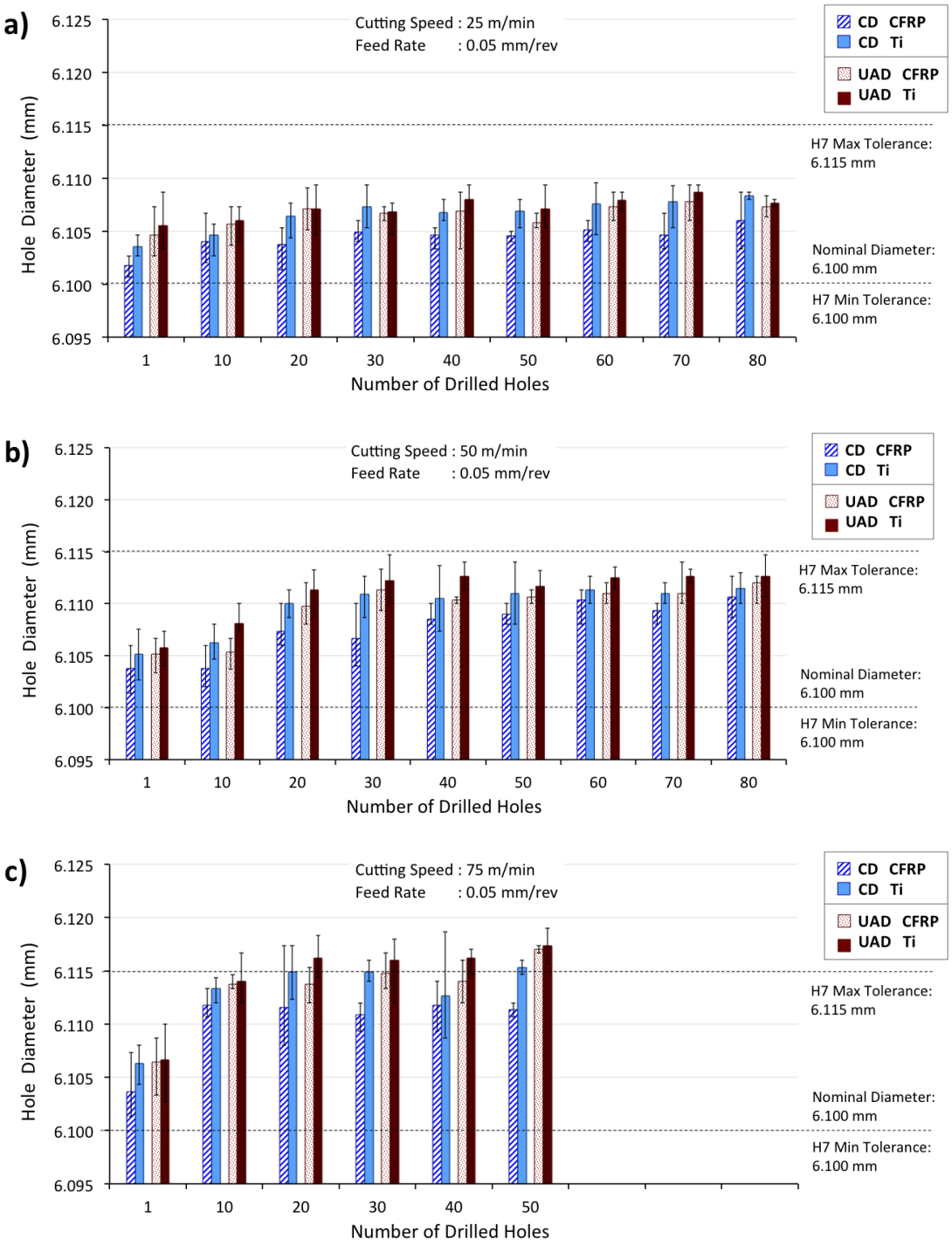

Figure 4.48: Comparison of hole diameters in CFRP/Ti stacks produced by CD and UAD using cutting speeds of 25, 50 and 75 m/min and a constant feed rate of 0.05 mm/rev. Range bars indicate variation for three consecutive holes (e.g. hole 1-3, hole 9-11, hole 19-21 etc.)

At 50 m/min (CD and UAD), initially, for the first holes up to 20 holes, the hole diameters were closer to the drill nominal diameter, Figure 4.48 (b). However, the hole

diameters increased as the number of holes and the adherent Ti on the cutting edges increased (hole 30 – hole 80). This observation indicated that the adherent Ti on the cutting edges was detrimental for hole quality as it enlarged the hole diameters by removing more material.

Similarly, at the highest cutting speed of 75 m/min (CD and UAD), diameters of the first three holes were closer to the drill nominal diameter, Figure 4.48 (c). However, as the number of holes increased (hole 10 – hole 50), the diameters increased (CD: 6.108 – 6.117 mm, UAD: 6.112 – 6.118 mm) and 30% of the holes were out of the tolerance limit. This was attributed to the drilling with the cutting edges with adherent Ti. ANOVA established that the effect of increasing cutting speeds on hole diameters was statistically significant, Appendix A, Tables A.3 and A.4.

An important finding was that the holes produced by UAD at all cutting speeds exhibited smaller diameter difference (Figure 4.49) compared to those of CD, as summarised in Table 4.3. All holes in CFRP produced by CD at all cutting speeds exhibited 1 – 4 μm smaller diameter than the holes in Ti. For UAD, the diameters of the holes in CFRP were either equal or 1 – 2 μm smaller than the hole diameters of Ti, Table 4.3. The smaller diameter in CFRP compared to Ti was attributed to the removal of the adhered Ti on the cutting edges by abrasion when drilling CFRP of the stacks, as discussed in Section 4.2.1. However, Ti adhesion on the cutting edges increased when drilling the Ti component of the stacks, which then caused larger hole diameters in Ti.

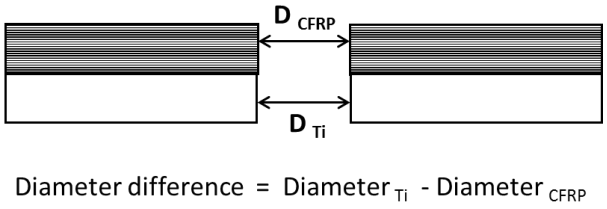

Figure 4.49: Schematic showing diameter difference between the holes in CFRP and Ti in a stack

Table 4.3: Comparison of diameter difference between holes in Ti and CFRP of the stacks produced by CD and UAD; 80 holes (for 25 and 50 m/min) and 50 holes (for 75 m/min)

Cutting Speed (m/min)	CD	UAD
25	1 – 3 μm	0 – 1 μm
50	1 – 4 μm	1 – 2 μm
75	1 – 4 μm	1 – 2 μm

In regard to the comparison between CD and UAD, the holes in CFRP produced by UAD of CFRP/Ti stacks at all cutting speeds were 1 – 5 μm larger than the holes produced by CD. The larger holes in CFRP produced by UAD compared to CD was confirmed to be statistically significant by ANOVA, Appendix A, Table A.3. The hole diameters in Ti produced by UAD were observed to be either equal or 1 – 2 μm larger than the holes produced by CD, which was confirmed to be not statistically significant by ANOVA, Appendix A, Table A.4. This result indicated that the application of UAD has a significant effect on producing larger holes in CFRP, however not for Ti.

UAD is regarded as a combination of shearing by the main cutting edges and rubbing by the outer part of the drill due to the oscillation of the drill [149]. A burnishing action of the machined surfaces by the margin of the drill took place as the drill oscillated back and forth, consequently resulted in larger hole diameter in CFRP compared to CD. This is the reason for observing lower diameter difference between the holes in CFRP and Ti during UAD compared to CD, Table 4.3. There was a concern that the larger holes observed during UAD compared to CD was due to the more adherent Ti on the drills. However, as shown in Section 4.2.1, (Figures 4.23, 4.24 and 4.25), drills used for UAD exhibited no marked difference in terms of Ti adhesion compared to the drills used for CD. Hence, the larger hole diameter observed in UAD was attributed to the additional mechanical movement of the drill, forth and backwards, against the hole wall.

In conclusion, the hole diameter was largely affected by the adherent Ti on the cutting edges as a result of increasing cutting speed and heat generation, leading to the removal of more material than intended, hence causing larger hole diameters further from the drill nominal diameter. Using lower cutting speeds of 25 and 50 m/min is important to produce holes that were within H7 tolerance limits (-0.000/+0.015 mm). It is not recommended to use the highest cutting speed of 75 m/min when H7 tolerance limit is required, despite shorter cutting time (and increased productivity), because only less than 10 holes can be drilled within tolerance, Figure 4.48 (c).

A requirement of tighter tolerance limit (e.g. H6: -0.000/+0.009 mm) requires the use of the lowest cutting speed of 25 m/min, however, it is important to note that this means longer cutting time hence a reduction in productivity. Using a higher cutting speed (e.g. 50 m/min) when a tighter tolerance (e.g. H6) is required would lead to part rejection due to oversized holes. An important finding was that at all cutting speeds, UAD caused smaller diameter difference (0 – 2 μm) between the holes in CFRP and Ti, compared to CD which exhibited a larger diameter difference within 1 – 4 μm. It is proposed that a consistent hole diameter between CFRP and Ti in a stack is achieved by applying the ultrasonic oscillation on the drill during the drilling in the feed direction.

4.2.4.2 CFRP delamination (hole entrance)

The ratio of CFRP delamination (F_D) at the hole entrance generated during CD and UAD of CFRP/Ti stacks at cutting speeds of 25, 50 and 75 m/min are compared in Figure 4.50. No apparent trend in the CFRP delamination when increasing cutting speeds was observed during CD and UAD. This observation is in agreement with Xu *et al*. [102], who also reported no distinctive trend in CFRP delamination with the change in cutting speed (from 15 to 60 m/min) when dry drilling of CFRP/Ti stacks although no further explanation was given. In the current study, even though reducing cutting

speed from 75 to 50 to 25 m/min resulted in less tool wear and Ti adhesion on cutting edges, CFRP delamination was not reduced. This means that CFRP delamination at the hole entrance when drilling CFRP/Ti stacks was not largely affected by tool wear and Ti adhesion.

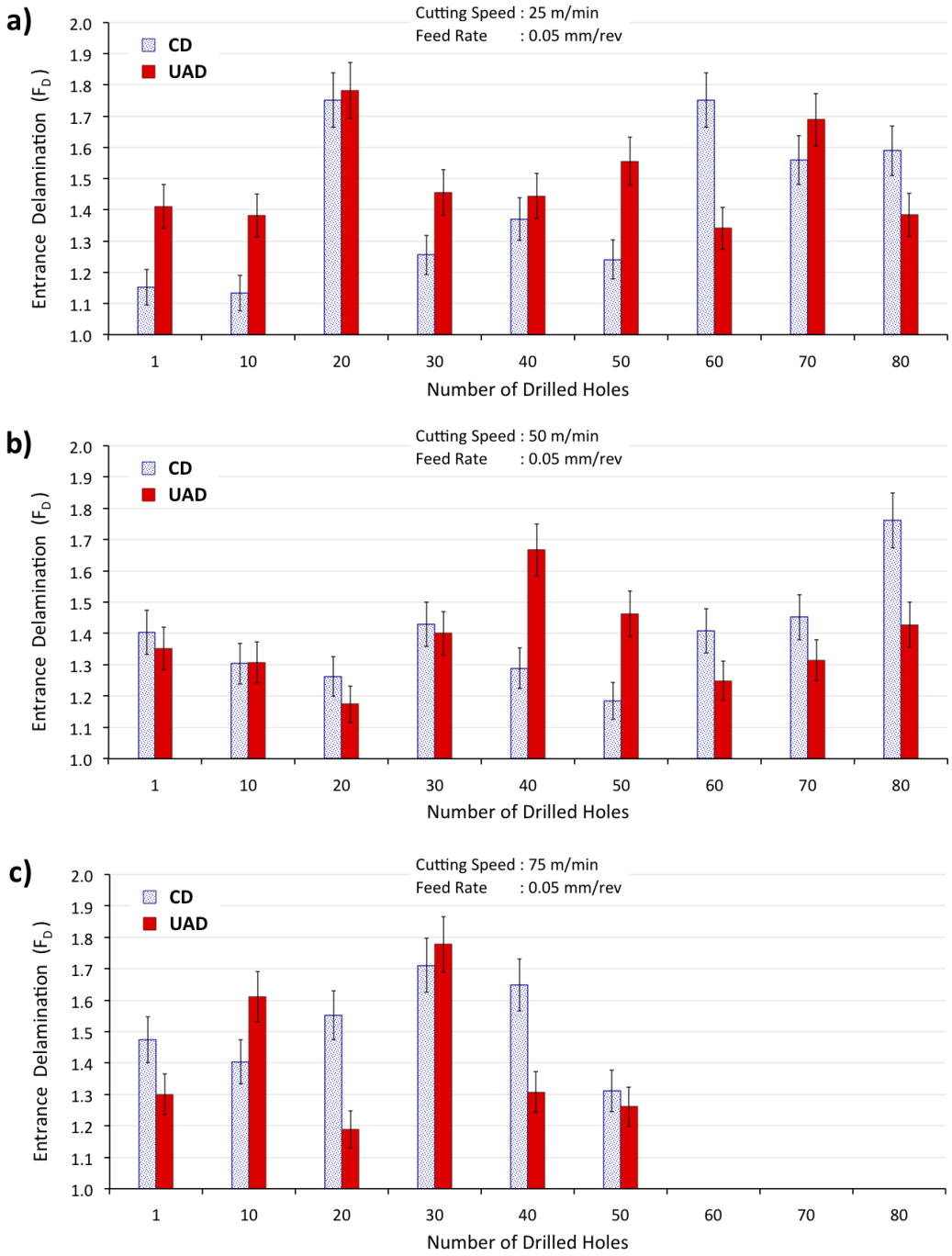

Figure 4.50: Comparison of delamination (F_D) of CFRP at the hole entrance produced by CD and UAD of CFRP/Ti stacks using cutting speeds of (a) 25 m/min, (b) 50 m/min and, (c) 75 m/min at a constant feed rate of 0.05 mm/rev. Range bars indicate variation for three consecutive holes (e.g. hole 1-3, hole 9-11, hole 19-21 etc.)

The CFRP delamination when drilling CFRP/Ti stacks at all cutting speeds was inconsistent and complex due to the interference of the Ti chips, entangling and moving around the drill and on CFRP surface as they evacuated through the CFRP, as discussed previously in Section 4.1.3.2. The fact that Ti chips produced during CD and UAD of CFRP/Ti stacks at all cutting speeds were long and spiral (Figure 4.44), with no marked difference in the morphology and length, justified no distinctive trend in CFRP delamination with respects to cutting speed when either CD or UAD was employed.

4.2.4.3 CFRP pull-out from machined surface

The topography of CFRP machined surfaces produced by CD and UAD at all cutting speeds is compared in Figure 4.51 for the first holes (minimal tool wear), and Figure 4.52 for the 20th holes (increased tool wear). The volume of CFRP pull-out (blue regions) was measured and compared in Figure 4.53. The 20th and 40th holes exhibited averagely 53% (CD) and 64% (UAD) more CFRP pull-out than the first holes, hence confirming the substantial influence of tool wear.

For the first holes drilled, the volume of CFRP pull-out caused by CD and UAD at the highest cutting speed of 75 m/min was 0.12 – 0.13 mm^3, which was 13% – 24% lower than those caused by the lower cutting speeds of 25 and 50 m/min (0.15 – 0.17 mm^3). However, for the 40th holes, the volume of CFRP pull-out caused by CD and UAD at 75 m/min increased to 0.24 – 0.29 mm^3, 17% - 28% higher than those produced at 25 m/min (0.20 – 0.24 mm^3) due to the dominant influence of tool wear. Nevertheless, ANOVA established that the difference in CFRP pull-out caused by different cutting speeds was not statistically significant, Appendix A, Table A.5.

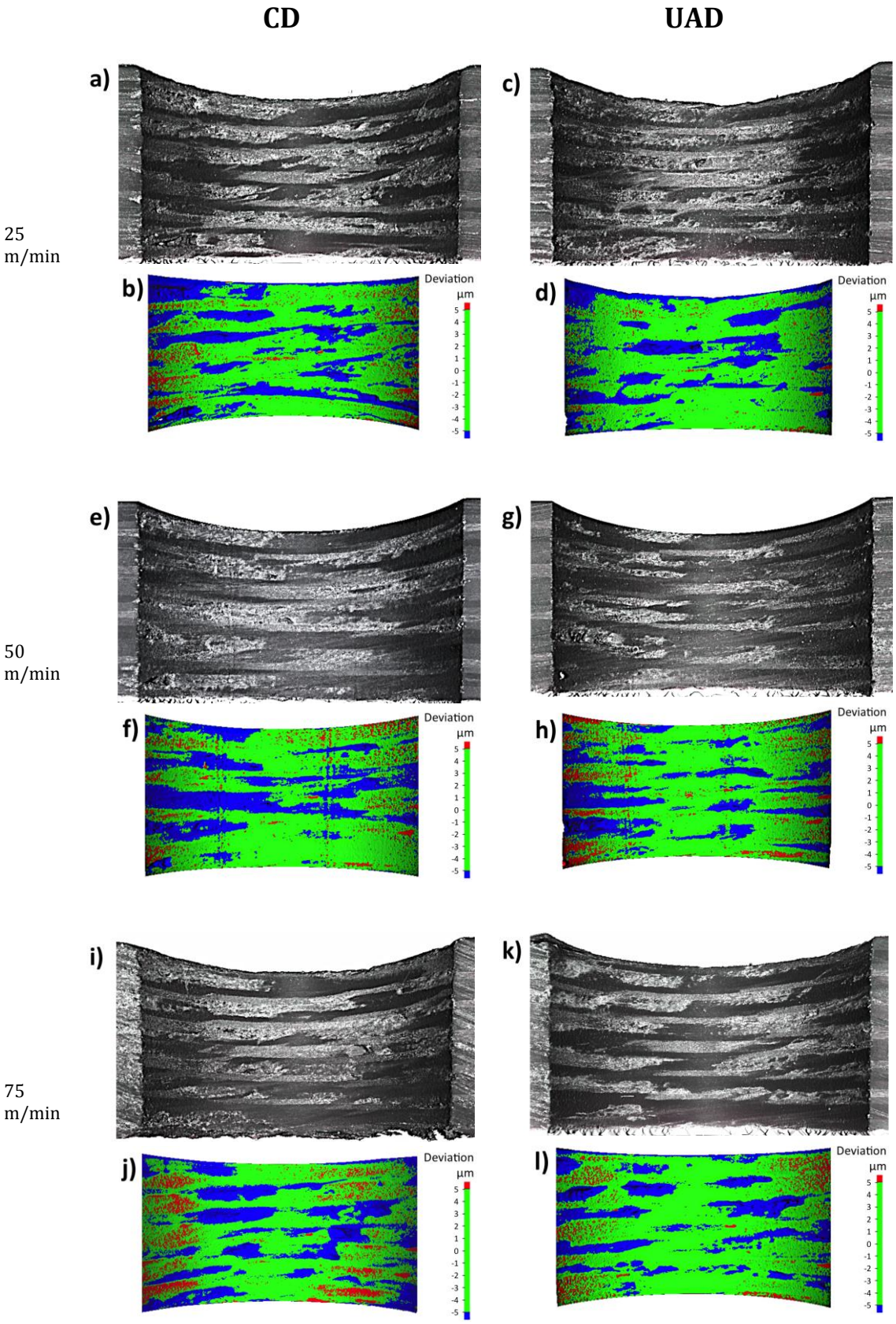

Figure 4.51: Surface topography of machined CFRP surfaces caused by CD and UAD of CFRP/Ti stacks using cutting speeds of (a, b, c, d) 25 m/min, (e, f, g, h) 50 m/min and (i, j, k, l) 75 m/min at a constant feed rate of 0.05 mm/rev – cross section of the 1st holes

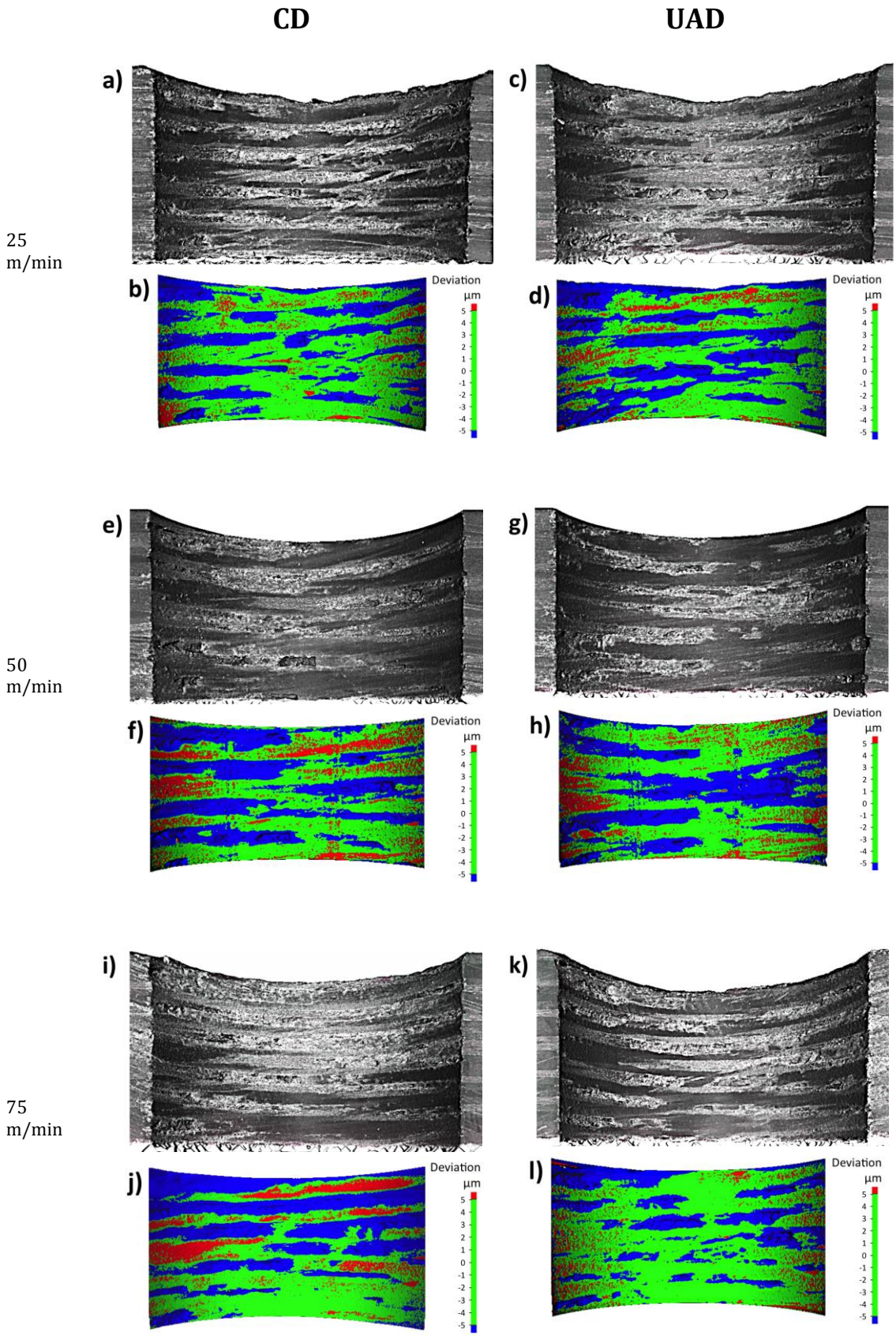

Figure 4.52: Surface topography of machined CFRP surfaces caused by CD and UAD of CFRP/Ti stacks using cutting speeds of (a, b, c, d) 25 m/min, (e, f, g, h) 50 m/min and (i, j, k, l) 75 m/min at a constant feed rate of 0.05 mm/rev – cross section of the 20th holes

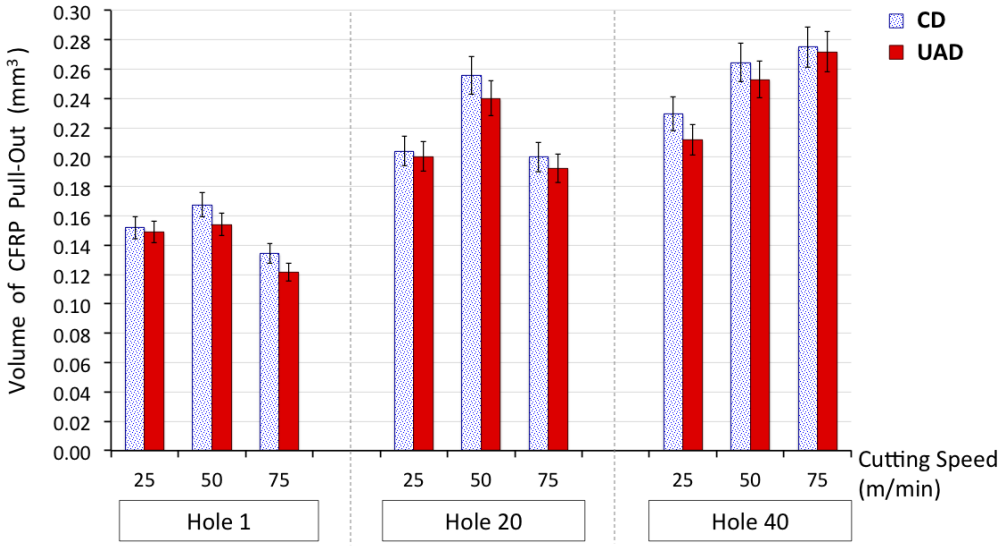

Figure 4.53: Comparison of volume of CFRP pull-out from the machined surfaces caused by CD and UAD of CFRP/Ti stacks using cutting speeds of 25, 50 and 75 m/min at a constant feed rate of 0.05 mm/rev

Although visually in Figure 4.53, there was a slight reduction (on average 5%) in CFRP pull-out during UAD compared to CD, ANOVA established that the difference in the volume of CFRP pull-out caused by UAD compared to CD was not statistically significant, Appendix A, Table A.5. This indicated that the drill oscillation during UAD has no significant influence on reducing CFRP pull-out compared to CD.

SEM images of the machined CFRP surfaces produced by CD and UAD at all cutting speeds, Figures 4.54 and 4.55, revealed the carbon fibres with 45° orientation with respect to cutting direction, suffered major pull out during the drilling operation, which is in agreement with the literature (Section 2.6.4.2). This was due to the direction of the cutting against the fibre orientation. Previous work [166] involving dry drilling of CFRP reported that the polymer matrix suffered thermal damage, which was indicated by observation of a burnt matrix. In the current study, no evidence of burnt polymer matrix was observed on the machined surface of CFRP produced by CD or UAD at all cutting speeds. This may suggest that the heat generated when drilling CFRP was not higher than the Tg of the polymer matrix, which was attributed to the use of cutting fluid, helping to cool the cutting zone.

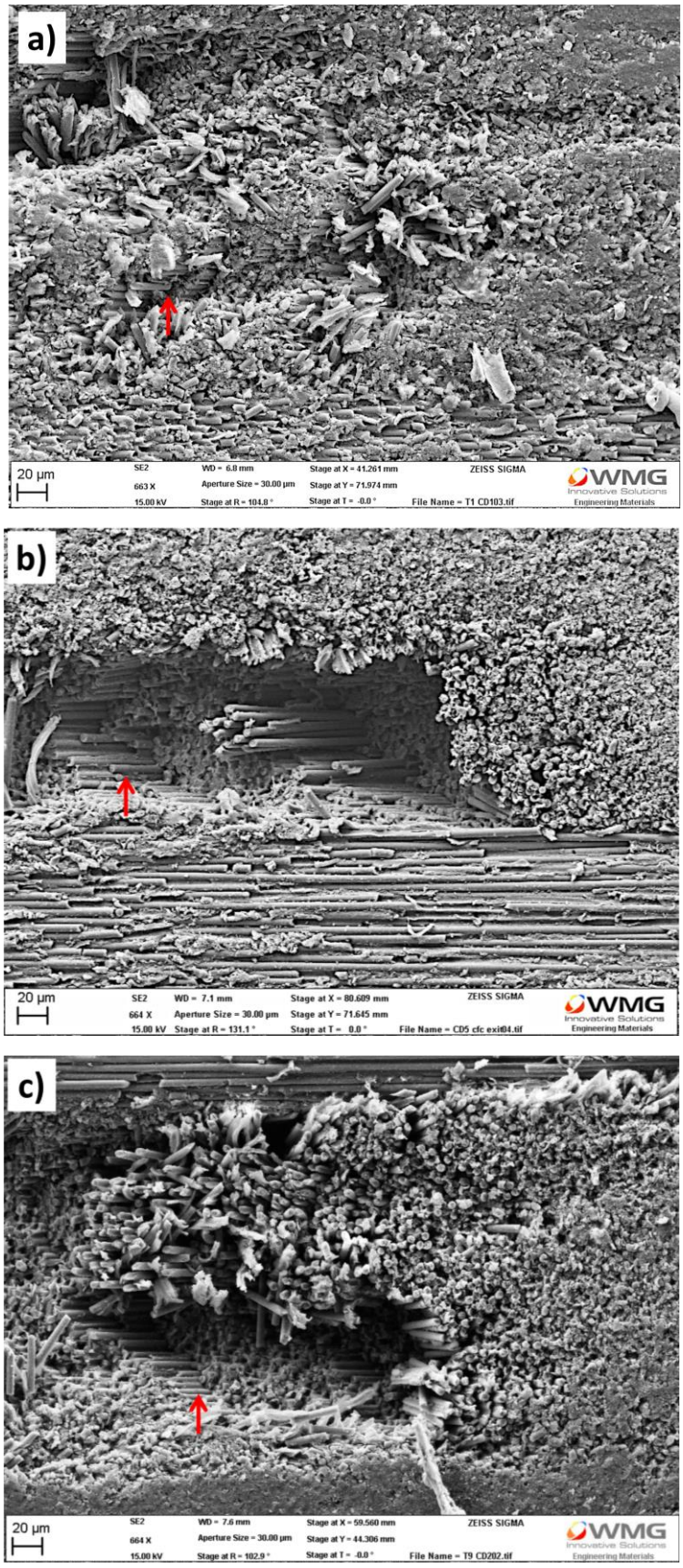

Figure 4.54: SEM micrographs showing typical machined CFRP surfaces in which carbon fibres with 45° orientation exhibiting major pull-out (indicated by the red arrows) during CD of CFRP/Ti stacks using cutting speeds of (a) 25 m/min, (b) 50 m/min and (c) 75 m/min at a constant feed rate of 0.05 mm/rev

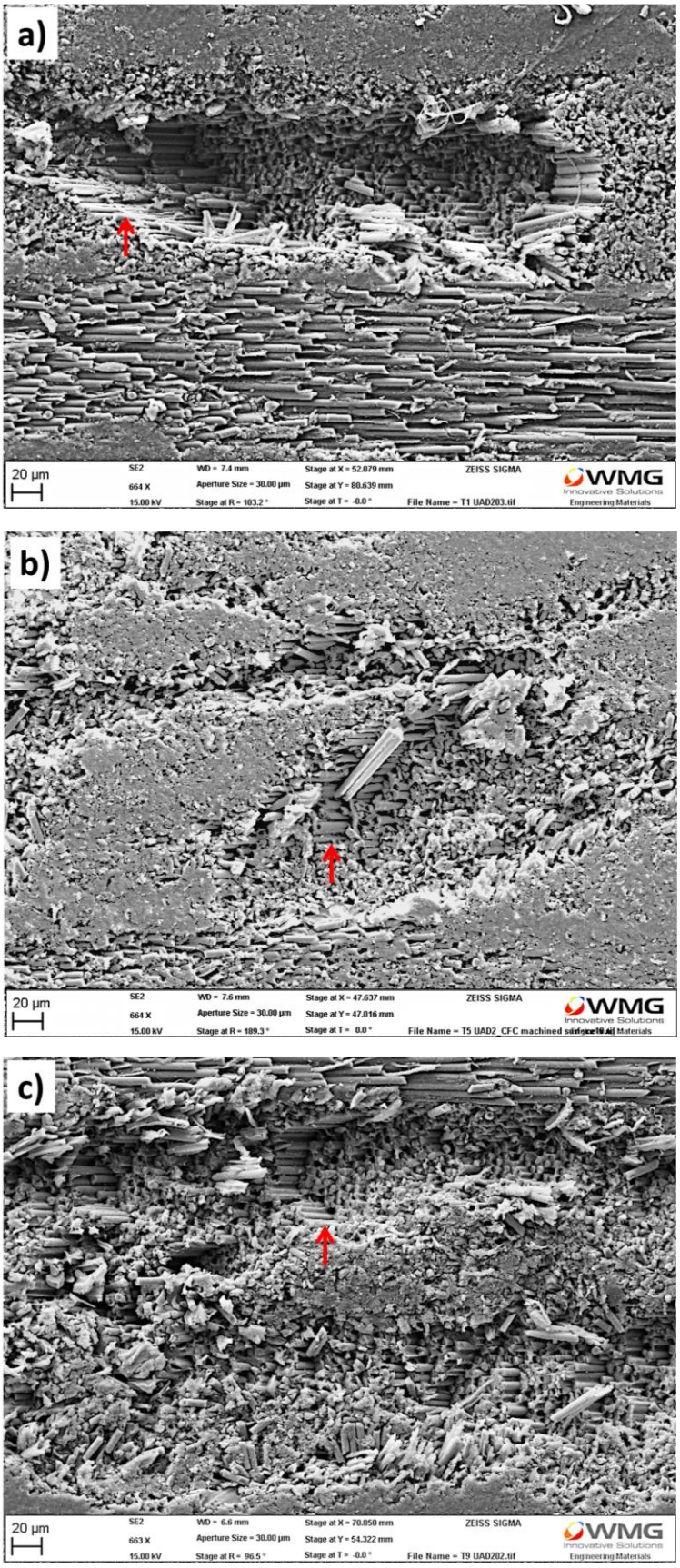

Figure 4.55: SEM micrographs showing typical machined CFRP surfaces in which carbon fibres with 45° orientation exhibiting major pull-out (indicated by the red arrows) during UAD of CFRP/Ti stacks using cutting speeds of (a, b) 25 m/min, (c, d) 50 m/min and (e, f) 75 m/min at a constant feed rate of 0.05 mm/rev

4.2.4.4 Titanium machined surface

The surface integrity of the machined Ti was investigated in terms of topography, surface roughness, sub-surface hardness and residual stress. Understanding the relationship of these features is necessary as a guideline to determine the functional performance of the machined parts. Figures 4.56 and 4.57 compare the surface finish / topography of the first holes produced by CD and UAD in the Ti layer of the stacks at cutting speeds of 25, 50 and 75 m/min.

The machined Ti surfaces produced by CD exhibited linear feed marks, Figure 4.56. The feed marks on the machined Ti surfaces produced by UAD was less visible, rather, the ultrasonic impression is evident, Figure 4.57. Figure 4.58 shows magnified views of the ultrasonic impression, taking the form of sinusoidal waves on the machined Ti surfaces. This was caused by the drill oscillation during UAD. The observation of sinusoidal waves imprinted on the machined surfaces proved that the drills oscillated continuously when the cutting edges touched and removed the workpiece material during UAD at all cutting speeds (which also supported the force data, Section 4.2.2).

It is important to ascertain that the measurement of the amplitude of ultrasonic vibration that was conducted on the non-rotating drill before drilling was consistent when the drill rotates and touches the workpiece. Measurement of the peak-to-peak amplitude of the sinusoidal waves on the machined surfaces of Ti produced by UAD, Figure 4.58, confirmed to be 11 μm, which was equal to the measurement conducted by an external laser device before performing the UAD trials. The length of one cycle of ultrasonic oscillation as indicated by the red sinusoidal waves in Figure 4.58, was observed to increase as the cutting speed increased from 25 m/min, Figure 4.58 (a), to 50 m/min, Figure 4.58 (b) and to 75 m/min, Figure 4.58 (c). This was expected as the drills were rotated faster.

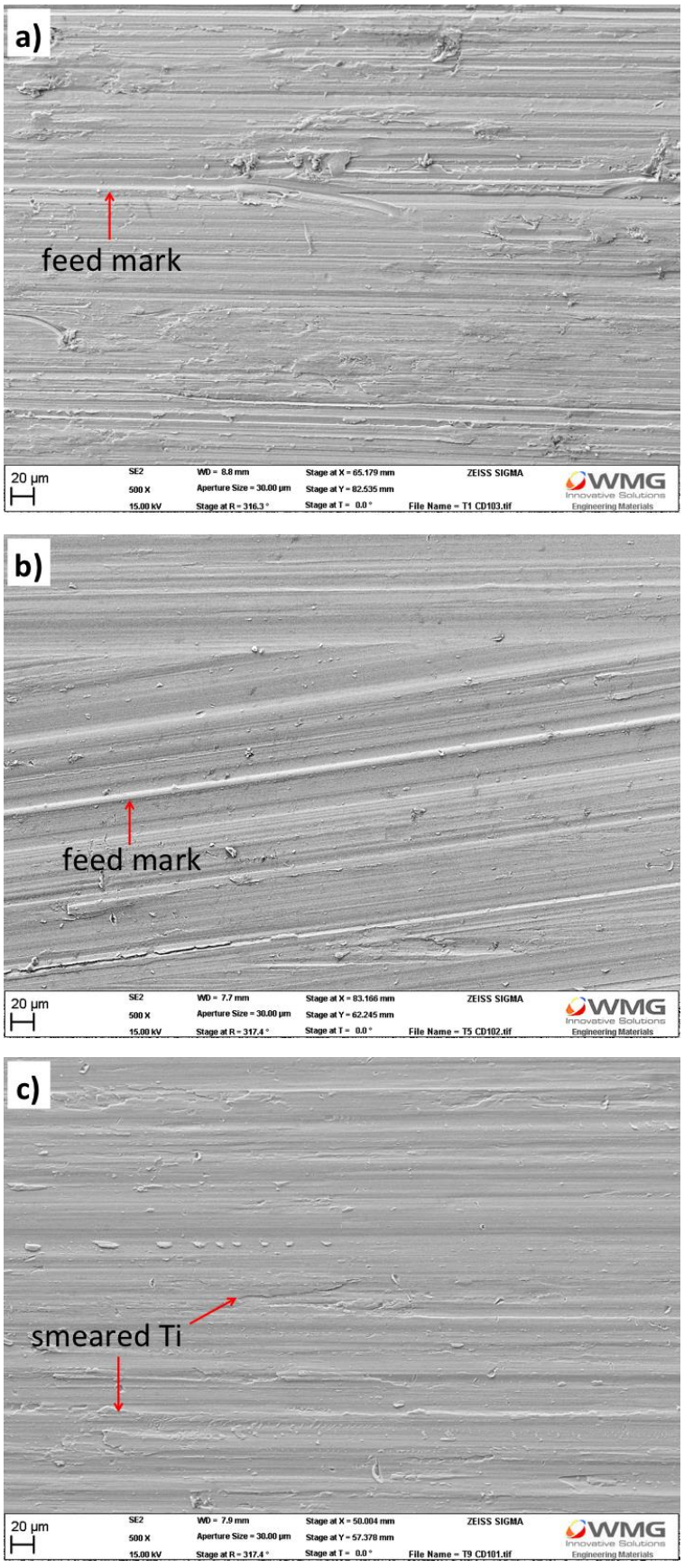

Figure 4.56: SEM micrographs showing machined Ti surfaces produced by CD of CFRP/Ti stacks using cutting speeds of (a) 25 m/min, (b) 50 m/min and (c) 75 m/min at a constant feed rate of 0.05 mm/rev – 1st holes

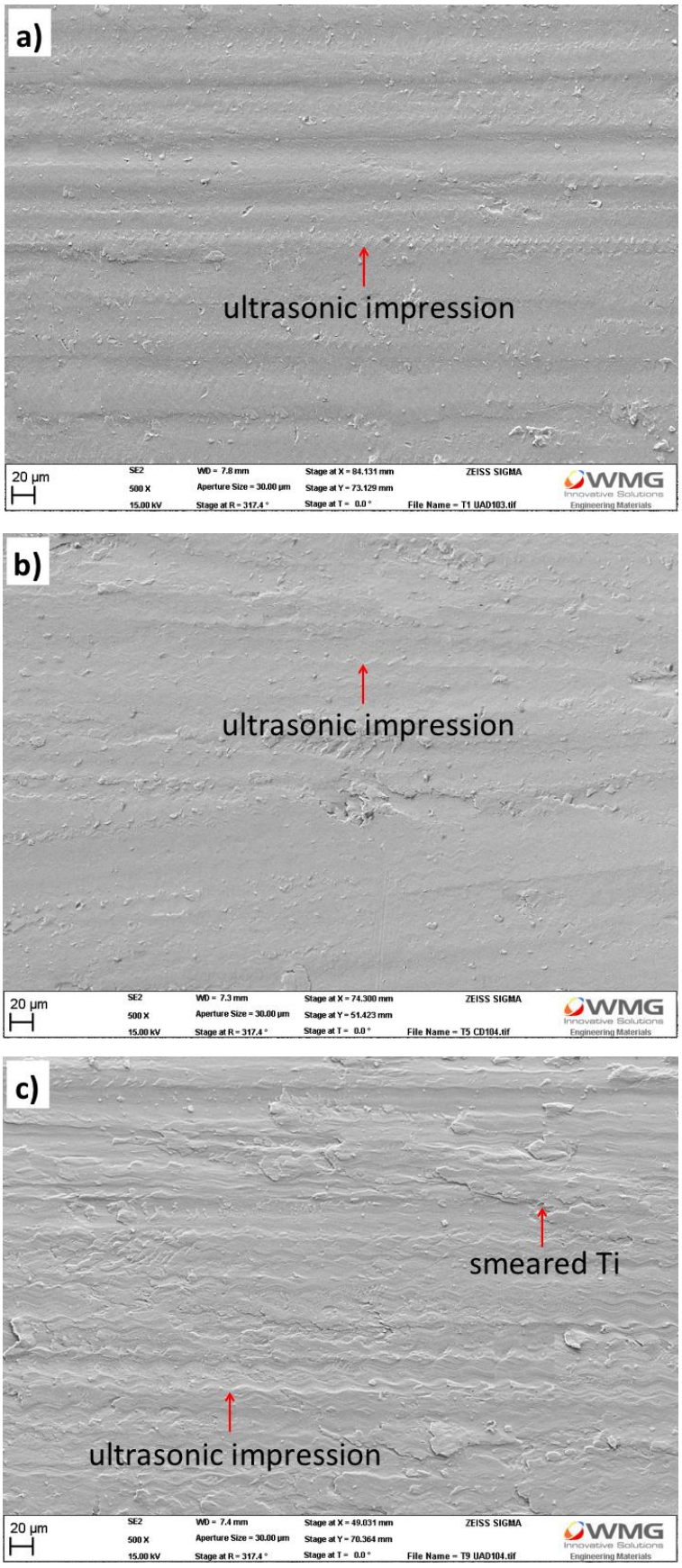

Figure 4.57: SEM micrographs showing machined Ti surfaces produced by UAD of CFRP/Ti stacks using cutting speeds of (a) 25 m/min, (b) 50 m/min and (c) 75 m/min at a constant feed rate of 0.05 mm/rev – 1st holes

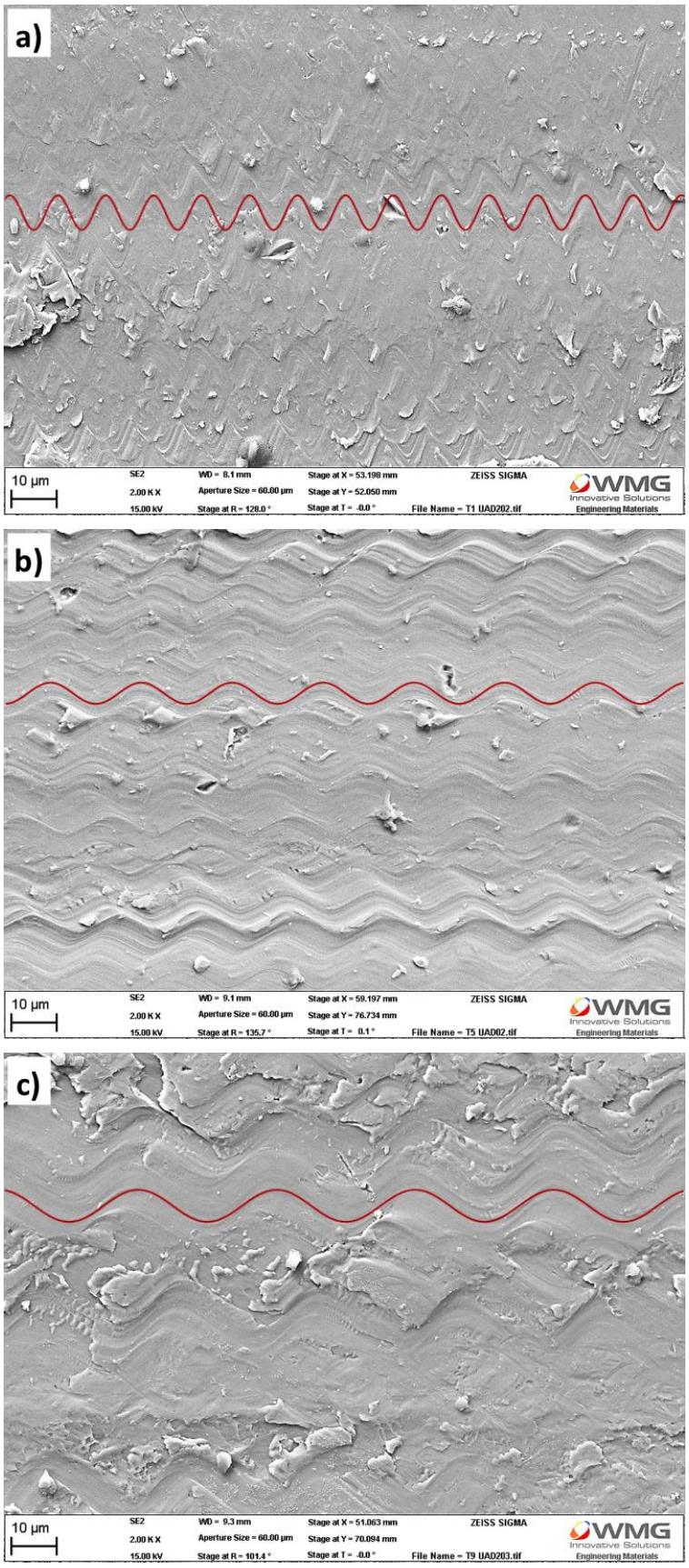

Figure 4.58: SEM micrographs showing ultrasonic impression on machined Ti surfaces, as indicated by red sinusoidal lines, produced by UAD of CFRP/Ti stacks using cutting speeds of (a) 25 m/min, (b) 50 m/min and (c) 75 m/min at a constant feed rate of 0.05 mm/rev – 1st holes

Notably, smeared material was observed on the machined Ti surfaces produced by CD and UAD at the highest cutting speeds of 75 m/min, Figures 4.56 (c) and 4.57 (c). The smeared material on the machined surfaces indicated more softening of the material, which was attributed to greater heat generation when using the higher cutting speed. For the first holes drilled, it is unlikely that the smeared material on the machined surfaces was due to deposition of the adhered Ti on the cutting edges. Even though it was demonstrated previously in Section 4.2.1 that Ti adhesion on the cutting edges was severe when using the higher cutting speeds of 50 and 75 m/min compared to 25 m/min, the severe Ti adhesion did not occur as early as drilling the 1st holes.

The machined surface roughness was quantified in terms of R_a (average roughness), R_z (average depth of peak to valley) and S_a (area roughness, considering measurement in both X and Y directions) and are compared in Figure 4.59. The results showed that the less intense feed marks (as the material was smeared) caused by CD at the highest cutting speed of 75 m/min for the first holes, contributed to lower surface roughness (R_a = 0.85 µm, R_z = 6.80 µm, S_a = 1.20 µm) compared to those produced by CD at the lower cutting speeds of 50 m/min (R_a = 0.96 µm, R_z = 7.00 µm, S_a = 1.33 µm) and 25 m/min (R_a = 1.28 µm, R_z = 12.00 µm, S_a = 1.75 µm), Figure 4.59. The observation of reduced surface roughness of Ti with increasing cutting speed is consistent with previous studies [37, 121, 132]. In contrast, the combination of ultrasonic impression and smeared material on the machined surface of the first hole due to UAD at the highest cutting speed of 75 m/min contributed to higher surface roughness (R_a = 0.83 µm, R_z = 5.00 µm, S_a = 1.14 µm) than those produced by UAD at lower cutting speeds of 50 m/min (R_a = 0.62 µm, R_z = 4.95 µm, S_a = 1.08 µm) and 25 m/min (R_a = 0.75 µm, R_z = 4.80 µm, S_a = 0.96 µm), Figure 4.59. With increasing hole number and adherent Ti on the cutting edges (hole 40), the surface roughness measurement

was observed to fluctuate, Figure 4.59. This was the reason for ANOVA not seeing any significant effect of cutting speed on surface roughness, Appendix A, Table A.6.

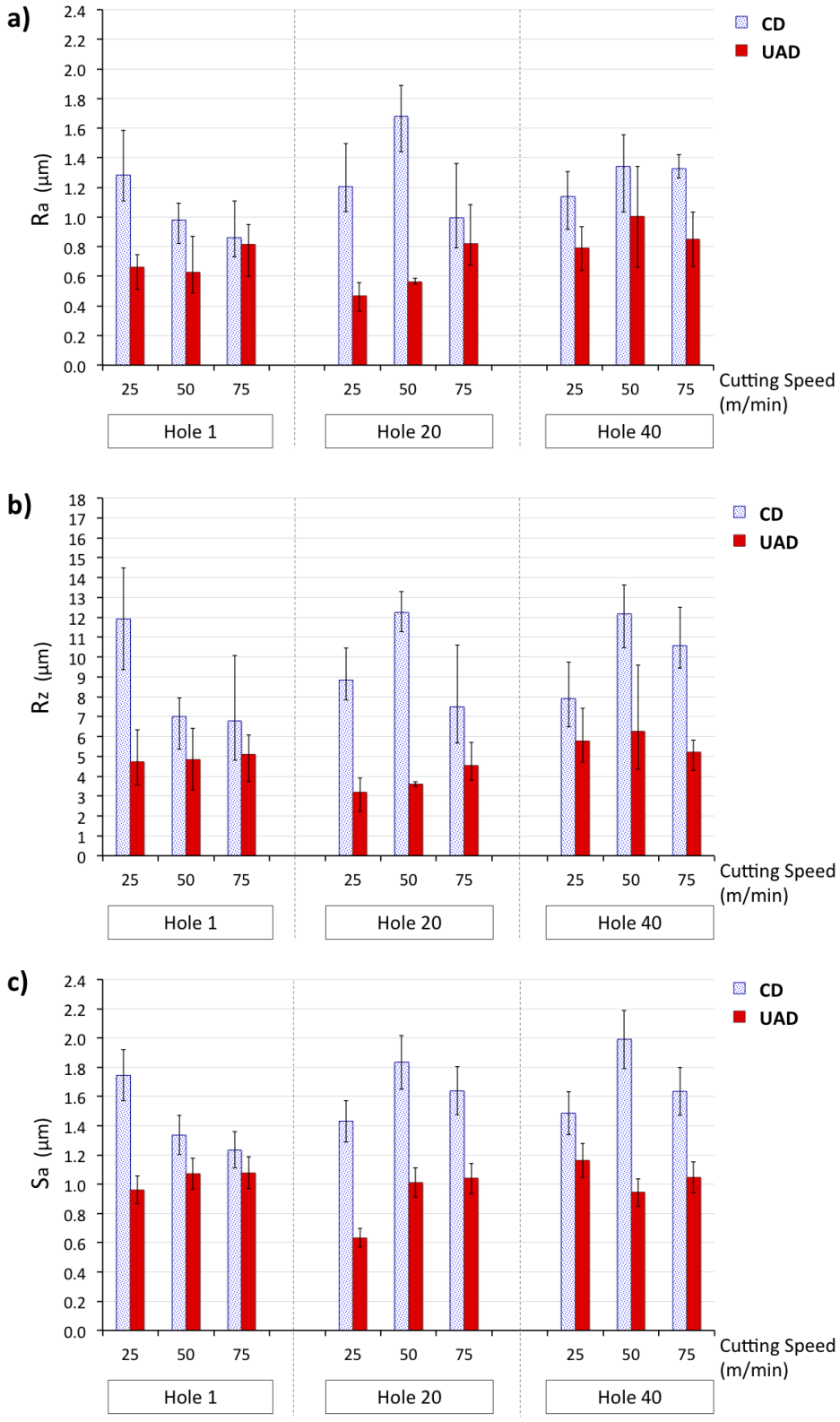

Figure 4.59: Surface roughness, R_a, R_z and S_a of machined Ti surfaces produced by CD and UAD of CFRP/Ti stacks using cutting speeds of 25, 50 and 75 m/min at a constant feed rate of 0.05 mm/rev

Notably, as seen in Figure 4.59, for the first holes and with increasing hole number (hole 20 and hole 40), UAD at all cutting speeds resulted in on average, 34% lower Ti surface roughness (regardless of surface roughness parameters R_a, R_z or S_a) compared to CD. This is in agreement with the previous study [141], which also reported lower R_a (1.2 μm) during UAD of Ti-only compared to CD (R_a = 2.8 μm). The effect of UAD on producing lower Ti surface roughness than CD in the current research was confirmed to be statistically significant by ANOVA, Appendix A, Table A.6. This thesis also presents more evidence, in terms of roughness parameters (R_a, R_z or S_a) and machined surfaces topography.

Ti alloys are known to work harden when subjected to deformation. In any conventional drilling operation, it is typical for the temperature to increase when deforming the material as a result of the mechanical energy being converted into thermal energy. If the heat generation is below the hot working temperature, plastic deformation during drilling causes work hardening of the Ti, which made it stronger and harder. To ascertain the effect of cutting speed and UAD on work hardening or softening of Ti subjected to plastic deformation during drilling, the machined sub-surface hardness of Ti was measured and compared as shown in Figures 4.60 and 4.61.

CD at 25 and 50 m/min resulted in on average 10% – 22% higher hardness (374 – 415 HK) within 10 μm beneath the machined surfaces, for the first holes, Figure 4.60 (a, b), and for the 40th holes, Figure 4.61 (a, b), compared to the bulk Ti workpiece before machining (average hardness of 340 HK). UAD at 25 and 50 m/min was also found to result in 15% – 22% harder (392 – 415 HK) machined Ti sub-surfaces (within 10 μm), Figures 4.60 (a, b) and 4.61 (a, b) than the bulk Ti workpiece. The higher hardness of the machined surfaces than the bulk Ti workpiece is indicative of grain deformation and hardening of Ti during drilling. The grain deformation beneath the machined surfaces is shown in Figure 4.62 and Appendix B, Figure B.7.

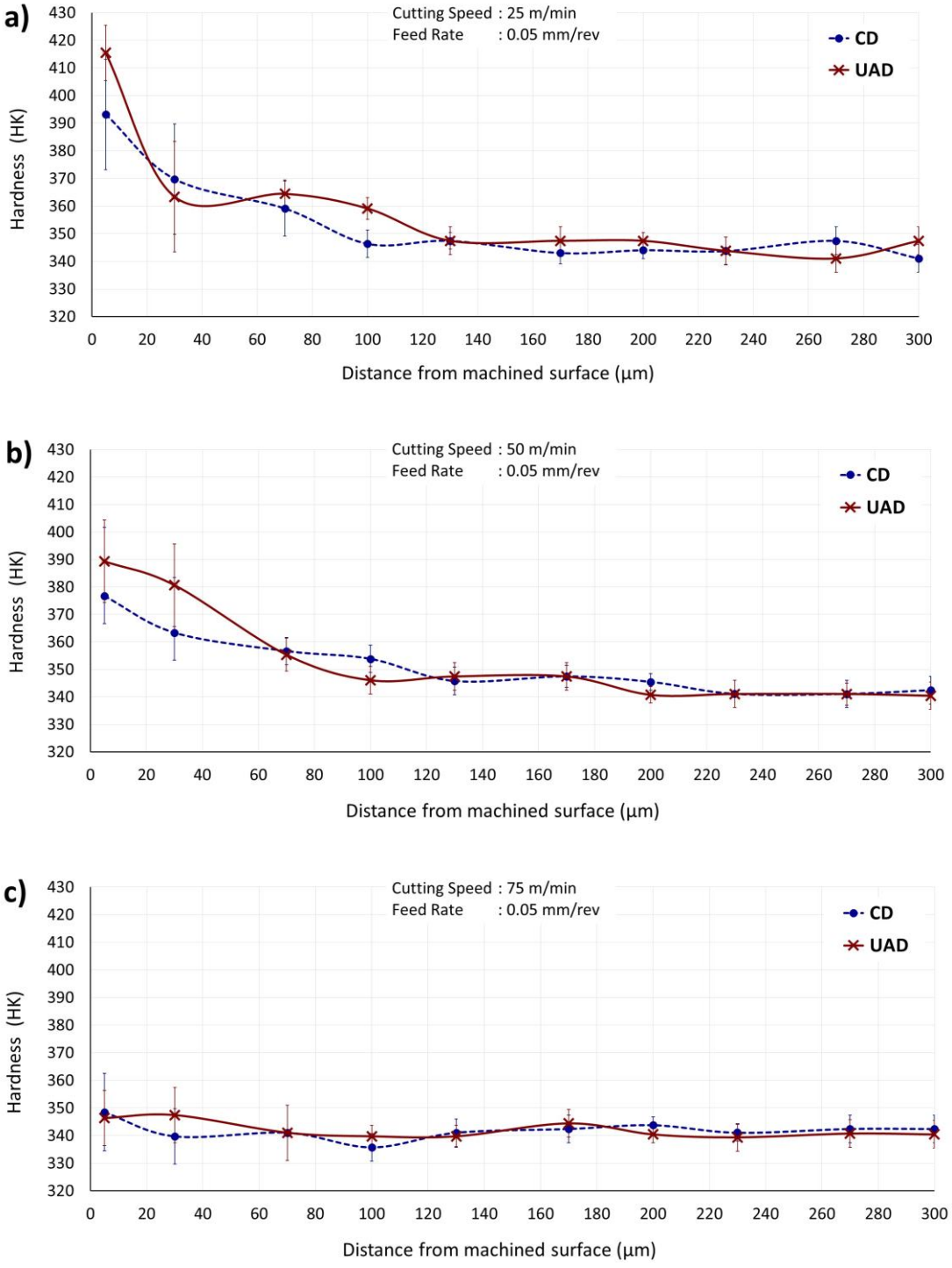

Figure 4.60: Comparison of sub-surface hardness of Ti cross section (within 300 µm from the machined surface) produced by CD and UAD of CFRP/Ti stacks using cutting speeds of 25, 50 and 75 m/min at a constant feed rate of 0.05 mm/rev (Initial Ti hardness before machining = 340 HK) – 1st holes

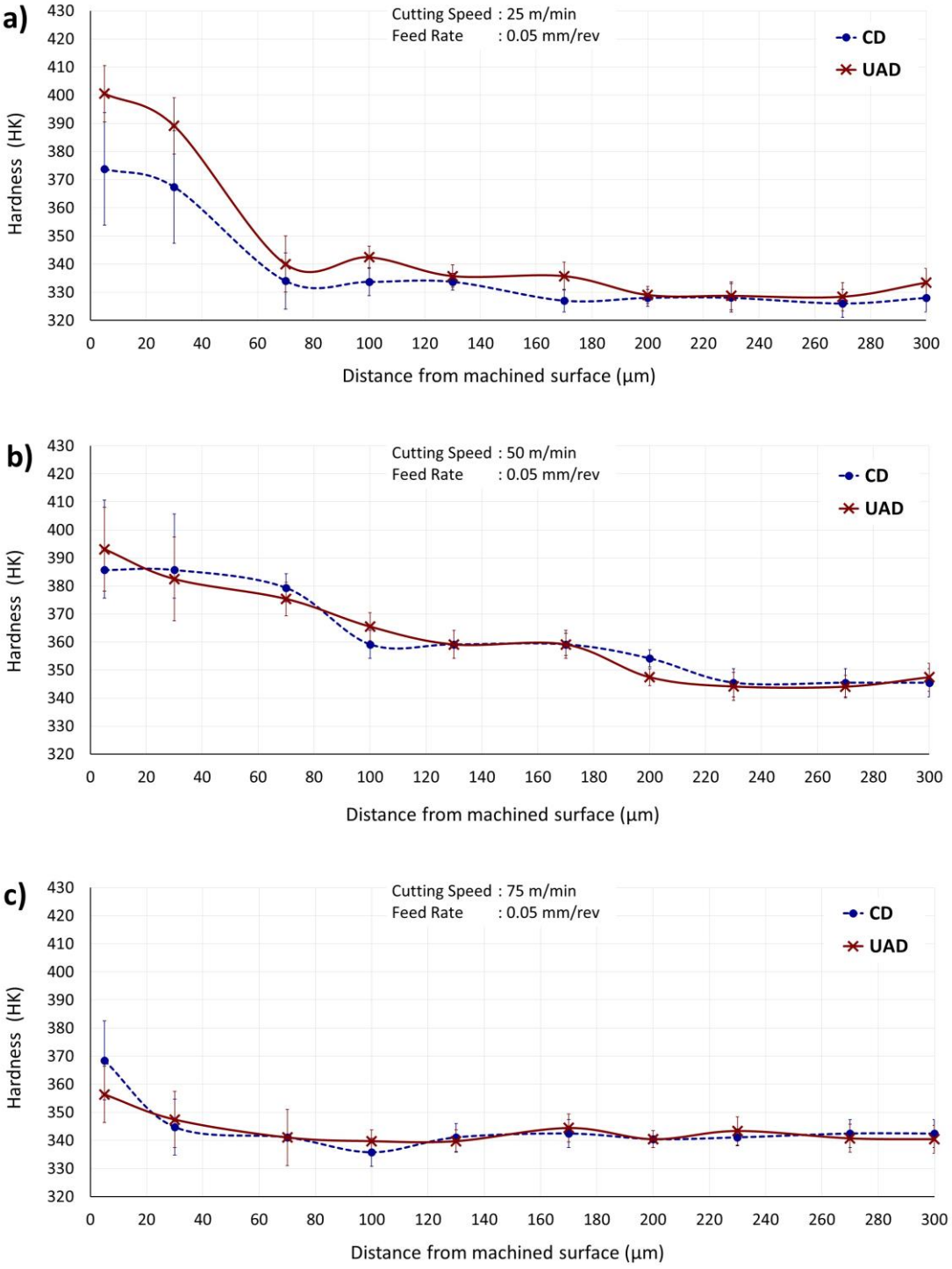

Figure 4.61: Comparison of sub-surface hardness of Ti cross section (within 300 µm from the machined surface) produced by CD and UAD of CFRP/Ti stacks using cutting speeds of 25, 50 and 75 m/min at a constant feed rate of 0.05 mm/rev (Initial Ti hardness before machining = 340 HK) – 40th holes

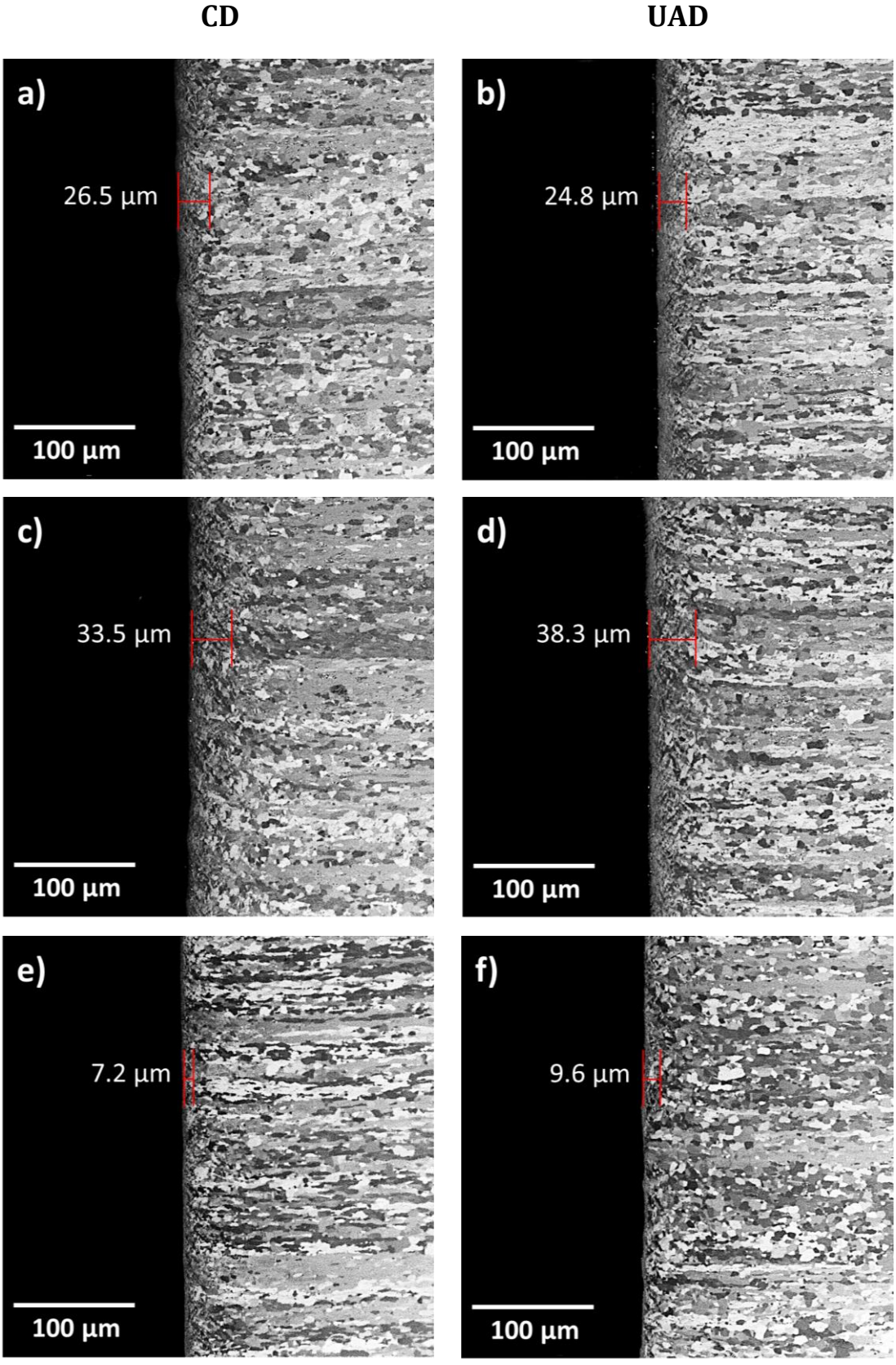

Figure 4.62: Optical microscopy images showing grain deformation beneath machined Ti surfaces when CD and UAD of CFRP/Ti stacks using (a) 25 m/min, (b) 50 m/min and (c) 75 m/min at a constant feed rate of 0.05 mm/rev – 1st holes

As seen in Figures 4.60 (a, b) and 4.61 (a, b), UAD at 25 and 50 m/min caused slightly harder machined Ti sub-surfaces (3% – 6%) than CD. This was likely attributed to more plastic deformation caused by oscillation of the drill during UAD, as shown by the machined Ti surfaces exhibiting ultrasonic impression and less apparent feed marks, Figure 4.57 (a, b).

At the highest cutting speed of 75 m/min, there was no marked difference observed between the hardness of machined Ti sub-surfaces (within 300 μm) produced by CD and UAD (hardness of 330 – 350 HK), Figures 4.60 (c) and 4.61 (c), as well as compared to the Ti workpiece before machining (average hardness of 340 HK). This observation suggests that at the highest cutting speed of 75 /min, the influence of thermal softening exceeding the work hardening of the Ti. As seen in Figures 4.56 (c) and 4.57 (c), material smearing on the machined surface is apparent which supported the effect of dominant thermal softening when drilling using the highest cutting speed of 75 m/min.

The increased hardness of the sub-machined surfaces at lower cutting speeds (25 and 50 m/min) is suggestive of stronger machined components. The increased hardness has been associated with compressive residual stress produced within the material during machining [124-126]. However, it must be noted that whilst work hardening is "permanent" (unless the material is heated), which is governed by plastic deformation of the material and involves microstructural deformation, the presence of residual stress is usually "elastic". This means that the effect would change if the residual stress is relieved.

A limited investigation of the residual stress beneath the machined surfaces of Ti produced by CD and UAD at 50 m/min (1st holes) was conducted. The result, Figure 4.63, shows that the machined surfaces (up to 400 μm beneath the surfaces)

exhibited tensile residual stress, which is indicated by positive values (a negative value indicates compressive residual stress). CD and UAD exhibited no marked difference in the value of tensile residual stress, Figure 4.63. Tensile residual stress is usually undesirable as it may suggest a weakening of the surface. There was no evidence of compressive residual stress, hence this result does not support the association of hardness and compressive residual stress which was suggested by previous work [124-126]. However, this result is in accordance with Paulsen *et al*. [127] involving drilling of Ti-only, which also reported the presence of tensile residual stress (100 - 550 MPa), despite the machined surfaces exhibiting increased hardness than the bulk workpiece. It must be noted that the result of residual stress in this thesis was only based on measurement of two samples (and there was no replication). The limited access to the facilities precluded measurement of more samples. Therefore, further measurement and investigation of the residual strain state around the drilled holes (with increasing hole number and tool wear) will be beneficial and is recommended to allow more accurate characterisation of the residual strain/stress state and its effect on the machined surface integrity.

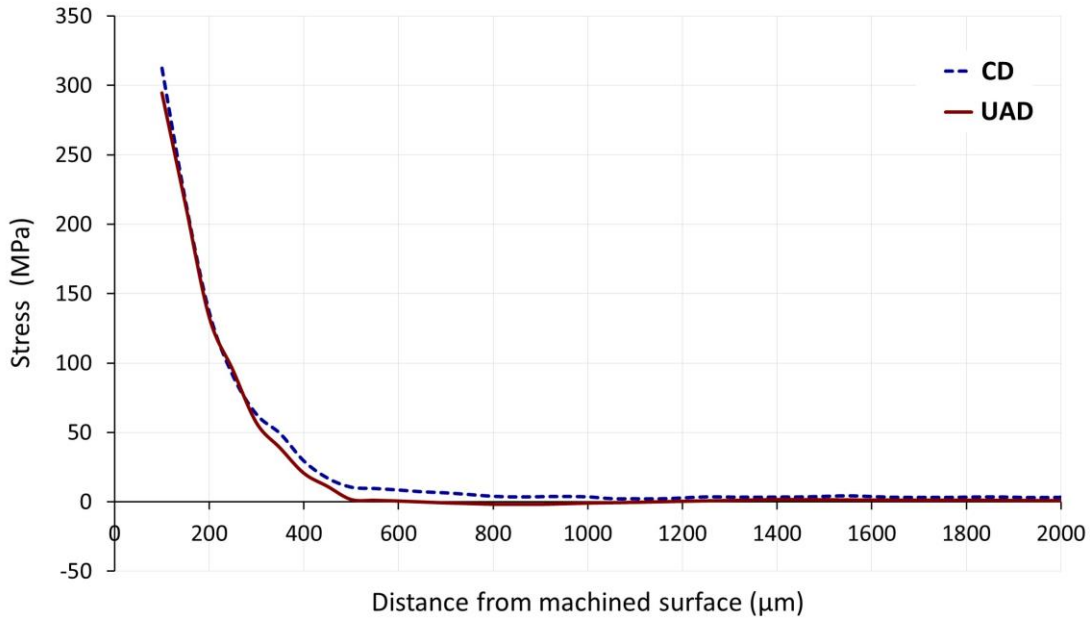

Figure 4.63: Comparison of residual stress of sub-machined surfaces of Ti produced by CD and UAD of CFRP/Ti stacks at a cutting speed of 50 m/min and feed rate of 0.05 mm/rev – 1st holes

4.2.4.5 Titanium burr height (hole exit)

Figure 4.64 shows that Ti burr height increased as the number of holes increased for CD and UAD of CFRP/Ti stacks at all cutting speeds due to increased tool wear.

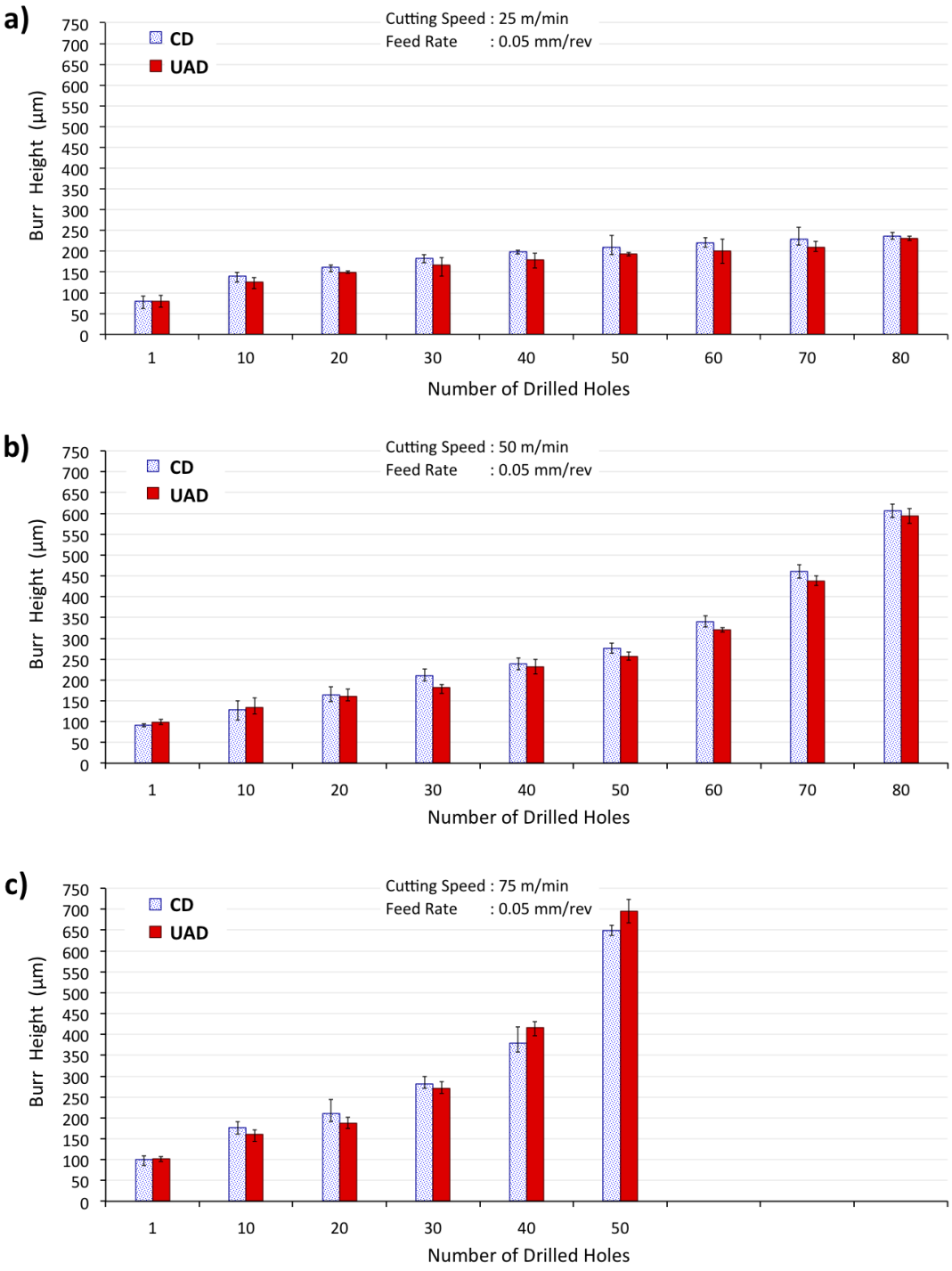

Figure 4.64: Comparison of Ti burr height at the hole exit caused by CD and UAD of CFRP/Ti stacks using cutting speeds of (a) 25 m/min, (b) 50 m/min and, (c) 75 m/min, at a constant feed rate of 0.05 mm/rev. Range bars indicate variation for three consecutive holes (e.g. hole 1-3, hole 9-11, hole 19-21 etc.)

When tool wear was minimal (first holes), no marked difference in Ti burr height produced by all cutting speeds was observed, Figure 4.64. As more holes were drilled, CD and UAD at the lowest cutting speed of 25 m/min was observed to cause the slowest rate of Ti burr height progression up to 80 holes, Figure 4.64 (a). Whereas, drilling with the highest cutting speed of 75 m/min resulted in the fastest increase in Ti burr height, Figure 4.64 (c). On average, Ti burr height increased by 56% with increasing cutting speed from 25 to 50 m/min. Further increasing cutting speed from 50 to 75 m/min increased the Ti burr height by 65%.

The trend in Ti burr height caused by CD and UAD of CFRP/Ti stacks at all cutting speeds, Figure 4.64, was observed to mirror the trend in tool wear, Figure 4.22. ANOVA established that the difference between Ti burr height data generated by drilling with different cutting speeds was statistically significant, Appendix A, Table A.7. This indicated that Ti burr height was significantly affected by cutting speed and tool wear. However, the difference in Ti burr height produced by CD and UAD at respective cutting speeds was found to be not statistically significant by ANOVA, Appendix A, Table A.7. This indicated that the use of UAD on CFRP/Ti stacks at all cutting speeds did not significantly change the burr formation compared to CD, which was consistent with the results of tool wear. The observation of no significant difference in Ti burr between CD and UAD is in agreement with Sanda *et al*. [141], although they did not provide further explanation. In this thesis, ANOVA was used to establish the non-significant effect of UAD on Ti burr height, and the result was correlated to the result of tool wear.

Burr during drilling occurs due to incomplete shearing of the workpiece materials, which is attributed to drilling with worn cutting edges, higher thrust forces as well as increased ductility or plastic flow of the workpiece material [32]. Optical micrographs of the Ti burr cross-section (of the 40th holes) produced by CD and UAD at all cutting speeds are shown in Figure 4.65. For all drilling tests, evident deformation and flow of

Ti grains was observed along the machined surfaces, indicative of resistance in cutting and shearing the material. This indicated that rather than shearing, the Ti grains were "pushed" (deformed to higher strain) by the worn cutting tool, thereby resulting in a burr at the hole exit.

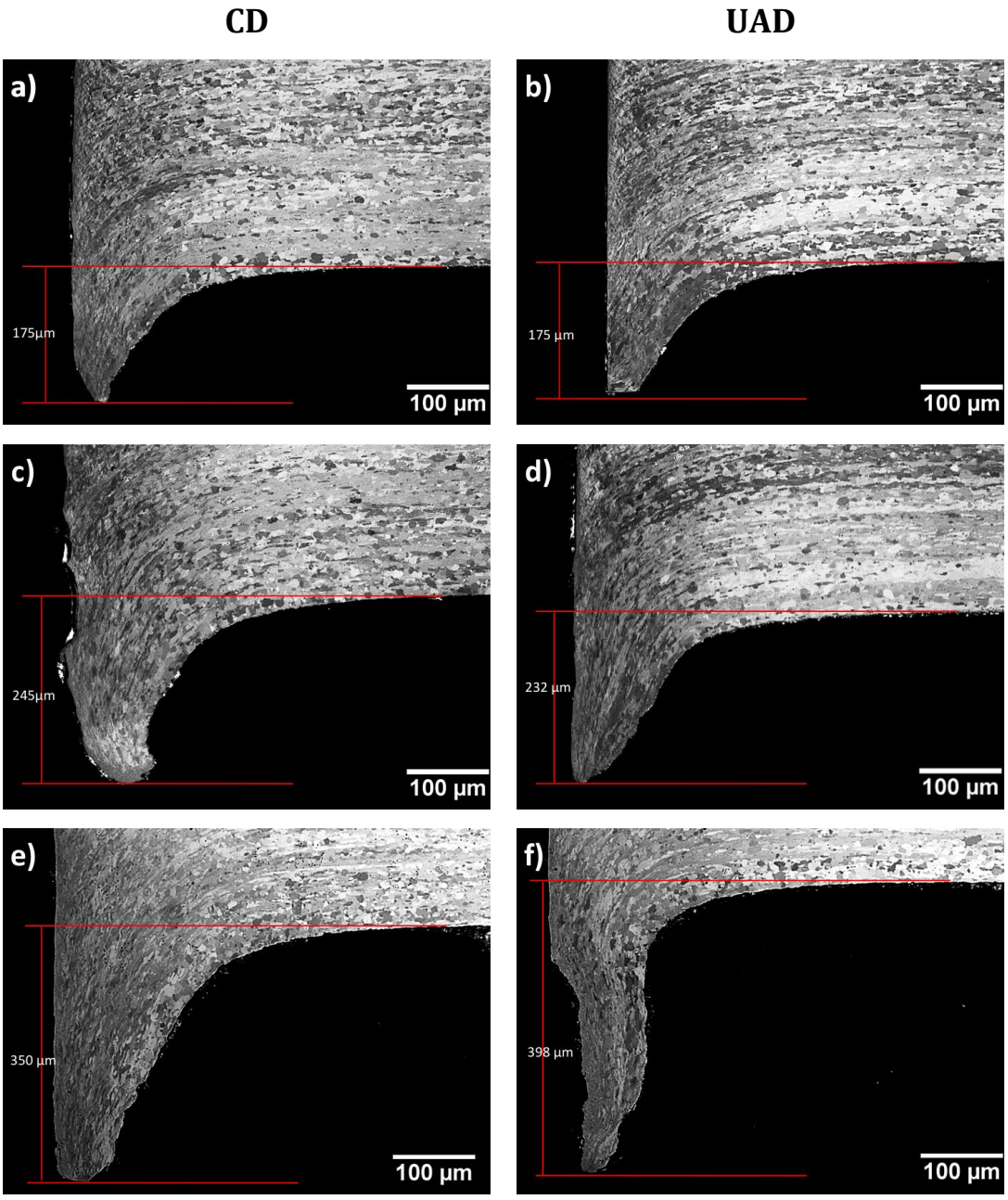

Figure 4.65: Cross section of Ti burr at the exit of the 40th holes caused by CD and UAD of CFRP/Ti stacks using cutting speeds of (a, b) 25 m/min, (c, d) 50 m/min and (e, f) 75 m/min at a constant feed rate of 0.05 mm/rev

Specifically, for the 40th holes, the drills used for drilling at the highest cutting speed of 75 m/min exhibited the highest tool wear (flank wear CD = 220 µm, UAD = 260 µm, as in Figure 4.22), consequently the Ti grains were "pushed" to a higher extent, leading to the highest burr of 350 µm for CD, and 398 µm for UAD, Figure 4.65 (e, f). Whereas, at the lowest cutting speed of 25 m/min, after 40th holes, Figure 4.65 (a, b), lower Ti burr of 175 µm for CD and UAD was observed due to the lowest tool wear (CD = 80 µm, UAD = 77 µm, Figure 4.22). This observation is consistent with the literature [37, 39], which reported a significant effect of increasing tool wear on increasing Ti burr height.

Although this research has shown that decreasing cutting speed reduced the Ti burr due to less tool wear rate, producing a burr-free hole in this work was not possible. The burr formation having a height of 78 – 100 µm was noted as early as drilling the first holes for all cutting speeds, Figure 4.64, despite the sharp cutting edges. This suggests that the geometry of the drills employed in the current study was not optimal to produce burr-free holes. The burr formation is suggested to be governed by drill geometry; a drill that has a smaller point angle with chamfered margin edge was reported to reduce the burr formation [167]. The point angle of the drills in the current work was 140° (Figure 3.4), considered large enough to create a higher resistance between the cut at the margin edge during drilling, consequently leaving higher burr, compared to the drill with a smaller point angle [114]. Nevertheless, when drilling Ti alloy, the large point angle is preferable to strengthen the drill in order to avoid rapid drill fracture. Since no significant difference in Ti burr produced by CD and UAD (at respective cutting speeds) was observed, it is concluded that oscillating the drills (with a peak-to-peak amplitude of 11 µm and frequency of 40 kHz) in UAD was not able to eliminate the Ti burr formation during drilling with this drill geometry. To produce burr-free holes, further research on drill geometry would be beneficial.

4.2.5 Conclusions from Study 2

In summary, when drilling CFRP/Ti stacks, cutting speed has a significant effect on tool wear, hole diameter and Ti burr height, as confirmed by ANOVA. The effect of cutting speed on CFRP damage and Ti surface roughness was confirmed to be not statistically significant by ANOVA. Tool wear reduced and longer tool life was achieved when drilling CFRP/Ti stacks with decreasing cutting speed. The longest tool life (extrapolated = 160 holes) was achieved when drilling (CD and UAD) with the lowest cutting speed of 25 m/min due to minor Ti adhering to the cutting edges, and the cutting edges wore gradually and uniformly by abrasive wear mechanism. Consequently, consistent hole diameter within H7 tolerance (-0.000/+0.015 mm), closer to the drill nominal diameter and the least Ti burr was achieved when using the lowest cutting speed of 25 m/min. In contrast, drilling with the highest cutting speed of 75 m/min caused the shortest tool life (35 holes) due to severe Ti adhering to the cutting edges leading to substantial cutting edge fragmentation. This caused larger hole diameter (by 10 – 18 μm), 30% of the holes were out of H7 tolerance, and rapid increase in Ti burr height.

With regards to UAD application as compared to CD, no marked difference in tool wear, Ti adhering to the cutting edges and cutting edges condition was observed when using cutting speeds of 25 and 50 m/min. However, at the highest cutting speed of 75 m/min, UAD caused more rapid and substantial cutting edges fragmentation compared to CD. Investigation of cutting force profile and Ti chip morphology established that the cutting during UAD at all cutting speeds was continuous similar to CD, although UAD exhibited 24% – 43% larger force variation compared to CD at all cutting speeds.

UAD did not significantly reduce tool wear, CFRP delamination, CFRP pull-out and Ti burr height compared to CD. Nevertheless, the application of UAD was favourable in

producing consistent hole diameters between CFRP and Ti, as well as improving machined surface integrity (increased hardness and lower roughness) compared to CD particularly at 25 and 50 m/min. It must be noted that even though using a lower cutting speed (25 m/min) is favourable for reducing tool wear and Ti adhesion on the cutting edges, this also increased cutting time, hence reducing productivity. Productivity when drilling is increased with an increase in feed rate. Therefore, the effect of feed rate during CD and UAD of CFRP/Ti stacks on tool wear and hole quality were investigated and discussed in the following Section 4.3.

4.3 Study 3: The effect of feed rate during CD and UAD of CFRP/Ti stacks

This study was designed to investigate the effect of feed rate during Conventional Drilling (CD) and Ultrasonic Assisted Drilling (UAD) of CFRP/Ti stacks using reground cemented carbide (WC-Co) drills on tool wear and hole quality. The feed rate was varied at 0.025, 0.05 and 0.075 mm/rev with a constant cutting speed of 50 m/min.

4.3.1 Tool wear mechanisms

Figure 4.66 shows that the flank wear when drilling CFRP/Ti stacks decreased with increasing feed rate. Using the highest feed rate of 0.075 mm/rev during CD and UAD of CFRP/Ti stacks was advantageous as it resulted in the longest tool life of 130 holes (extrapolated), Figure 4.66.

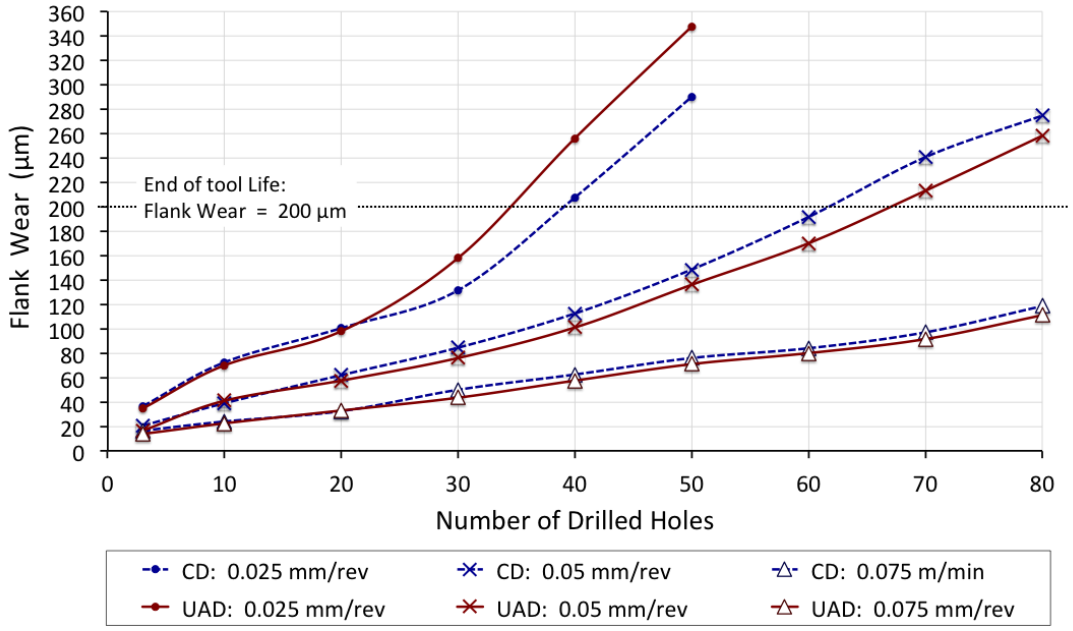

Figure 4.66: Comparison of flank wear during CD and UAD of CFRP/Ti stacks using feed rates of 0.025, 0.05 and 0.075 mm/rev at a constant cutting speed of 50 m/min

ANOVA was used to establish that the difference between flank wear when drilling with different feed rates of 0.025, 0.05 and 0.075 mm/rev was statistically significant, although the difference between CD and UAD was confirmed to be not statistically

significant, Appendix A, Table A.8. As can be seen in Figure 4.66, the results of flank wear during UAD of CFRP/Ti stacks replicated those of CD at respective feed rates.

It is interesting to note that tool wear reduced when drilling CFRP/Ti stacks with increasing feed rate, which contradicted the effect of cutting speed. Increasing feed rate during drilling means removing more materials with reduced cutting time. Increasing feed rate from 0.025 to 0.05 to 0.075 mm/rev reduced the cutting time from 7.2 to 3.7 to 2.5 seconds per hole in a CFRP/Ti stack (for both CD and UAD). The reduction in cutting or contact time between the cutting edges and the workpiece when drilling (CD and UAD) with higher feed rate is beneficial to minimise the heat build-up in the cutting zone. In addition, using a higher feed rate indicated that there was less contact between cutting edges and abrasive CFRP, which contributed to less tool wear.

Figure 4.67 shows cutting edge condition after CD and UAD of 30 and 80 holes through CFRP/Ti stacks using the highest feed rate of 0.075 mm/rev. Limited Ti adhesion on the cutting edges was observed. SEM investigation as shown in Figure 4.68 confirmed that Ti masked the cutting edges, nevertheless, no visible Ti adhesion was observed on flank face of the drills. CD and UAD were observed to exhibit no marked difference in Ti adhesion on the cutting edges, Figures 4.67 and 4.68.

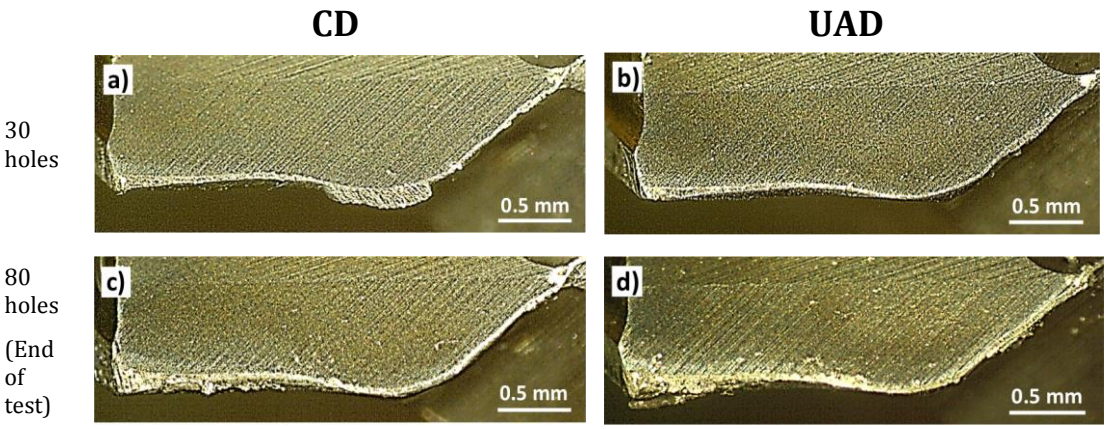

Figure 4.67: Cutting edge condition after CD and UAD of (a, b) 30 holes and (c, d) 80 holes through CFRP/Ti stacks using a feed rate of 0.075 mm/rev and cutting speed of 50 m/min

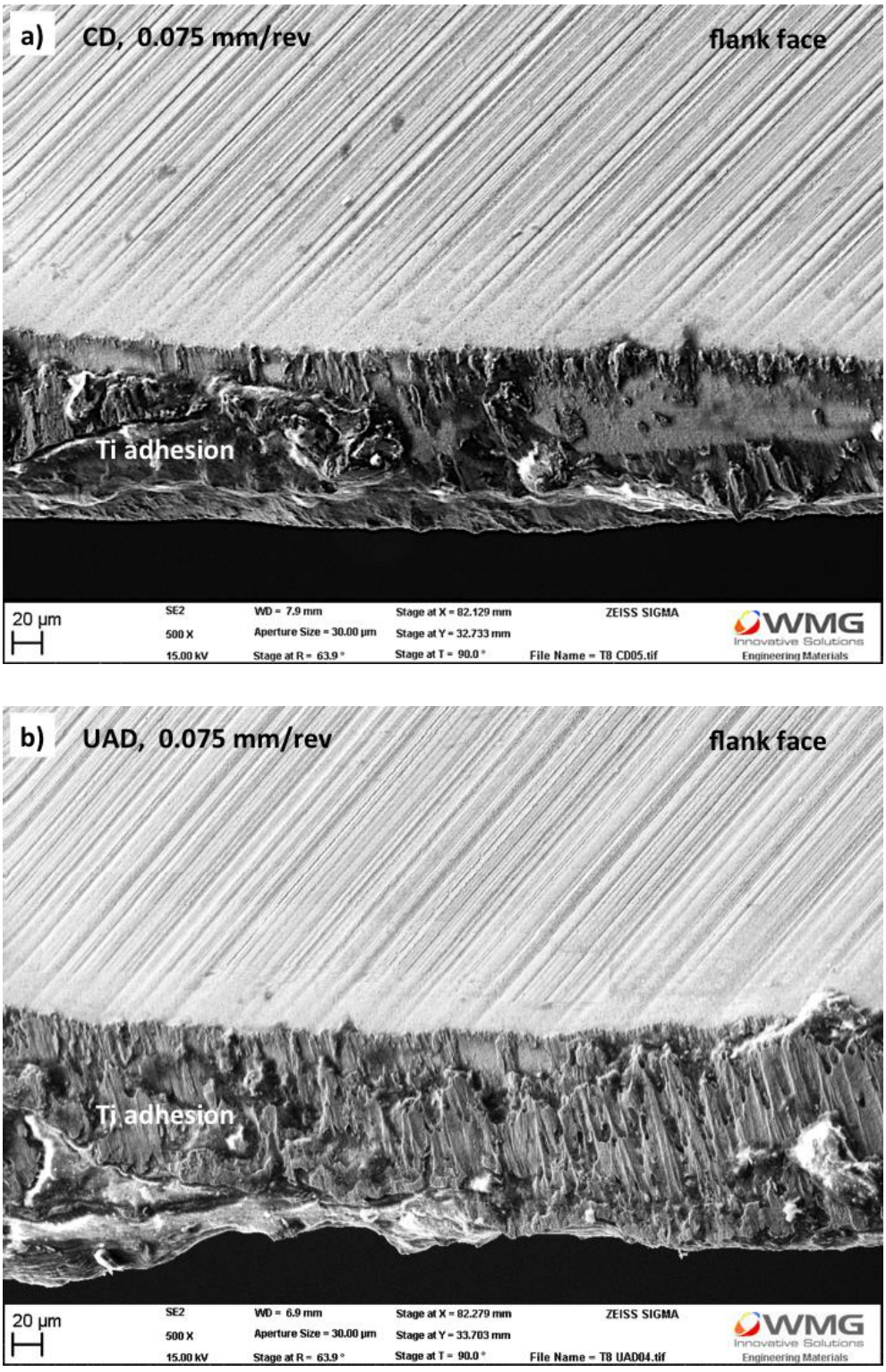

Figure 4.68: SEM micrographs showing morphology of adhered Ti on the cutting edge, and flank face condition after (a) CD and (b) UAD, of 80 holes through CFRP/Ti stacks using a feed rate of 0.075 mm/rev and cutting speed of 50 m/min

Following removal of the adherent Ti (by drilling through a hole in CFRP) on the cutting edges used for CD and UAD at the highest feed rate of 0.075 mm/rev, minor fragmentation (width of 28 – 40 μm) at few areas along the cutting edges was observed, Figure 4.69. The fragmentation of cutting edges was attributed to the effect of exerting a higher load on the cutting edges when using the high feed rate of 0.075 mm/rev. Yet, the fragmentation is regarded as minor up to drilling 80 holes, since it did not substantially change the shape of the cutting edges. The fragmentation was within the cutting edges and it did not extend beyond the width of cutting edges (the width of the cutting edge was 70 μm), Figure 4.69.

Further SEM investigation, showing preferential removal of Co binder between WC grains at the worn cutting edges for the feed rate of 0.075 mm/rev is attached in Appendix B, Figure B.5. The preferential removal of Co binder was attributed to the abrasion by carbon fibres as discussed previously in Sections 4.1.1.1 and 4.2.1.

Further SEM investigation on the rake face of the drills used for CD and UAD with the highest feed rate of 0.075 mm/rev was conducted, Figure 4.70. The TiAlN coating at the rake face remained intact, and no fracture and crater was observed on other part of the drills used for CD, Figure 4.70 (a) and UAD, Figure 4.70 (b). No marked difference was observed between CD and UAD drills.

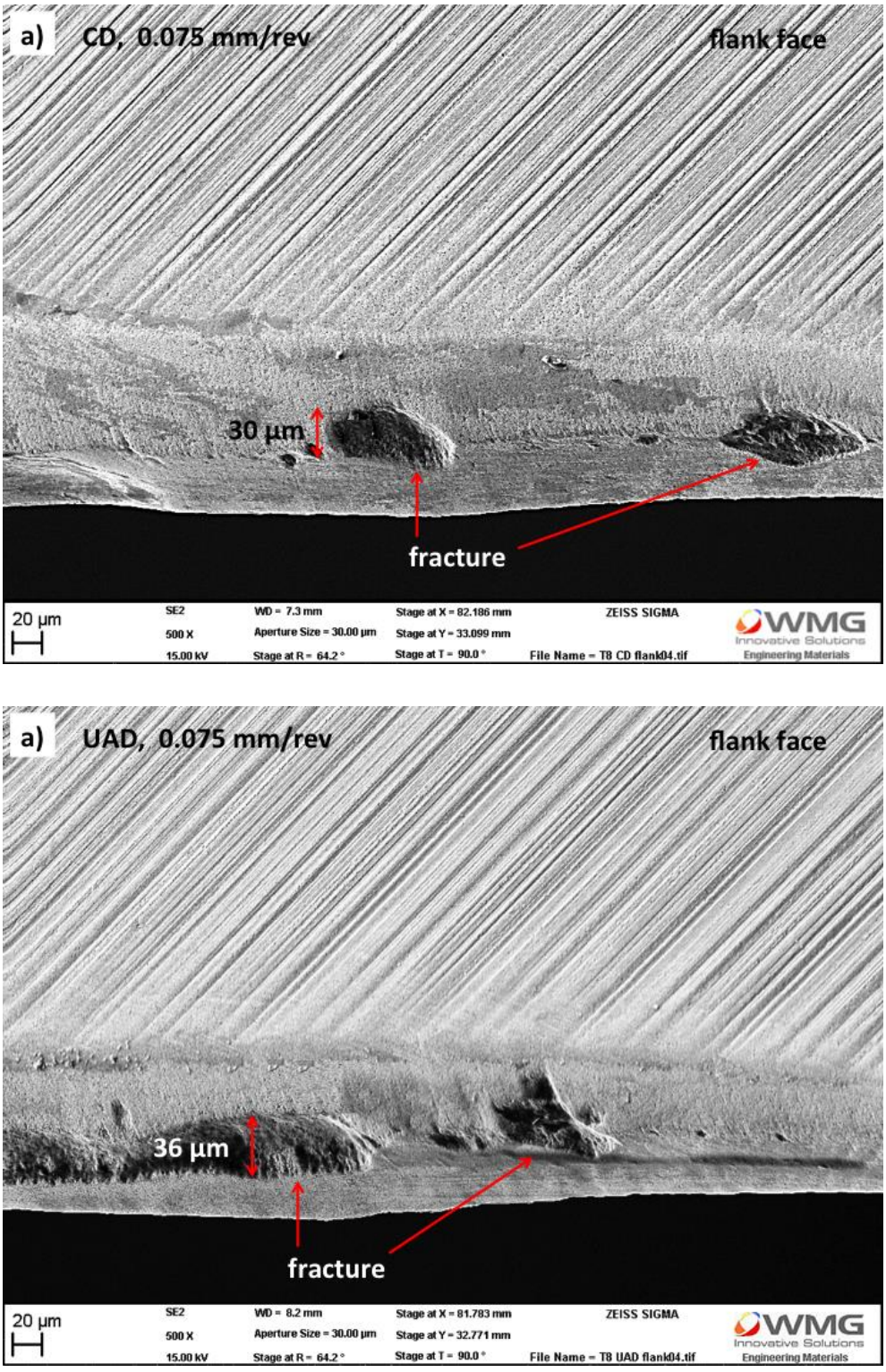

Figure 4.69: SEM micrographs showing cutting edge and flank face condition after (a) CD and (b) UAD, of 80 holes through CFRP/Ti stacks using a feed rate of 0.075 mm/rev and cutting speed of 50 m/min; following removal of the adhered Ti

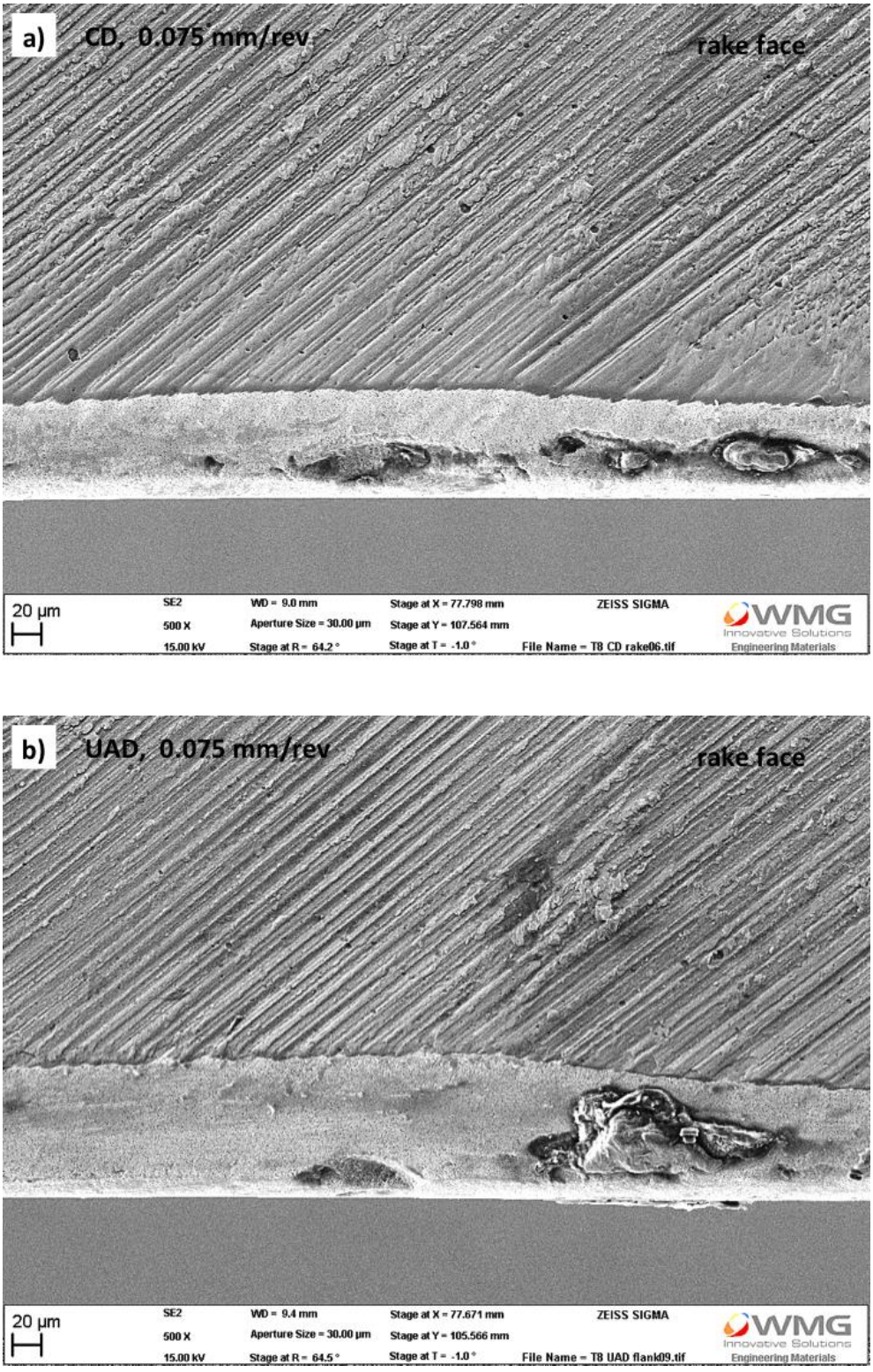

Figure 4.70: SEM micrographs showing rake face condition after (a) CD and (b) UAD, of 80 holes through CFRP/Ti stacks using a feed rate of 0.075 mm/rev and cutting speed of 50 m/min

In contrast, drilling with the lowest feed rate of 0.025 mm/rev caused the fastest drill failure (CD = 40 holes, UAD = 35 holes; Figure 4.66) due to Ti adhesion and cutting edge chipping, Figure 4.71. A longer contact time between the cutting edges and the workpiece (due to lower feed rate) caused more contact between cutting edges and workpiece, and also more heat build-up. This weakened the cutting edges and caused substantial Ti adhering strongly on the cutting edges, and makes the cutting edges prone to fracture. It is important to note that the drill used for UAD of CFRP/Ti stacks at 0.025 mm/rev exhibited earlier substantial cutting edge chipping (width = 200 µm, length = 1185 µm), Figure 4.71 (b), compared to CD which exhibited no visible edge chipping after 30 holes, Figure 4.71 (a). This was the reason for a sudden increase in flank wear during UAD, higher than CD, as seen in Figure 4.66. This observation suggests that the combination of a longer cutting time and drill oscillation at high frequency (40 kHz) during UAD was detrimental as it caused earlier drill failure.

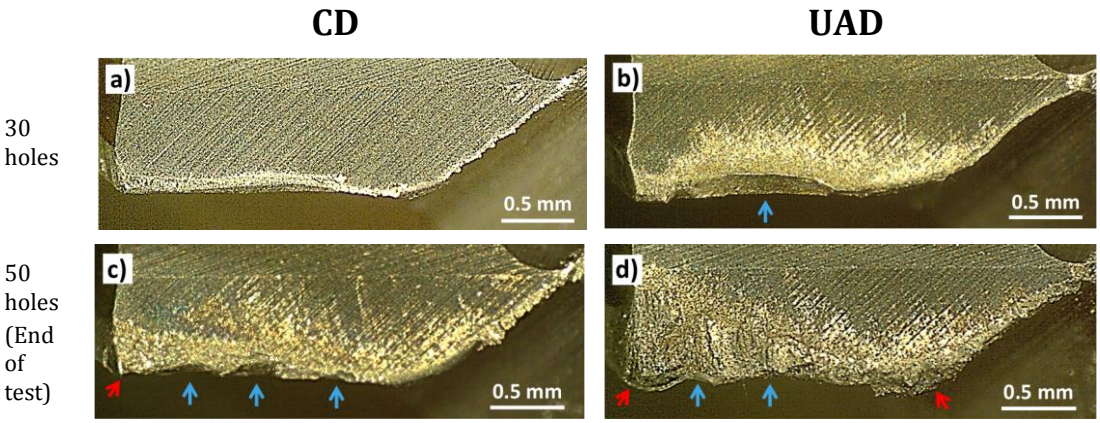

Figure 4.71: Condition of cutting edges after CD and UAD of (a, b) 30 holes and (c, d) 50 holes through CFRP/Ti stacks using feed rate of 0.025 mm/rev and cutting speed of 50 m/min. Red arrows show Ti adhesion on the cutting edge and blue arrows show edge chipping

Figure 4.72 shows magnified views of the cutting edges at the end of CD and UAD trials of CFRP/Ti stacks using the lowest feed rate of 0.025 mm/rev. For CD drill, substantial cutting edge chipping and adhered Ti on the cutting edge and flank face are evident, Figure 4.72 (a). For UAD drill, it was observed that Ti masked the worn cutting edges and the flank face, Figure 4.72 (b).

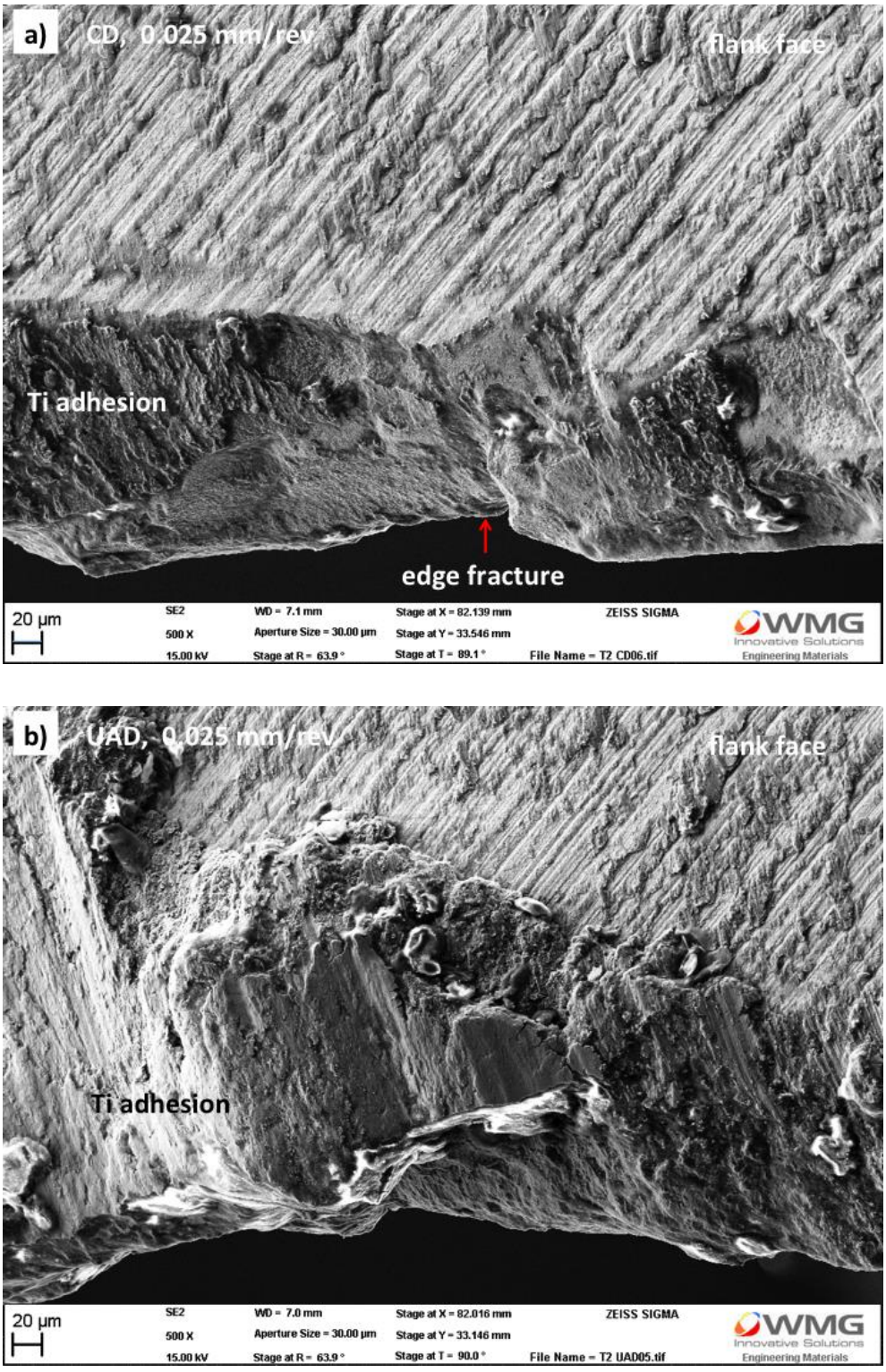

Figure 4.72: SEM micrographs showing cutting edge and flank face condition after (a) CD and (b) UAD, through CFRP/Ti stacks using a feed rate of 0.025 mm/rev and cutting speed of 50 m/min

Figures 4.73 shows the cutting edge condition and flank face (of 0.025 mm/rev) after the adhered Ti was removed (by drilling CFRP). The fractured and worn cutting edge as well as flank face of the drill used for CD, Figure 4.73 (a), and UAD, Figure 4.73 (b), were still largely covered by the adhering Ti. This observation indicated that the Ti was strongly bonded to the tool substrate, which was due to the harsh drilling condition. Magnified views of the worn and fractured edges are attached in Appendix B, Figure B.6, showing pull-out of WC-Co, preferential removal of Co binder by abrasion (as discussed previously in Sections 4.1.1 and 4.2.1) and fractured WC grains. The rake face of the drills, Figure 4.74, exhibited substantial fracture with width up to 226 μm (CD) and 220 μm (UAD) along the cutting edges. Therefore, CFRP/Ti stacks should not be drilled with lower feed rates as it caused more rapid tool wear by a combination of abrasion, severe Ti adhesion and cutting edge fracture.

In summary, the fact that increasing feed rate from 0.025 to 0.05 to 0.075 mm/rev resulted in a reduction in tool wear and increased tool life, indicated that productivity can be increased when drilling CFRP/Ti stacks using this approach. This result contradicted previous study [132], which found that flank wear increased from 0.02 to 0.4 mm with increasing feed rate from 0.03 to 0.25 mm/rev at a constant cutting speed of 12 m/min after 20th holes. It was not stated in their report [132], how the cutting edges wore, but it is reasonable to assume that the feed rate of 0.25 mm/rev was too high (233% higher than the highest feed rate used in the current study) for drilling CFRP/Ti stacks. It must be noted that increasing feed rate will also cause an increase in cutting force, which can cause cutting edges' fracture and drills' breakage if they are not strong enough to withstand the stress. Hence, when using the high feed rate, the load and cutting forces should constantly be monitored. It is suggested that using the highest feed rate of 0.075 mm/rev is practical to prolong the tool life when drilling CFRP/Ti stacks as the cutting edges were found to wear gradually and uniformly.

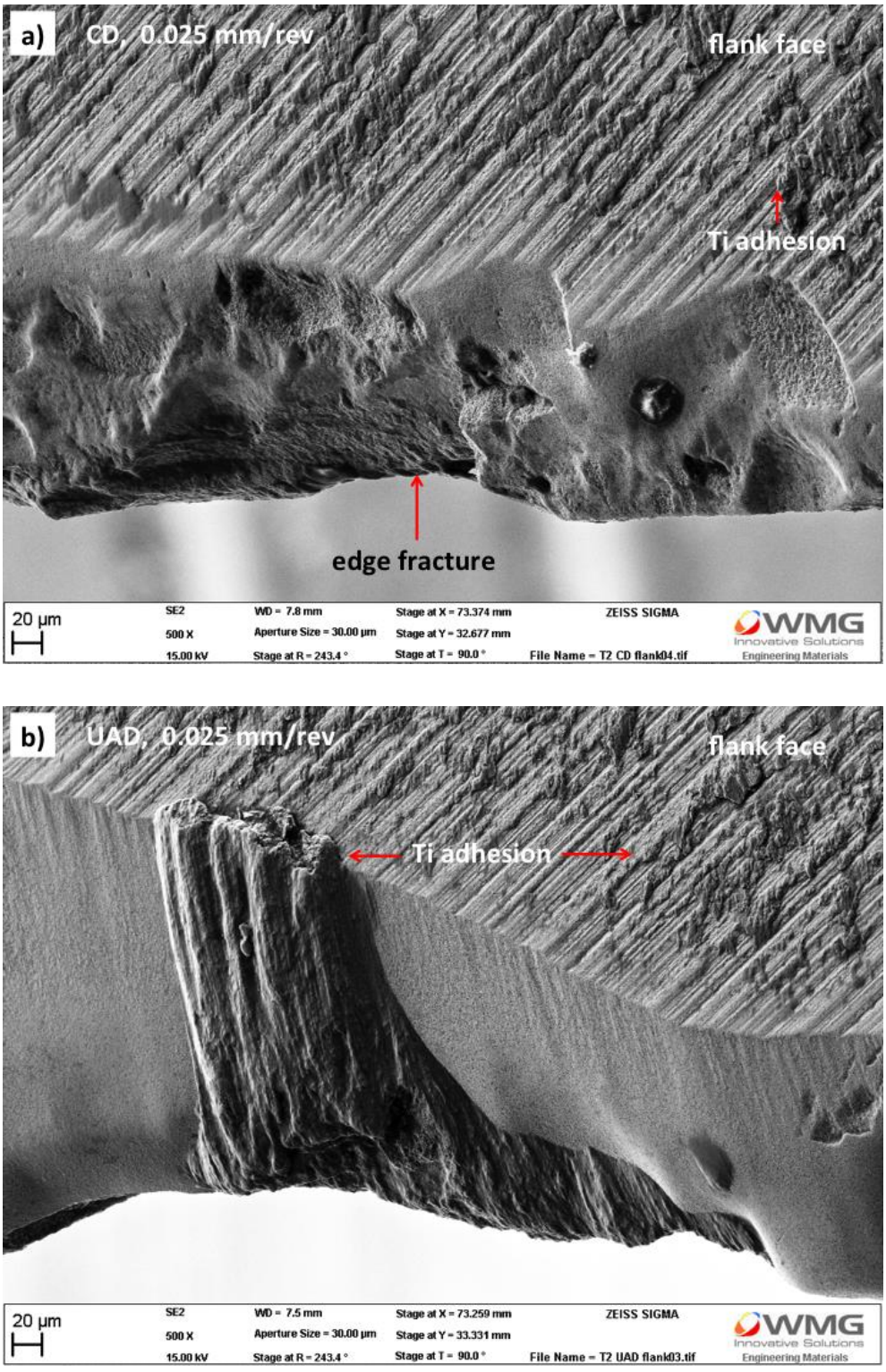

Figure 4.73: SEM micrographs showing cutting edge and flank face condition after (a) CD and (b) UAD, through CFRP/Ti stacks using a feed rate of 0.025 mm/rev and cutting speed of 50 m/min; following removal of adhered Ti

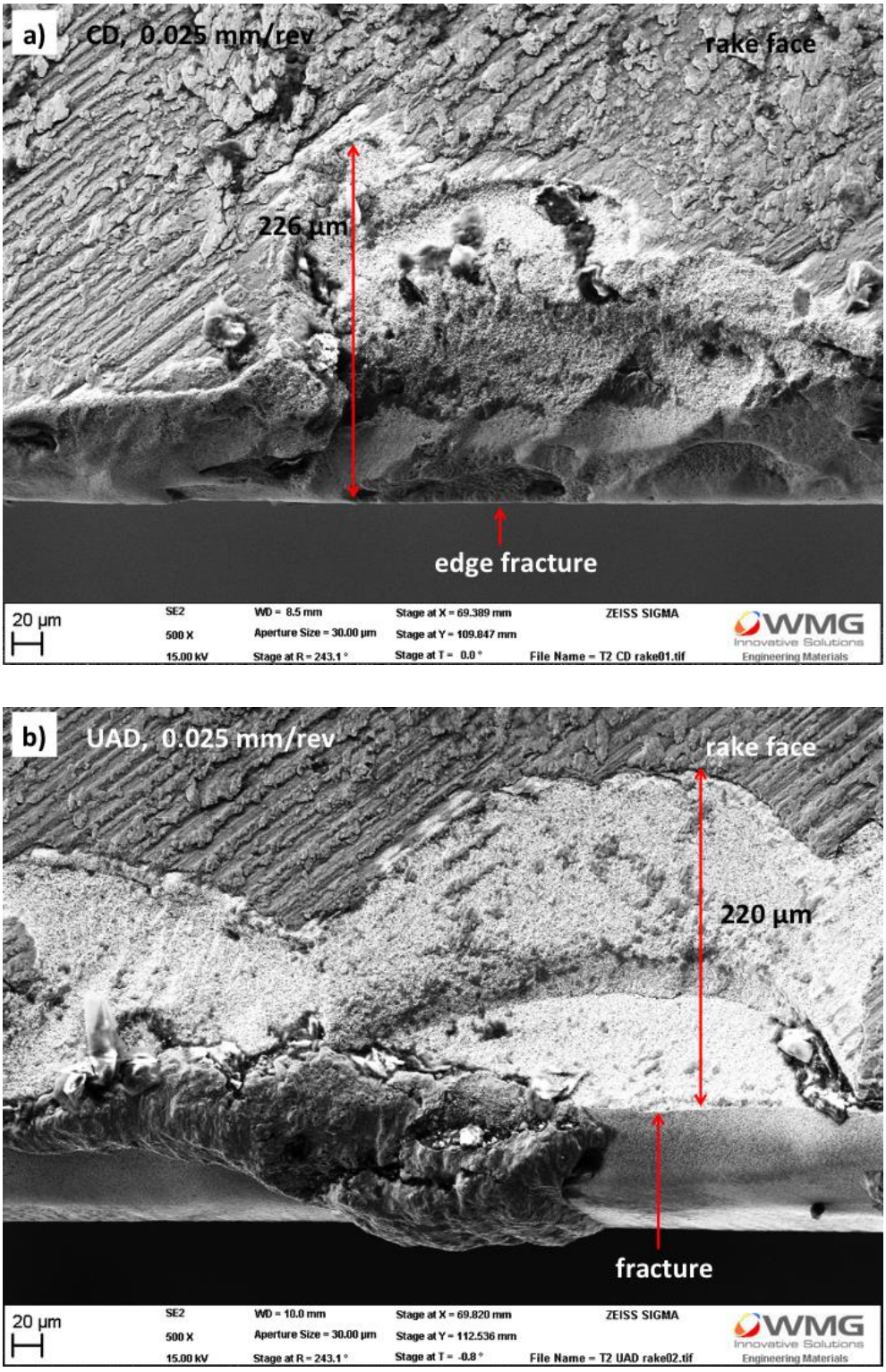

Figure 4.74: SEM micrographs showing rake face condition after (a) CD and (b) UAD, through CFRP/Ti stacks using a feed rate of 0.025 mm/rev and cutting speed of 50 m/min

4.3.2 Thrust force and torque

Figure 4.75 compares thrust force profiles during CD and UAD of CFRP/Ti stacks at 0.025, 0.05 and 0.075 mm/rev. At all feed rates, UAD was observed to exhibit 24% – 45% larger differences between the minimum and maximum thrust forces (or variation) in thrust forces compared to CD, which is summarised in Table 4.4.

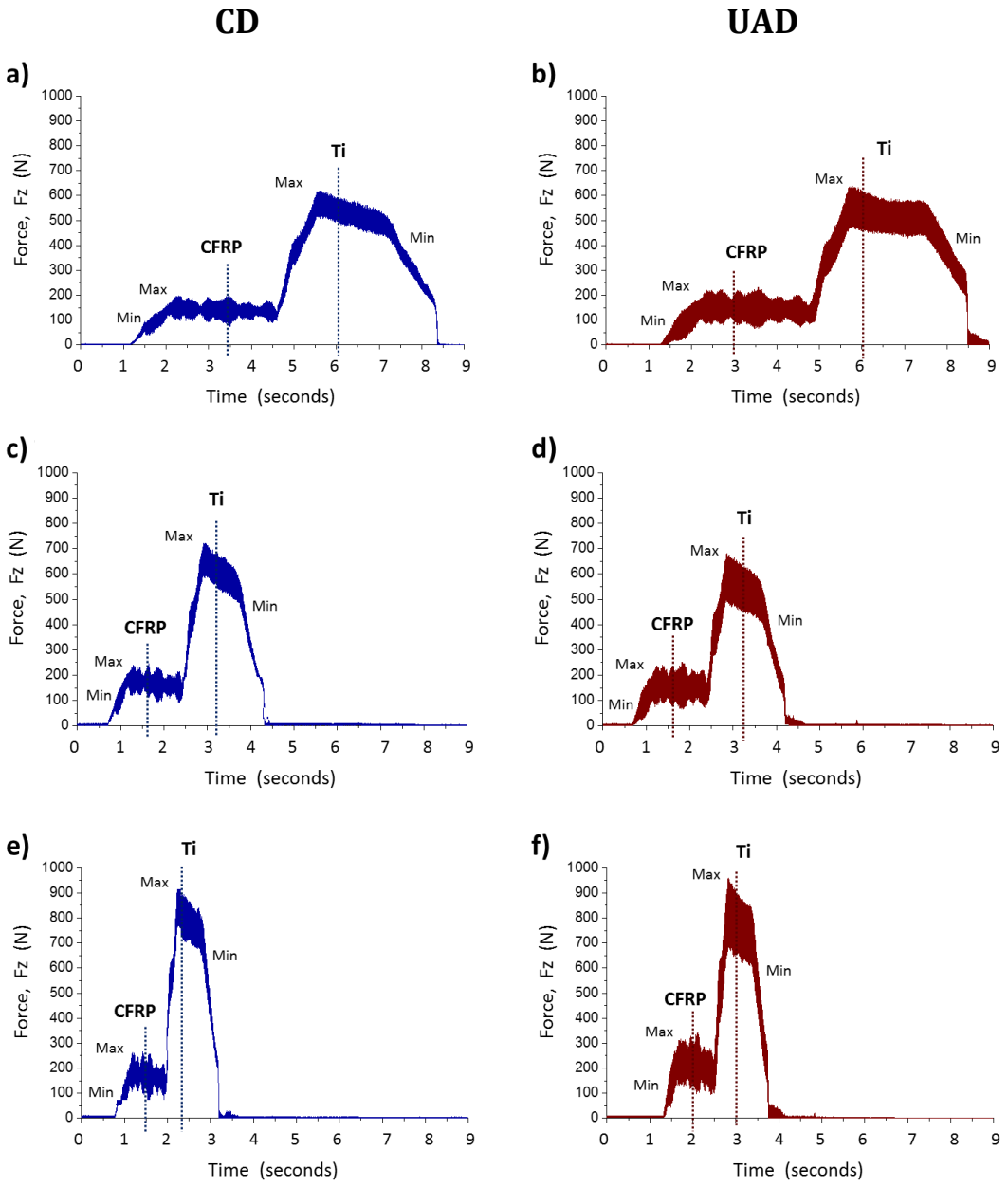

Figure 4.75: Thrust force profiles during CD and UAD of the 1st holes in CFRP/Ti stacks using feed rates of (a, b) 0.025 mm/rev, (c, d) 0.05 mm/rev and (e, f) 0.075 mm/rev at a constant cutting speed of 50 m/min (sampling rate = 80,000 Hz)

Table 4.4: Difference between minimum and maximum thrust forces during CD and UAD of CFRP/Ti stacks using feed rates of 0.025, 0.05 and 0.075 mm/rev at a constant cutting speed of 50 m/min - 1st holes

Feed Rate	CFRP			Ti (N)		
	CD (N)	UAD (N)	* UAD – CD	CD (N)	UAD (N)	* UAD – CD
0.025 mm/rev	110	158	44%	133	193	45%
0.05 mm/rev	138	188	36%	220	273	24%
0.075 mm/rev	155	222	43%	272	370	36%

*** Indicates that UAD exhibited a larger force variation compared to CD, by the percentage shown.**

The larger force variation during UAD compared to CD was attributed to the drill oscillation, back and forth during the cutting. Figures 4.76 and 4.77 show magnified views of thrust force profiles during CD and UAD of CFRP and Ti (at the dashed lines in Figure 4.75). It was confirmed that UAD exhibited interference waves patterns confirming the oscillation of the drills during drilling at all feed rates, Figures 4.76 (b, d, f) and 4.77 (b, d, f). In contrast, interference wave patterns were not observed during CD at all feed rates, Figures 4.76 (a, c, e) and 4.77 (a, c, e). This was similar to the observation in Study 2, as discussed previously in Section 4.2.2. In summary, these observations indicated that the UAD application using the machine tool in the current study for all cutting parameters employed is robust to continuously oscillate the drills throughout UAD process.

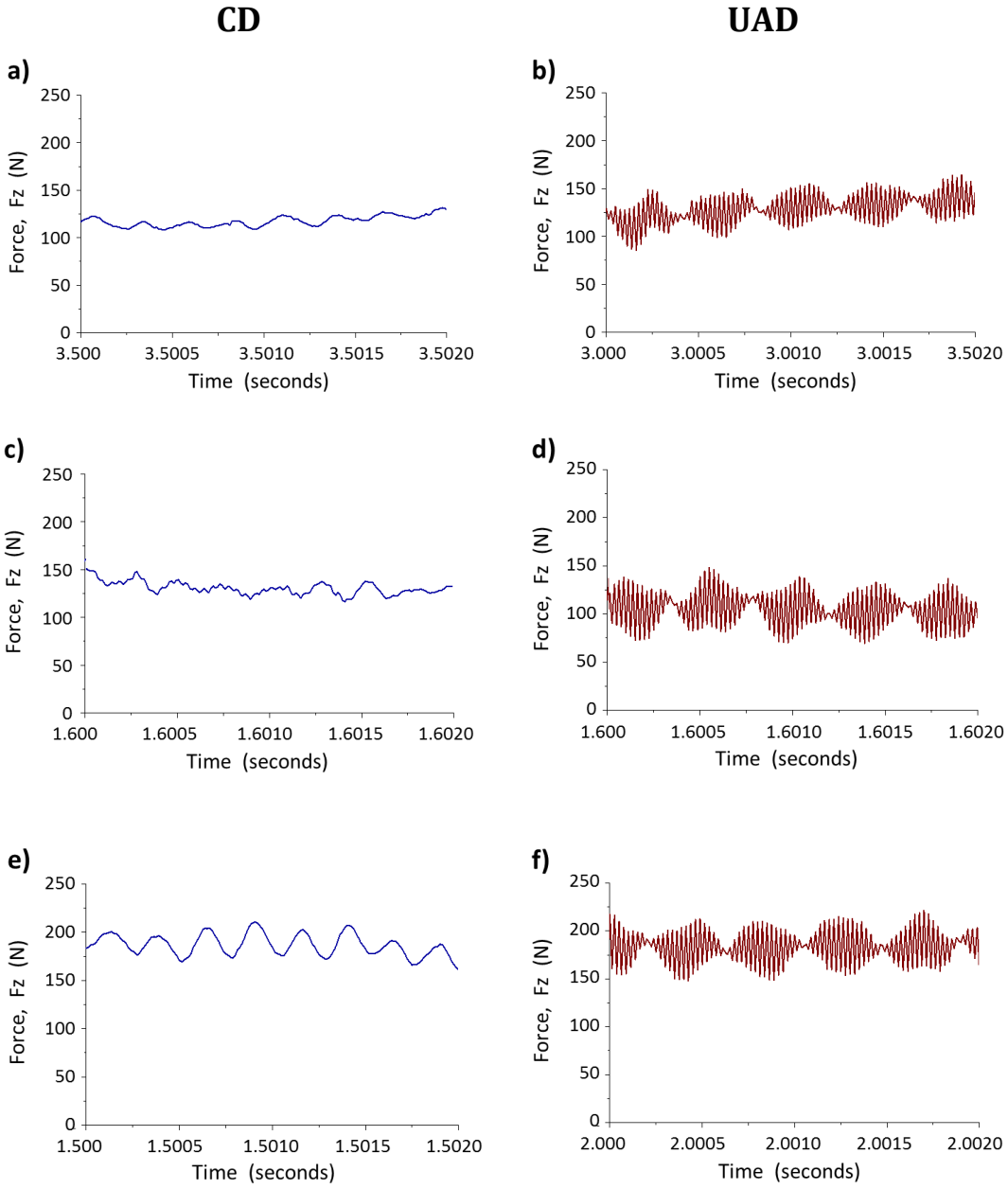

Figure 4.76: Thrust force profiles during CD and UAD of the 1st holes through CFRP component of the stack using feed rates of (a, b) 0.025 mm/rev, (c, d) 0.05 mm/rev, and (e, f) 0.075 mm/rev at a constant cutting speed of 50 m/min (sampling rate = 80,000 Hz)

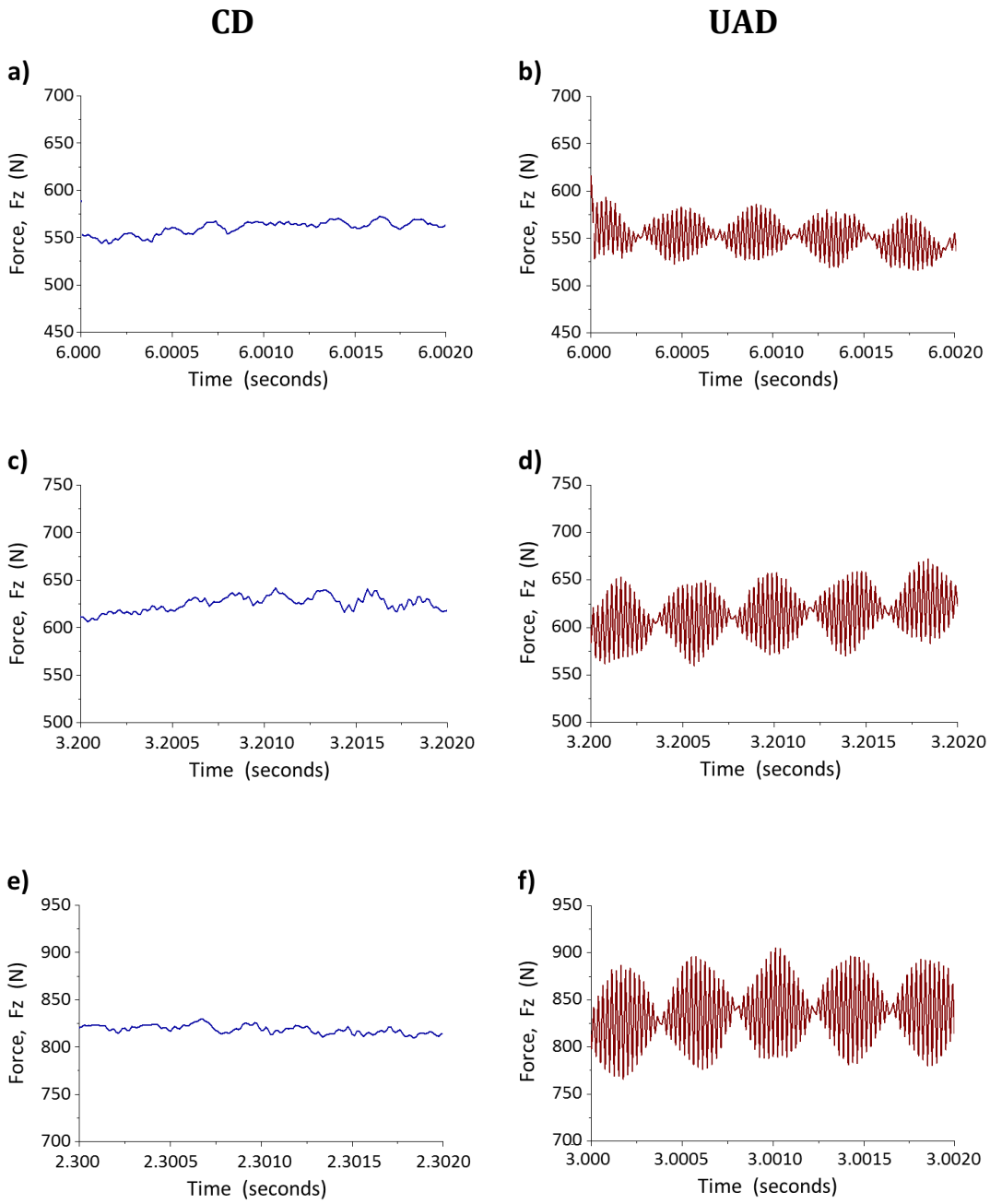

Figure 4.77: Thrust force profiles during CD and UAD of the 1st holes through Ti component of the stack using feed rates of (a, b) 0.025 mm/rev, (c, d) 0.05 mm/rev, and (e, f) 0.075 mm/rev at a constant cutting speed of 50 m/min (sampling rate = 80,000 Hz)

Figures 4.78 and 4.79 compare the average thrust forces during CD and UAD of CFRP/Ti stacks at all feed rates with respect to increasing hole number. For the first holes, when tool wear was minimal, increasing the feed rate from 0.025 to 0.05 to 0.075 mm/rev during CD and UAD of CFRP/Ti stacks resulted in increasing average

thrust forces. The higher feed rate means that more material was removed per unit time, which consequently required more force.

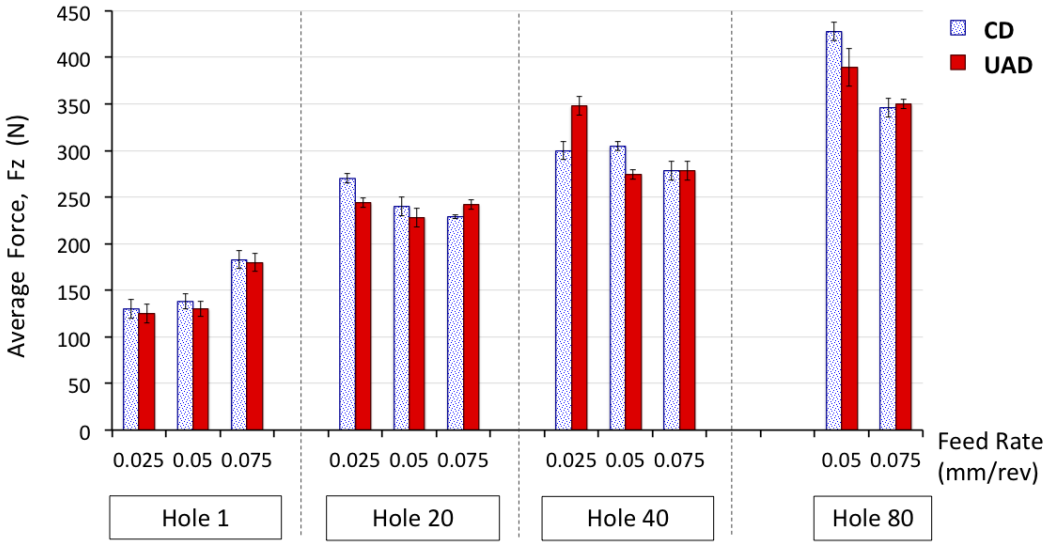

Figure 4.78: Comparison of average thrust forces during CD and UAD of CFRP in the stacks using feed rates of 0.025, 0.05 and 0.075 mm/rev at a constant cutting speed of 50 m/min. Range bars indicate variation for three consecutive holes (e.g. hole 1-3, hole 19-21, hole 39-41)

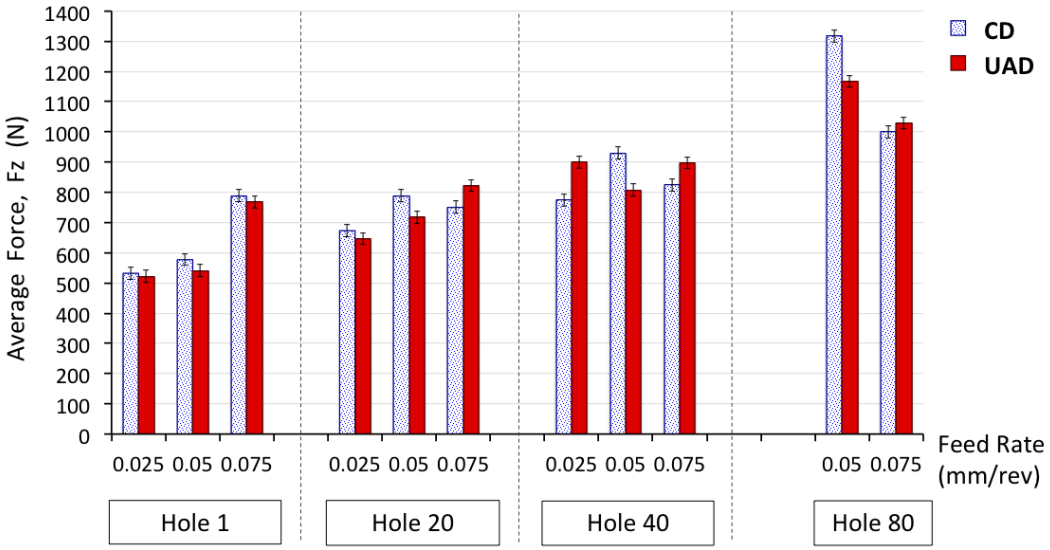

Figure 4.79: Comparison of average thrust forces during CD and UAD of Ti in the stacks using feed rates of 0.025, 0.05 and 0.075 mm/rev at a constant cutting speed of 50 m/min. Range bars indicate variation for three consecutive holes (e.g. hole 1-3, hole 19-21, hole 39-41)

With increasing hole number (holes 20, 40, 80), the average thrust forces at the lower feed rates of 0.025 and 0.05 mm/rev increased, higher than those of 0.075 mm/rev,

Figures 4.78 and 4.79, due to dominating influence of tool wear. Notably, when drilling the 80th holes, CD and UAD with the highest feed rate of 0.075 mm/rev resulted in 14% – 26% lower average thrust forces compared to when using the lower feed rate of 0.05 mm/rev. This result was consistent with the observation of tool wear in which the highest feed rate of 0.075 mm/rev caused the least tool wear, Section 4.3.1. There was no marked difference in the average thrust forces generated during UAD compared to CD.

Figure 4.80 compares torque profiles during CD and UAD of CFRP/Ti stacks. UAD was observed to exhibited larger (24% – 40%) torque variation compared to CD, which is consistent with the observation of thrust forces. Further examination of the torque profiles confirmed that UAD of both CFRP and Ti exhibited standing waves patterns, Figures 4.81 (b, d, f) and 4.82 (b, d, f). Whereas, this was not observed during CD, Figures 4.81 (a, c, e) and 4.82 (a, c, e).

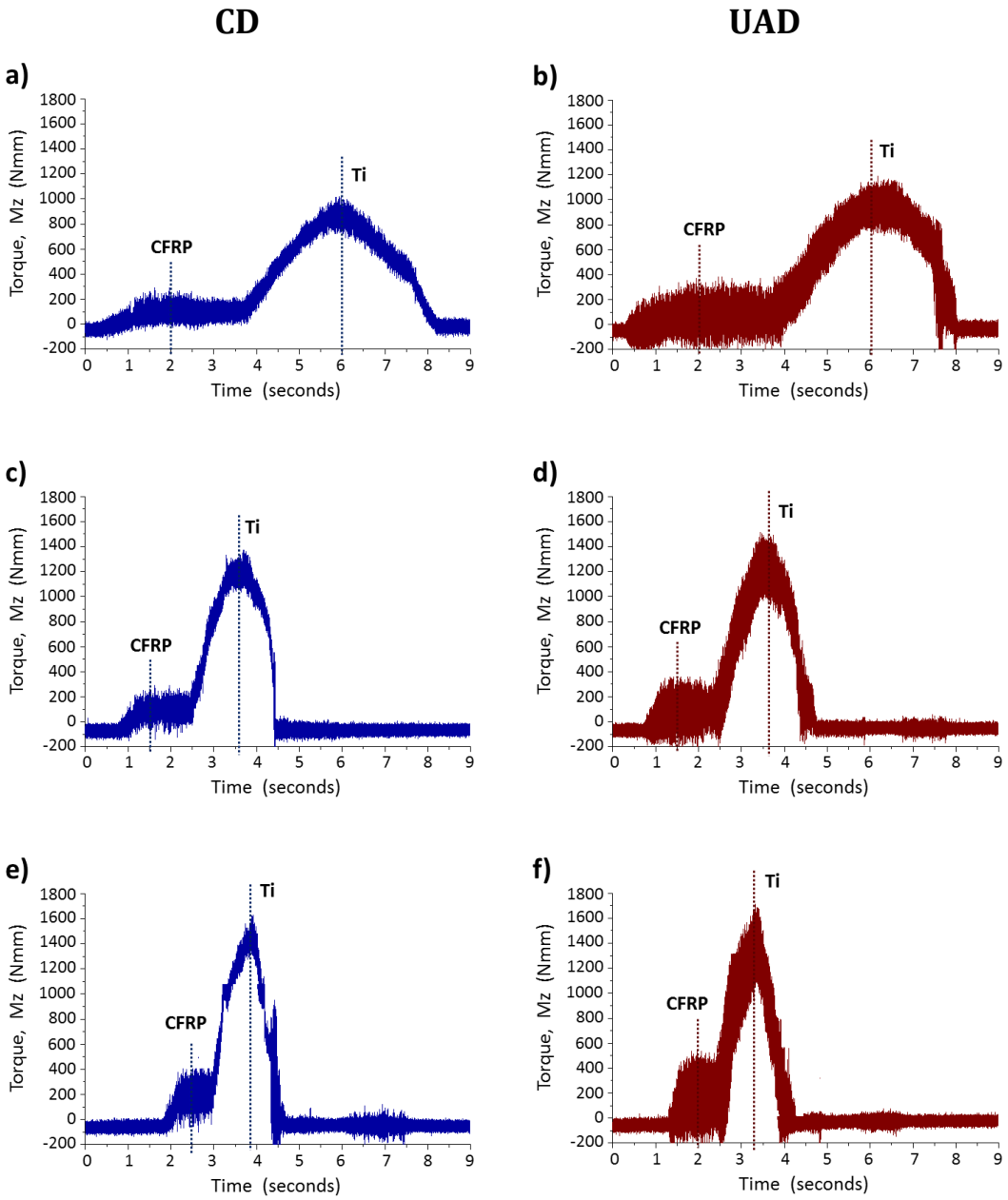

Figure 4.80: Torque profiles during CD and UAD of the 1st holes in CFRP/Ti stacks using feed rates of (a, b) 0.025 mm/rev, (c, d) 0.05 mm/rev and (e, f) 0.075 mm/rev at a constant cutting speed of 50 m/min (sampling rate = 80,000 Hz)

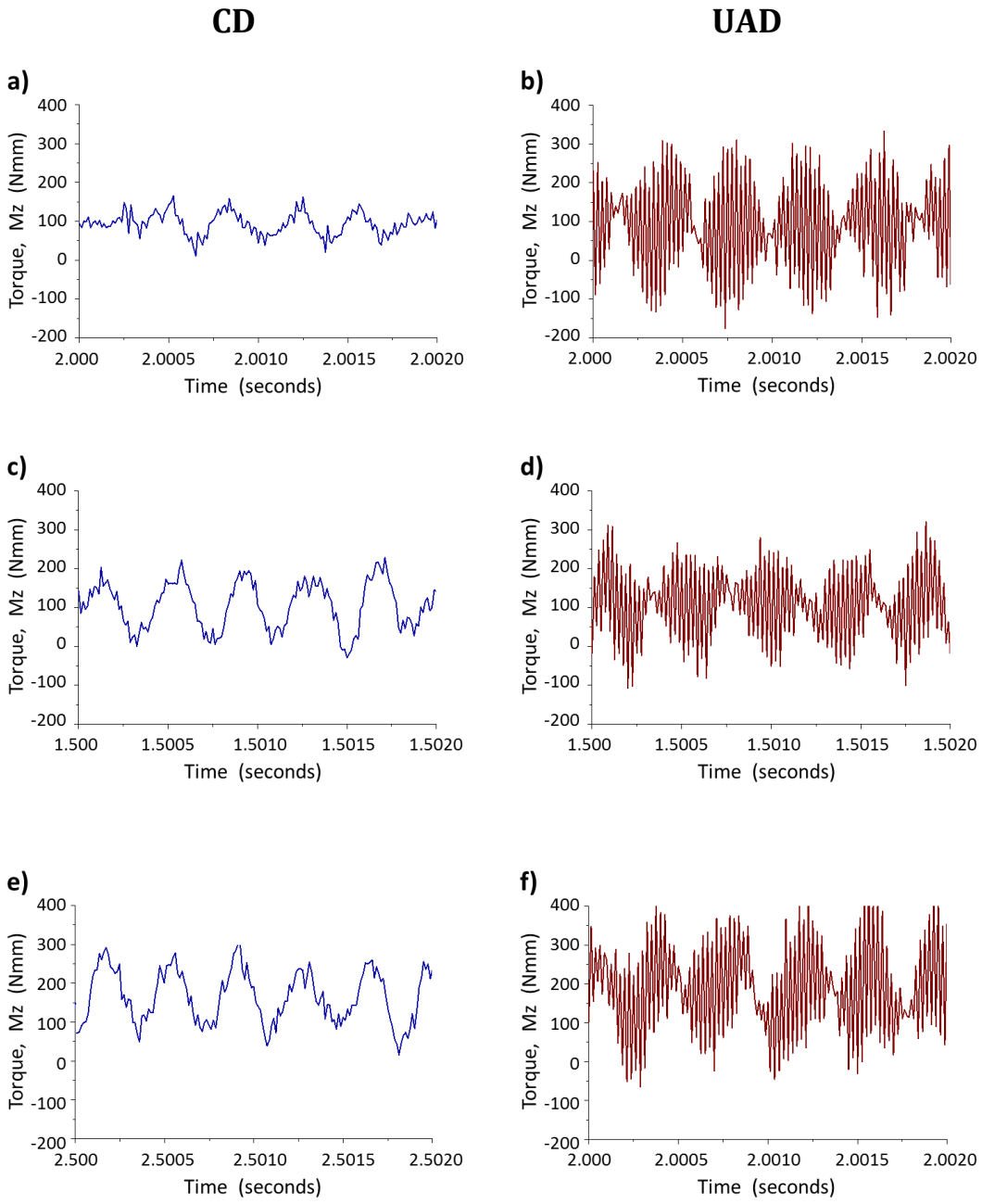

Figure 4.81: Torque profiles during CD and UAD of the 1st holes in CFRP component of the stacks using feed rates of (a, b) 0.025 mm/rev, (c, d) 0.05 mm/rev and (e, f) 0.075 mm/rev at a constant cutting speed of 50 m/min (sampling rate = 80,000 Hz)

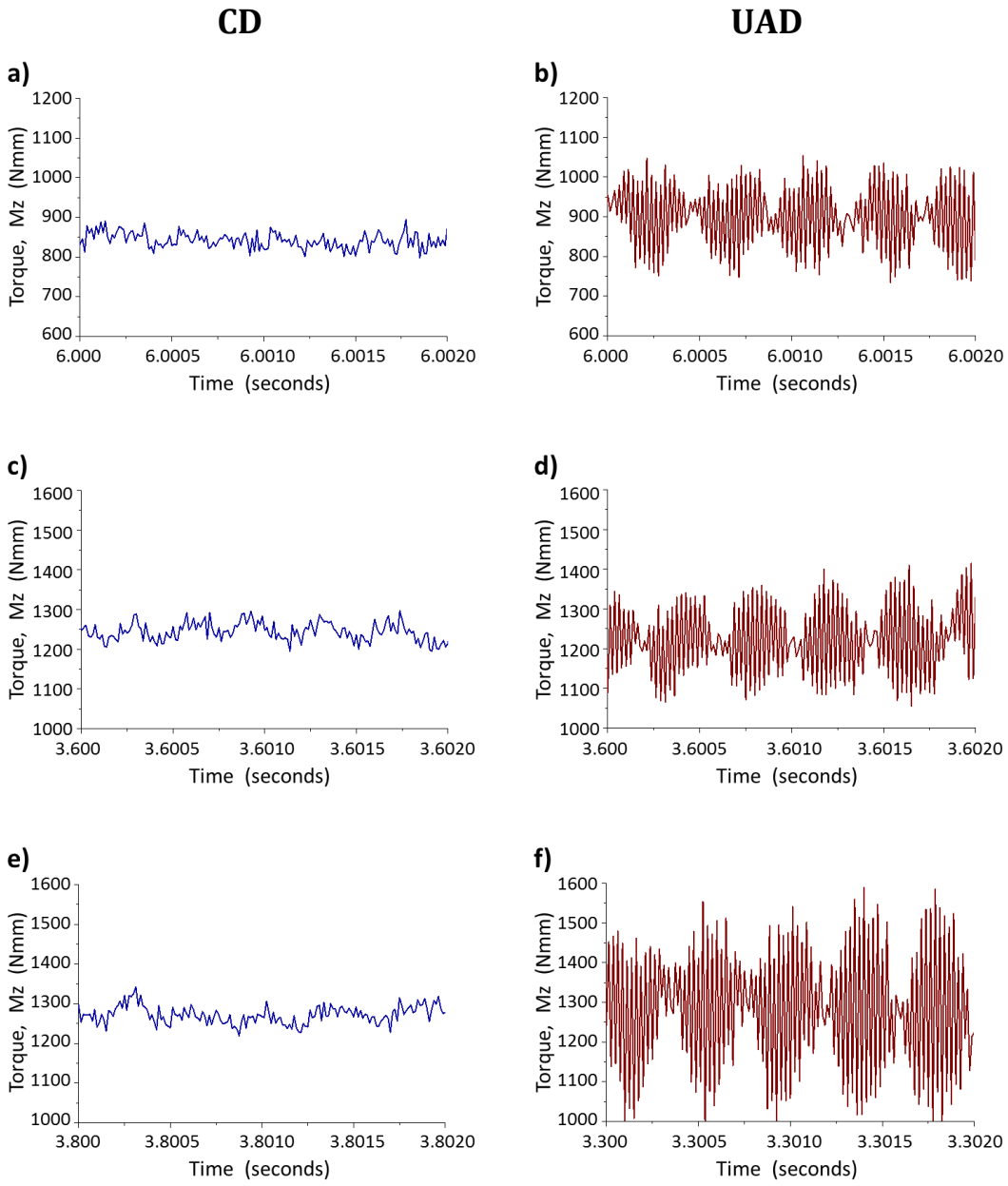

Figure 4.82: Torque profiles during CD and UAD of the 1st holes in Ti component of the stacks using feed rates of (a, b) 0.025 mm/rev, (c, d) 0.05 mm/rev and (e, f) 0.075 mm/rev at a constant cutting speed of 50 m/min (sampling rate = 80,000 Hz)

Figures 4.83 and 4.84 compare the average torque when the drills were in full engagement during CD and UAD of CFRP/Ti stacks at all feed rates. Up to 40 holes, the average torque in CD and UAD of both CFRP and Ti was observed to increase with increasing feed rates from 0.025 to 0.05 to 0.075 mm/rev, indicative of increasing load on the cutting edges as more materials were removed in one revolution of the drills. At 80th holes, the average torque when drilling at 0.05 mm/rev, was equivalent to those at 0.075 mm/rev due to dominating influence of tool wear.

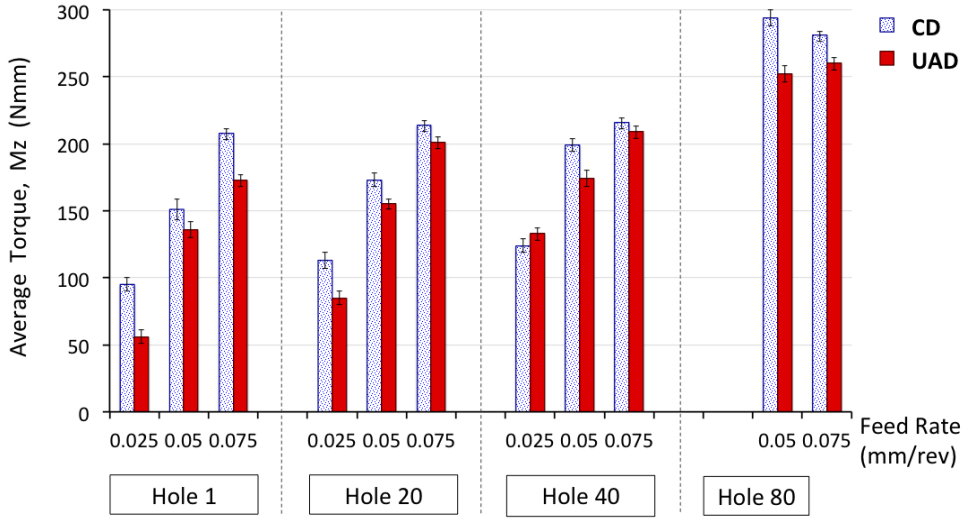

Figure 4.83: Comparison of average torque during CD and UAD of CFRP component of the stacks using feed rates of 0.025, 0.05 and 0.075 mm/rev at a constant cutting speed of 50 m/min. Range bars indicate variation for three consecutive holes (e.g. hole 1-3, hole 19-21, hole 39-41)

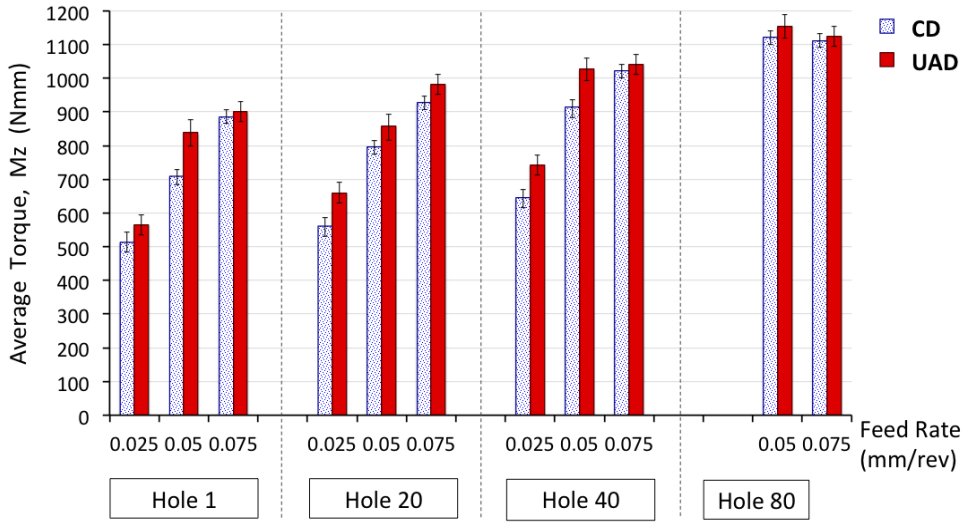

Figure 4.84: Comparison of average torque during CD and UAD of Ti component of the stacks using feed rates of 0.025, 0.05 and 0.075 mm/rev at a constant cutting speed of 50 m/min. Range bars indicate variation for three consecutive holes (e.g. hole 1-3, hole 19-21, hole 39-41)

For all feed rates, the average torque generated during UAD of CFRP was 13% (on average) lower than those of CD of CFRP. In contrast, the average torque during UAD of Ti was 9% higher than those of CD of Ti due to hardening of Ti caused by drill vibration against the workpiece. Further evidence of the hardened machined Ti surfaces is shown in Section 4.3.4.4.

4.3.3 Titanium chip morphology

Figure 4.85 shows the morphology of Ti chips produced during CD and UAD of CFRP/Ti stacks using feed rates of 0.025, 0.05 and 0.075 mm/rev.

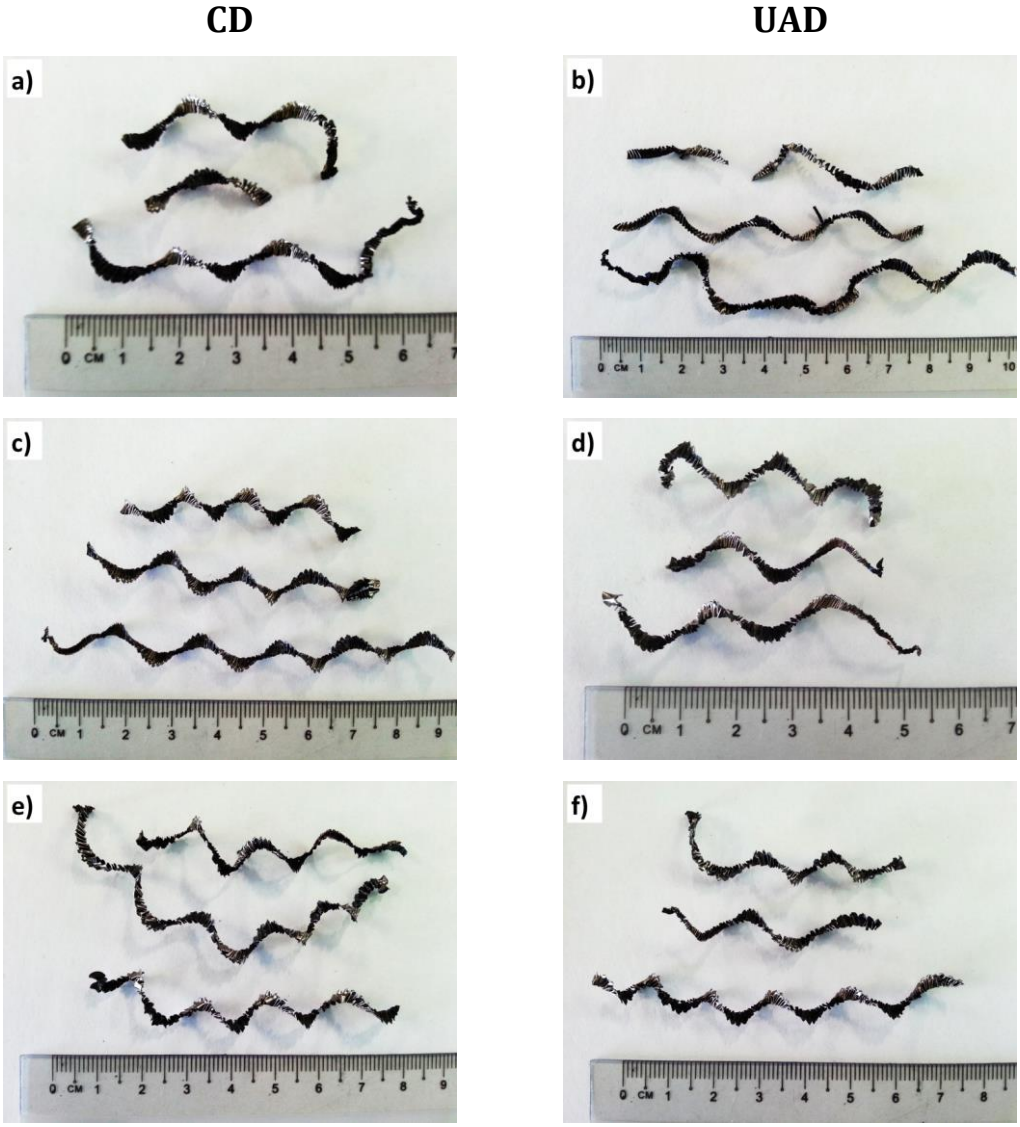

Figure 4.85: Ti chips produced by CD and UAD of CFRP/Ti stacks at feed rates of (a, b) 0.025 mm/rev, (c, d) 0.05 mm/rev and (e, f) 0.075 mm/rev at a constant cutting speed of 50 m/min

For all drilling tests, the Ti chips were in the form of a long spiral, ribbon and folded shape, Figure 4.85. This result indicated that changing the feed rate did not alter the shape of the chips, regardless of CD or UAD. To further understand the chip formation mechanism in CD and UAD with respect to changing feed rate, the Ti chips were cross-sectioned, polished and compared as shown in Figure 4.86.

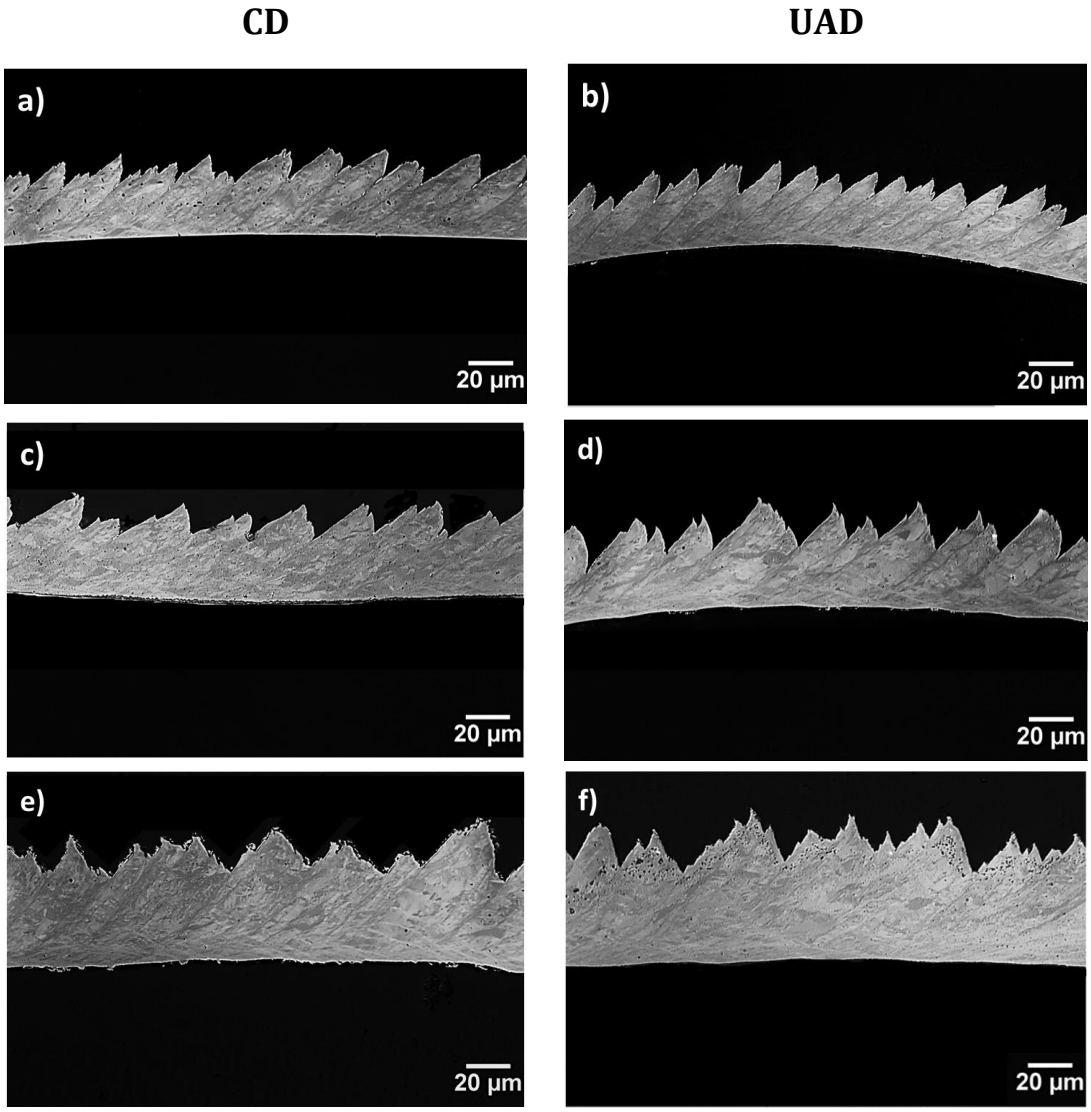

Figure 4.86: Cross section of Ti chips produced by CD and UAD of CFRP/Ti stacks using feed rates of (a, b) 0.025 mm/rev, (c, d) 0.05 mm/rev and (e, f) 0.075 mm/rev at a constant cutting speed of 50 m/min

The Ti chip produced at the lowest feed rate of 0.025 mm/rev exhibited apparent segmentation, Figure 4.86 (a, b), with the smallest shear band angle, as detailed in Figure 4.87, and the lowest thickness, as detailed in Figure 4.88. In contrast, the Ti chip

segmentation became less visible when using the highest feed rate of 0.075 mm/rev, Figure 4.86 (e, f). This suggests less heat generation in the shear region when using a higher feed rate, hence less thermal localisation and the grain deformed more homogenously. The thickness of the Ti chip was observed to increase with increasing feed rate, which is expected, Figure 4.86 and 4.88. The difference between the Ti chip thickness data produced by different feed rates was confirmed to be statistically significant by ANOVA, Appendix A, Table A.9.

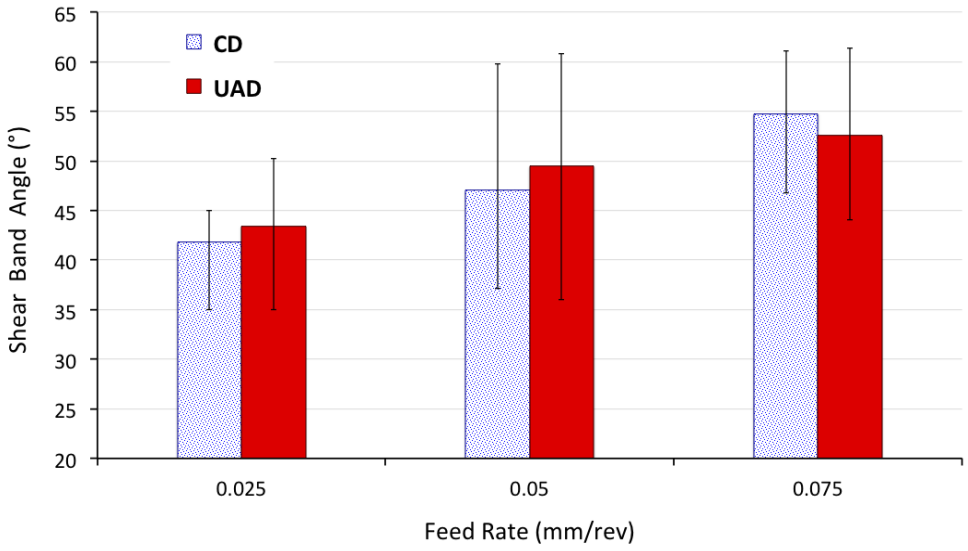

Figure 4.87: Comparison of average shear band angles of Ti chips produced by CD and UAD of CFRP/Ti stacks using feed rates of 0.25, 0.05 and 0.075 mm/rev at a constant cutting speed of 50 m/min

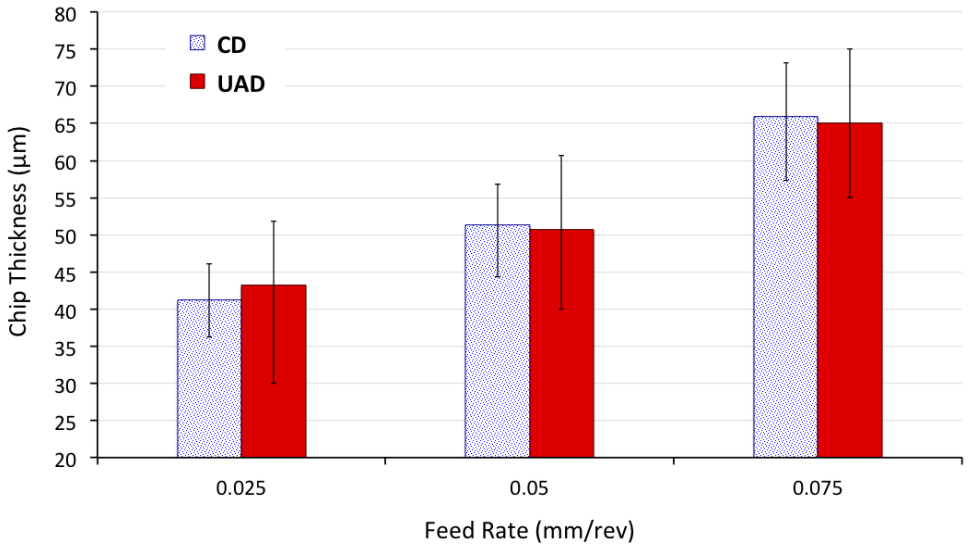

Figure 4.88: Comparison of average thickness of Ti chips produced by CD and UAD of CFRP/Ti stacks using feed rates of 0.25, 0.05 and 0.075 mm/rev at a constant cutting speed of 50 m/min

Comparing the chip thickness and shear band angle produced between CD and UAD, on average, no discernible difference was observed, however, the chips produced by UAD at all feed rates exhibited 48% larger variation in thickness and shear band angle (indicated by larger range bars) compared to those of CD, Figures 4.87 and 4.88. The effect of UAD on producing larger chip thickness variation was confirmed to be statistically significant by ANOVA, Appendix A, Table A.9. This observation is similar to the case when varying cutting speeds with a constant feed rate as in Study 2, Section 4.2.3. Therefore, this confirmed that UAD caused larger variation in the feed rates, hence larger variation in the chip thickness, compared to CD.

4.3.4 Hole quality

The hole quality of CFRP/Ti stacks produced by CD and UAD with respect to the change in feed rates of 0.025, 0.05 and 0.075 mm/rev at a constant cutting speed of 50 m/min were compared and evaluated in terms of:

- accuracy and consistency of diameter between the holes in CFRP and Ti
- the extent of CFRP entrance delamination
- fibre pull-out from the bore machined surfaces of CFRP
- topography, roughness and sub-surface hardness of machined Ti
- Ti burr height

4.3.4.1 Hole diameter

Figure 4.89 compares hole diameters in CFRP/Ti stacks produced by CD and UAD using feed rates of 0.025, 0.05 and 0.075 mm/rev at a constant cutting speed of 50 m/min. The hole diameter became more consistent and closer to the drill nominal diameter as the feed rate increased from 0.025 to 0.05 to 0.075 mm/rev, Figure 4.89. This result positively correlated with the tool wear observation. As seen in Figure 4.89 (c), the

diameter of all holes produced using the highest feed rate of 0.075 mm/rev were within H7 tolerance limits and closer to the drill nominal diameter of 6.100 mm (CD: 6.104 – 6.112 mm, UAD: 6.105 – 6.111 mm). This was attributed to drilling with the drills that exhibited the least wear and Ti adhering to the cutting edges.

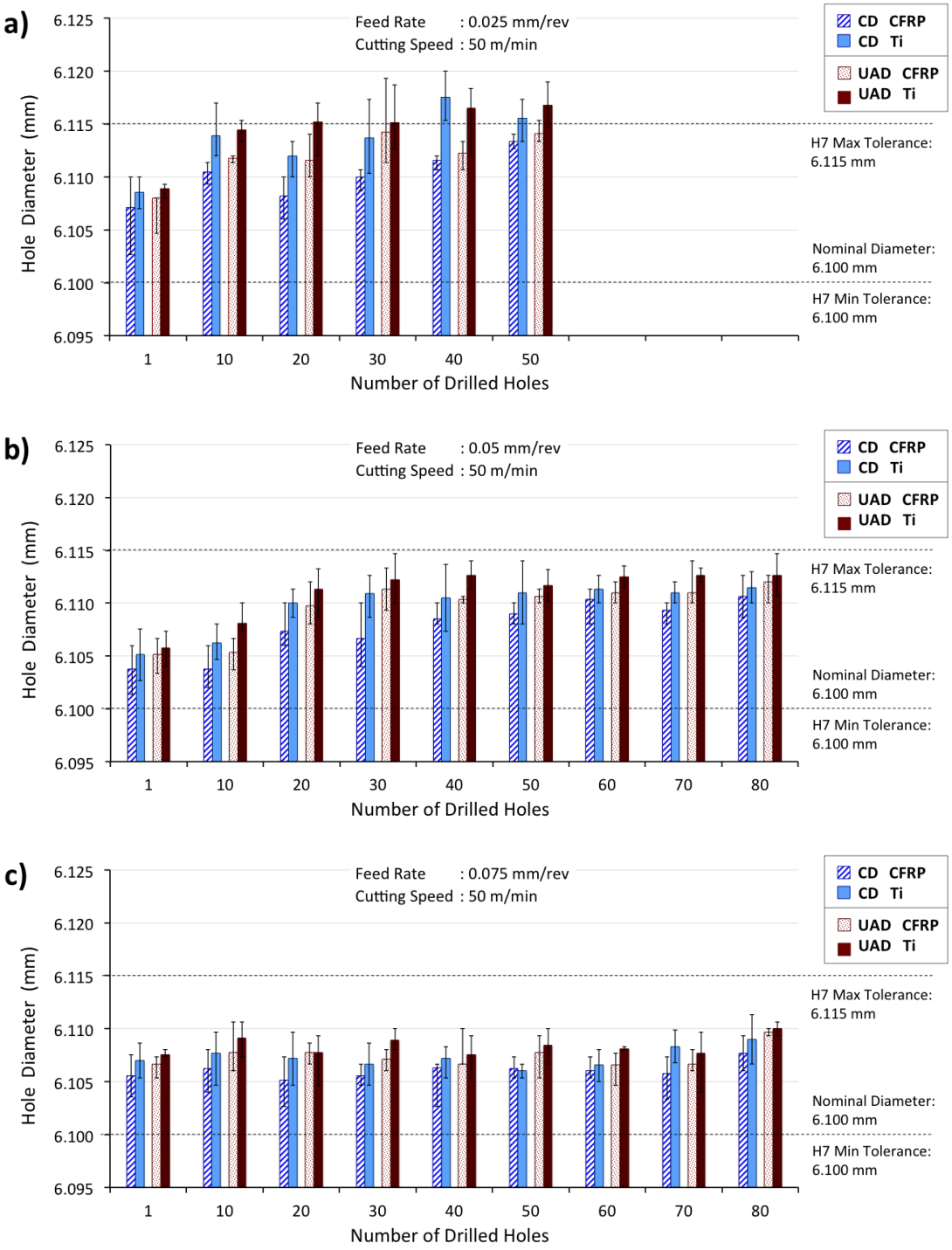

Figure 4.89: Comparison of hole diameters in CFRP/Ti stacks produced by CD and UAD using feed rates of (a) 0.025 mm/rev, (b) 0.05 mm/rev and (c) 0.075 mm/rev at a constant cutting speed of 50 m/min. Range bars indicate variation for three consecutive holes (e.g. hole 1-3, hole 9-11, hole 19-21 etc.)

In contrast, for CD and UAD with the lowest feed rate of 0.025 mm/rev, initially (holes 1-3) the hole diameters were closer to the drill nominal diameter, however, the hole diameter increased with increasing hole number. Moreover, at the lowest feed rate of 0.025 mm/rev, 38% and 55% of the holes produced by CD and UAD, respectively, exceeded the tolerance limit due to Ti chips adhering on the cutting edges causing oversized holes. The effect of increasing feed rate on producing holes with smaller diameters in CFRP/Ti stacks was confirmed to be statistically significant by ANOVA, Appendix A, Tables A.10 and A.11. Comparing CD and UAD, the holes in CFRP and Ti produced by UAD exhibited smaller diameter difference at all feed rates, Table 4.5, compared to those of CD. UAD caused 1 – 6 μm larger hole diameter in CFRP than CD of CFRP, which was confirmed to be statistically significant by ANOVA, Appendix A, Table A.10. Whereas, there was no significant difference between the hole diameter in Ti produced by CD and UAD, ANOVA, Appendix, Table A.11.

Table 4.5: Comparison of diameter difference between holes in Ti and CFRP of the stacks produced by CD and UAD at 0.025, 0.05 and 0.075 mm/rev (50 holes)

Feed Rate (mm/rev)	CD	UAD
0.025	1 – 6 μm	1 – 3 μm
0.05	1 – 4 μm	1 – 2 μm
0.075	1 – 3 μm	0 – 2 μm

In summary, with regard to obtaining holes that are consistent in diameters and within H7 tolerance limits when drilling CFRP/Ti stacks, it is recommended to use a higher feed rate (0.075 mm/rev). This would reduce the tendency of parts being rejected due to oversized holes. In addition, using the higher feed rate (e.g. 0.075 mm/rev) during drilling has a practical implication on improving productivity as more holes with accurate and consistent diameter can be produced within a shorter time (2.5 seconds per hole), compared to when a lower feed rate is employed (e.g. 0.025 mm/rev, 7.2 seconds per hole).

4.3.4.2 CFRP delamination (hole entrance)

Figure 4.90 compares CFRP delamination, F_D, at the hole entrance produced during CD and UAD of CFRP/Ti stacks using feed rates of 0.025, 0.05 and 0.075 mm/rev.

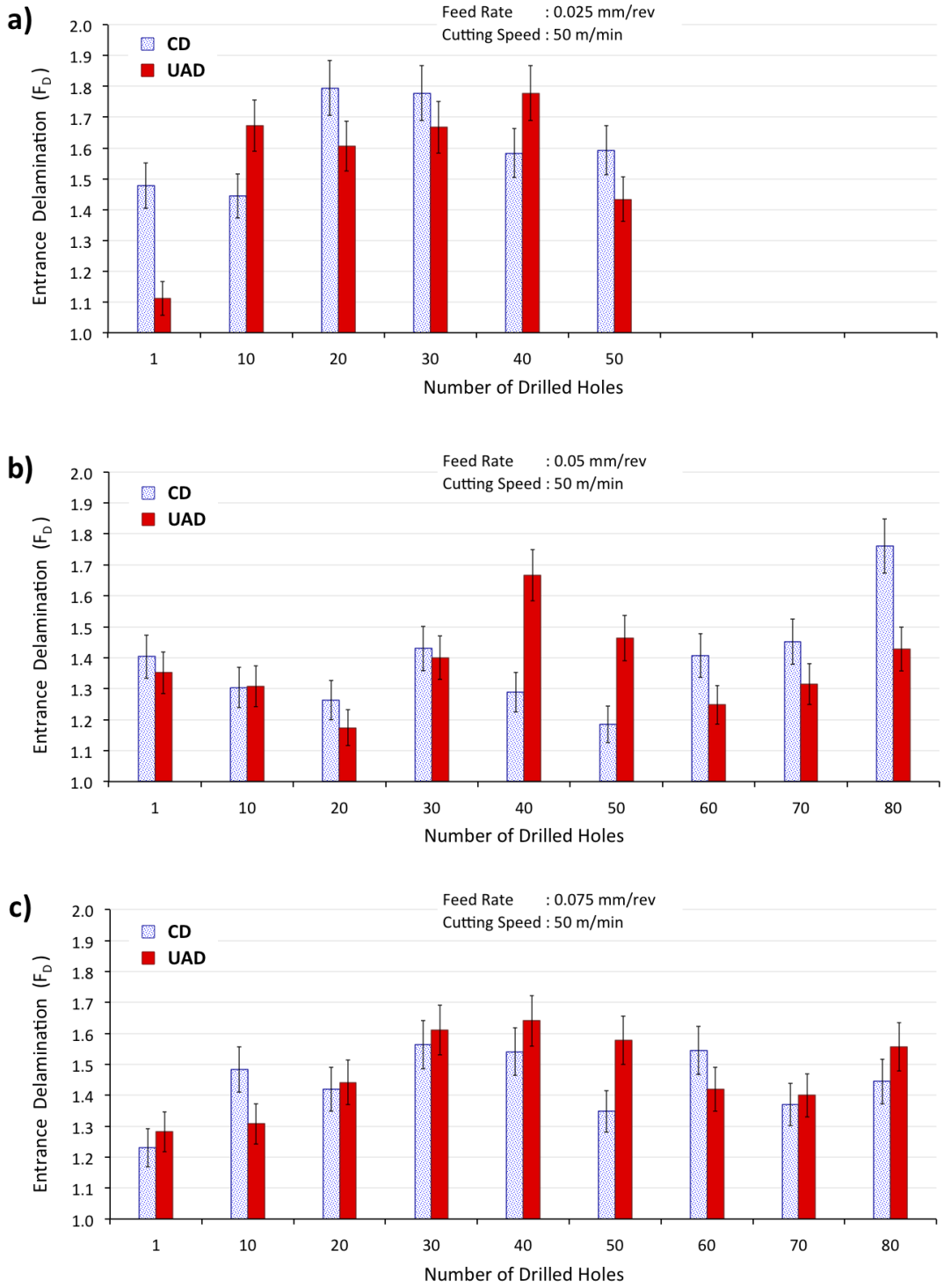

Figure 4.90: Comparison of delamination of CFRP at the hole entrance produced by CD and UAD of CFRP/Ti stacks using feed rates of (a) 0.025, (b) 0.05 and, (c) 0.075 mm/rev at a constant cutting speed of 50 m/min. Range bars indicate variation for three consecutive holes (e.g. hole 1-3, hole 9-11, hole 19-21 etc.)

No definite trend in CFRP delamination was observed when varying the feed rate. Also, there was no definite trend when comparing delamination caused by CD and UAD at all feed rates of 0.025 mm/rev, Figure 4.90 (a), 0.05 mm/rev, Figure 4.90 (b), and 0.075 mm/rev, Figure 4.90 (c). The inconsistency of CFRP delamination with varying feed rate and drilling operations (CD and UAD) was attributed to the substantial influence of Ti chips in damaging the CFRP.

When drilling the CFRP individually (not in a stack with Ti), reducing feed rate has been reported to reduce the entrance and exit CFRP delamination [11, 76, 81, 168]. This was explained in terms of reducing the feed rate caused a reduction in thrust force, which exerted less pressure on the materials. In the current study, when CFRP was drilled in a stack with Ti, the effect of minimising the delamination by reducing the feed rate was not observed.

Notably, when the tool wear was negligible (1^{st} – 10^{th} holes), no significant difference was observed between the entrance delamination during drilling using the low feed rate (0.025 mm/rev) compared to the higher feed rate (0.075 mm/rev), although lower thrust force and torque was observed at the lower feed rate (Figures 4.78 and 4.83). This observation was due to the dominating influence of titanium chips, which damaging the CFRP material as they evacuated from the hole.

4.3.4.3 CFRP pull-out from machined surface

Figures 4.91 and 4.92 show topography of the machined surfaces of CFRP produced by CD and UAD after drilling the first and 20^{th} holes using feed rates of 0.025, 0.05 and 0.075 mm/rev. The pull-out of CFRP materials is evident, as highlighted in blue colour, when drilling at all feed rates, Figures 4.91 and 4.92. The volume of CFRP being pulled out from the surfaces was quantified and compared in Figure 4.93.

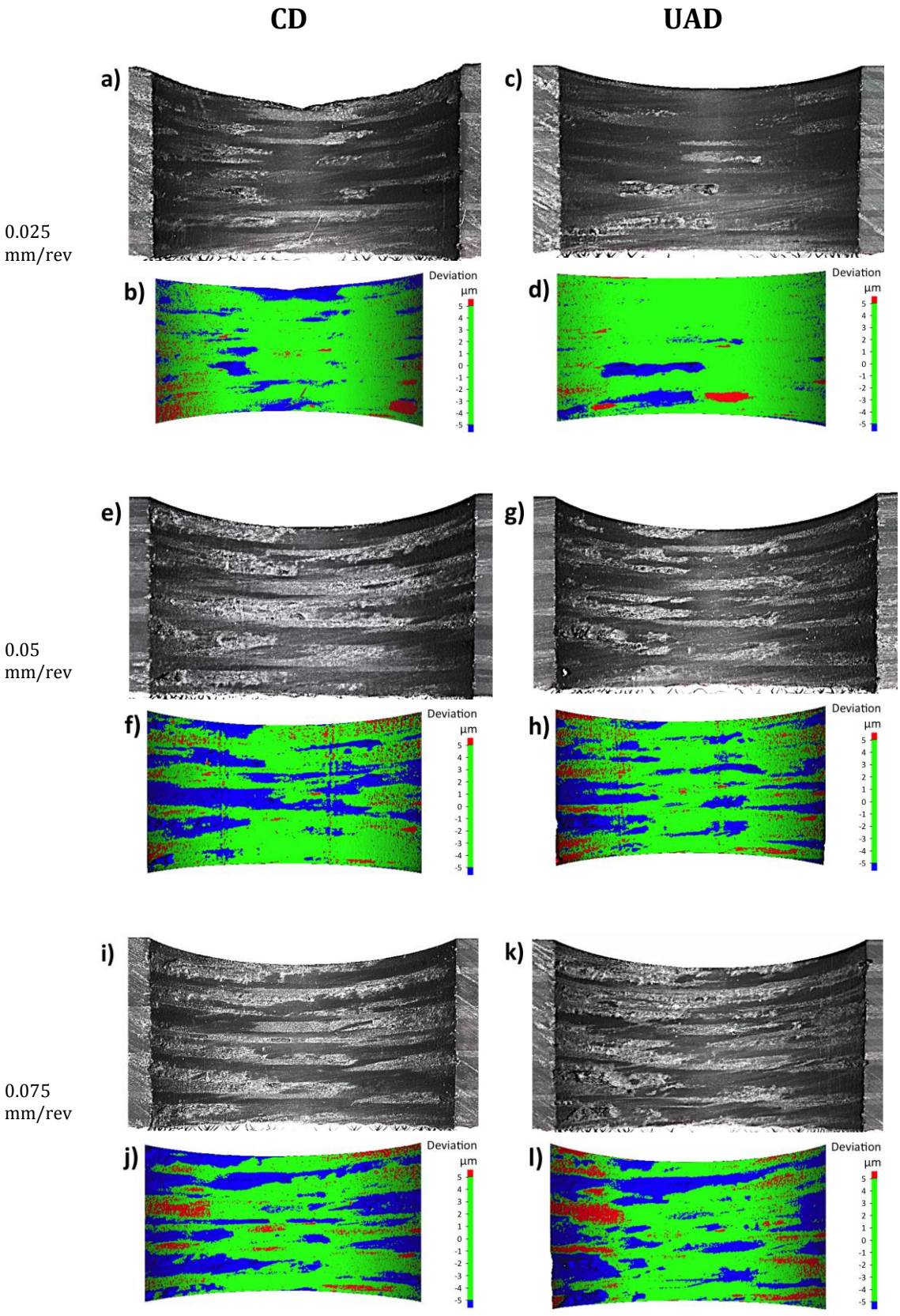

Figure 4.91: Surface topography of machined CFRP surfaces caused by CD and UAD of CFRP/Ti stacks using cutting speeds of (a, b, c, d) 0.025 mm/rev, (e, f, g, h) 0.05 mm/rev and (i, j, k, l) 0.075 mm/rev at a constant cutting speed of 50 m/min – 1st holes

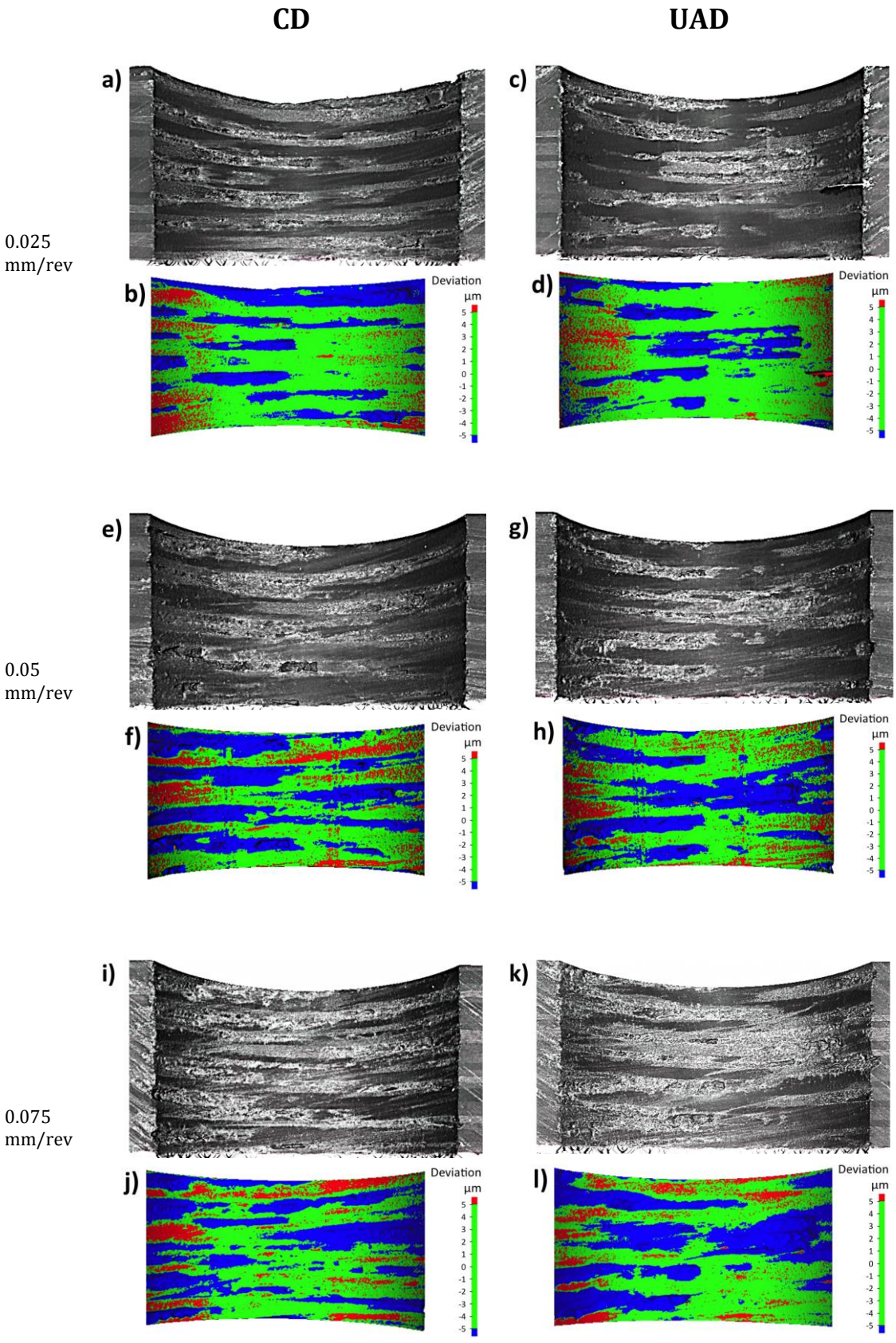

Figure 4.92: **Surface topography of machined CFRP surfaces caused by CD and UAD of CFRP/Ti stacks using cutting speeds of (a, b, c, d) 0.025 mm/rev, (e, f, g, h) 0.05 mm/rev and (i, j, k, l) 0.075 mm/rev at a constant cutting speed of 50 m/min – 20th holes**

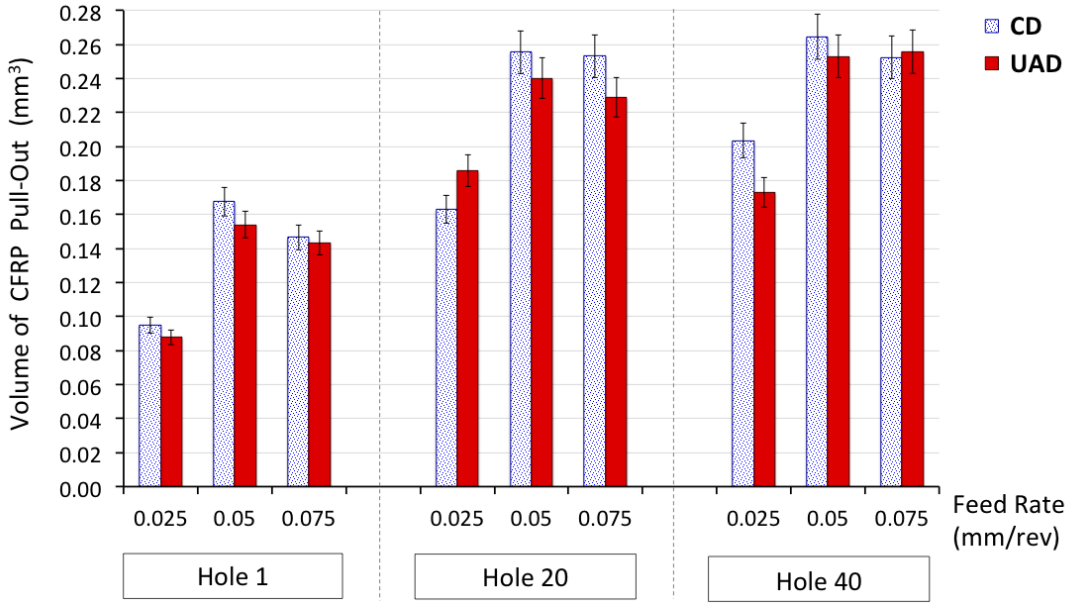

Figure 4.93: Comparison of the volume of CFRP pull-out from the machined surfaces caused by CD and UAD of CFRP/Ti stacks using feed rates of 0.025, 0.05 and 0.075 mm/rev at a constant cutting speed of 50 m/min

CD and UAD of CFRP/Ti stacks using the lowest feed rate of 0.025 mm/rev were observed to cause the least CFRP being pulled-out, consistently from the beginning (hole 1) until the drill has worn out (holes 20 and 40), Figure 4.93. Using the higher feed rates of 0.05 and 0.075 mm/rev when drilling CFRP/Ti stacks resulted in, on average, 48% and 45% larger volume of CFRP pull-out, respectively, compared to the lowest feed rate of 0.025 mm/rev, despite exhibiting lower tool wear (Section 4.3.1). The difference in the volume of CFRP pull-out caused by using different feed rates of 0.025, 0.05 and 0.075 mm/rev was confirmed to be statistically significant by ANOVA, Appendix A, Table A.12. This indicated the significant influence of using a lower feed rate (0.025 mm/rev) to reduce CFRP pull-out when drilling CFRP/Ti stacks. The observation of reducing feed rate on causing less fibre pull-out when drilling CFRP/Ti stacks is in agreement with the previous study [132]. Notably, the current study has provided more evidence with quantitative analysis, which was lacking in the previous study.

The least volume of CFRP pull-out when drilling with the lowest feed rate of 0.025 mm/rev was due to the least amount of material removed in one revolution of the drill and the least cutting forces (Section 4.3.2). The difference in the volume of CFRP pull out caused by CD and UAD was found to be not statistically significant by ANOVA, Appendix A, Table A.12. This indicated that CFRP pull-out was not significantly affected by the drill oscillation during UAD at all feed rates, compared to CD.

It is important to note that drilling CFRP/Ti stacks using the lowest feed rate of 0.025 mm/rev exhibited larger volume of CFRP pull-out within 0.08 – 0.22 mm^3, Figure 4.93, compared to the case of drilling CFRP-only at a higher feed rate of 0.05 mm/rev which exhibited lower volume of CFRP pull-out, 0.02 – 0.05 mm^3 (Study 1, Section 4.1.3.3, Figure 4.20). Hence, this observation emphasised the marked influence of Ti chip that flowed through the CFRP machined surfaces on causing more CFRP pull-out, compared to when Ti chip was absent as in the case of drilling CFRP-only.

4.3.4.4 Titanium machined surface

Linear feed marks are evident on the machined Ti surfaces produced by CD at 0.025, 0.05 and 0.075 mm/rev, Figure 4.94. In contrast, the machined Ti surfaces produced by UAD at all feed rates exhibited ultrasonic impression in the form of sinusoidal waves, Figures 4.95 and 4.96, confirming oscillation of the drills during UAD. Figure 4.96 (a, b, c) are the magnified views of Figure 4.95 (a, b, c).

Measurement of the amplitude of sinusoidal waves on the machined surfaces was confirmed to be consistent with the measurement of the amplitude (peak-to-peak amplitude = 11 μm) on the non-rotating drills prior to drilling. No marked difference in the length of sinusoidal waves on the machined surfaces was observed, Figure 4.96, since the cutting speed was constant.

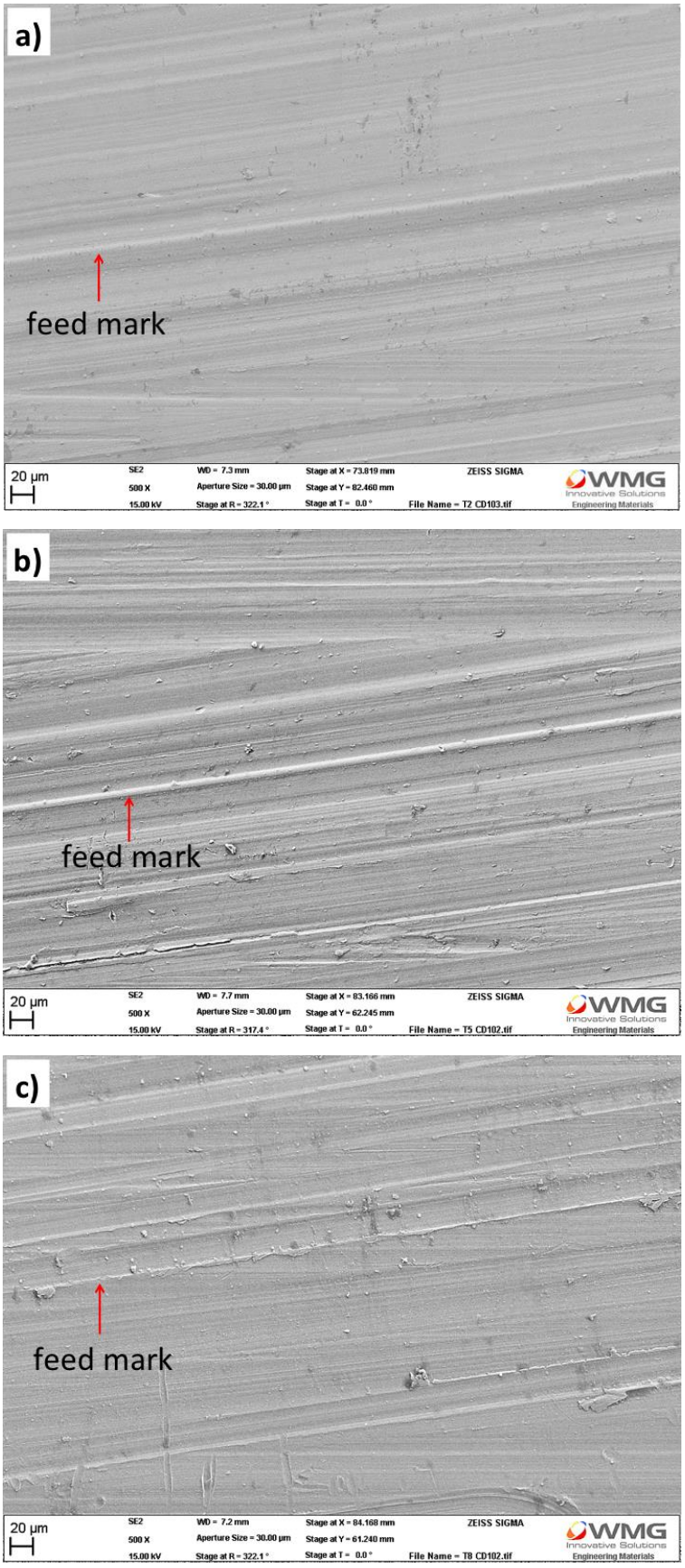

Figure 4.94: SEM micrographs showing machined Ti surfaces produced by CD of CFRP/Ti stacks using feed rates of (a) 0.025 mm/rev, (b) 0.05 mm/rev and (c) 0.075 mm/rev at a constant cutting speed of 50 m/min – 1st holes

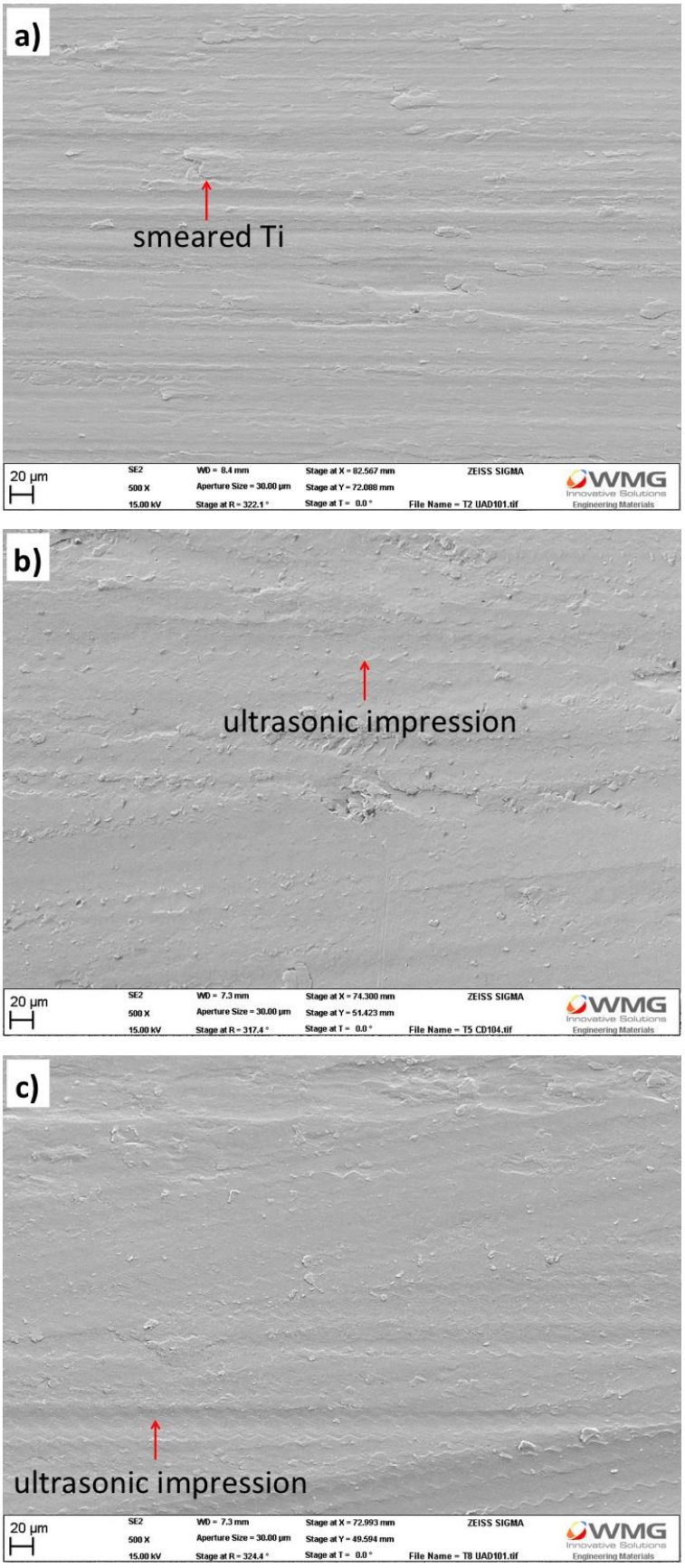

Figure 4.95: SEM micrographs showing machined Ti surfaces produced by UAD of CFRP/Ti stacks using feed rates of (a) 0.025 mm/rev, (b) 0.05 mm/rev and (c) 0.075 mm/rev at a constant cutting speed of 50 m/min – 1st holes

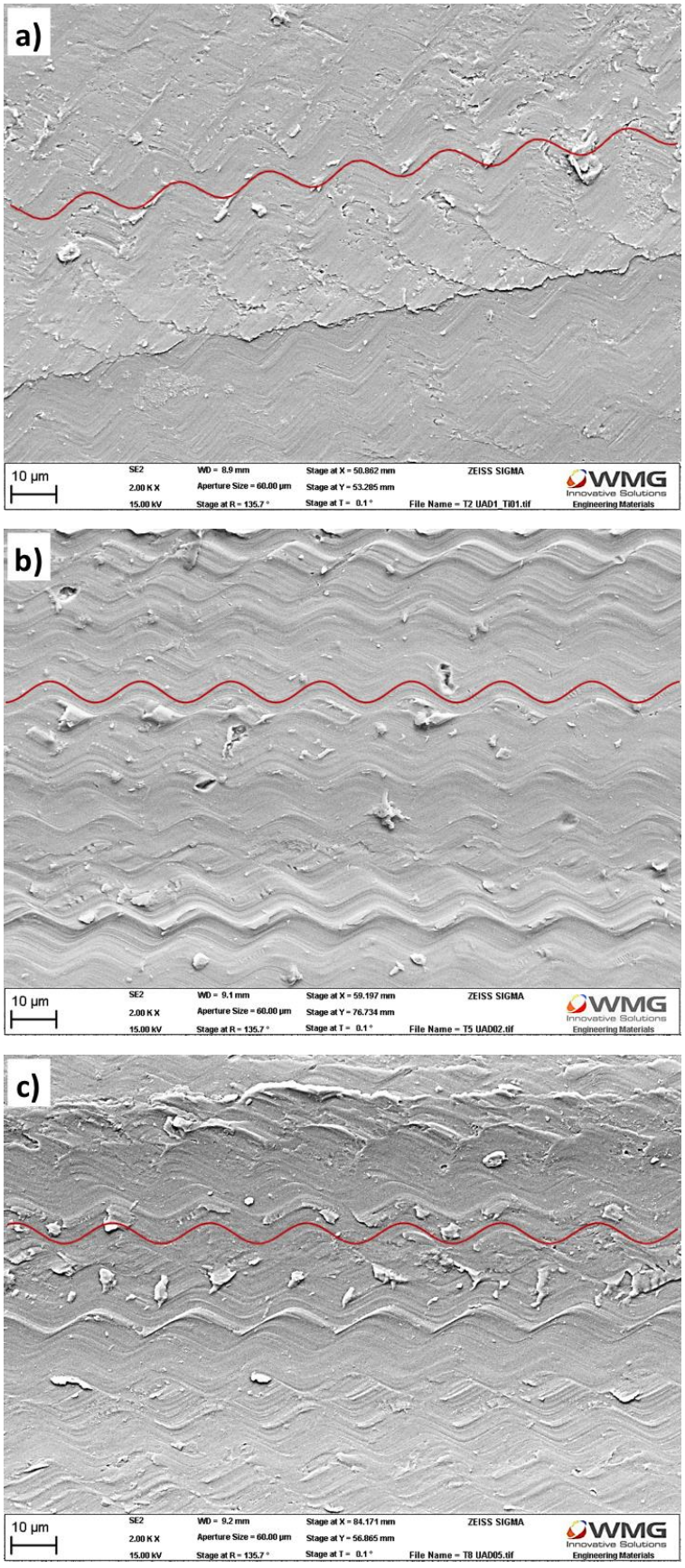

Figure 4.96: SEM micrographs showing ultrasonic impression on machined Ti surfaces, as indicated by red sinusoidal lines, produced by UAD of CFRP/Ti stacks using feed rates of (a) 0.025 mm/rev, (b) 0.05 mm/rev and (c) 0.075 mm/rev at a constant cutting speed of 50 m/min – 1st holes

The surface roughness of the machined Ti surfaces was quantified and the results are compared in Figure 4.97.

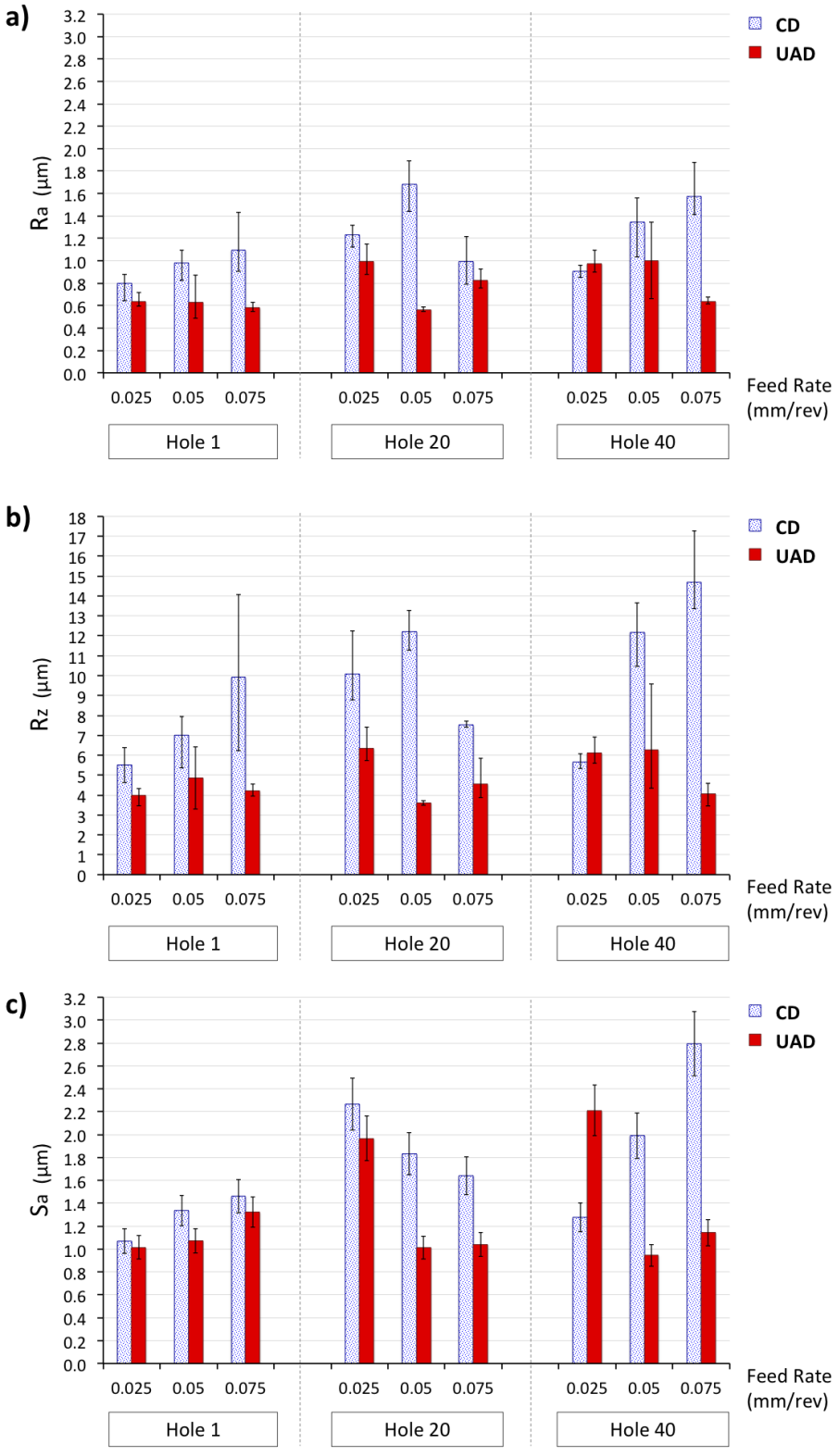

Figure 4.97: Surface roughness of machined Ti surfaces produced by CD and UAD of CFRP/Ti stacks using feed rates of 0.025, 0.05 and 0.075 mm/rev with a constant cutting speed of 50 m/min

When tool wear was minimal, increasing feed rate during CD resulted in increasing machined Ti surface roughness, R_a, R_z and S_a, Figure 4.97, which is in agreement with previous studies [37, 121]. However, with increasing tool wear (hole number), the surface roughness measurement was observed to fluctuate, Figure 4.97. The fluctuation in the surface roughness was the reason for ANOVA showing no significant difference in the effect of feed rate, Appendix A, Table A.13. Comparing CD and UAD, Figure 4.97 shows that the machined Ti surfaces produced by UAD at all feed rates exhibited on average, 32% lower surface roughness than those of CD, which was confirmed to be statistically significant by ANOVA, Appendix, Table A.13. The lower surface roughness in UAD was attributed to less intense feed marks, as shown in Figure 4.95, due to drill oscillation, compared to CD, Figure 4.94.

Investigation of the hardness of cross section of the holes in Ti, within 300 μm from the machined surfaces was conducted, and the results are shown in Figures 4.98 and 4.99. Drilling using the lower feed rates of 0.025 and 0.05 mm/rev resulted in 20 – 40 HK harder machined surfaces than those produced by the highest feed rate of 0.075 mm/rev. This observation indicates that reducing the feed rate when drilling Ti caused more work hardening of the machined Ti surfaces. Lower feed rate means that lower amount material was removed in one revolution of the drill, which suggests more rubbing of the drill against the machined surface, hence more plastic deformation that hardened the surface. Comparing UAD and CD when the tool wear was negligible (1^{st} holes), the machined surfaces produced by UAD were 20 – 30 HK harder than those produced by CD, Figure 4.98. The observation of more hardening of the machined surface caused by UAD than CD is consistent with Study 2 in the case when cutting speed was varied, as discussed previously in Section 4.2.4.4. For the 40^{th} holes, it is plausible that the dominant influence of tool wear was the reason for not seeing a marked difference between UAD and CD, Figure 4.99.

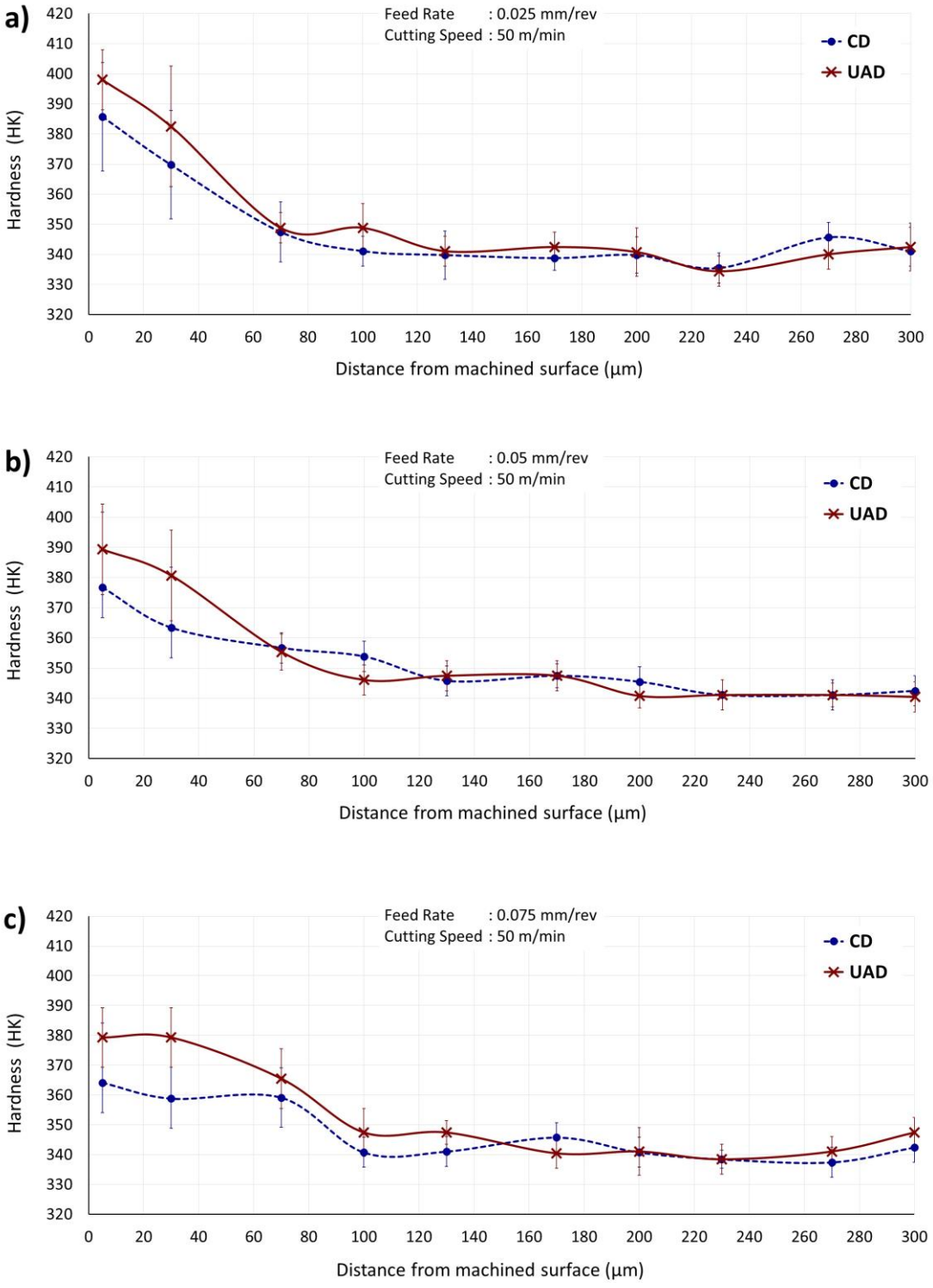

Figure 4.98: Comparison of sub-surface hardness of Ti cross section produced by CD and UAD of CFRP/Ti stacks using feed rates of 0.025, 0.05 and 0.075 mm/rev at a constant cutting speed of 50 m/min (Initial Ti hardness before machining: 340 HK) – 1st holes

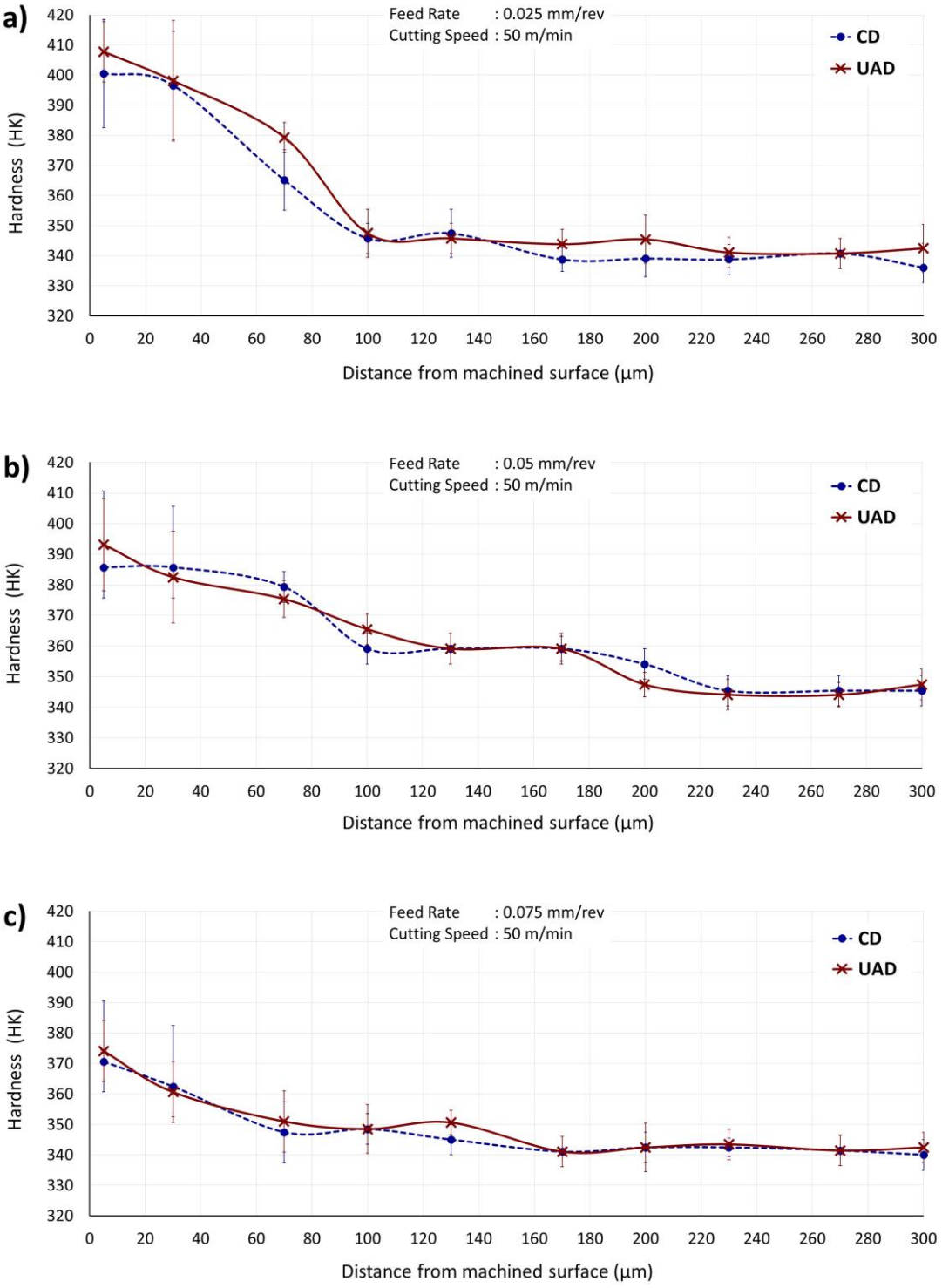

Figure 4.99: Comparison of sub-surface hardness of Ti cross section produced by CD and UAD of CFRP/Ti stacks feed rates of 0.025, 0.05 and 0.075 mm/rev at a constant cutting speed of 50 m/min (Initial Ti hardness before machining: 340 HK) – 40th holes

4.3.4.5 Titanium burr height (hole exit)

Figure 4.100 compares the progression of Ti burr height during CD and UAD of CFRP/Ti stacks when varying feed rates.

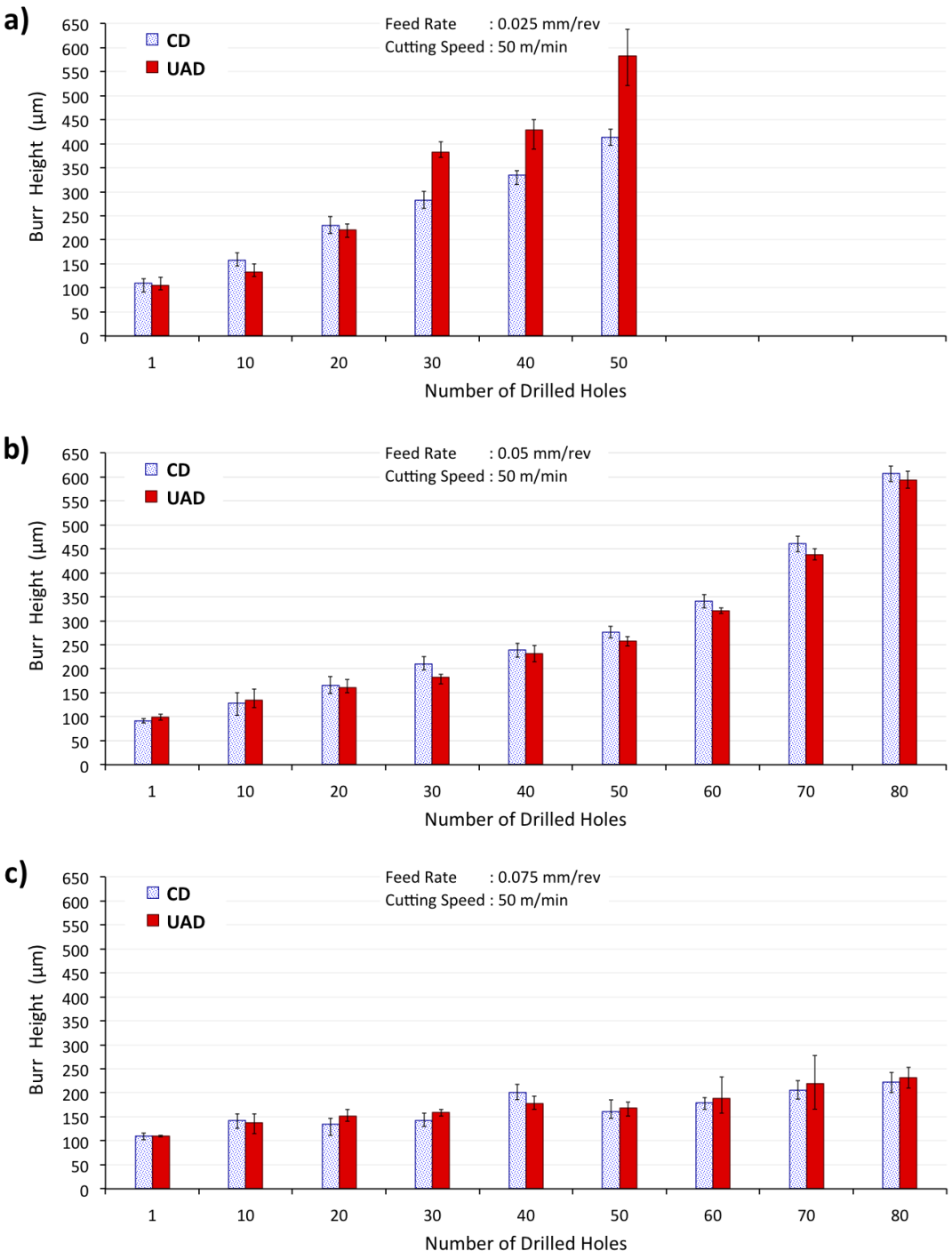

Figure 4.100: Comparison of Ti burr height at the hole exit caused by CD and UAD of CFRP/Ti stacks using feed rates of (a) 0.025 mm/rev, (b) 0.05 mm/rev and (c) 0.075 mm/rev at a constant cutting speed of 50 m/min. Range bars indicate variation for three consecutive holes (e.g. hole 1-3, hole 9-11, hole 19-21 etc.)

Increasing feed rate from 0.025 to 0.05 mm/rev reduced Ti burr height by on average of 19% and 36% during CD and UAD, respectively. Increasing feed rate further from 0.05 to 0.075 mm/rev reduced Ti burr height further by on average of 26% and 11% during CD and UAD, respectively. The result of Ti burr height in Figure 4.100 is consistent with the tool wear result, Figure 4.66. The Ti burr height was observed to be more consistent and progressed gradually when drilling using the highest feed rate of 0.075 mm/rev, Figure 4.100 (c), due to the lowest tool wear rate.

The difference between Ti burr height data produced by different feed rates was confirmed to be statistically significant by ANOVA, Appendix A, Table A.14. This means that Ti burr height was significantly affected by feed rate and tool wear. However, ANOVA established that the difference between Ti burr height data produced by CD and UAD at all feed rates was not statistically significant, Appendix A, Table A.14. This confirmed that the use of UAD did not significantly affect the Ti burr height at all feed rates employed compared to CD, which is consistent with the result of tool wear (Section 4.3.1).

The Ti burr morphology and grain flow of the 40th holes for all feed rates are compared in Figure 4.101. Drilling using the lowest feed rate of 0.025 mm/rev caused larger amount of Ti grain deformation / flow, hence higher burr (CD = 330 µm, UAD = 410 µm), Figure 4.101 (a, b), compared to the case of using the highest feed rate of 0.075 mm/rev (CD = 205 µm, UAD = 190 µm), Figure 4.101 (e, f). The higher Ti burr with decreasing feed rate was due to more material being "pushed" and extruded by the worn cutting edges, instead of being sheared during the drilling. Therefore, to obtain the least Ti burr when drilling CFRP/Ti stacks, using a higher feed rate (e.g. 0.075 mm/rev) is recommended.

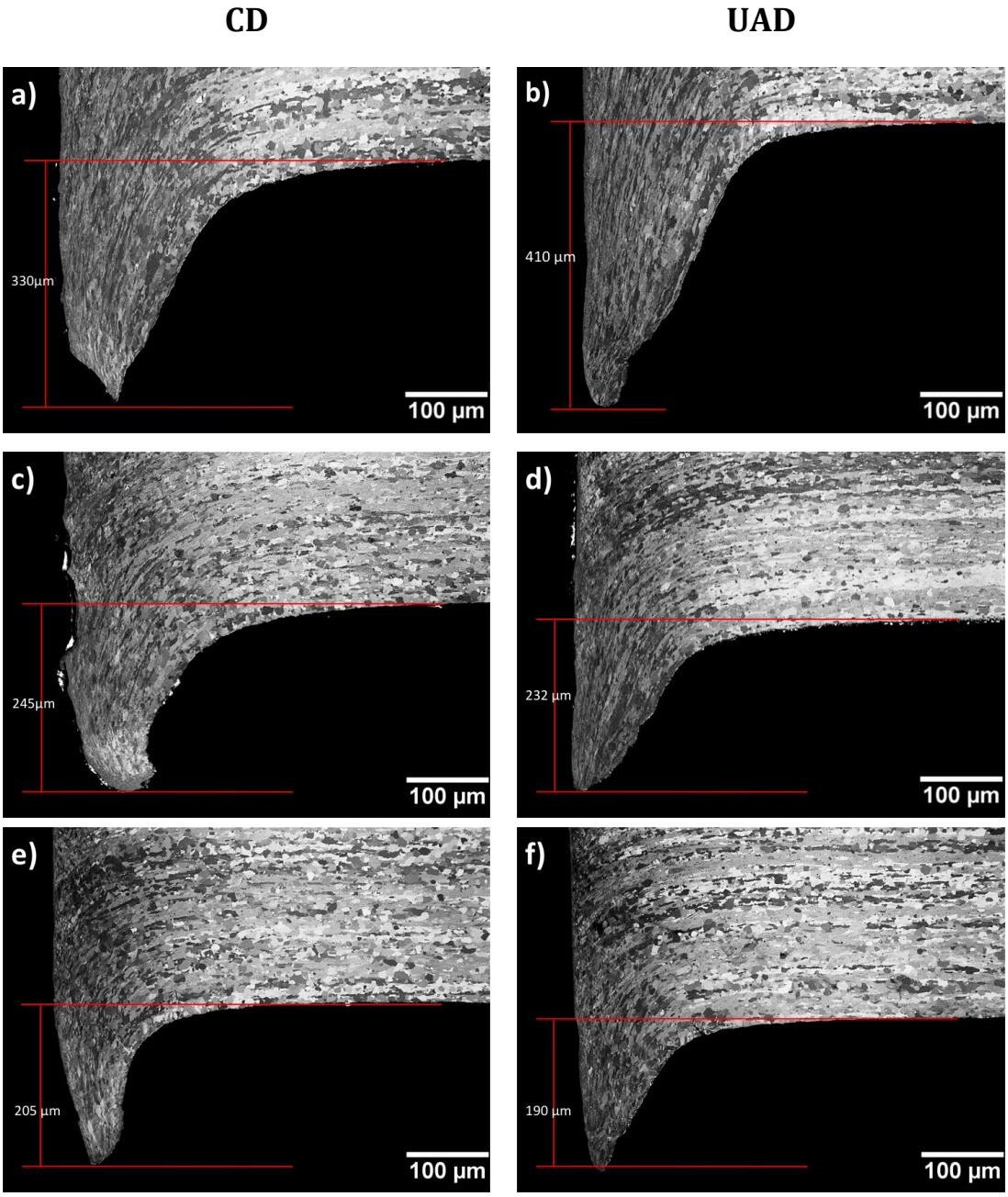

Figure 4.101: Cross section of Ti burr at the exit of the 40th holes caused by CD and UAD of CFRP/Ti stacks using feed rates of (a, b) 0.025 mm/rev, (c, d) 0.05 mm/rev and, (e, f) 0.075 mm/rev at a constant cutting speed of 50 m/min

4.3.5 Conclusions from Study 3

In summary, tool wear, hole diameter, CFRP pull-out and Ti burr height when drilling CFRP/Ti stacks were significantly affected by feed rate. However, CFRP delamination and Ti surface roughness were not significantly affected by feed rate. Tool wear reduced and longer tool life was achieved with increasing feed rate. The longest tool life (CD and UAD = 130 holes) was achieved when drilling with the highest feed rate of 0.075 mm/rev due to minor Ti adhering to the cutting edges and the cutting edges wore gradually and uniformly by abrasive wear mechanism. In contrast, drilling with the lowest feed rate caused the shortest tool life (CD = 40 holes, UAD = 35 holes) due to severe Ti adhering to the cutting edges leading to substantial cutting edge fragmentation.

In terms of hole quality, due to the least tool wear and Ti adhesion, using the highest feed rate of 0.075 mm/rev (cutting speed = 50 m/min) is favourable for producing consistent hole diameter, closer to the drill nominal diameter (up to 80 holes) and the least Ti burr height. Using the high feed rate of 0.075 mm/rev did not significantly affect CFRP entrance delamination and machined Ti surface roughness, however, it caused 45% more fibre pull-out, despite lower tool wear than the case of using the lower feed rate of 0.025 mm/rev.

At all feed rates, the application of UAD on CFRP/Ti stacks did not significantly improve tool life compared to CD. At the lowest feed rate of 0.025 mm/rev, UAD caused more rapid and substantial cutting edge fragmentation compared to CD. There was no significant difference in CFRP delamination, CFRP pull-out and Ti burr height between UAD and CD. Nevertheless, UAD resulted in smaller diameter difference between the holes in CFRP and Ti, as well as improved machined Ti surfaces in terms of lower roughness and increased hardness.

Chapter 5 Discussion

5.1 Tool wear

Previous studies [37, 41, 133, 136] reported a mixture of cutting edge rounding (abrasive wear), material adhesion on cutting edges and edge chipping (adhesive wear) when drilling CFRP/Ti stacks, however, it was difficult to determine in which event they occurred as various cutting tools, cutting parameters and drilling condition were employed. The current research has extended the knowledge of tool wear mechanisms when drilling CFRP/Ti stacks. In this research, it was shown that drilling CFRP/Ti stacks in one-shot using uniform cutting parameters (cutting speed = 50 m/min, feed rate = 0.05 mm/rev) is more difficult than drilling the materials individually. This was attributed to a complex interaction between two different tool wear mechanisms causing severe Ti adhesion to the cutting edges, thereby rapid tool failure due to cutting edge fragmentation. Obtaining manageable Ti adhesion, uniform and gradual tool wear (by edge rounding) when drilling CFRP/Ti stacks is possible by minimising the heat generation and reducing contact time. This was achieved by reducing cutting speed and increasing feed rate. A change in the wear mechanisms when drilling CFRP/Ti stacks from severe adhesive wear and cutting edges fracture to abrasive wear (edge rounding) was observed as cutting speed decreased from 75 to 25 m/min (at a constant feed rate of 0.05 mm/rev) and as feed rate increased from 0.025 to 0.075 mm/rev (at a constant cutting speed of 50 m/min).

A limited amount of Ti adhered uniformly to the cutting edges when drilling the Ti layer of the stack was beneficial as it protected the cutting edges and is gradually abraded away when drilling CFRP. This is the key to gradual tool wear when drilling CFRP/Ti stacks, rather than substantial Ti adhesion being built up which is not easily abraded, thereby suddenly fractured causing cutting edge fragmentation. The stable,

gradual and predictable tool failure when using a lower cutting speed of 25 m/min (feed rate = 0.05 mm/rev) and a higher feed rate of 0.075 mm/rev (cutting speed = 50 m/min) is vital for better tool life and less tool changes during drilling operations. In contrast, employing a higher cutting speed of 75 m/min (feed rate = 0.05 mm/rev) or lower feed rate of 0.025 mm/rev (cutting speed = 50 m/min) when drilling CFRP/Ti stacks could lead to scrapping a very expensive component as the drill may fail or break abruptly, and there is no operator to stand by the machine tool to monitor the operation at all time in the event it occurs.

With regards to UAD application on CFRP/Ti stacks, it was found that vibrating the drill (frequency = 40 kHz, peak-to-peak amplitude = 11 μm) did not reduce the amount of Ti adhesion to the cutting edges and tool wear compared to CD. This indicated that with the employed cutting tools and parameters, it is not possible to improve tool life and productivity when drilling CFRP/Ti stacks by applying ultrasonic assistance. The oscillation of the drill back and forth during UAD caused rapid fluctuation in the feed rate, which may cause earlier drill failure compared to CD if the cutting edge is not strong. Oscillation of the drill during UAD in this research was not observed to cause intermittent cutting (periodic separation of the cutting edges and workpiece). Instead, the cutting mechanism in UAD was continuous as in the case of CD, with the employed cutting tools, cutting parameters, and ultrasonic vibration parameter, which was the reason for not seeing a discernible difference in Ti adhesion and tool wear in UAD compared to CD. Previous studies [143, 145] reported that intermittent cutting during drilling CFRP/Ti stacks which was achieved by employing Low Frequency Vibration Assisted Drilling (LFVAD) is favourable to facilitate Ti chip removal, hence less Ti adhesion on the cutting edges and longer tool life compared to CD. Despite a similar concept of drill vibration during LFVAD and UAD, it important to note that LFVAD uses

10 times higher amplitude (e.g. 100 – 300 μm) and 1000 times lower frequency (e.g. 10 – 40 Hz) than UAD (e.g. amplitude = 2 – 20 μm, frequency = 10,000 – 40,000 Hz).

5.2 Hole quality

Obtaining a total improvement in hole quality in CFRP/Ti stacks is difficult. When the hole quality in Ti component of the stacks was improved, the hole quality in CFRP was not. Previous studies [37, 39, 102, 103] have reported that CFRP delamination, fibre pull out and Ti burr were common damage observed when drilling CFRP/Ti stacks which deteriorated hole quality, however, factors which caused the damage was not detailed. Whilst obtaining uniform and gradual tool wear is important to prolong the tool life, this does not necessarily improve the overall hole quality in CFRP/Ti stacks. In fact, controlling the hole quality in CFRP/Ti stacks is complex because of two different materials. The consistency of hole diameter and Ti burr height growth were found to be positively correlated and were significantly affected by the progressive increase in Ti adhesion and tool wear due to increased cutting speed and decreased feed rate. Using a lower cutting speed of 25 m/min (feed rate = 0.05 mm/rev) and a higher feed rate of 0.075 mm/rev (cutting speed = 50 m/min) is important to obtain consistent hole diameters within H7 tolerance (-0.000/+0.015 mm) and the least Ti burr (height of less than 250 μm up to 80 holes).

However, the extent of damage to the holes in CFRP in terms of delamination and fibre pull was not found to be significantly affected by tool wear. Rather, CFRP entrance delamination and fibre pull-out were primarily governed by the Ti chip flow. Although longer tool life, hence consistent hole diameter and least Ti burr height were achieved by reducing cutting speed and increasing feed rate, CFRP delamination at the hole entrance when drilling CFRP/Ti stacks was not reduced. The inconsistency and lack of definite trend in CFRP entrance delamination with respect to the change in cutting

speed and feed rate were attributed to the sharp Ti chips, which caused unpredictability, variation and additional damage to the CFRP as the Ti chip evacuated through the CFRP workpiece and whirling (entangling and moving around the drill) on the hole entrance. The fibre pull-out from the machined surfaces of CFRP was largely affected by feed rate, in addition to the factor of Ti chip. Even though using a higher feed rate (0.075 mm/rev) when drilling CFRP/Ti stacks was beneficial to obtain a longer tool life, the larger amount of material removed per drill revolution caused more CFRP pull-out from the machined surfaces. This indicates that there is no single solution to improve both productivity and hole quality in the CFRP component of the stacks, with respect to the change in feed rate; based on cutting parameters, cutting tool and drilling environment employed in this research. Therefore, further finishing operation would still be needed to improve the hole quality.

The implementation of UAD did not substantially improve the overall hole quality in CFRP/Ti stacks. UAD did not significantly reduce the CFRP damage as similarly long, continuous and spiral Ti chips were produced since the cutting mechanism remained continuous. Notably, the oscillation of the drill back and forth during UAD has potential to cause more consistent diameter between the holes in CFRP and Ti in stacks. In terms of the surface integrity of Ti workpiece, evidence showed that UAD generated lower surface roughness and harder machined surface compared to CD (Sections 4.2.4.4 and 4.3.4.4), which was attributed to more plastic deformation on the machined surfaces caused by the drill oscillation during UAD. This suggests that UAD is favourable for Ti individually for improving the strength of the machined component. No reported data of machined surface integrity of Ti caused by UAD was found, therefore, this finding contributed to the body of knowledge regarding the effect of drill oscillation during drilling on the machined surface of Ti. Even though no further work to check the fatigue life of the machined Ti was conducted due to time constraint and it was not the

focus of this research, the hardness data and limited data of residual stress obtained from this study can be used as a benchmark to initiate a further work focussing on the potential of UAD to improve the fatigue strength of the machined component, particularly titanium alloy.

Eliminating Ti burr formation was not possible during UAD in this work. The fact that the Ti burr was formed as early as drilling the first hole in all CD and UAD at all cutting speeds and feed rates indicated that the geometry of the drill is not optimal for producing a free-burr hole to begin with. This indicated that a secondary finishing operation is still required to remove the burr, regardless of cutting parameters employed in this research. Therefore, further work on the drill geometry, which can produce holes with zero or minimal burr in order to improve hole quality, would be beneficial.

With the range of parameters employed in the current study, the application of UAD for CFRP/Ti stacks does not eliminate the requirement for a secondary finishing operation. In order to obtain a significant advantage in hole quality of CFRP/Ti stacks, further research on the drill geometry to break the long Ti chip should be incorporated. Whilst this study has provided the basis for understanding the cutting mechanism during UAD, further work is required to maximise the potential of UAD in improving tool wear and hole quality compared to CD.

Chapter 6 Conclusions

The aim of this work was to develop the fundamental knowledge and yield understanding of machinability of CFRP/Ti stacks in terms of tool wear and hole quality during CD and UAD using tungsten carbide (WC-Co) drills. The following conclusions were drawn from this work:

6.1 Conclusions from the literature review

- The main critical issues when drilling CFRP-only has been associated with rapid abrasive tool wear, CFRP delamination and fibre pull-out. CFRP has been recommended to be drilled with low feed rates (e.g. lower than 0.05 mm/rev) to minimise the thrust forces and hence CFRP damage. Whereas, the thrust force and CFRP damage typically are less affected by cutting speed, thereby permits the use of high cutting speed (e.g. higher than 100 m/min), which is favourable for improving productivity.

- The main issue when drilling Ti-only is high cutting temperature (higher than 500 °C), which is typically due to the use of high cutting speed, causing rapid weakening of cutting edges and accelerating drill failure. Therefore, titanium has been recommended to be drilled with a low cutting speed (e.g. 20 – 60 m/min) and high feed rate (e.g. higher than 0.1 mm/rev) with cutting fluid / coolant to minimise cutting temperature and contact time.

- The different requirement of cutting parameters when drilling CFRP-only and Ti-only has resulted in the majority of studies involving drilling CFRP/Ti stacks to change cutting speed and feed rate between the CFRP and titanium layers of the stacks. However, this is impractical in industry. A uniform set of cutting parameters when drilling through the stacks is preferable, however, the limited

research precluded understanding the machinability of CFRP/Ti stacks in terms of tool wear and hole quality.

- Ultrasonic Assisted Drilling (UAD) has attracted industry and researchers' attention as it has been demonstrated to produce lower thrust force, which it was suggested may improve tool wear and hole quality of CFRP/Ti stacks. However, because of the lack of reported research and machining data regarding UAD of CFRP/Ti stacks, there is a lack of understanding of the cutting mechanisms involved and its functional performance.

6.2 Conclusions from experimental work

6.2.1 Tool wear mechanisms and hole quality during conventional drilling of CFRP/Ti stacks compared to drilling CFRP and Ti alloy individually using a cutting speed of 50 m/min and feed rate of 0.05 mm/rev

- When drilling CFRP-only, tools wore uniformly by an abrasive wear mechanism. In contrast, a limited adhesive tool wear was observed when drilling Ti-only. The interaction between abrasive and adhesive wear mechanisms during one-shot drilling of CFRP/Ti stacks was identified as the reason for severe adhesive wear, hence causing 90% and 1038% higher tool wear than drilling CFRP-only and Ti-only, respectively after 80 holes. Ti adhered strongly on the abraded cutting edges. The strong metallic bonding between the drill substrate (WC-Co) and the Ti caused substantial WC-Co fracture, hence rapid tool failure. A delay between drilling CFRP and Ti caused less Ti adhesion and reduced tool wear, which was attributed to the presence of protective oxide layer on the cutting edges.

- For one-shot drilling of CFRP/Ti stacks, as the number of holes increased, hole diameter became increasingly inconsistent. CFRP pull-out increased and Ti burr height increased due to the increase in tool wear and Ti adhesion. CFRP entrance

delamination was not substantially affected by tool wear, rather, it was substantially affected by the Ti chip evacuated through the CFRP layer of the stacks. In contrast, for drilling CFRP-only, hole diameters were consistent, whereas, CFRP entrance delamination and CFRP pull-out progressed gradually with increasing tool wear until the end of drilling test (80 holes). In the case of drilling Ti-only, hole diameter and Ti burr height were consistent from the beginning until the end of drilling test due to the least tool wear.

6.2.2 The effect of cutting parameters during one-shot CD and UAD of CFRP/Ti stacks on tool wear and hole quality

- Decreasing cutting speed from 75 to 50 to 25 m/min (at a constant feed rate = 0.05 mm/rev), and increasing feed rate from 0.025 to 0.05 to 0.075 mm/rev (at a constant cutting speed = 50 m/min) when drilling CFRP/Ti stacks was found to significantly reduce the titanium adhesion on the cutting edges and tool wear, hence longer tool life was achieved. Consequently, consistent hole diameter within tolerance closer to the nominal diameter of 6.1 mm and reduced Ti burr height were obtained. There was no significant difference in tool life and Ti burr height produced by CD and UAD at all cutting parameters. Nevertheless, the use of UAD was found to produce more consistent diameter with smaller (by 0 – 2 μm) diameter difference between the holes in CFRP and Ti of the stacks, compared to CD, which produced larger diameter difference (of 1 – 6 μm).

- No significant difference in CFRP delamination was found irrespective of cutting parameters employed and whether CD or UAD were employed. CFRP delamination was not reduced despite the limited Ti adhesion and reduction in tool wear with decreasing cutting speed and increasing feed rate. This was due to the fact that CFRP delamination was largely affected by the titanium chip

evacuating through the CFRP layer of the stacks, rather than tool wear, irrespective of cutting parameters.

- Carbon fibre pull-out from the machined surfaces during CD and UAD of CFRP/Ti stacks was not significantly affected by cutting speed. However, there was 45% reduction in carbon fibre pull-out as the feed rate reduced from 0.075 to 0.025 mm/rev, despite the drill exhibiting 270% higher tool wear. The volume of CFRP pull-out caused by UAD exhibited no significant difference than CD.

- When tool wear was minimal (1st holes), the roughness of machined titanium surfaces reduced with increasing cutting speed and decreasing feed rate. However, with increasing hole number and tool wear, the surface roughness of titanium fluctuated. At all cutting parameters, the use of UAD was found to generate on average 33% lower titanium surface roughness than those of CD.

- The hardness of the machined titanium surface increased with decreasing cutting speed as well as with decreasing feed rate when drilling CFRP/Ti stacks. The use of UAD was found to have potential to generate harder and stronger machined surface of Ti than those produced by CD.

6.2.3 Cutting forces profiles and chip formation during UAD of CFRP/Ti stacks compared to CD

- Ultrasonic Assisted Drilling (UAD) of CFRP/Ti stacks at all cutting parameters exhibited 24% – 45% larger forces variation compared to CD, which was attributed to oscillation of the drills during UAD causing variation in feed rate. Intermittent cutting did not occur during UAD, rather the cutting was continuous similar to the case of conventional drilling (CD).

- Both CD and UAD at all cutting parameters produced titanium chips having similar morphology taking the form of spiral and folded. Cross sectioning,

polishing and etching the chips revealed segmentation, i.e. apparent shear bands. The shear bands in the titanium chips became more evident with increasing cutting speed from 25 to 50 to 75 m/min, and with reducing feed rate from 0.075 to 0.05 to 0.025 mm/rev, indicative of increased variation in thermal softening and hardening of the workpiece during chip formation.

- UAD and CD at all cutting parameters produced continuous titanium chips having a similar length within the range of 4 to 12 cm. No broken titanium chips were observed during UAD at all cutting parameters. This indicated that the chips during UAD were formed continuously as the cutting was continuous similar to the case of CD. However, titanium chips produced by UAD exhibited on average 46% larger variation in thickness compared to CD, which supported the observation of larger forces variation due to drill oscillation during UAD.

6.3 Final conclusions

This research has developed the knowledge and understanding of machinability of CFRP/Ti stacks in terms of tool wear and hole quality when drilling. The overall conclusions about this thesis are:

- Evidence of complex tool wear mechanisms when drilling CFRP/Ti stacks were presented and explained. The rapid drill failure during one-shot drilling of CFRP/Ti stacks using uniform cutting parameters was due to the interaction between abrasive and adhesive wear mechanisms causing strong Ti adhesion, and hence cutting edge fracture.

- The effect of cutting parameters when one-shot drilling of CFRP/Ti stacks on tool wear and subsequently its influence on hole quality was established, which was often ignored in the previous literature. Cutting speed and feed rate are vital

parameters, which have to be carefully controlled since they significantly affect tool wear mechanism and hence tool life. The use of low cutting speed and high feed rate, which caused less heat generation is beneficial for obtaining less Ti adhesion, gradual tool wear and hence longer tool life when drilling CFRP/Ti stacks. The less Ti adhesion on the cutting edges and gradual tool wear are favourable for obtaining consistent hole diameter in CFRP/Ti stacks within tolerance and less Ti burr formation. However, the gradual tool wear did not resolve CFRP damage as the damage was found to be substantially affected by the Ti chips evacuating through the CFRP layer of the stacks.

- Evidence of continuous cutting and drill oscillation during UAD of CFRP/Ti stacks were presented, which was lacking in the previous literature, and its effect on tool wear / life and hole quality was established. The application of UAD did not provide any significant advantage in tool life compared to CD, as the cutting remains continuous. It is concluded that tool wear is significantly governed by cutting parameters, rather than by drill oscillation (peak-to-peak amplitude = 11 μm, frequency = 40 kHz). However, the oscillation of the drill during UAD caused larger variation in cutting forces compared to CD and can lead to earlier cutting edge fracture if the cutting edges are not strong enough. Furthermore, UAD did not completely resolve the hole quality issue of CFRP/Ti stacks. The oscillation of the drill during UAD is beneficial to produce consistent diameter between the holes in CFRP and Ti of the stacks, lower machined Ti surface roughness and harder Ti sub-surface, compared to CD. However, CFRP damage during UAD was not reduced compared to CD since the damage is affected by long Ti chips, similarly produced by CD and UAD. Therefore, within this research context, finishing operations would be needed to improve the hole quality after either CD or UAD.

Chapter 7 Future Work

- Earlier cutting edge fracture that was observed during UAD at high cutting speed and low feed rate indicated that UAD required strong cutting edges compared to CD. Therefore, further work to investigate a stronger cutting tool material (e.g. development of mixed carbide) and geometry for UAD application particularly for titanium alloy is recommended.

- This work has shown that UAD has potential to produce machined Ti surfaces with lower surface roughness and marginal improvement in hardness compared to CD, however, there was limited data on residual stress. Further work focusing on the residual stress and fatigue strength of the machined surfaces produced by drilling operations is recommended. Extensive analysis on fatigue life and mechanical properties of the machined component would be beneficial to determine whether improvement in the functional performance of the machined component can be achieved by UAM application.

- Further investigation of UAD parameters (amplitude and frequency) is required to see if intermittent cutting can be achieved. Consequently, investigation of its implication on tool wear and the machined surfaces would be beneficial.

- It would be beneficial to examine the way in which the cutting tool oscillates during UAM influences the way the workpiece material behaves in the cutting zone, i.e. on the primary shear plane and rake face of the tool.

- Experimental work is costly and very time consuming. Therefore, modelling of drilling operations (CD and UAD) would be beneficial as a guideline to determine the optimised parameters for achieving better tool life and improved hole quality. The machining data presented in this thesis can be used as the input, reference and benchmark for modelling work.

References

1. Mouritz, A.P., *Introduction to Aerospace Materials*. 2012: Elsevier. ISBN 9781855739468.
2. Chawla, K., *Composite Materials: Science and Engineering*. Third Edition. 2012, New York Springer. ISBN 9780387743646.
3. Murray, G., C. White, and W. Weise, *Introduction to Engineered Materials*. Second Edition. 2008, Boca Raton: CRC Press, Taylor & Francis Group. ISBN 9781574446838.
4. Mortensen, A., *Concise Encyclopedia of Composite Materials.* Second Edition. 2007, Oxford: Elsevier. ISBN 9780080451268.
5. Astrom, B.T., *Manufacturing of Polymer Composites*. 1997: CRC Press. ISBN 0748770763.
6. Sheikh-Ahmad, J.Y., *Machining of Polymer Composites*. 2009: Springer. ISBN 9780387355399.
7. Campbell, F.C., *Structural Composite Materials*. 2010: ASM International. ISBN 9781615030378.
8. Karpat, Y., B. Değer, and O. Bahtiyar, "Drilling thick fabric woven CFRP laminates with double point angle drills", *Journal of Materials Processing Technology*, 2012, **212**(10): pp. 2117-2127.
9. Lazar, M. and P. Xirouchakis, "Experimental analysis of drilling fiber reinforced composites", *International Journal of Machine Tools and Manufacture*, 2011, **51**(12): pp. 937-946.
10. Gay, D., *Composite Materials: Design and Applications*. Third Edition. 2014: CRC press. ISBN 9781466584877.
11. Liu, D., Y. Tang, and W. Cong, "A review of mechanical drilling for composite laminates", *Composite Structures*, 2012, **94**(4): pp. 1265-1279.
12. Zhao, Y.H., Y.F. Zhang, S.L. Bai, and X.W. Yuan, "Carbon fibre/graphene foam/polymer composites with enhanced mechanical and thermal properties", *Composites Part B: Engineering*, 2016, **94**: pp. 102-108.
13. He, H.W. and F. Gao, "Effect of fiber volume fraction on the flexural properties of unidirectional carbon fiber/epoxy composites", *International Journal of Polymer Analysis and Characterization*, 2015, **20**(2): pp. 180-189.
14. Hamza, M.S., "Study the effect of carbon fiber volume fraction and their orientations on the thermal conductivity of the polymer composite materials", *Al-Khwarizmi Engineering Journal*, 2008, **4**(1): pp. 80-89.
15. Ward, I.M. and D.W. Hadley, *An Introduction to the Mechanical Properties of Solid Polymers*. Second Edition. 2004: John Wiley & Sons Ltd. ISBN 9780471496267.
16. Schwartz, M.M., *Composite Materials. Volume 1: Properties, Non-Destructive Testing, and Repair*. 1997: Prentice Hall. ISBN 9780133000474.

17. Bolton, W. and R.A. Higgins, *Materials for Engineers and Technicians*. 2014: Routledge. ISBN 1317676130.

18. Liaw, D.J., P.N. Hsu, W.H. Chen, and S.L. Lin, "High glass transitions of new polyamides, polyimides, and polyamide-imides containing a triphenylamine group: synthesis and characterization", *Macromolecules*, 2002, **35**(12): pp. 4669-4676.

19. Lin, K.-F., J.-S. Lin, and C.-H. Cheng, "High temperature resins based on allylamine/bismaleimides", *Polymer*, 1996, **37**(21): pp. 4729-4737.

20. Davim, J.P., *Machining: Fundamentals and Recent Advances*. 2008: Springer. ISBN 1848002130.

21. Leyens, C. and M. Peters, *Titanium and Titanium Alloys*. 2003: Wiley Online Library. ISBN 9783527305346.

22. Moiseyev, V.N., *Titanium Alloys Russian Aircraft and Aerospace Applications*. 2005: CRC Press. ISBN 9780849332739.

23. Lütjering, G. and J.C. Williams, *Engineering Materials and Processes: Titanium*. Second Edition. 2003: Springer. ISBN 9783540713975.

24. Davim, J.P., *Machining of Titanium Alloys*. Materials Forming, Machining and Tribology. 2014, Verlag Berlin Heidelberg: Springer. ISBN 9783662439012.

25. Grzesik, W., *Advanced Machining Processes of Metallic Materials: Theory, Modelling and Applications*. 2008: Elsevier. ISBN 9780080557496.

26. Donachie, M.J., *Titanium: A Technical Guide*. Second Edition. 2000: ASM international. ISBN 9780871706867.

27. Hosseini, A. and H. Kishawy, *Cutting tool materials and tool wear*, in *Machining of Titanium Alloys*, J.P. Davim, Editor. 2014, Springer: Berlin, Heidelberg. ISBN 9783662439012.

28. Grzesik, W., *Machining of hard materials*, in *Machining: Fundamentals and Recent Advances*, P. Davim, Editor. 2008, Springer: London.

29. Sharif, S., E.A. Rahim, and H. Sasahara, *Machinability of titanium alloys in drilling*, in *Titanium Alloys - Towards Achieving Enhanced Properties for Diversified Applications*, A.K.M.N. Amin, Editor. 2012, Intech Open. ISBN 9789535103547.

30. Welsch, G., R. Boyer, and E. Collings, *Materials Properties Handbook: Titanium Alloys*. 1993: ASM international. ISBN 0871704811.

31. Klocke, F., *Manufacturing Processes 1: Cutting*. 2011, Berlin Heidelberg: Springer. 503. ISBN 9783642119798.

32. Stephenson, D.A. and J.S. Agapiou, *Metal Cutting Theory and Practice*. Third Edition. 2016, Boca Raton: CRC press. ISBN 9781466587540.

33. Yang, X. and C. Richard Liu, "Machining titanium and its alloys", *Machining Science and Technology*, 1999, **3**(1): pp. 107-139.

34. Smith, G.T., *Cutting Tool Technology: Industrial Handbook*. 2008: Springer. ISBN 9781848002043.

35. Trent, E.M. and P.K. Wright, *Metal Cutting*. Fourth Edition. 2000: Butterworth-Heinemann. ISBN 9780080511450.

36. Sandvik. *Cemented Carbide, Sandvik New Developments and Applications*. 2006, Sandvik Group. Available from: http://pdf.directindustry.com/pdf/sandvik-hyperion/cemented-carbide/14464-89403-_3.html (Assessed 24 September 2016).

37. Isbilir, O. and E. Ghassemieh, "Comparative study of tool life and hole quality in drilling of CFRP/titanium stack using coated carbide drill", *Machining Science and Technology*, 2013, **17**(3): pp. 380-409.

38. Niknam, S.A., R. Khettabi, and V. Songmene, *Machinability and machining of titanium alloys: A review*, in *Machining of Titanium Alloys*, J.P. Davim, Editor. 2014, Springer: Berlin, Heidelberg. ISBN 9783662439029.

39. Shyha, I.S., S.L. Soo, D.K. Aspinwall, S. Bradley, R. Perry, P. Harden, and S. Dawson, "Hole quality assessment following drilling of metallic composite stacks", *International Journal of Machine Tools and Manufacture*, 2011, **51**(7–8): pp. 569-578.

40. Sharif, S. and E. Rahim, "Performance of coated-and uncoated carbide tools when drilling titanium alloy Ti6Al4V", *Journal of materials processing technology*, 2007, **185**(1): pp. 72-76.

41. Wang, X., P.Y. Kwon, C. Sturtevant, D. Kim, and J. Lantrip, "Comparative tool wear study based on drilling experiments on CFRP/Ti stack and its individual layers", *Wear*, 2014, **317**: pp. 265-276.

42. Kurlov, A.S. and A.I. Gusev, *Tungsten Carbides : Structure, Properties and Application in Hardmetals*. 2013: Springer. ISBN 9783319343921.

43. Astakhov, V.P., *Drills: Science and Technology of Advanced Operations*. 2014: CRC Press. ISBN 9781466584341.

44. Boothroyd, G. and W. Knight, *Fundamentals of Machining and Machine Tools*. Third Edition. 2006, Boca Raton: Taylor & Francis Group. ISBN 9781574446593.

45. Park, K.-H., A. Beal, D. Kim, P. Kwon, and J. Lantrip, "Tool wear in drilling of composite/titanium stacks using carbide and polycrystalline diamond tools", *Wear*, 2011, **271**(11–12): pp. 2826-2835.

46. Garrick, R. *Drilling advanced aircraft structures with PCD (Poly-Crystalline Diamond) drills*. 2007, SAE Technical Paper.

47. Astakhov, V.P., *Geometry of single-point turning tools and drills: fundamentals and practical applications*. 2010: Springer. ISBN 1849960534.

48. Shaw, M.C., *Metal Cutting Principles*. Second Edition. 2005: Oxford University Press New York. ISBN 9788123901367.

49. Davim, J.P., *Machining Composite Materials*. 2010, London; Hoboken: Wiley. ISBN 9781848211704.

50. Krishnaraj, V., R. Zitoune, and J.P. Davim, *Drilling of Polymer Matrix Composites*. 2013: Springer Berlin Heidelberg. ISBN 9783642383441.

51. Faraz, A., D. Biermann, and K. Weinert, "Cutting edge rounding: An innovative tool wear criterion in drilling CFRP composite laminates", *International Journal of Machine Tools and Manufacture*, 2009, **49**(15): pp. 1185-1196.

52. Wang, X., P.Y. Kwon, C. Sturtevant, D. Kim, and J. Lantrip, "Tool wear of coated drills in drilling CFRP", *Journal of Manufacturing Processes*, 2013, **15**(1): pp. 127-135.

53. Rawat, S. and H. Attia, "Wear mechanisms and tool life management of WC–Co drills during dry high speed drilling of woven carbon fibre composites", *Wear*, 2009, **267**(5–8): pp. 1022-1030.

54. Ramirez, C., G. Poulachon, F. Rossi, and R. M'Saoubi, "Tool wear monitoring and hole surface quality during CFRP drilling", *Procedia CIRP*, 2014, **13**: pp. 163-168.

55. Stachowiak, G. and A.W. Batchelor, *Engineering Tribology*. Fourth Edition. 2013: Butterworth-Heinemann. ISBN 9780123977762.

56. Masuda, M., Y. Kuroshima, and Y. Chujo, "Failure of tungsten carbide-cobalt alloy tools in machining of carbon materials", *Wear*, 1993, **169**(2): pp. 135-140.

57. Teti, R., "Machining of Composite Materials", *CIRP Annals - Manufacturing Technology*, 2002, **51**(2): pp. 611-634.

58. Gaugel, S., P. Sripathy, A. Haeger, D. Meinhard, T. Bernthaler, F. Lissek, M. Kaufeld, V. Knoblauch, and G. Schneider, "A comparative study on tool wear and laminate damage in drilling of carbon-fiber reinforced polymers (CFRP)", *Composite Structures*, 2016, **155**: pp. 173-183.

59. Henerichs, M., R. Voß, D. Harsch, F. Kuster, and K. Wegener, "Tool life time extension with nano-crystalline diamond coatings for drilling carbon fibre reinforced plastics (CFRP)", *Procedia CIRP*, 2014, **24**: pp. 125-129.

60. Iliescu, D., D. Gehin, M. Gutierrez, and F. Girot, "Modeling and tool wear in drilling of CFRP", *International Journal of Machine Tools and Manufacture*, 2010, **50**(2): pp. 204-213.

61. Barnes, S., P. Bhudwannachai, and A.N. Dahnel. *Drilling performance of carbon fiber reinforced epoxy composite when machined dry, with conventional cutting fluid and with a cryogenically cooled tool*. in *ASME 2013 International Mechanical Engineering Congress and Exposition*. 15 - 21 Nov 2013, American Society of Mechanical Engineers, pp. V02BT02A063.

62. Chen, W.C., "Some experimental investigations in the drilling of carbon fiber-reinforced plastic (CFRP) composite laminates", *International Journal of Machine Tools and Manufacture*, 1997, **37**(8): pp. 1097-1108.

63. Sorrentino, L., S. Turchetta, and C. Bellini, "In process monitoring of cutting temperature during the drilling of FRP laminate", *Composite Structures*, 2017, **168**: pp. 549-561.

64. Liu, D., C. Zhang, and W. HY, "Study of Cutting Temperature in Drilling Carbon Fibre Reinforced Plastic (CFRP)", *4th International Conference on Intelligent Information Technology Application*, 2010: pp. 5-8.

65. Merino-Pérez, J., R. Royer, S. Ayvar-Soberanis, E. Merson, and A. Hodzic, "On the temperatures developed in CFRP drilling using uncoated WC-Co tools Part I: Workpiece constituents, cutting speed and heat dissipation", *Composite Structures*, 2015, **123**: pp. 161-168.

66. Karpat, Y. and O. Bahtiyar, "Comparative analysis of PCD drill designs during drilling of CFRP laminates", *Procedia CIRP*, 2015, **31**: pp. 316-321.

67. Xu, J., Q. An, and M. Chen, "A comparative evaluation of polycrystalline diamond drills in drilling high-strength T800S/250F CFRP", *Composite Structures*, 2014, **117**: pp. 71-82.

68. Davim, J.P. and P. Reis, "Study of delamination in drilling carbon fiber reinforced plastics (CFRP) using design experiments", *Composite structures*, 2003, **59**(4): pp. 481-487.

69. Mayuet, P., A. Gallo, A. Portal, P. Arroyo, M. Alvarez, and M. Marcos, "Damaged area based study of the break-in and break-out defects in the dry drilling of Carbon Fiber Reinforced Plastics (CFRP)", *Procedia Engineering*, 2013, **63**(0): pp. 743-751.

70. Krishnaraj, V., A. Prabukarthi, A. Ramanathan, N. Elanghovan, M. Senthil Kumar, R. Zitoune, and J.P. Davim, "Optimization of machining parameters at high speed drilling of carbon fiber reinforced plastic (CFRP) laminates", *Composites Part B: Engineering*, 2012, **43**(4): pp. 1791-1799.

71. Shyha, I., S.L. Soo, D. Aspinwall, and S. Bradley, "Effect of laminate configuration and feed rate on cutting performance when drilling holes in carbon fibre reinforced plastic composites", *Journal of Materials Processing Technology*, 2010, **210**(8): pp. 1023-1034.

72. Hocheng, H. and C. Tsao, "The path towards delamination-free drilling of composite materials", *Journal of materials processing technology*, 2005, **167**(2): pp. 251-264.

73. Feito, N., J. López-Puente, C. Santiuste, and M.H. Miguélez, "Numerical prediction of delamination in CFRP drilling", *Composite Structures*, 2014, **108**(0): pp. 677-683.

74. Enemuoh, E.U., A.S. El-Gizawy, and A. Chukwujekwu Okafor, "An approach for development of damage-free drilling of carbon fiber reinforced thermosets", *International Journal of Machine Tools and Manufacture*, 2001, **41**(12): pp. 1795-1814.

75. Haeger, A., G. Schoen, F. Lissek, D. Meinhard, M. Kaufeld, G. Schneider, S. Schuhmacher, and V. Knoblauch, "Non-destructive detection of drilling induced delamination in CFRP and its effect on mechanical properties", *Procedia Engineering*, 2016, **149**: pp. 130-142.

76. Gaitonde, V.N., S.R. Karnik, J.C. Rubio, A.E. Correia, A.M. Abrão, and J.P. Davim, "Analysis of parametric influence on delamination in high-speed drilling of carbon fiber reinforced plastic composites", *Journal of Materials Processing Technology*, 2008, **203**(1–3): pp. 431-438.

77. Aurich, J.C., B. Kirsch, C. Müller, and L. Heberger, "Quality of drilled and milled rivet holes in carbon fiber reinforced plastics", *Procedia CIRP*, 2014, **24**: pp. 56-61.

78. Sardinas, R.Q., P. Reis, and J.P. Davim, "Multi-objective optimization of cutting parameters for drilling laminate composite materials by using genetic algorithms", *Composites Science and Technology*, 2006, **66**(15): pp. 3083-3088.

79. Davim, J.P. and P. Reis, "Drilling carbon fiber reinforced plastics manufactured by autoclave experimental and statistical study", *Materials & Design*, 2003, **24**(5): pp. 315-324.

80. Bonnet, C., G. Poulachon, J. Rech, Y. Girard, and J.P. Costes, "CFRP drilling: Fundamental study of local feed force and consequences on hole exit damage", *International Journal of Machine Tools and Manufacture*, 2015, **94**: pp. 57-64.

81. Karnik, S.R., V.N. Gaitonde, J.C. Rubio, A.E. Correia, A.M. Abrão, and J.P. Davim, "Delamination analysis in high speed drilling of carbon fiber reinforced plastics (CFRP) using artificial neural network model", *Materials & Design*, 2008, **29**(9): pp. 1768-1776.

82. Dahnel, A.N., C. Kibbler, S. Barnes, and H. Ascroft. *Study of cutting forces and surface roughness in milling of Carbon Fibre Composite (CFC) with conventional and pressurized CO2 cutting fluids*. in *ASME 2015 International Mechanical Engineering Congress and Exposition*. Houston, Texas, USA: 13 - 19 Nov 2015, American Society of Mechanical Engineers, pp. V02BT02A042.

83. Li, M., S. Soo, D. Aspinwall, D. Pearson, and W. Leahy, "Influence of lay-up configuration and feed rate on surface integrity when drilling carbon fibre reinforced plastic (CFRP) composites", *Procedia CIRP*, 2014, **13**: pp. 399-404.

84. Poulachon, G., J. Outeiro, C. Ramirez, V. André, and G. Abrivard, "Hole surface topography and tool wear in CFRP drilling", *Procedia CIRP*, 2016, **45**: pp. 35-38.

85. Li, R. and A.J. Shih, "Tool temperature in titanium drilling", *Journal of Manufacturing Science and Engineering*, 2007, **129**(4): pp. 740-749.

86. Ezugwu, E. and Z. Wang, "Titanium alloys and their machinability - a review", *Journal of materials processing technology*, 1997, **68**(3): pp. 262-274.

87. Wu, H. and S. To, "Serrated chip formation and their adiabatic analysis by using the constitutive model of titanium alloy in high speed cutting", *Journal of Alloys and Compounds*, 2015, **629**: pp. 368-373.

88. Pramanik, A., "Problems and solutions in machining of titanium alloys", *The International Journal of Advanced Manufacturing Technology*, 2014, **70**(5-8): pp. 919-928.

89. Sutter, G. and G. List, "Very high speed cutting of Ti6Al4V titanium alloy - change in morphology and mechanism of chip formation", *International Journal of Machine Tools and Manufacture*, 2013, **66**: pp. 37-43.

90. Batista, M., J. Salguero, A. Gomez-Parra, S. Fernández-Vidal, and M. Marcos, "SOM based methodology for evaluating shrinkage parameter of the chip developed in titanium dry turning process", *Procedia CIRP*, 2013, **8**: pp. 533-538.

91. Sun, S., M. Brandt, and M. Dargusch, "Characteristics of cutting forces and chip formation in machining of titanium alloys", *International Journal of Machine Tools and Manufacture*, 2009, **49**(7): pp. 561-568.

92. Komanduri, R., "Some clarifications on the mechanics of chip formation when machining titanium alloys", *Wear*, 1982, **76**(1): pp. 15-34.

93. Bäker, M., "An investigation of the chip segmentation process using finite elements", *Technische Mechanik*, 2003, **23**(1): pp. 1-9.

94. Vyas, A. and M. Shaw, "Mechanics of saw-tooth chip formation in metal cutting", *Journal of Manufacturing Science and Engineering, Transactions of the ASME*, 1999, **121**(2): pp. 163-172.

95. Cantero, J., M. Tardio, J. Canteli, M. Marcos, and M. Miguelez, "Dry drilling of alloy Ti6Al4V", *International Journal of Machine Tools and Manufacture*, 2005, **45**(11): pp. 1246-1255.

96. Li, R., P. Hegde, and A.J. Shih, "High-throughput drilling of titanium alloys", *International Journal of Machine Tools and Manufacture*, 2007, **47**(1): pp. 63-74.

97. Dahnel, A.N., H. Ascroft, S. Barnes, and M. Gloger. *Analysis of tool wear and hole quality during Ultrasonic Assisted Drilling (UAD) of Carbon Fibre Composite (CFC)/titanium alloy (Ti6Al4V) stacks*. in *ASME 2015 International Mechanical Engineering Congress and Exposition*. Houstan, Texas, USA: 13 - 19 Nov 2015, American Society of Mechanical Engineers, pp. V02BT02A041.

98. Bermingham, M., S. Palanisamy, D. Kent, and M. Dargusch, "A comparison of cryogenic and high pressure emulsion cooling technologies on tool life and chip morphology in Ti6Al4V cutting", *Journal of Materials Processing Technology*, 2012, **212**(4): pp. 752-765.

99. Debnath, S., M.M. Reddy, and Q.S. Yi, "Environmental friendly cutting fluids and cooling techniques in machining: A Review", *Journal of Cleaner Production*, 2014: pp. 33-47.

100. Costa, E.S., M.B.d. Silva, and A.R. Machado, "Burr produced on the drilling process as a function of tool wear and lubricant-coolant conditions", *Journal of the Brazilian Society of Mechanical Sciences and Engineering*, 2009, **31**(1): pp. 57-63.

101. Nandgaonkar, S., T. Gupta, and S. Joshi, "Effect of Water Oil Mist Spray (WOMS) Cooling on Drilling of Ti6Al4V Alloy Using Ester Oil Based Cutting Fluid", *Procedia Manufacturing*, 2016, **6**: pp. 71-79.

102. Xu, J. and M. El Mansori, "Experimental study on drilling mechanisms and strategies of hybrid CFRP/Ti stacks", *Composite Structures*, 2016, **157**: pp. 461-482.

103. Kim, D. and M. Ramulu, "Drilling process optimization for graphite/bismaleimide–titanium alloy stacks", *Composite Structures*, 2004, **63**(1): pp. 101-114.

104. Abdelhafeez, A., S. Soo, D. Aspinwall, A. Dowson, and D. Arnold, "Burr formation and hole quality when drilling titanium and aluminium alloys", *Procedia CIRP*, 2015, **37**: pp. 230-235.

105. Shetty, P.K., R. Shetty, D. Shetty, N.F. Rehaman, and T.K. Jose, "Machinability study on dry drilling of titanium alloy Ti-6Al-4V using L9 orthoganal array", *Procedia Materials Science*, 2014, **5**: pp. 2605-2614.

106. Arulkirubakaran, D. and V. Senthilkumar, "Performance of TiN and TiAlN coated micro-grooved tools during machining of Ti6Al4V alloy", *International Journal of Refractory Metals and Hard Materials*, 2017, **62**: pp. 47-57.

107. Dearnley, P. and A. Grearson, "Evaluation of principal wear mechanisms of cemented carbides and ceramics used for machining titanium alloy IMI 318", *Materials Science and Technology*, 1986, **2**(1): pp. 47-58.

108. Biermann, D. and I. Terwey, "Cutting edge preparation to improve drilling tools for HPC processes", *CIRP Journal of Manufacturing Science and Technology*, 2008, **1**(2): pp. 76-80.

109. Shokrani Chaharsooghi, A., H. Sun, V. Dhokia, and S. Newman. *High speed cryogenic drilling of grade 5 ELI titanium alloy*. in *26th International Conference on Flexible Automation and Intelligent Manufacturing*. 2016. University of Bath.

110. Zhang, S., J.F. Li, J. Deng, and Y. Li, "Investigation on diffusion wear during high-speed machining Ti6Al4V alloy with straight tungsten carbide tools", *The International Journal of Advanced Manufacturing Technology*, 2009, **44**(1): pp. 17-25.

111. Bai, D., J. Sun, W. Chen, and D. Du, "Molecular dynamics simulation of the diffusion behaviour between Co and Ti and its effect on the wear of WC/Co tools when titanium alloy is machined", *Ceramics International*, 2016, **42**(15): pp. 17754-17763.

112. Chang, S.S.F. and G.M. Bone, "Burr height model for vibration assisted drilling of aluminum 6061-T6", *Precision Engineering*, 2010, **34**(3): pp. 369-375.

113. Aurich, J.C., D. Dornfeld, P. Arrazola, V. Franke, L. Leitz, and S. Min, "Burrs - analysis, control and removal", *CIRP Annals Manufacturing Technology*, 2009, **58**(2): pp. 519-542.

114. Dornfeld, D., J. Kim, H. Dechow, J. Hewson, and L. Chen, "Drilling burr formation in titanium alloy, Ti6AI4V", *CIRP Annals-Manufacturing Technology*, 1999, **48**(1): pp. 73-76.

115. Zhang, P., N. Churi, Z.J. Pei, and C. Treadwell, "Mechanical drilling processes for titanium alloys: a literature review", *Machining Science and Technology*, 2008, **12**(4): pp. 417-444.

116. Min, S., J. Kim, and D.A. Dornfeld, "Development of a drilling burr control chart for low alloy steel, AISI 4118", *Journal of materials processing technology*, 2001, **113**(1): pp. 4-9.

117. Niknam, S.A., *Surface treatment, finishing and integrity: Special case of machined edge finishing - burr and deburring*, in *Lecture Slides Presentation*. 2014: Laboratory of Products, Processes and Systems Engineering (LPPSE) Department of Mechanical Engineering Ecole de technologie superieure (ETS).

118. Percin, M., K. Aslantas, I. Ucun, Y. Kaynak, and A. Cicek, "Micro-drilling of Ti6Al4V alloy: The effects of cooling/lubricating", *Precision Engineering*, 2016, **45**: pp. 450-462.

119. Davim, J.P., *Surface Integrity in Machining*. Vol. 1848828742. 2010: Springer.

120. Isbilir, O. and E. Ghassemieh, "Numerical investigation of the effects of drill geometry on drilling induced delamination of carbon fiber reinforced composites", *Composite Structures*, 2013, **105**(0): pp. 126-133.

121. Celik, Y.H., "Investigating the effects of cutting parameters on the hole quality in drilling the Ti6Al4V alloy", *Materiali in Tehnologije*, 2014, **48**(5): pp. 653-659.

122. Che-Haron, C. and A. Jawaid, "The effect of machining on surface integrity of titanium alloy Ti6Al4V", *Journal of Materials Processing Technology*, 2005, **166**(2): pp. 188-192.

123. Li, R., L. Riester, T.R. Watkins, P.J. Blau, and A.J. Shih, "Metallurgical analysis and nanoindentation characterization of Ti6Al4V workpiece and chips in high-throughput drilling", *Materials Science and Engineering: A*, 2008, **472**(1): pp. 115-124.

124. Jawahir, I., E. Brinksmeier, R. M'Saoubi, D. Aspinwall, J. Outeiro, D. Meyer, D. Umbrello, and A. Jayal, "Surface integrity in material removal processes: Recent advances", *CIRP Annals Manufacturing Technology*, 2011, **60**(2): pp. 603-626.

125. Sun, J. and Y. Guo, "A comprehensive experimental study on surface integrity by end milling Ti6Al4V", *Journal of Materials Processing Technology*, 2009, **209**(8): pp. 4036-4042.

126. Yang, X., C. Ren, Y. Wang, and G. Chen, "Experimental study on surface integrity of Ti6Al4V in high speed side milling", *Transactions of Tianjin University*, 2012, **18**(3): pp. 206-212.

127. Paulsen, T., O. Pecat, and E. Brinksmeier, "Influence of different machining conditions on the subsurface properties of drilled TiAl6V4", *Procedia CIRP*, 2016, **46**: pp. 472-475.

128. Chen, L., T. El-Wardany, and W. Harris, "Modelling the effects of flank wear land and chip formation on residual stresses", *CIRP Annals-Manufacturing Technology*, 2004, **53**(1): pp. 95-98.

129. Durão, L.M.P., D.J. Gonçalves, J.M.R. Tavares, V.H.C. de Albuquerque, A.A. Vieira, and A.T. Marques, "Drilling tool geometry evaluation for reinforced composite laminates", *Composite Structures*, 2010, **92**(7): pp. 1545-1550.

130. Isbilir, O. and E. Ghassemieh, "Finite element analysis of drilling of titanium alloy", *Procedia Engineering*, 2011, **10**: pp. 1877-1882.

131. Brinksmeier, E., O. Pecat, and R. Rentsch, "Quantitative analysis of chip extraction in drilling of Ti6Al4V", *CIRP Annals Manufacturing Technology*, 2015.

132. Ramulu, M., T. Branson, and D. Kim, "A study on the drilling of composite and titanium stacks", *Composite Structures*, 2001, **54**(1): pp. 67-77.

133. SenthilKumar, M., A. Prabukarthi, and V. Krishnaraj, "Study on tool wear and chip formation during drilling carbon fiber reinforced polymer (CFRP)/titanium alloy Ti6Al4V stacks", *Procedia Engineering*, 2013, **64**: pp. 582-592.

134. Beal, A., D.D.W. Kim, K.H. Park, and P. Kwon. *A comparative study of carbide tools in drilling of CFRP and CFRP-Ti stacks*. in *ASME 2011 International Manufacturing Science and Engineering Conference*. Corvallis, Oregon, USA: 13 – 17 June 2011, American Society of Mechanical Engineers, pp. 145-152.

135. Park, K.-H. and P. Kwon, "Wear characteristic on BAM coated carbide tool in drilling of composite/titanium stack", *International Journal of Precision Engineering and Manufacturing*, 2012, **13**(7): pp. 1073-1076.

136. Park, K.-H., A. Beal, P. Kwon, and J. Lantrip, "A comparative study of carbide tools in drilling of CFRP and CFRP-Ti stacks", *Journal of Manufacturing Science and Engineering*, 2014, **136**(1): pp. 014501.

137. Poutord, A., F. Rossi, G. Poulachon, R. M'Saoubi, and G. Abrivard, "Local Approach of Wear in Drilling Ti6Al4V/CFRP for Stack Modelling", *Procedia CIRP*, 2013, **8**(0): pp. 316-321.

138. *Ultrasonic Series*. 2014, DMG Mori. Available from: http://uk.dmgmori.com/blob/127642/d0e7715c390265e3a0d5d224d5aa5e3f/pu0uk13-ultrasonic-pdf-data.pdf (Assessed 10 June 2015).

139. Baghlani, V., P. Mehbudi, J. Akbari, and M. Sohrabi, "Ultrasonic Assisted Deep Drilling of Inconel 738LC Superalloy", *Procedia CIRP*, 2013, **6**: pp. 571-576.

140. Makhdum, F., V.A. Phadnis, A. Roy, and V.V. Silberschmidt, "Effect of ultrasonically assisted drilling on carbon fibre reinforced plastics", *Journal of Sound and Vibration*, 2014, **333**(23): pp. 5939-5952.

141. Sanda, A., I. Arriola, V.G. Navas, I. Bengoetxea, and O. Gonzalo, "Ultrasonically assisted drilling of carbon fibre reinforced plastics and Ti6Al4V", *Journal of Manufacturing Processes*, 2016, **22**: pp. 169-176.

142. Phadnis, V.A., F. Makhdum, A. Roy, and V.V. Silberschmidt, "Experimental and numerical Investigations in conventional and ultrasonically assisted drilling of CFRP Laminate", *Procedia CIRP*, 2012, **1**: pp. 455-459.

143. Pecat, O. and E. Brinksmeier, "Tool wear analyses in low frequency vibration assisted drilling of CFRP/Ti6Al4V stack material", *Procedia CIRP*, 2014, **14**: pp. 142-147.

144. Pecat, O. and E. Brinksmeier, "Low damage drilling of CFRP/titanium compound materials for fastening", *Procedia CIRP*, 2014, **13**: pp. 1-7.

145. Lonfier, J. and C. De Castelbajac, "A comparison between regular and vibration assisted drilling in CFRP/Ti6Al4V stack", *SAE International Journal of Materials and Manufacturing*, 2014, **8**(2014-01-2236): pp. 18-26.

146. Makhdum, F., L.T. Jennings, A. Roy, and V.V. Silberschmidt. *Cutting forces in ultrasonically assisted drilling of carbon fibre-reinforced plastics*. in *Journal of Physics: Conference Series*. 2012. IOP Publishing, pp. 012019.

147. Pujana, J., A. Rivero, A. Celaya, and L.N. López de Lacalle, "Analysis of ultrasonic-assisted drilling of Ti6Al4V", *International Journal of Machine Tools and Manufacture*, 2009, **49**(6): pp. 500-508.

148. Babitsky, V.I., V.K. Astashev, and A. Meadows, "Vibration excitation and energy transfer during ultrasonically assisted drilling", *Journal of Sound and Vibration*, 2007, **308**(3–5): pp. 805-814.

149. Astashev, V.K., K. Khusnutdinova, and V. Babitsky, *Ultrasonic Processes and Machines: Dynamics, Control and Applications*. 2007: Springer. ISBN 9783540720614.

150. Maurotto, A., R. Muhammad, A. Roy, and V.V. Silberschmidt, "Enhanced ultrasonically assisted turning of a β-titanium alloy", *Ultrasonics*, 2013, **53**(7): pp. 1242-1250.

151. *ISO 3685: 1993 (E)*. Tool life testing with single-point turning tools 1993. p. 11.

152. Ladonne, M., M. Cherif, Y. Landon, J.-Y. K'Nevez, O. Cahuc, and C. de Castelbajac, "Modelling the vibration-assisted drilling process: identification of influential phenomena", *The International Journal of Advanced Manufacturing Technology*, 2015, **81**(9-12): pp. 1657-1666.

153. Neugebauer, R. and A. Stoll, "Ultrasonic application in drilling", *Journal of materials processing technology*, 2004, **149**(1): pp. 633-639.

154. Cytec. *CYCOM 5250-4 Pre-preg System: Technical Data Sheet*. 2012. Available from: https://www.cytec.com/sites/default/files/datasheets/CYCOM_5250-4_032012.pdf (Assessed 5 July 2014).

155. *CoroDrill® Delta-C high precision carbide drill* Rotating Tools: Drilling 2012, Sandvik Coromant. p. 10. Available from: http://www2.coromant.sandvik.com/coromant/downloads/catalogue/us/ROT_E.pdf (Assessed 10 April 2015).

156. *Laser sensors*. 2016; Available from: http://www.keyence.co.uk/products/sensor/laser/index.jsp (Assessed 3 March 2016).

157. Raath, N., D. Norman, I. McGregor, R. Dashwood, and D. Hughes, "Effect of Weld Schedule on the Residual Stress Distribution of Boron Steel Spot Welds", *Metallurgical and Materials Transactions A*, 2017, **48**(6): pp. 2900-2914.

158. *LAMP, the Large Array Manipulation Program*. Available from: http://www.ill.cu/data_treat/lamp/the-lamp-book/ (Assessed 6 August 2017).

159. Private Communication with Cook, A., Specialist Development Engineer at BAE Systems Samlesbury, June 2014.

160. Montgomery, D.C. and G.C. Runger, *Applied Statistics and Probability for Engineers*. 2010: John Wiley & Sons. ISBN 0470053046.

161. Bhudwannachai, P., *Performance evaluation and analysis of the use of CO2 cooling for conventional drilling of carbon fibre reinforced plastics*. 2014, PhD Thesis, University of Warwick.

162. Chelliah, N. and S.V. Kailas, "Synergy between tribo-oxidation and strain rate response on governing the dry sliding wear behavior of titanium", *Wear*, 2009, **266**(7): pp. 704-712.

163. Fan, Y., Z. Hao, J. Lin, and Z. Yu, "New observations on tool wear mechanism in machining Inconel 718 under water vapor + air cooling lubrication cutting conditions", *Journal of Cleaner Production*, 2015, **90**: pp. 381-387.

164. Gurbatov, S.N., O.V. Rudenko, and A. Saichev, *Waves and Structures in Nonlinear Nondispersive Media: General Theory and Applications to Nonlinear Acoustics*. 2012: Springer Science & Business Media. ISBN 9783642236174.

165. Karpat, Y., "Temperature dependent flow softening of titanium alloy Ti6Al4V: An investigation using finite element simulation of machining", *Journal of Materials Processing Technology*, 2011, **211**(4): pp. 737-749.

166. Ismail, S.O., H.N. Dhakal, I. Popov, and J. Beaugrand, "Comprehensive study on machinability of sustainable and conventional fibre reinforced polymer composites", *Engineering Science and Technology, an International Journal*, 2016, **19**(4): pp. 2043-2052.

167. Ko, S.-L., J.-E. Chang, and S. Kaipakjian, "Development of drill geometry for burr minimization in drilling", *CIRP Annals Manufacturing Technology*, 2003, **52**(1): pp. 45-48.

168. Tsao, C. and H. Hocheng, "Computerized tomography and C-Scan for measuring delamination in the drilling of composite materials using various drills", *International Journal of Machine Tools and Manufacture*, 2005, **45**(11): pp. 1282-1287.

Appendix A

Appendix A presents statistical analysis, i.e. ANOVA (Analysis of Variance) for data / results in Chapter 4 (Sections 4.2 and 4.3). The difference between the data generated is statistically significant when the value of calculated F_{ratio} is higher than the value of $F_{critical}$. The ANOVA was conducted using Microsoft Excel Data Analysis Pack Software.

Table A.1: ANOVA for flank wear data produced due to CD and UAD of CFRP/Ti stacks at cutting speeds 25, 50 and 75 m/min and a constant feed rate of 0.05 mm/rev

Source of variations	Sum of squares	Degree of freedom	Mean sum of squares	F_{ratio}	$F_{critical}$	Remark
Between cutting speed	53515.04	2	26757.52	5.13	3.32	Significant
Between CD and UAD	1072.56	1	1072.56	0.21	4.17	Not significant

Table A.2: ANOVA for Ti chip thickness data produced during CD and UAD of CFRP/Ti stacks at cutting speeds 25, 50 and 75 m/min and a constant feed rate of 0.05 mm/rev

Source of variations	Sum of squares	Degree of freedom	Mean sum of squares	F_{ratio}	$F_{critical}$	Remark
Between cutting speed	107.25	2	53.62	11.23	3.17	Significant
Between CD and UAD	27.07	1	27.07	5.67	4.02	Significant

Table A.3: ANOVA for hole diameter in CFRP produced during CD and UAD of CFRP/Ti stacks at cutting speeds 25, 50 and 75 m/min and a constant feed rate of 0.05 mm/rev

Source of variations	Sum of squares	Degree of freedom	Mean sum of squares	F_{ratio}	$F_{critical}$	Remark
Between cutting speed	8.0×10^{-4}	2	4.0×10^{-4}	45.91	3.09	Significant
Between CD and UAD	1.3×10^{-4}	1	1.3×10^{-4}	15.06	3.94	Significant

Table A.4: ANOVA for hole diameter in Ti produced during CD and UAD of CFRP/Ti stacks at cutting speeds 25, 50 and 75 m/min and a constant feed rate of 0.05 mm/rev

Source of variations	Sum of squares	Degree of freedom	Mean sum of squares	F_{ratio}	$F_{critical}$	Remark
Between cutting speed	8.8×10^{-4}	2	4.4×10^{-4}	44.05	3.09	Significant
Between CD and UAD	2.8×10^{-4}	1	2.8×10^{-5}	2.80	3.94	Not Significant

Table A.5: ANOVA for volume of CFRP pull-out caused by CD and UAD of CFRP/Ti stacks at cutting speeds 25, 50 and 75 m/min and a constant feed rate of 0.05 mm/rev

Source of variations	Sum of squares	Degree of freedom	Mean sum of squares	F_{ratio}	$F_{critical}$	Remark
Between cutting speed	7.3×10^{-3}	2	3.6×10^{-3}	1.70	3.19	Not Significant
Between CD and UAD	1.5×10^{-4}	1	1.5×10^{-4}	0.07	4.04	Not Significant

Table A.6: ANOVA for R_a data produced by CD and UAD of CFRP/Ti stacks at cutting speeds 25, 50 and 75 m/min and a constant feed rate of 0.05 mm/rev

Source of variations	Sum of squares	Degree of freedom	Mean sum of squares	F_{ratio}	$F_{critical}$	Remark
Between cutting speed	0.12	2	0.059	1.78	3.19	Not Significant
Between CD and UAD	2.96	1	2.96	88.31	4.04	Significant

Table A.7: ANOVA for Ti burr height data produced by CD and UAD of CFRP/Ti stacks at cutting speeds 25, 50 and 75 m/min and a constant feed rate of 0.05 mm/rev

Source of variations	Sum of squares	Degree of freedom	Mean sum of squares	F_{ratio}	$F_{critical}$	Remark
Between cutting speed	298435	2	149218	12.51	3.09	Significant
Between CD and UAD	4467	1	4467	0.37	3.94	Not Significant

Table A.8: ANOVA for flank wear data produced by CD and UAD of CFRP/Ti stacks at feed rates of 0.025, 0.05 and 0.075 mm/rev and a constant cutting speed of 50 m/min

Source of variations	Sum of squares	Degree of freedom	Mean sum of squares	F_{ratio}	$F_{critical}$	Remark
Between feed rates	41889	2	20945	4.78	3.32	Significant
Between CD and UAD	46.69	1	46.69	0.01	4.17	Not Significant

Table A.9: ANOVA for Ti chip thickness data produced by CD and UAD of CFRP/Ti stacks at feed rates of 0.025, 0.05 and 0.075 mm/rev and a constant cutting speed of 50 m/min

Source of variations	Sum of squares	Degree of freedom	Mean sum of squares	F_{ratio}	$F_{critical}$	Remark
Between feed rates	10607	2	5303	365	3.11	Significant
Between CD and UAD	62.03	1	62.03	4.27	3.95	Significant

Table A.10: ANOVA for hole diameter in CFRP produced by CD and UAD of CFRP/Ti stacks at feed rates of 0.025, 0.05 and 0.075 mm/rev and a constant cutting speed of 50 m/min

Source of variations	Sum of squares	Degree of freedom	Mean sum of squares	F_{ratio}	$F_{critical}$	Remark
Between feed rates	1.1×10^{-4}	2	5.6×10^{-5}	9.58	3.09	Significant
Between CD and UAD	9.2×10^{-5}	1	9.2×10^{-5}	15.71	9.94	Significant

Table A.11: ANOVA for hole diameter in Ti produced by CD and UAD of CFRP/Ti stacks at feed rates of 0.025, 0.05 and 0.075 mm/rev and a constant cutting speed of 50 m/min

Source of variations	Sum of squares	Degree of freedom	Mean sum of squares	F_{ratio}	$F_{critical}$	Remark
Between feed rates	1.0×10^{-3}	2	5.2×10^{-4}	59.86	3.09	Significant
Between CD and UAD	2.8×10^{-5}	1	2.8×10^{-5}	3.25	3.94	Not Significant

Table A.12: ANOVA for volume of CFRP pull-out produced by CD and UAD of CFRP/Ti stacks at feed rates of 0.025, 0.05 and 0.075 mm/rev and a constant cutting speed of 50 m/min

Source of variations	Sum of squares	Degree of freedom	Mean sum of squares	F_{ratio}	$F_{critical}$	Remark
Between feed rates	0.05	2	0.025	10.94	3.19	Significant
Between CD and UAD	4.9 x 10-4	1	4.9 x 10-4	0.21	4.04	Not Significant

Table A.13: ANOVA for R_a data produced by CD and UAD of CFRP/Ti stacks at feed rates of 0.025, 0.05 and 0.075 mm/rev and a constant cutting speed of 50 m/min

Source of variations	Sum of squares	Degree of freedom	Mean sum of squares	F_{ratio}	$F_{critical}$	Remark
Between feed rates	0.12	2	0.059	1.24	3.19	Not Significant
Between CD and UAD	2.36	1	2.36	49.41	4.04	Significant

Table A.14: ANOVA for Ti burr height data produced by CD and UAD of CFRP/Ti stacks at feed rates of 0.025, 0.05 and 0.075 mm/rev and a constant cutting speed of 50 m/min

Source of variations	Sum of squares	Degree of freedom	Mean sum of squares	F_{ratio}	$F_{critical}$	Remark
Between feed rates	146784	2	73392	9.26	3.09	Significant
Between CD and UAD	4767	1	4767	0.60	3.94	Not Significant

Appendix B

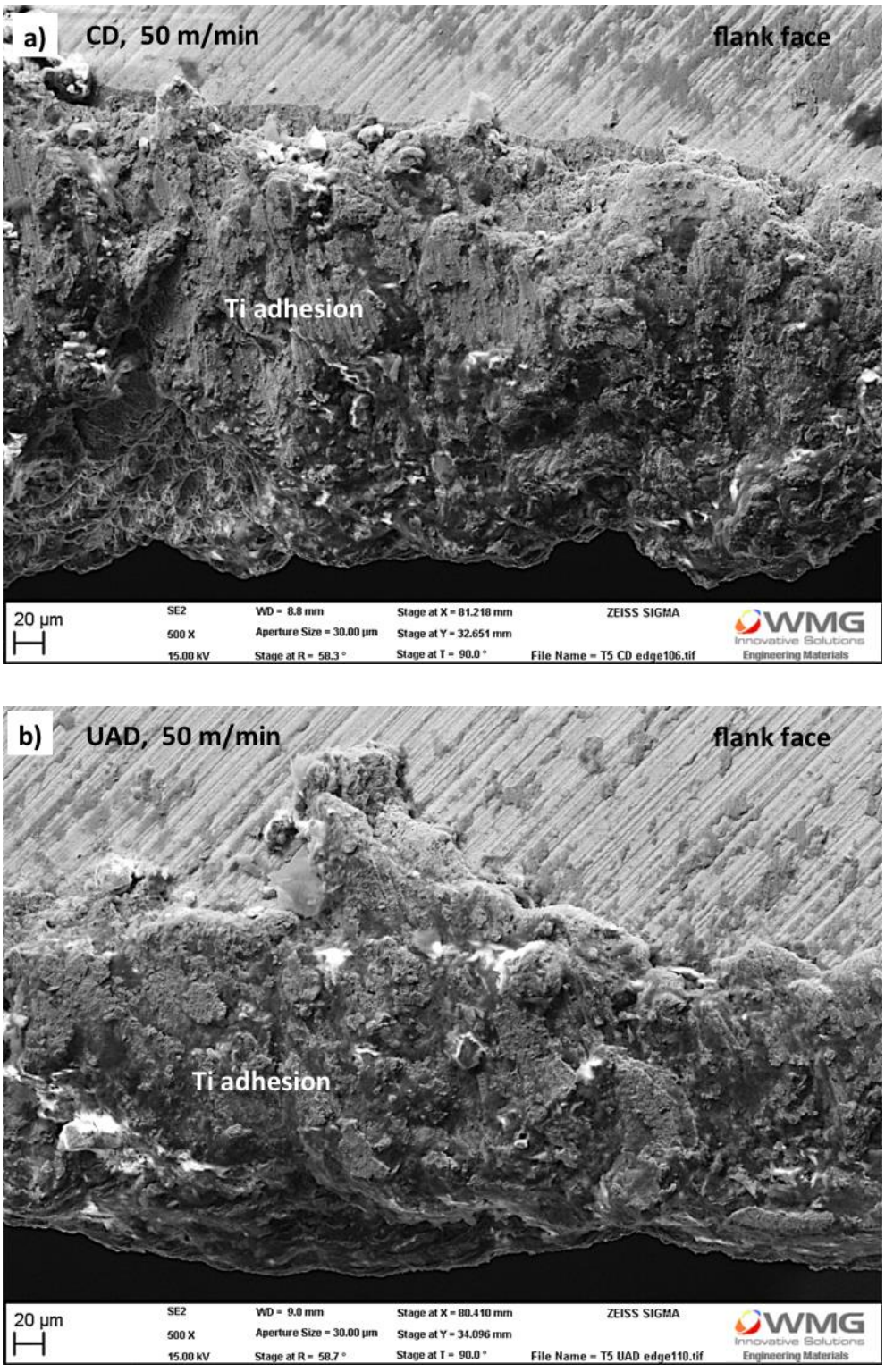

Figure B.1: SEM micrographs showing morphology of adhered Ti on the cutting edge and flank face condition after (a) CD and (b) UAD, of 80 holes through CFRP/Ti stacks using a cutting speed of 50 m/min and feed rate of 0.05 mm/rev

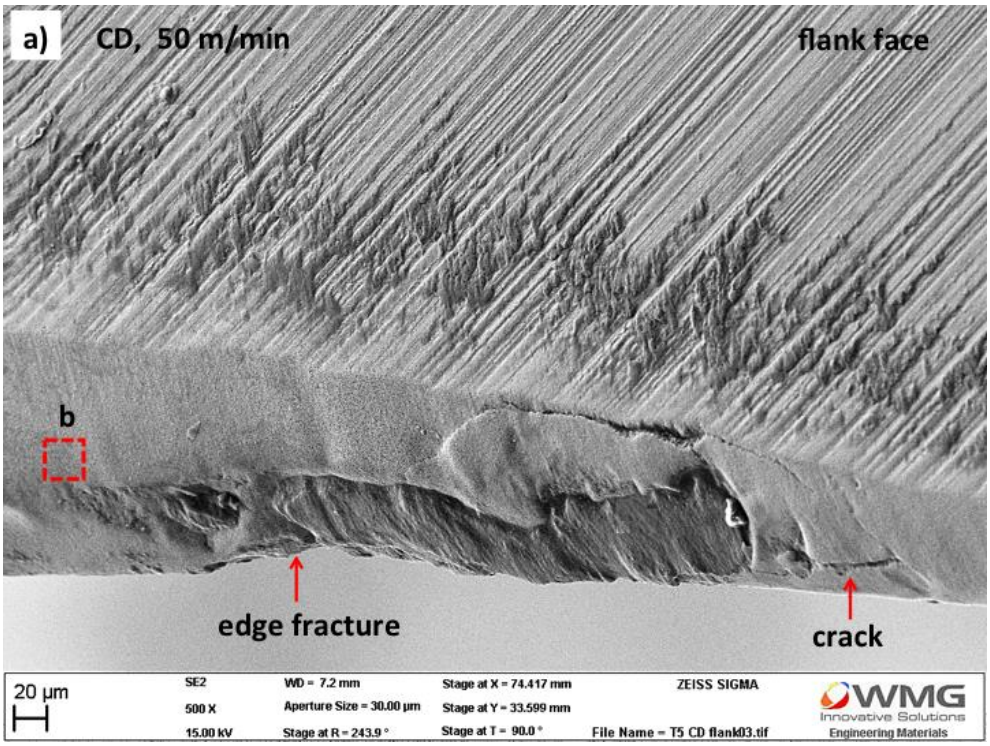

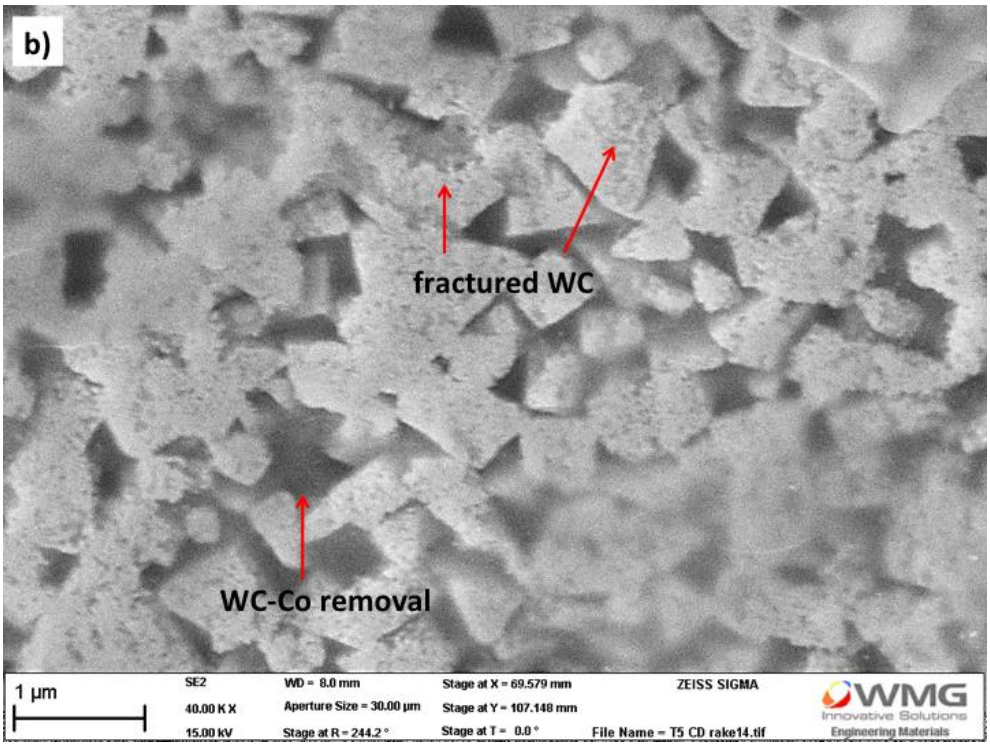

Figure B.2: SEM micrographs showing cutting edge and flank face condition after CD of 80 holes through CFRP/Ti stacks using a cutting speed of 50 m/min and feed rate of 0.05 mm/rev; following removal of the adhered Ti

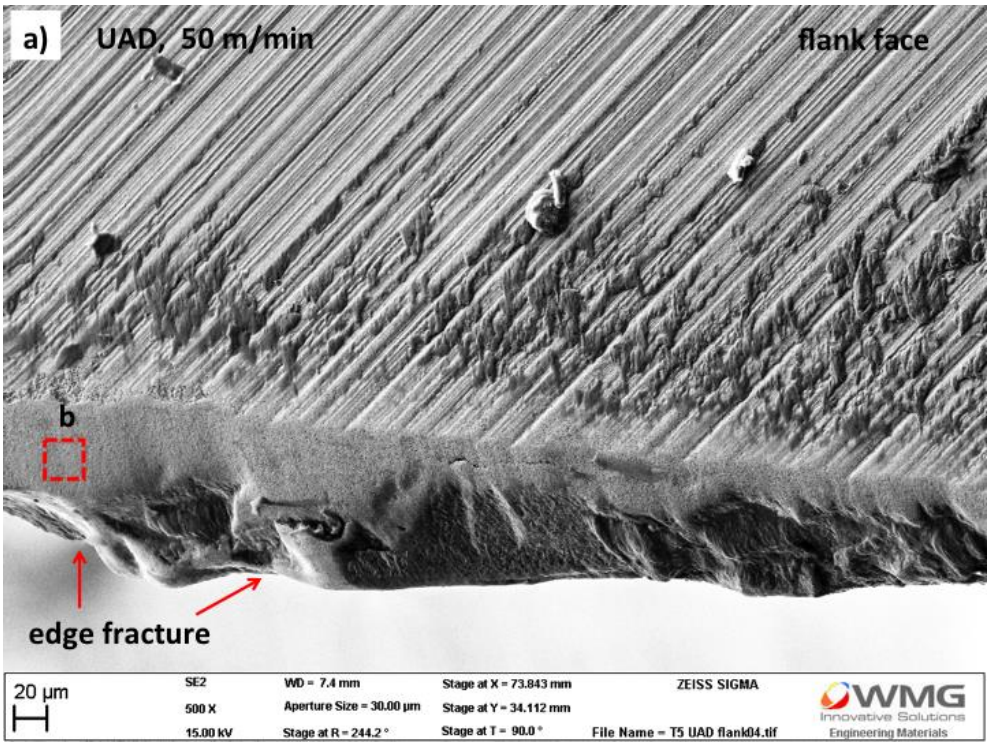

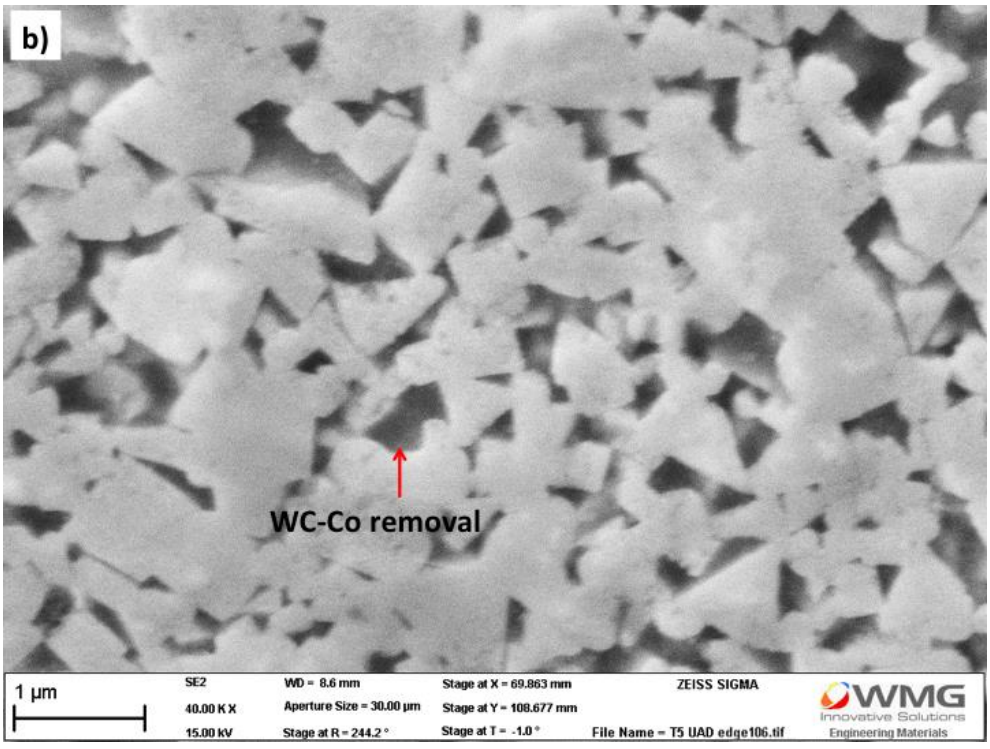

Figure B.3: SEM micrographs showing cutting edge and flank face condition after UAD of 80 holes through CFRP/Ti stacks using a cutting speed of 50 m/min and feed rate of 0.05 mm/rev; following removal of the adhered Ti

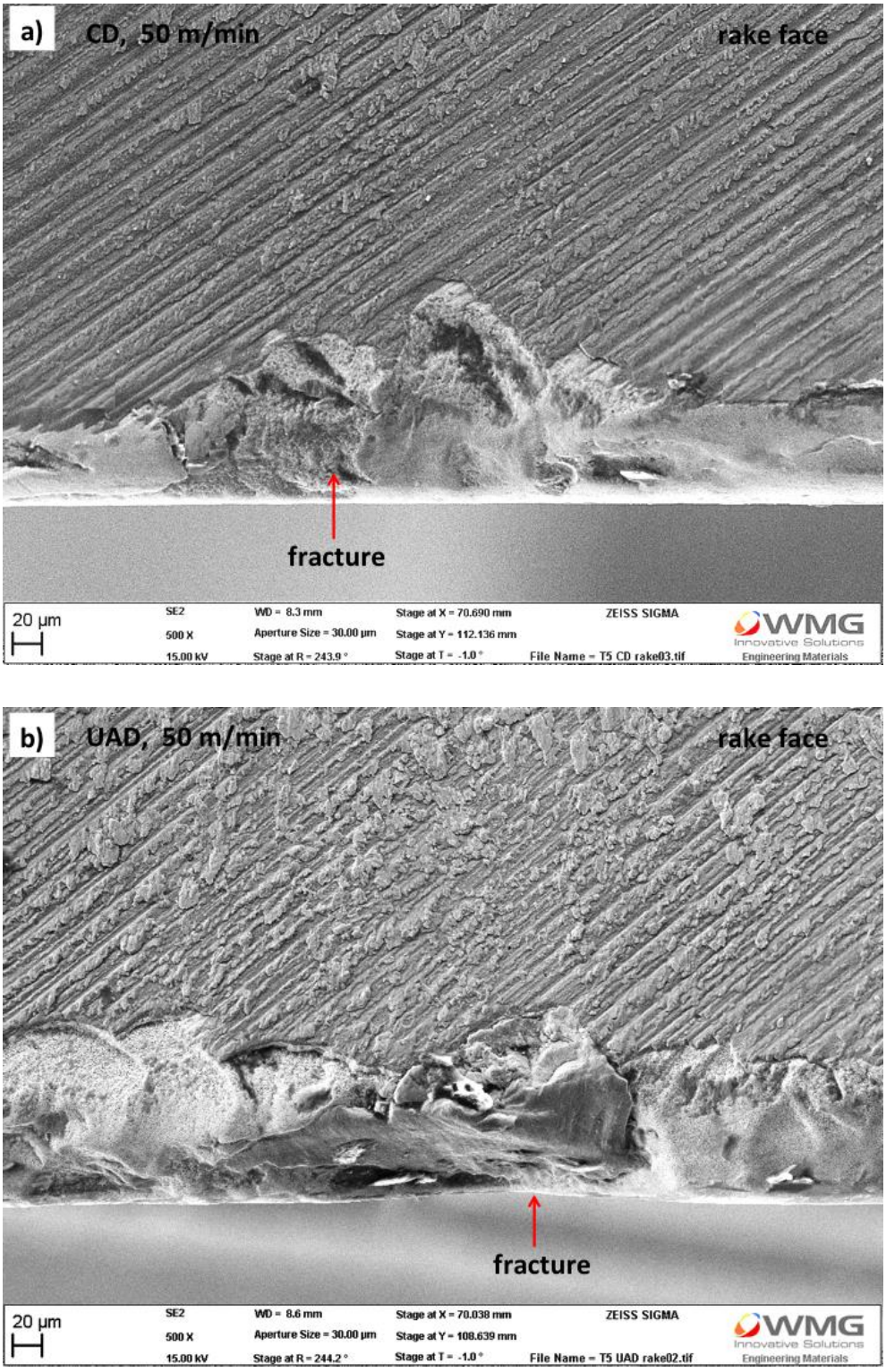

Figure B.4: SEM micrographs showing rake face condition after UAD of 80 holes through CFRP/Ti stacks using a cutting speed of 25 m/min and feed rate of 0.05 mm/rev; following removal of the adhered Ti

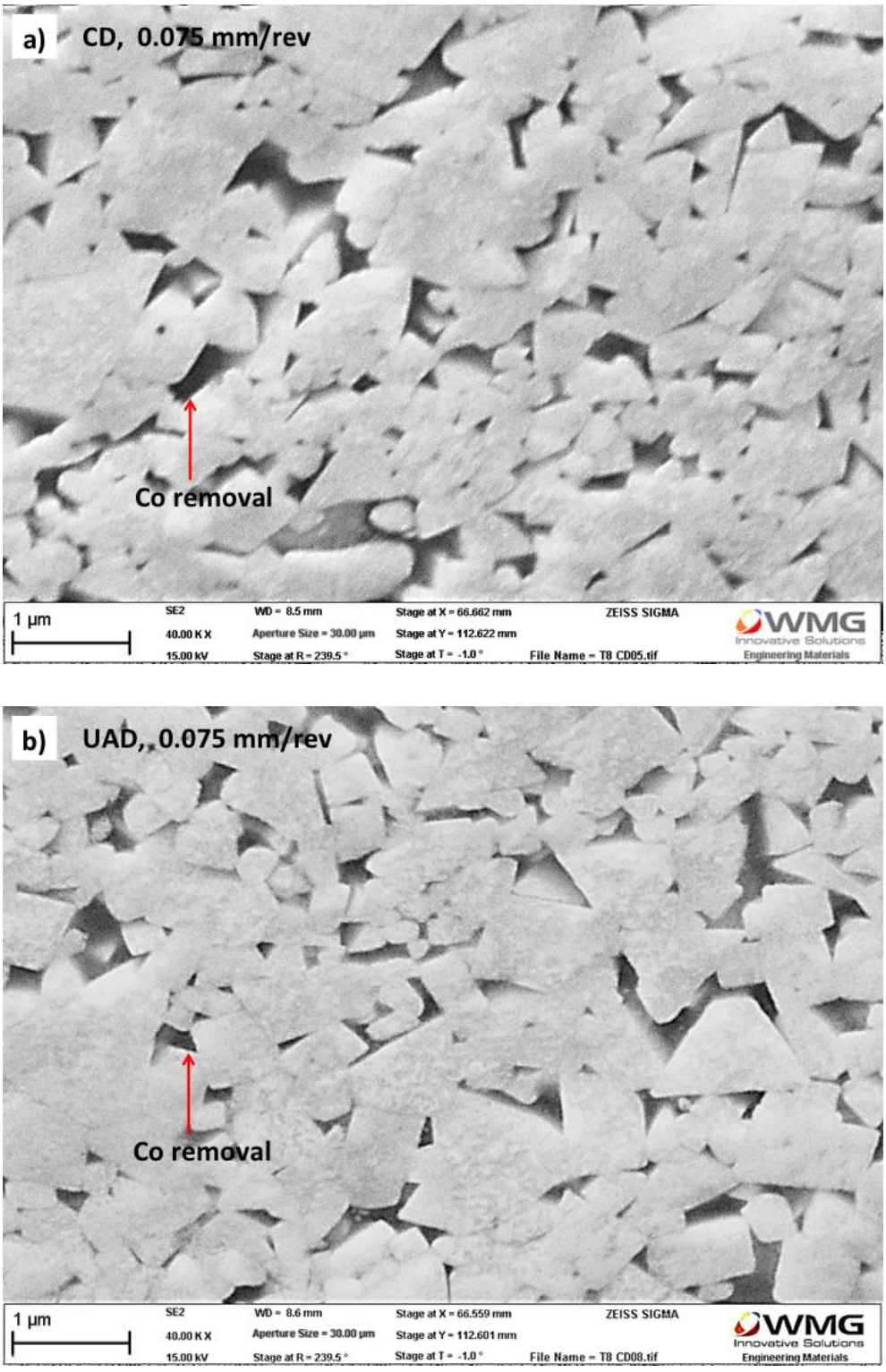

Figure B.5: SEM micrographs showing Co removal at the worn cutting edges after (a) CD and (b) UAD, of 80 holes through CFRP/Ti stacks using a feed rate of 0.075 mm/rev and cutting speed of 50 m/min

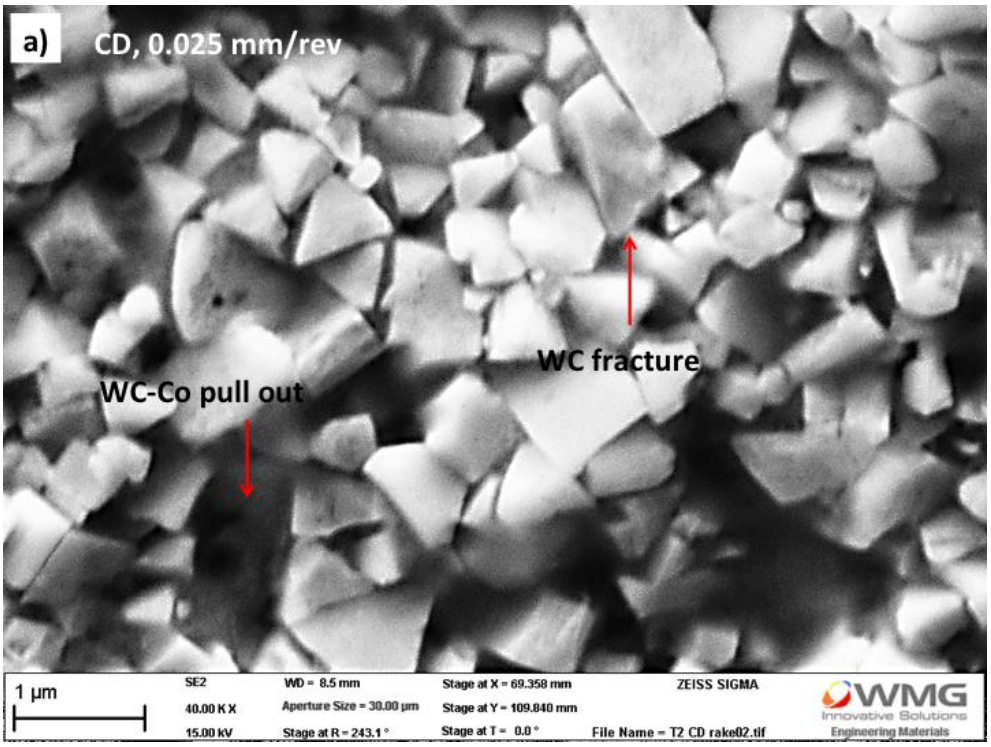

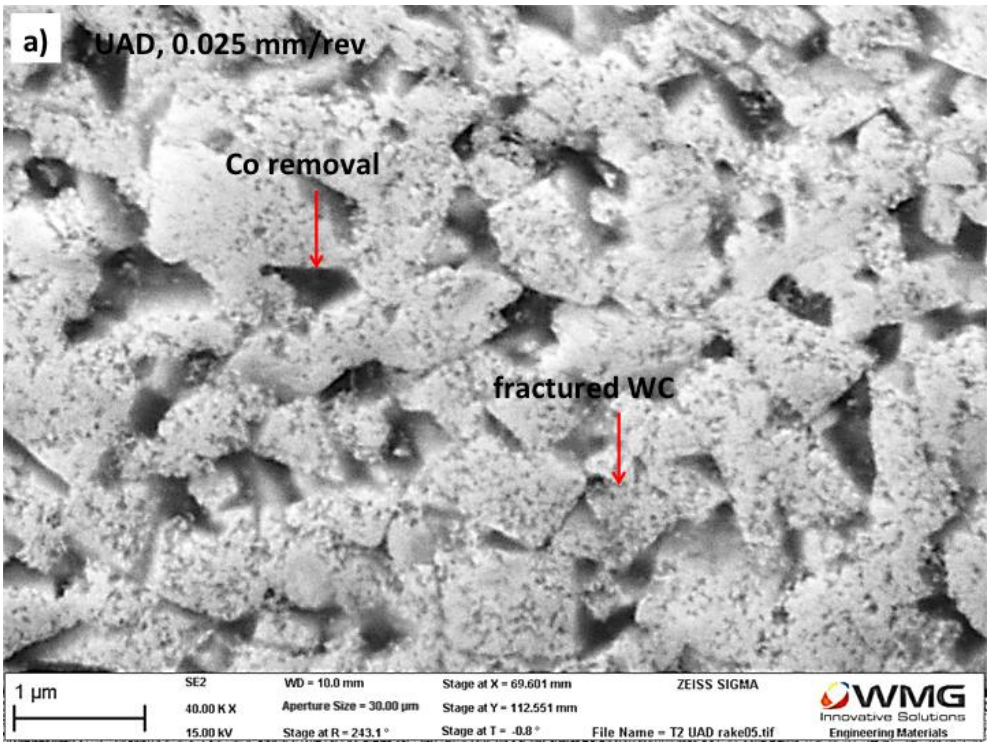

Figure B.6: SEM micrographs showing Co removal at the worn cutting edges after (a) CD and (b) UAD, of 80 holes through CFRP/Ti stacks using a feed rate of 0.025 mm/rev and cutting speed of 50 m/min

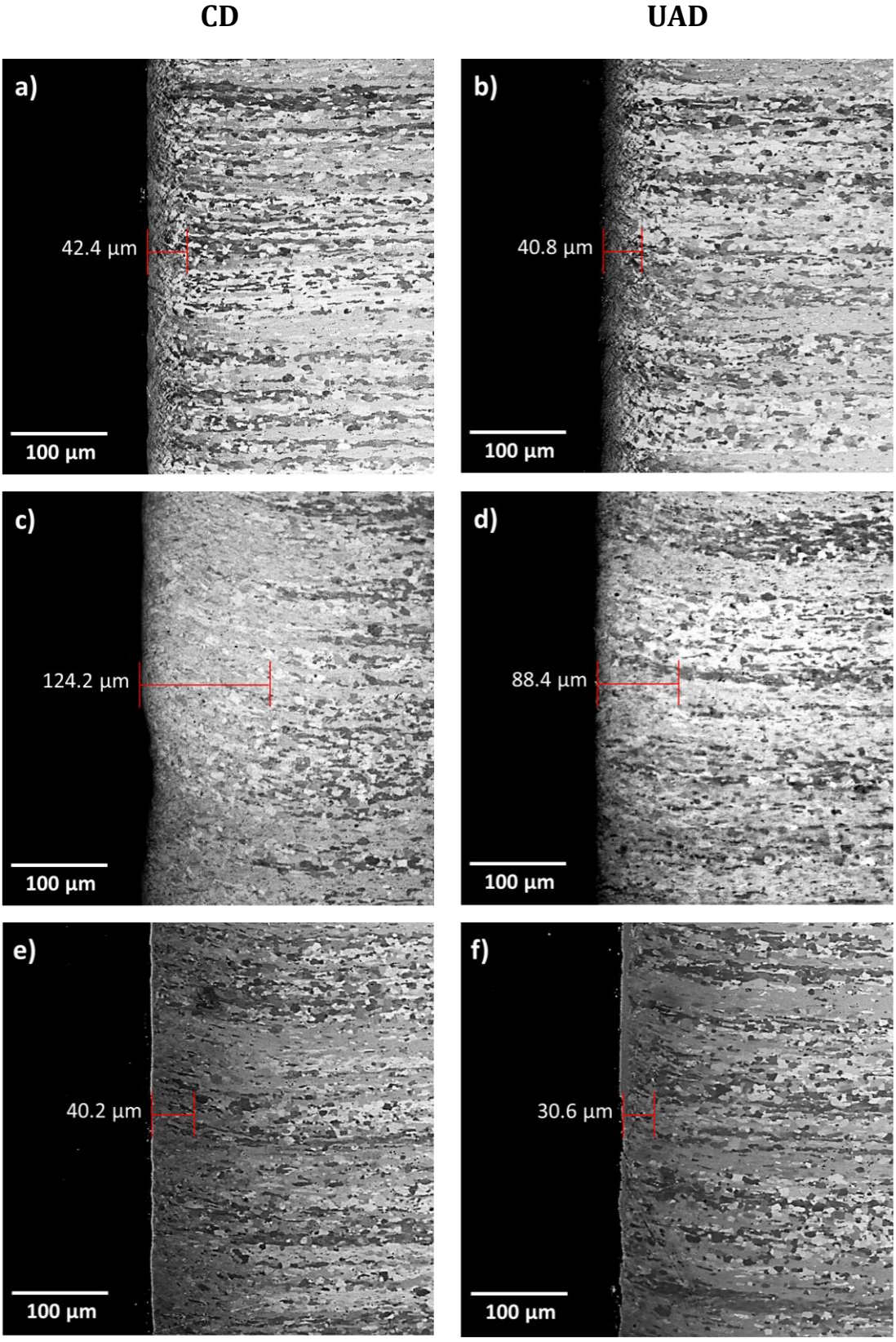

Figure B.7: Optical microscopy images showing grain deformation beneath machined Ti surfaces when CD and UAD of CFRP/Ti stacks using (a) 25 m/min, (b) 50 m/min and (c) 75 m/min at a constant feed rate of 0.05 mm/rev – 40th holes

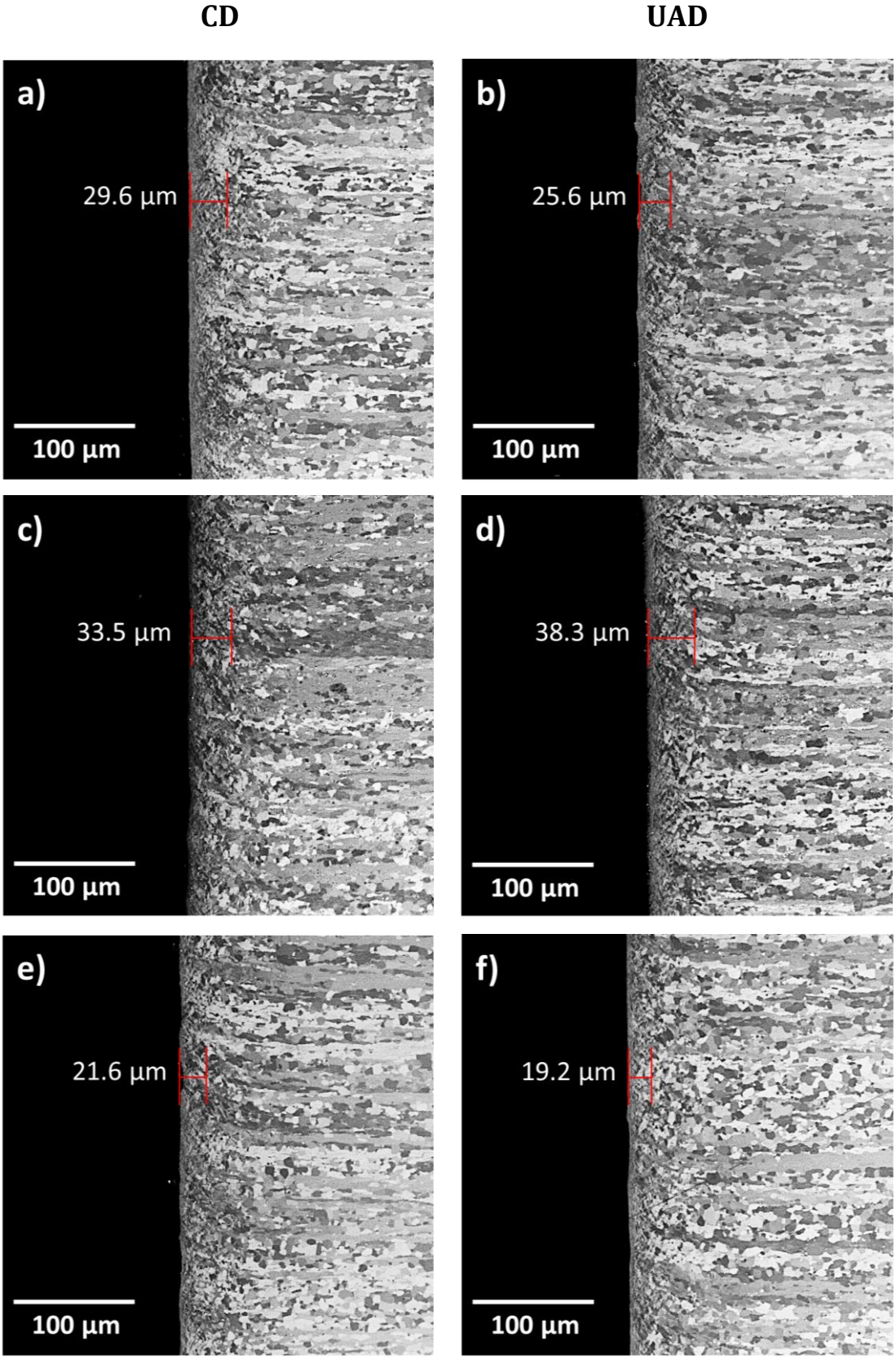

Figure B.8: Optical microscopy images showing grain deformation beneath machined Ti surfaces when CD and UAD of CFRP/Ti stacks using (a) 0.025 mm/rev, (b) 0.05 mm/rev and (c) 0.075 mm/rev at a constant cutting speed of 50 m/min – 1st holes

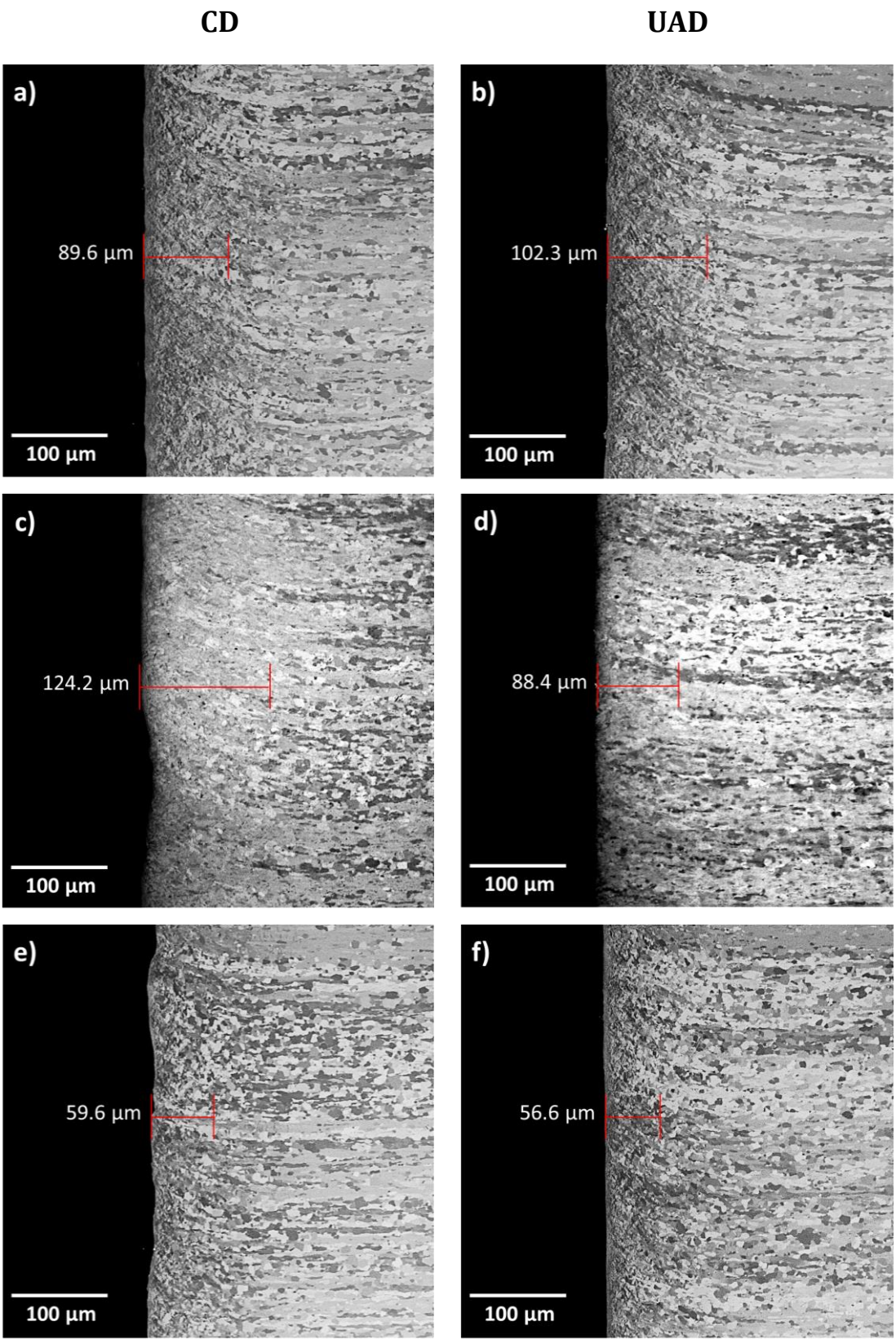

Figure B.9: Optical microscopy images showing grain deformation beneath machined Ti surfaces when CD and UAD of CFRP/Ti stacks using (a) 0.025 mm/rev, (b) 0.05 mm/rev and (c) 0.075 mm/rev at a constant cutting speed of 50 m/min – 40th holes